

CHARACTERIZATION AND FUNCTION OF THE NEK11 KINASE IN CANCER CELLS

Thesis submitted for the degree of

Doctor of Philosophy

at the University of Leicester

by

Sarah R. Sabir BSc (Hons) (Leicester)

Department of Biochemistry

University of Leicester

September 2014

DECLARATION

The accompanying thesis submitted for the degree of Doctor of Philosophy, entitled "Characterization and Function of the Nek11 Kinase in cancer cells" is based on work conducted by the author in the Department of Biochemistry at the University of Leicester mainly during the period between October 2010 and September 2014. All work recorded in this thesis is original unless otherwise acknowledged in the text or by references. None of the work has been submitted for another degree in this or any other University.

Signed:

Date:

Department of Biochemistry

University of Leicester

Lancaster road

Leicester

LE1 9HN

CHARACTERIZATION AND FUNCTION OF THE NEK11 KINASE IN CANCER CELLS

Sarah R. Sabir

ABSTRACT

The human serine/threonine NIMA-related protein kinase family comprises eleven members, named Nek1 to Nek11. Of these, Nek1, Nek4, Nek8, Nek10 and Nek11 are implicated in the DNA damage response (DDR) with Nek11 playing a central role in the G2/M checkpoint. In response to DNA damage, Chk1 is activated by the ATM/ATR kinases. Chk1 then phosphorylates and activates Nek11 before both Chk1 and Nek11 phosphorylate Cdc25A. This promotes binding of SCF^{B-TrCP} and subsequent degradation of Cdc25A resulting in cell cycle arrest at G2/M. Nek11 protein expression is also increased in colorectal cancers. This study focuses on the role of Nek11 in colorectal cancer cells to examine whether targeting Nek11 in combination with DNA damaging agents may have a clinical benefit for colorectal cancer patients. Using RNAi to deplete Nek11 in HCT116 colorectal cancer cells we show that Nek11 is required for the G2/M arrest in response to ionizing radiation and chemotherapeutically relevant drugs, oxaliplatin and irinotecan. Furthermore, depletion of Nek11 alone and in combination with IR results in apoptosis and loss of cell survival. Nek11 exists as several closely related but distinct isoforms in colorectal cancer cells: Nek11 Long (L), Nek11 Short (S), Nek11C and Nek11D. We reveal that depletion of Nek11S results in a more substantial abrogation of the G2/M checkpoint, as compared to depletion of the Nek11L or D isoforms. Furthermore, through the use of stable cell lines, we show Nek11 isoforms exhibit distinct localisation patterns and all isoforms are able to undergo nucleocytoplasmic shuttling, regulated by the C-terminal domain. Excitingly, we observe Nek11 localisation at sites of DNA damage foci in response to IR exposure. Overall, our findings reveal an essential role for Nek11 at the G2/M checkpoint in HCT116 cells contributing not only to their arrest but also their survival after DNA damage. Hence, Nek11 could be an exciting target for the development of novel anti-cancer drugs.

ACKNOWLEDGEMENTS

I would like to start off by saying a huge thank you to my supervisor, Professor Andrew Fry. Andrew has played a key role in my science career so far and his guidance and enthusiasm over the past years have been invaluable. He has always been approachable and helpful in times of great urgency (!) and never ceases to amaze me with his wealth of knowledge. So, thank you for all of your support and wisdom, Andrew, and making my PhD experience a useful and enjoyable one. I would also like to thank my co-supervisor, Dr Don Jones, for useful advice throughout my project and for his enthusiasm during discussions. Many thanks also go to my committee members, Professor Marion MacFarlane and Professor Maggie Manson for helpful and insightful discussions throughout my PhD.

Lab work just wouldn't have been the same without all of the past and present members of the Fry lab. I would like to thank Navdeep, Laura, Suzy, Magali, Joelle, Jo, Carla, Xavier and Tara for welcoming me to the lab and for always being willing to help and provide support. To present lab members, Jess, Tammy, Josephina and Karolin, my final year would not have been the same without you so thank you for creating an enjoyable working environment, and for your support and friendship.

To my other fellow biochemists, Emma, Ellie, Jesvin, Jen, Deep and Sam thank you for your friendship and making the biochemistry department a great place to work. I have thoroughly enjoyed going on my PhD journey with you.

Finally, but definitely not least, endless thanks goes to my Mum, Dad and Sister, Lisa, whose love and support have seen me through many ups and downs. You know you have awesome parents when they listen to science ramblings frequently over the phone! I wouldn't be here without your encouragement, wisdom and understanding.

CONTENTS

Declaration	I
Abstract	II
Acknowledgements	III
Contents	IV
Abbreviations	XI
Tables and Figures	XV
CHAPTER 1 Introduction	1
1.1 The eukaryotic cell cycle	1
1.2 Cell cycle regulation	3
1.2.1 Cyclins and Cdks	5
1.2.2 Checkpoints and control of cell cycle progression	8
1.2.2.1 G1/S regulation	8
1.2.2.2 S-phase regulation	9
1.2.2.3 G2/M regulation	10
1.2.2.4 SAC	10
1.3 DNA damage signalling and the DNA damage response	11
1.3.1 Sources of DNA damage	11
1.3.2 Types of DNA damage	14
1.3.3 The DNA damage response	16
1.3.3.1 Transcription	19
1.3.3.2 Cell cycle arrest at DNA damage checkpoints	20
1.3.3.3 DNA Repair	20
1.3.3.4 Senescence and apoptosis induction	22

1.4	DNA damage induced cell cycle checkpoints	23
1.4.1	The G1/S checkpoint	24
1.4.2	Intra-S.....	25
1.4.3	G2/M.....	27
1.4.4	The DDR, cell cycle checkpoints and relevance to cancer	29
1.5	NIMA-related protein kinases.....	30
1.5.1	NIMA	30
1.5.2	NIMA homologues in lower eukaryotes	33
1.5.3	The Mammalian NIMA-related kinase family	34
1.5.3.1	Mitotic Neks	36
1.5.3.2	Ciliary Neks.....	38
1.5.3.3	Signal transducing Neks	40
1.5.3.4	Neks implicated in the DNA damage response (DDR).....	40
1.5.4	Nek11	43
1.5.4.1	Nek11 and the DNA damage response	43
1.5.4.2	Nek11 localisation and interaction with Nek2.....	47
1.5.4.3	Nek11 as a potential cancer drug target	48
1.6	Colorectal cancer	50
1.6.1	Colorectal cancer incidence	50
1.6.2	Development of colorectal cancer	50
1.6.3	Current treatments.....	51
1.7	Aims and objectives	52
CHAPTER 2	Materials and Methods	54
2.1	Materials	54
2.1.1	Chemical suppliers	54

2.1.2	Vectors	55
2.1.3	Antibodies.....	56
2.1.3.1	Primary antibodies	56
2.1.3.2	Secondary antibodies	57
2.1.4	Drugs.....	57
2.1.5	siRNAs	58
2.1.6	qRT-PCR primers.....	58
2.2	Molecular biology techniques.....	59
2.2.1	Cloning	59
2.2.1.1	Oligonucleotide design.....	59
2.2.1.2	Polymerase chain reaction.....	59
2.2.1.3	Agarose gel electrophoresis.....	60
2.2.1.4	Purification of PCR products.....	60
2.2.1.5	DNA ligation into pGEM-T Easy vector	60
2.2.1.6	Bacterial transformation	61
2.2.1.7	Colony PCR	61
2.2.1.8	Isolation of plasmid DNA by miniprep purification.....	62
2.2.1.9	DNA quantification	62
2.2.1.10	DNA sequencing	62
2.2.2	Generation of eGFP tagged Nek11 constructs.....	62
2.2.3	Site-directed mutagenesis	63
2.2.3.1	Oligonucleotide design.....	63
2.2.3.2	Site-directed mutagenesis reaction.....	63
2.2.4	Isolation of plasmid DNA by maxiprep purification.....	64
2.3	Real-time quantitative RT-PCR	64
2.3.1	RNA extraction	64

2.3.2	First strand cDNA synthesis	65
2.3.3	qRT-PCR	65
2.3.3.1	Oligonucleotide design.....	65
2.3.3.2	qRT-PCR amplification conditions	66
2.3.3.3	Data analysis	66
2.4	Cell culture techniques.....	67
2.4.1	Human cell line maintenance	67
2.4.2	Cell line storage and recovery	67
2.4.3	Cell counting.....	68
2.4.4	Transient transfections	68
2.4.4.1	Lipofectamine transfection	68
2.4.4.2	FuGENE HD transfection.....	69
2.4.5	Generation of U2OS:GFP-Nek11 and U2OS:GFP stable cell lines...	69
2.4.5.1	G418 kill curve	69
2.4.5.2	Stable cell line generation	69
2.4.6	RNA interference	70
2.4.7	Irradiation treatment	70
2.4.8	Clonogenic assay	70
2.5	Flow cytometry.....	71
2.5.1	Cell cycle analysis	71
2.5.2	Annexin V assay.....	71
2.6	Protein analysis	72
2.6.1	Preparation of cell lysates	72
2.6.2	BCA protein assay.....	72
2.6.3	SDS polyacrylamide gels.....	73

2.6.4	Staining of protein gels	73
2.6.4.1	Standard Coomassie Blue staining	73
2.6.4.2	Brilliant blue colloidal stain for mass spectrometry (MS)	74
2.6.5	Western blotting.....	74
2.6.6	Immunoprecipitation	75
2.6.7	Indirect immunofluorescence microscopy.....	75
2.7	Immunohistochemistry.....	76
2.7.1	Generation of cytoblocks from cell suspensions.....	76
2.7.2	Immunohistochemical analysis	77
2.7.3	Ethical approval	77
2.8	Statistical analysis.....	78
CHAPTER 3	Nek11 is required for G2/M checkpoint activation in colorectal cancer cells.....	79
3.1	Introduction	79
3.2	Results	81
3.2.1	Optimisation of RNAi-mediated depletion of Nek11.....	81
3.2.2	Nek11 depletion has no effect on cell cycle progression in HCT116 cells.....	84
3.2.3	G2/M checkpoint activation in HCT116 cells is Chk1 dependent .	84
3.2.4	Nek11 is required for IR-induced DNA damage response in HCT116 WT and p53 null.....	87
3.2.5	Nek11 depletion enhances cell death in HCT116 cells.....	87
3.2.6	Nek11 is required for G2/M arrest induced by chemotherapeutic agents.....	93
3.2.6.1	Oxaliplatin-induced G2/M arrest is Nek11 dependent in HCT116 WT but not p53-null cells.....	93

3.2.6.2	Irinotecan-induced G2/M arrest is Nek11-dependent in HCT116 cells.....	97
3.2.7	Depletion of Nek11S results in a greater checkpoint abrogation	100
3.3	Discussion.....	103
CHAPTER 4	Localisation and function of Nek11 isoforms.....	108
4.1	Introduction	108
4.2	Results	111
4.2.1	Isolation of Nek11S and Nek11D cDNA from U2OS cells	111
4.2.2	Generation of GFP Nek11 stable cell lines.....	111
4.2.3	Nek11D is degraded by the proteasome	117
4.2.4	Subcellular localisation of recombinant Nek11 isoforms.....	117
4.2.5	Nek11 isoforms exhibit nucleocytoplasmic shuttling.....	125
4.2.6	IR exposure leads to Nek11 recruitment to sites of DNA damage....	131
4.2.7	Overexpression of Nek11L causes G2/M arrest and polyploidy .	133
4.3	Discussion.....	135
CHAPTER 5	Identification of novel Nek11 binding partners using IP-MS analysis.....	141
5.1	Introduction	141
5.2	Results	144
5.2.1	Small-scale optimisation of Nek11 immunoprecipitation.....	144
5.2.2	Large-scale immunoprecipitation of GFP-Nek11L for LC-MS/MS analysis	144
5.2.3	GFP-Nek11L co-immunoprecipitates with Ku70.....	149
5.3	Discussion.....	153

5.3.1	DNA damage response and repair proteins	154
5.3.1.1	Nek11L interacts with Ku70	156
5.3.2	mRNA processing factors	157
5.3.3	Nucleolar proteins.....	159
5.3.4	Comparison of partners identified in the presence or absence of DNA damage	160
CHAPTER 6	assessment of nek11 expression in colorectal cancer cells and tissue.....	161
6.1	Introduction	161
6.2	Results	163
6.2.1	Nek11 isoforms are expressed in colorectal cancer cell lines	163
6.2.2	Nek11 protein expression in colorectal cancer tissue compared to normal tissue.....	171
6.3	Discussion.....	178
CHAPTER 7	Discussion.....	181
7.1	Does Nek11 have a role in the DNA damage response?	181
7.1.1	Nek11 is required for G2/M accumulation in response to DNA damaging agents	181
7.1.2	Nek11 is required for cell survival.....	182
7.2	What's the relevance of different Nek11 isoform expression? ...	183
7.3	What's the purpose of nucleocytoplasmic shuttling of Nek11? .	184
7.4	Why does Nek11 overexpression result in aneuploidy?	185
7.5	Is Nek11 a validated chemotherapeutic target?	186
7.6	Concluding remarks	187
CHAPTER 8	Bibliography.....	189

ABBREVIATIONS

µg	microgram
µl	microlitre
µM	micromolar
5-FU	5-fluorouracil
aa	amino acid
ab	antibody
APC/C	anaphase promoting complex/cyclosome
APS	ammonium persulfate
ATM	ataxia telangiectasia mutated
ATR	ATM- and Rad3-related
bp	base pairs
BRCA1	Breast cancer type 1 susceptibility protein
BSA	bovine serum albumin
C-	carboxy
CCB	Colloidal Coomassie Blue
Cdc25	cell division cycle 25
CDK	cyclin-dependent kinase
cDNA	complementary deoxyribonucleic acid
Chk	checkpoint kinase
CKI	Cdk inhibitor
CRC	Colorectal cancer

Ct	crossing threshold
DDR	DNA damage response
DMSO	dimethylsulfoxide
DNA	deoxyribonucleic acid
DNA-PK	DNA-activated protein kinase
DNA-PK	DNA-dependent protein kinase
DSB	double-stranded break
EDTA	ethylene diamine tetraacetic acid
EGTA	ethylene glycol tetraacetic acid
FACS	fluorescence-activated cell sorting
FBS	foetal bovine serum
G418	geneticin
GFP	green fluorescent protein
GL2	firefly luciferase
Gy	Gray
Hrs	hours
IF	immunofluorescence microscopy
IP	immunoprecipitation
IR	ionising radiation
kDa	kilo Daltons
LMB	Leptomycin B
M	molar
m. wt	molecular weight

mg	milligram
Mins	minutes
ml	millilitre
mM	millimolar
mRNA	messenger ribonucleic acid
N-	amino
Nek	NIMA-related kinase
Nek11L	Nek11 Long
Nek11S	Nek11 Short
NES	nuclear export sequence
ng	nanogram
NIMA	never in mitosis A
NLS	nuclear localisation sequence
nm	nanometer
nM	nanomolar
PBS	phosphate buffered saline
PCR	polymerase chain reaction
pH3	phospho-histone H3
PI	propidium iodide
Rb	Retinoblastoma protein
RNA	ribonucleic acid
ROS	reactive oxygen species
Rpm	revolutions per minute

SAC	spindle assembly checkpoint
SCF	Skp1-Cullin-F-box
SDS	sodium dodecyl sulfate
SDS-PAGE	SDS polyacrylamide gel electrophoresis
siRNA	small interfering RNA
SSB	single strand break
ssDNA	single stranded DNA
U	unit
U2OS	human osteosarcoma
UV	ultraviolet
V	volts
v/v	volume per volume ratio
w/v	weight per volume ratio
WT	wild-type

TABLES AND FIGURES

Table 1.1 Activation, localisation and function of human Neks	35
Table 5.1 Proteins identified in Nek11L immunoprecipitates by LC-MS/MS analysis	150
Figure 1.1 The eukaryotic cell cycle	2
Figure 1.2 Mitosis and cytokinesis	4
Figure 1.3 Regulation of cell cycle progression	6
Figure 1.4 The DDR signal-transduction pathway	12
Figure 1.5 DNA damage induction and repair processes	15
Figure 1.6 The G1/S DNA damage checkpoint	26
Figure 1.7 The G2/M DNA damage checkpoint	28
Figure 1.8 <i>Aspergillus</i> NIMA and the human NIMA-related protein kinase family	31
Figure 1.9 Nek11 exists as at least four alternatively spliced isoforms	44
Figure 1.10 Proposed role for Nek11 at the G2/M DNA damage checkpoint ...	46
Figure 1.11 Exploiting DNA damage checkpoints for cancer treatment	49
Figure 3.1 siRNA-mediated depletion of recombinant GFP-Nek11L	82
Figure 3.2 siRNA mediated depletion of endogenous Nek11	83
Figure 3.3 Depletion of Nek11 does not affect normal cell cycle progression ..	85
Figure 3.4 Optimisation of G2/M checkpoint activation in HCT116 WT cells ...	86
Figure 3.5 G2/M arrest in response to IR in HCT116 cells is Chk1 dependent	88
Figure 3.6 Nek11 is required for G2/M arrest in response to IR in HCT116 WT and p53-null cells	89
Figure 3.7 Loss of Nek11 induces apoptosis and this is enhanced in combination with IR in HCT116 cells	91

Figure 3.8 Nek11 depletion in combination with IR affects cell proliferation.....	92
Figure 3.9 Oxaliplatin induces a dose-dependent G2/M arrest in HCT116 WT cells.....	94
Figure 3.10 Oxaliplatin induced G2/M arrest is Nek11 dependent in HCT116 WT but not p53-null cells	95
Figure 3.11 Oxaliplatin treatment results in a reduction of S-phase cells in HCT116 WT but an increase in HCT116 p53-null cells.....	96
Figure 3.12 Irinotecan induces a dose-dependent G2/M arrest in HCT116 WT cells.....	98
Figure 3.13 Irinotecan-induced G2/M arrest is Nek11-dependent in HCT116 WT and p53-null cells	99
Figure 3.14 Validation of isoform specific RNAi using qRT-PCR	101
Figure 3.15 Cell cycle response to Nek11 isoform specific depletions in combination with DNA damaging agents in HCT116 WT and p53-null cells..	102
Figure 4.1 Isolation of Nek11S cDNA.....	112
Figure 4.2 Isolation of Nek11D cDNA	113
Figure 4.3 G418 dose response curve	115
Figure 4.4 Generation of U2OS:GFP-Nek11 and GFP-only stable cell lines .	116
Figure 4.5 Nek11D is subject to proteasomal degradation.....	118
Figure 4.6 Nek11 isoforms exhibit distinct localisation patterns	119
Figure 4.7 Nek11 isoforms do not show localisation to the microtubule network	120
Figure 4.8 Nek11 isoforms show weak localisation to centrosomes during interphase	122
Figure 4.9 Endogenous Nek11 localises to centrosomes in interphase and spindle poles during mitosis	123
Figure 4.10 GFP-Nek11L localises to nucleoli	124
Figure 4.11 Nek11 splice variants exhibit nucleocytoplasmic shuttling	126

Figure 4.12 Cytoplasmic localisation of Nek11L is not affected by mutation of a putative nuclear export sequence	128
Figure 4.13 The non-catalytic domain of Nek11L is responsible for nuclear localisation	129
Figure 4.14 Non-catalytic domain constructs reveal nuclear targeting and export sequences.....	130
Figure 4.15 Nek11 is recruited to DNA damage foci upon IR treatment.....	132
Figure 4.16 Nek11L overexpression induces G2/M arrest and polyploidy	134
Figure 4.17 The non-catalytic domain of Nek11 contains both nuclear import and export sequences.....	137
Figure 5.1 Immunoprecipitation of endogenous Nek11 protein with Nek11 (3216) antibody	145
Figure 5.2 Small-scale optimisation of GFP-Nek11 immunoprecipitation.....	146
Figure 5.3 Large-scale GFP IP for the identification of novel binding partners by mass spectrometry analysis	148
Figure 5.4 Ku70 co-immunoprecipitates with Nek11L but not Nek11S or inactive Nek11L.....	152
Figure 6.1 Exon organisation of Nek11 isoforms.....	164
Figure 6.2 Presence of a single amplification product with Nek11 isoform-specific primers was determined by melt curve and agarose gel analysis	166
Figure 6.3 Nek11L is the most highly expressed isoform across a panel of cell lines.....	167
Figure 6.4 Validation of GAPDH as a suitable normalisation gene for qRT-PCR analysis	169
Figure 6.5 Expression of Nek11 isoforms in a panel of CRC cell lines compared to HCEC cells.....	170
Figure 6.6 Optimization of the Nek11 antibody, 3216, for immunohistochemistry	172

Figure 6.7 Expression of Nek11 in normal colorectal and colorectal cancer tissue.....	173
Figure 6.8 Nek11 monoclonal antibody, Origene, detects Nek11L and Nek11D isoforms only	175
Figure 6.9 Optimization of the Origene Nek11 antibody for immunohistochemistry	176
Figure 6.10 Competition assay with Origene antibody confirms detection of Nek11 is specific	177
Figure 7.1 Cellular roles and mechanisms for Nek11.....	188

CHAPTER 1 INTRODUCTION

1.1 The eukaryotic cell cycle

The eukaryotic cell cycle describes a set of highly complex, ordered events required to accurately produce two identical daughter cells. Great emphasis has been placed on understanding the molecular mechanisms of the cell cycle since its discovery, since defects and misregulation can result in progression of diseases such as cancer. Furthermore, greater understanding of the mechanisms of regulation has led to the identification of novel drug targets for cancer therapies.

Broadly, the cell cycle consists of four distinct phases: Gap1 (G1), Synthesis (S), Gap2 (G2), and the mitotic phase (M) (Figure 1.1). In addition, there is a fifth stage, G0, also known as the quiescent stage, where cells exit the cell cycle and no longer divide due to differentiation or the lack of growth factors or nutrients. However, cells remain active and may re-enter the cell cycle upon meeting of growth requirements. The G1, S and G2 phases collectively occupy around 90% of the cell cycle and together are known as interphase. It is during these stages that the cells grow and prepare for entry into cell division. During the first growth phase, G1, the cell synthesises proteins and organelles required for DNA replication, resulting in an increase in cell size. In addition, throughout this stage the cell also monitors its intracellular and extracellular environment to determine whether the conditions are suitable for cell division to proceed. If they are, the cell passes the restriction point (R point) and becomes committed to entry into S phase during which the genetic material is accurately duplicated to produce pairs of identical sister chromatids. The final growth phase, G2, involves continuing cell growth and synthesis of proteins required during cell division. Finally, the cell enters mitosis for the production of two identical daughter cells.

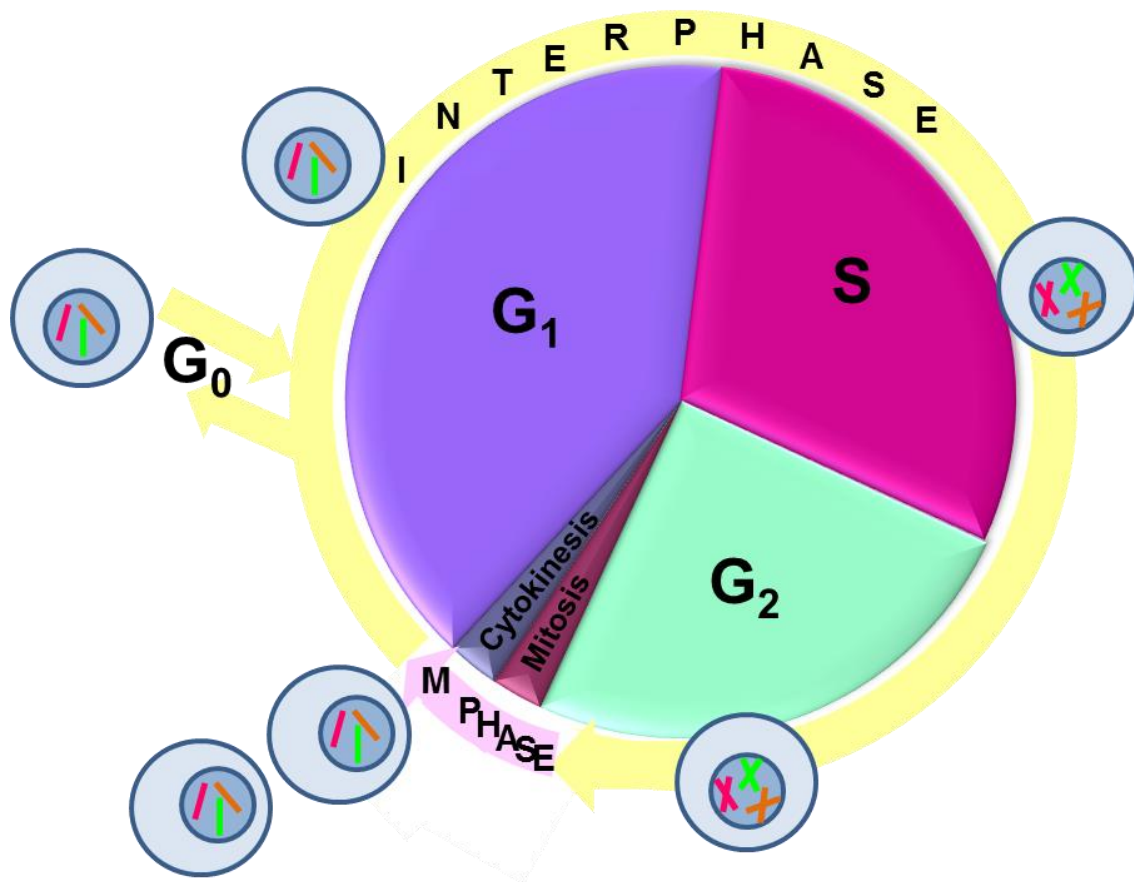


Figure 1.1 The eukaryotic cell cycle

The eukaryotic cell cycle is broadly divided into interphase and mitosis. Interphase consists of two growth phases, G₁ and G₂, as well as a DNA synthesis phase (S-phase). The M-phase includes mitosis and cytokinesis and sees the division of a cell to create two identical daughter cells. A further phase, G₀ (quiescence), is entered when growth conditions are unfavourable.

Broadly, the M-phase consists of two stages: mitosis and cytokinesis. Mitosis can then be further divided into 5 stages: prophase, prometaphase, metaphase, anaphase and telophase (Figure 1.2). During prophase, sister chromatids condense and form distinct chromosomes. In addition, previously duplicated centrosomes, or microtubule organising centres (MTOC), separate and migrate to opposite poles of the cell where they nucleate the formation of microtubules in order to form the mitotic spindle structure (Salaun *et al.*, 2008). Prometaphase sees the breakdown of the nuclear envelope, allowing chromosomes to attach to the dynamic mitotic spindle apparatus through their kinetochore structures found at the centromere. During metaphase, sister chromatids become attached to microtubules from opposite spindle poles, thus creating a stable bipolar attachment and chromosomal alignment midway between the poles, also known as the metaphase plate. Sister chromatids are then pulled to opposite poles of the cell during anaphase before chromosomes decondense and a nuclear envelope reforms around each set of DNA during telophase (Nigg, 2001). The final stage, cytokinesis, is the physical separation of the daughter cells and involves division of the cytoplasm and organelles. A contractile ring made of myosin and actin forms and acts to pinch the two cells apart through constriction of the plasma membrane. Typically, for a human cell in culture the whole process of growth and cell division takes around 24 hours (Salaun *et al.*, 2008).

1.2 Cell cycle regulation

Cell cycle regulation is well conserved across species, from yeast to humans (Malumbres, 2011). Timing and progression of cell cycle events need to be tightly controlled to ensure the production of identical daughter cells and hence minimise the generation and segregation of DNA errors that can lead to uncontrolled cell division, loss of genomic stability and cancer cell formation. Mechanisms of regulation occur through a vast network of cellular proteins that are controlled both temporally and spatially and that together act at various checkpoints throughout the cell cycle. Events coordinated include commitment to the cell cycle, initiation of DNA replication, formation of mitotic spindles,

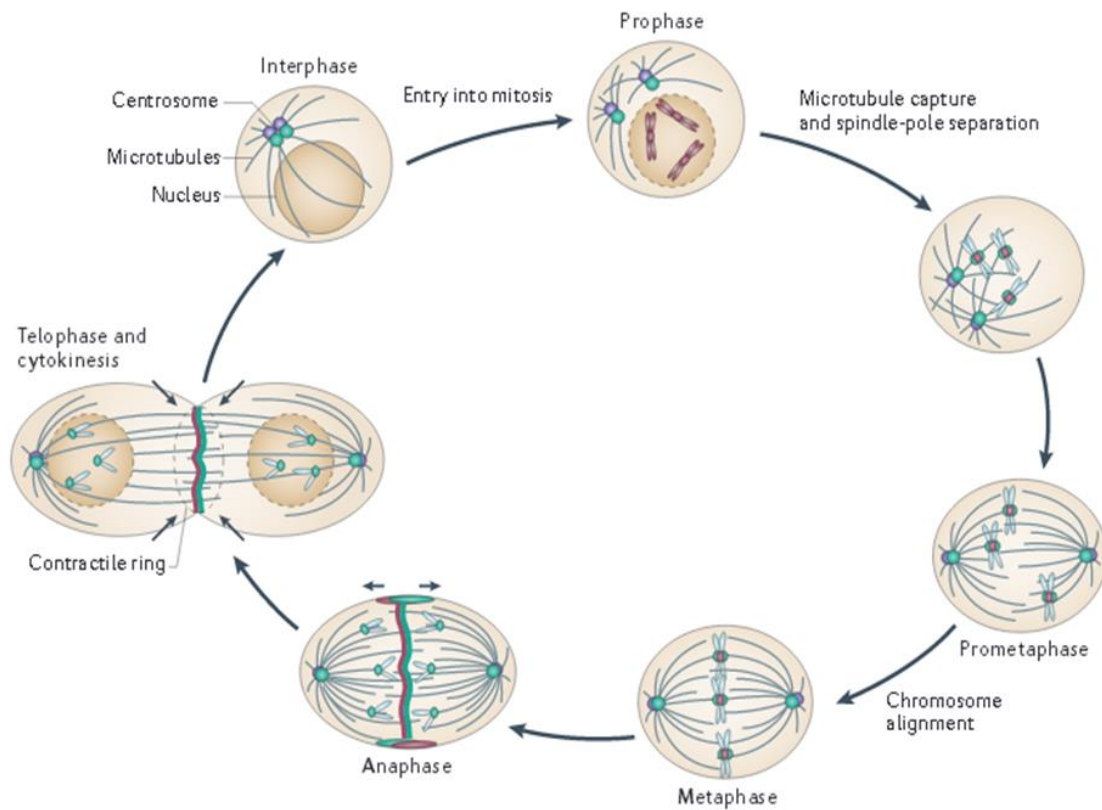


Figure 1.2 Mitosis and cytokinesis

The M-phase involves two key events: nuclear division (mitosis) followed by cytoplasmic division (cytokinesis). Mitosis can be further divided into prophase, prometaphase, metaphase, anaphase and telophase. Adapted by permission from Macmillan Publishers Ltd. (Rath et al., 2012).

nuclear envelope breakdown, sister chromatid separation and cytokinesis (Ma & Poon, 2011). A major component of these pathways are protein kinases, which control activity of downstream proteins through phosphorylation events. These events affect the activity, localisation, complex formation and conformation of proteins, to name a few. And because of their catalytic activity, these kinases have in recent years become attractive targets for drug development in the treatment of cancer (Malumbres, 2011).

1.2.1 Cyclins and Cdks

Key instigators of checkpoint control throughout the cell cycle are the serine/threonine protein kinases belonging to the Cyclin-dependent kinase (Cdk) family (Figure 1.3). Members of this kinase family regulate progression and entry into different stages of the cell cycle. However, since expression of Cdks show little variation throughout the cell cycle, activation is regulated through phosphorylation and dephosphorylation events, presence of inhibitors and through association with appropriate members of the cyclin protein family.

Based on sequence similarity the human genome contains 21 genes encoding CDKs (Malumbres *et al.*, 2009). However, of these, only Cdk1, Cdk2, Cdk4 and Cdk6 have been implicated directly in cell cycle control. Cdk1 (Cdc28/cdc2 in yeast) is the founding member of the Cdk family and is known as the master mitotic regulator. It is absolutely essential for cell cycle progression and is able to phosphorylate a wide range of proteins with around 200 Cdk1 substrates being identified in a budding yeast proteomic library (Malumbres & Barbacid, 2005; Ubersax *et al.*, 2003). In mammals, Cdk1 plays crucial roles during mitosis including nuclear envelope breakdown, condensation and cohesion of chromosomes, bipolar spindle formation and chromosome attachment (Malumbres, 2011). Furthermore, inactivation of this complex through degradation of cyclin B is required for proper mitotic exit (Harper *et al.*, 2002). The yeast variant of Cdk1 however, is also able to regulate a number of interphase events since it can also bind to cyclins present during G1 and S.

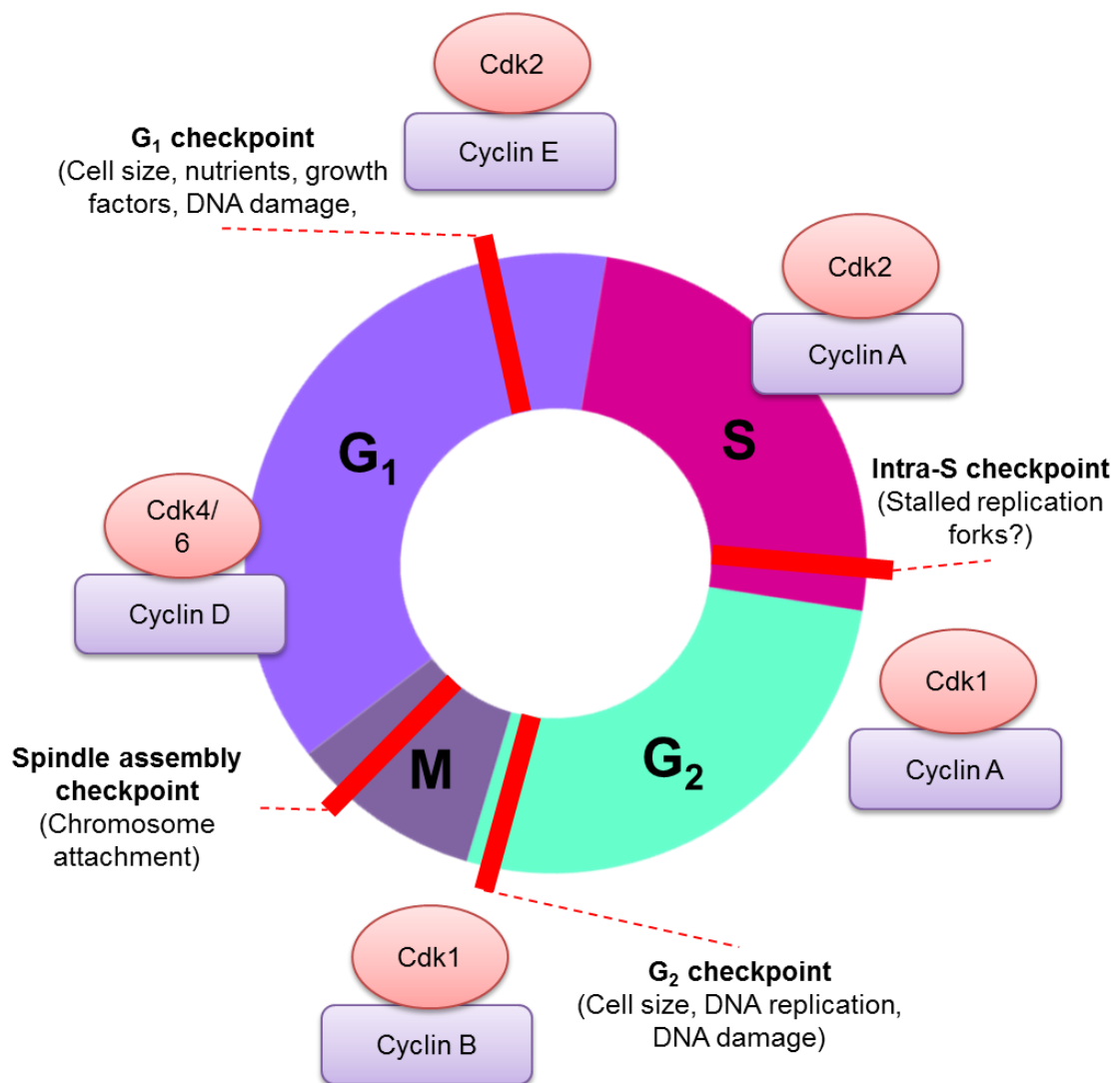


Figure 1.3 Regulation of cell cycle progression

Progression of the cell cycle is regulated by the activity of Cyclin-dependent kinases (Cdks) and their regulatory cyclin partners. Indicated are the stages at which each heterodimer plays key roles in cell cycle progression. Also shown (red bars), are the major eukaryotic cell cycle checkpoints at the G₁/S boundary, during S-phase, G₂/M and during mitosis at the metaphase to anaphase transition (spindle assembly checkpoint, SAC).

Throughout evolution, the number of family members has increased and as a result in mammals, Cdk4, Cdk6 and Cdk2 act to regulate interphase progression through binding to different cyclin members. As briefly discussed, monomeric Cdks have low kinase activity and become activated first by binding to cyclin subunits with studies showing that upon heterodimer formation Cdk activity is increased by 40,000-fold (Connell-Crowley *et al.*, 1993). As their name suggests cyclin expression varies in a cyclical fashion throughout the cell cycle, with different family members accumulating and being degraded at specific stages. Cdk proteins therefore become activated in a sequential manner throughout the cell cycle thus ensuring proper timing of phases and also the progression of cell division in a directional manner ensuring that processes are not repeated (Nurse, 1997).

Insights into Cdk/cyclin control came from studies carried out in early frog and sea urchin embryos (Masui & Markert, 1971; Smith & Ecker, 1969). In these experiments, cytoplasm from maturing oocytes was injected into immature oocytes resulting in their maturation. It was found that this was due to a protein component termed the maturation-promoting factor (MPF) which was later discovered to be the Cdk1/cyclin B complex (Masui & Markert, 1971; Rao & Johnson, 1970; Lohka *et al.*, 1988; Lee & Nurse, 1987). Furthermore, in sea urchin eggs, experiments identified a number of proteins (cyclins) which accumulated throughout the cell cycle and were then destroyed at each cleavage division (Evans *et al.*, 1983). In later years, additional cyclin members were identified in mammals through complementation studies using mutant yeast (Xiong & Beach, 1991).

In addition to heterodimer formation Cdks are also activated through phosphorylation of a threonine residue on the T-loop by CDK-activating kinase (CAK), and dephosphorylation at inhibitory sites Thr14 and Tyr15 by Cdc25 phosphatases. Additional regulatory mechanisms occur through association with Cdk inhibitors (CKIs), namely the family of INK4 proteins and the Cip/Kip family (Nurse, 1990; Morgan, 1995). The INK4 family consists of 4 members:

p16^{INK4a}, p15^{INK4b}, p18^{INK4c} and p19^{INK4d}, which negatively regulate Cdk4 and Cdk6, through binding to their monomeric forms. p21^{Cip1}, p27^{Kip1} and p57^{Kip2} of the Cip/Kip family on the other hand, are able to bind and inhibit heterodimeric Cdk/cyclin complexes (Sherr & Roberts, 1999).

1.2.2 Checkpoints and control of cell cycle progression

The concept of cell cycle checkpoints was first described by Weinert and Hartwell in 1988, who carried out experiments in budding yeast and found that cells with mutant checkpoint proteins continued through the cycle prematurely (Weinert & Hartwell, 1988). Checkpoints describe a set of feed-back mechanisms that are found at various stages throughout the cell cycle and act to monitor and control the entry into subsequent stages, where the initiation of events are dependent on completion of earlier cell cycle events (Peeper *et al.*, 1994). The main checkpoint controls are found at G1/S, during S-phase, G2/M and during mitosis and involve surveillance systems that detect DNA damage, ongoing replication and inappropriate conditions for cell division (Nurse, 2000). Interest in studying these controls has come about since many cancers acquire a proliferative advantage through defects in checkpoint control leading to accumulation of mutated genes. Furthermore, in recent years, checkpoint proteins have become attractive targets for combination therapies in the treatment of cancers, since their lack of function can make cells more sensitive to radio- and chemotherapies.

1.2.2.1 G1/S regulation

Progression of the cell through the majority of G1 is controlled by the continual monitoring of the extracellular and intracellular environments to ensure that growth conditions are met for cell division. The decision made here either commits the cell to cell division or entry into quiescence, and the point at which this occurs is known as the restriction (R) point in animal cells. Expression of D-type cyclins is induced in the presence of mitogenic signals thus allowing the formation of active Cdk4 and Cdk6 heterodimers (Malumbres & Barbacid,

2005). These active complexes then phosphorylate the tumour suppressor protein, retinoblastoma (Rb), which functions to inhibit the transcription of genes required for cell cycle progression by binding to and regulating the activity of transcription factors such as E2F family members, HDACs and chromatin remodelling factors (Cobrinik, 2005). In the presence of favourable cell cycle conditions then the phosphorylation of Rb leads to its release from transcription factors allowing for expression of key cell cycle genes. Dissociation from E2F, for example, allows it to upregulate the expression of E-type cyclins, which is required for the activation of Cdk2 and completion of late G1 (Malumbres & Barbacid, 2005). Indeed, many cancer cells lack or carry mutated versions of pRb resulting in a non-functional R-point and unregulated cell division irrespective of growth signals (Dannenberg *et al.*, 2000; Sage *et al.*, 2000).

Other aspects that affect progression of the cell into S-phase include the presence of DNA damage resulting in an arrest at the G1/S boundary to allow time for DNA repair (see section 1.4).

1.2.2.2 S-phase regulation

Cdk2/cyclin E is required for the initiation of DNA replication. However, once origins of replication are fired this complex is inactivated by degradation of cyclin E, to prevent re-firing and therefore re-replication of DNA (Hwang & Clurman, 2005). During S-phase, Cdk2/cyclin A becomes active through accumulation of A-type cyclins in response to inactivation of pRb, and functions to phosphorylate various proteins involved in the progression and completion of S-phase. This complex has also been found to co-localise to DNA replication sites, with its activity persisting through to G2 to prevent the assembly of new pre-replicative complexes (Cardoso *et al.*, 1993; Morgan, 1997).

1.2.2.3 G2/M regulation

Early G2 progression requires A-type cyclins to associate with Cdk1. A-type cyclins are then degraded during G2 and the accumulation of B-type cyclins is observed, leading to the formation and activation of the major mitotic regulator, Cdk1/cyclin B in late G2. Regulation of the activation of this complex is tightly controlled by a number of proteins, aside from cyclin B binding. The Cdk-activating kinase (CAK) phosphorylates Cdk1 at Thr161, however the complex remains inactive due to phosphorylation of Thr14 and Tyr15 sites by Myt1 and Wee1 kinases. It is only when the cell is satisfied that there is no DNA damage and that DNA replication is complete that these inhibitory phosphate groups are then removed by Cdc25A phosphatases, triggering progression into mitosis.

1.2.2.4 SAC

The spindle assembly checkpoint (SAC) prevents entry of a cell into anaphase until all kinetochores are properly attached to the mitotic spindle, thus ensuring that sister chromatids are correctly segregated and therefore preventing formation of cells exhibiting aneuploidy. Experiments whereby cells were blocked in mitosis upon displacement of chromosomes from the spindle, and isolation of yeast mutants that divide in the presence of an abnormal spindle led to the discovery of crucial players within the SAC (Nurse, 2000; Hoyt *et al.*, 1991; Li & Murray, 1991; Nicklas, 1997). The SAC ultimately controls the activity of the ubiquitin ligase, APC/C (anaphase-promoting complex/cyclosome) through regulation of one of its subunits, Cdc20 (Musacchio & Salmon, 2007). When the checkpoint is activated APC/C remains inactive due to inhibition of Cdc20 which means that targets of APC/C, such as cyclin B and securin, remain abundant in the cell. As discussed, cyclin B is required for activation of the mitotic kinase Cdk1, and its presence means that cells remain in mitosis. Securin on the other hand, is an inhibitor of separase, which cleaves the cohesin complex between sister chromatids (Peters, 2006). Therefore, activation of the SAC by unattached kinetochores allows cells to remain in early mitosis until all chromosomes are properly attached (Chen *et al.*, 1996). Once all chromosomes are attached to both spindle poles the checkpoint

is satisfied and the APC/C becomes activated thereby triggering anaphase and the segregation of sister chromatids.

Key players within the SAC mechanism include Mad1, Mad2, BubR1, Bub1, Bub3 and Mps1. Of these Mad2, BubR1 and Bub3 along with Cdc20 form the mitotic checkpoint complex (MCC) which binds to APC/C to keep it inactive, whereas Mad1, Bub1 and Mps1 act to amplify SAC signalling (Musacchio & Salmon, 2007). All of these proteins however show localisation to unattached kinetochores to some degree and are removed upon attachment to microtubules.

1.3 DNA damage signalling and the DNA damage response

The DNA damage response (DDR) describes a whole host of cellular responses that are initiated when a cell is subjected to DNA damage or by the presence of stalled replication forks. These events ensure the transmission of unmutated or undamaged DNA to daughter cells hence preventing the progression of harmful diseases such as cancer, neurological disorders, stem-cell dysfunction, cardiovascular disease and even ageing (Jackson & Bartek, 2009). In large, the majority of the protein networks involved are inter-linked and begin with the sensing of DNA damage followed by signal transduction and amplification, and then finally the activation of multiple cellular responses, including cell cycle arrest, transcription initiation, DNA repair and apoptosis. A basic overview of the DDR is shown in Figure 1.4, and discussed in further detail below.

1.3.1 Sources of DNA damage

Our cells receive tens of thousands of DNA lesions per day which if not properly repaired can lead to the accumulation of mutated DNA and serious consequences to the organism (Jackson & Bartek, 2009; Lindahl & Barnes, 2000). Our cells are subject to DNA damage induced by both intrinsic cellular

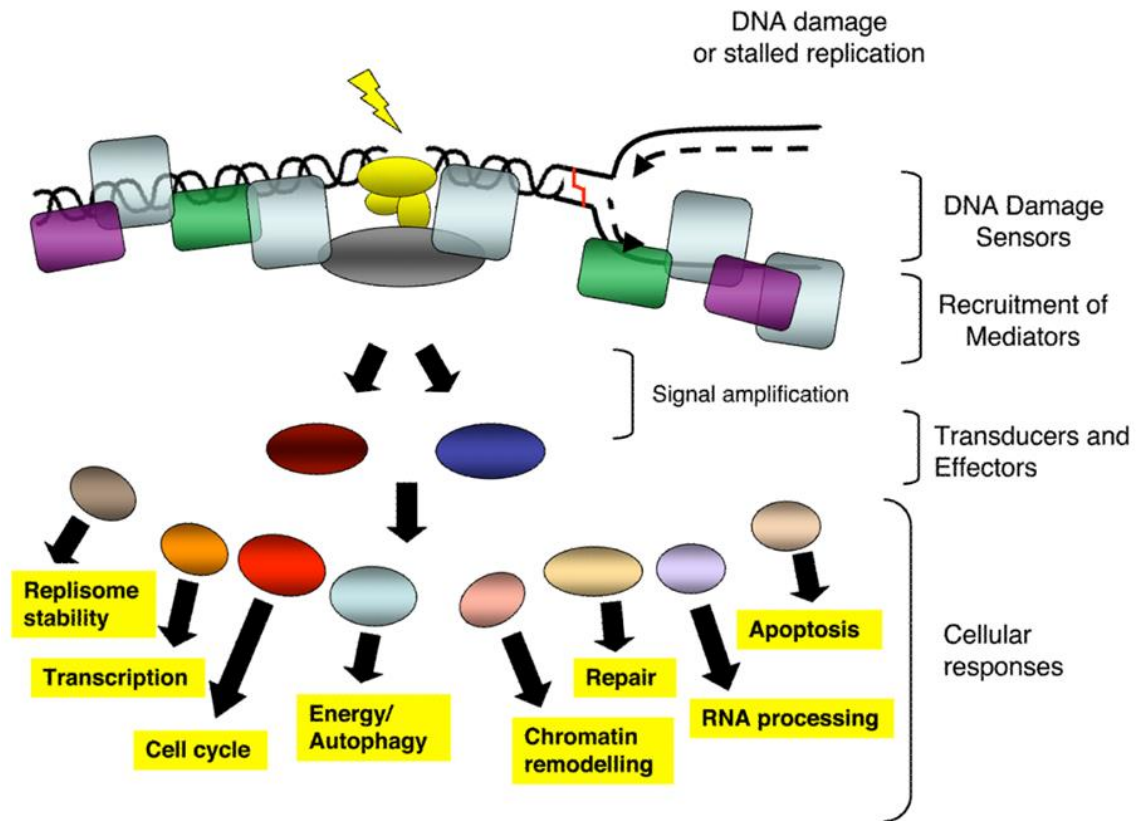


Figure 1.4 The DDR signal-transduction pathway

Presence of DNA damage or replication stress is detected by sensor proteins. These recruit and activate mediators to these sites which amplify the DDR signal through activation of transducers. Effector proteins then mediate the activation of a number of cellular responses as highlighted in yellow. Taken with permission from Jackson et al., 2009.

processes and extrinsic sources. One of the most harmful sources of intrinsic damage arises from the generation of reactive oxygen species (ROS) such as the superoxide ion, hydrogen peroxide and hydroxyl radical, during oxidative metabolism. Some of the ROS intermediates escape the site of respiration in the mitochondria and proceed to form covalent bonds with DNA amongst other cellular macromolecules (Bridge *et al.*, 2014). In addition, ROS are also able to induce DNA-protein crosslinks and single and double stranded breaks with over 100 oxidative modifications identified in DNA (Cadet *et al.*, 1997). Other forms of intrinsic DNA damage arise from mismatch during errors in DNA replication, abortive topoisomerase activity and reactive compounds produced at sites of infection/inflammation (Jackson & Bartek, 2009).

Genetic material is also subject to damage by exogenous sources, and probably the most well-known and common example is that by UV irradiation which can induce 100,000 lesions per cell per hour (Jackson & Bartek, 2009). Another environmental or man-made source is from X-rays or ionising radiation (IR), with the first suggestion that X-rays were able to cause mutations made in 1927 (Muller, 1927). As the name suggests, IR generates ionised and highly reactive molecules which leads to the formation of ROS. Harmful chemicals such as those found in tobacco smoke, and even some found in food such as aflatoxins (from contaminated peanuts and grains) and heterocyclic amines, are other examples of extrinsic sources (Wogan *et al.*, 2004).

The final source of DNA damage occurs from the spontaneous disintegration of DNA, resulting in abasic sites (AP site, apurinic/apyrimidinic), these are sites lacking a pyrimidine or purine base. In addition, deamination of bases, where amine groups from cytosine, adenine and guanine are lost, resulting in the formation of modified bases uracil, hypoxanthine and xanthine, respectively, resulting in the miscoding of nucleotide pairs and structural changes to DNA (Hoeijmakers, 2001). Furthermore, the methylated form of cytosine, 5-methylcytosine, results in formation of thymine upon deamination which is not

recognised as a foreign base by repair enzymes since it is one of the four common bases, therefore the resulting T:G mispairing often escapes detection.

1.3.2 Types of DNA damage

The range of DNA lesions incurred varies widely in severity depending on the source of DNA damage. A summary of the major sources of DNA damage as well as the lesions induced are shown in Figure 1.5; also shown are the major DNA repair processes for each lesion type and this is discussed in more detail in section 1.3.3.3. Endogenous sources commonly incur single nucleotide changes, for example as a result of DNA replication errors resulting in the incorporation of mismatched bases, or due to interconversion of bases through deamination, or even complete loss of a base at abasic sites through spontaneous disintegration (Ciccia & Elledge, 2010). However, more severe modifications are found to occur through ROS generated during metabolism and inflammatory responses, as well as by IR and UV exposure, and these have been linked to the initiation and progression of cancer (Klaunig & Kamendulis, 2004). ROS commonly induce oxidation of bases, the most studied example being the oxidation of guanine to 7,8-dihydro-8-oxoguanine (8-oxoG) which is often used as a biomarker to indicate the levels of oxidative stress (David *et al.*, 2007). In addition, ROS also leads to single and double DNA strand breaks, the latter of which is particularly detrimental to cells since it involves the complete break of DNA, thus making repair a much more error-prone process (see section 1.3.3.3). In addition to ROS, DSBs can also be induced by IR, replication blocks and chemotherapeutic drugs (such as bleomycin, topoisomerase inhibitors, etoposide and doxorubicin), as well as by normal cellular processes such as V(D)J recombination and meiosis. Focusing on IR in particular, it has been estimated that exposure to 1 Gy of IR induces approximately 1000 and 40 single and double stranded breaks, respectively, per cell (Ciccia & Elledge, 2010). Exposure to UV light from the sun, on the other hand, commonly induces the formation of pyrimidine dimers. These involve the covalent linkage between adjacent pyrimidine nucleotides thereby

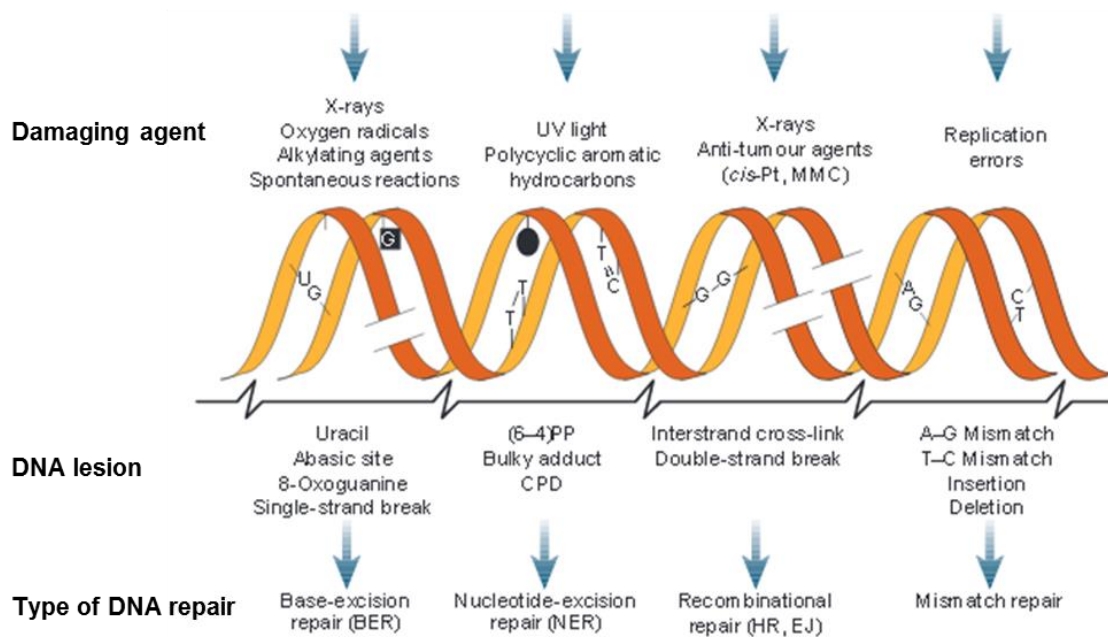


Figure 1.5 DNA damage induction and repair processes

DNA is continuously subject to damage from a variety of exogenous and endogenous sources, as shown above the DNA. These induce a variety of DNA lesion types (middle) and depending on the type of damage the DNA is repaired by the mechanisms shown below. Adapted from Hoeijmakers, 2001.

altering DNA structure and as a result affecting DNA polymerase action and DNA replication. Finally, DNA damaging agents used in cancer chemotherapies induce a wide range of DNA lesions including alkylation (by alkylating agents such as methyl methanesulfonate (MMS)), DNA crosslinking between and within DNA strands (intra- and interstrand crosslinking), SSBs and DSBs (Ciccia & Elledge, 2010).

1.3.3 The DNA damage response

The DNA damage response (DDR) describes a network of interacting pathways that are initiated upon detection of DNA lesions or stalled replication forks. These pathways are activated in a rapid manner to prevent cells continuing through the cell cycle with damaged genetic material, which could lead to the formation of cancer and other deleterious effects in multicellular organisms. Some responses to DDR signalling is the upregulation of DDR genes, cell cycle arrest, and importantly, activation of DNA repair pathways. However in some cases, where damage is severe, apoptotic pathways are also initiated. While these processes are distinct, activation of them occurs through signalling from the same or similar upstream pathways, with many proteins in the DDR playing multiple roles in a number of processes, as described below.

Upon DNA damage induction, 'sensor' or 'mediator' proteins are rapidly recruited to aberrant DNA sites to initiate the DDR. The type of proteins recruited to these sites depends on the type of DNA damage. For example, exposure of ssDNA results in binding of the single-stranded DNA-binding protein, replication protein A (RPA), which then acts to recruit the 9-1-1 heterotrimeric complex (Rad9-Hus1-Rad1, belonging to the PCNA-like family) before this recruits further proteins specific to this lesion type (Cortez *et al.*, 2001). The presence of DSBs on the other hand is sensed by the MRN complex (Mre11-Rad50-Nbs1) which recruits proteins specific to DSB response pathways, such as the ATM kinase through the C-terminus of Nbs1 (Falck *et al.*, 2005). In mammals, mediator proteins mainly belong to a family of BRCT-

containing proteins, and include the p53 binding protein (53BP1), Topoisomerase binding protein 1 (TopBP1), mediator of DNA damage checkpoint 1 (MDC1) and breast cancer susceptibility gene 1 (BRCA1) (Niida & Nakanishi, 2006).

Proteins recruited and activated by sensor proteins are known as transducers of the DNA damage response, with the most important family being the phosphatidylinositol 3-kinase-related kinases (PIKK). The serine/threonine kinases of the PIKK family play central and conserved roles within many DDR pathways, the key kinases being the large ataxia telangiectasia mutated (ATM, 350 kDa) and ATM and Rad3-related (ATR, 301 kDa) kinases (Kastan & Bartek, 2004). Whilst both, ATM and ATR kinases play interlinked roles in the DDR, ATR signalling occurs mainly in response to the detection of blocked transcription or replication and the detection of DNA repair intermediates as signalled by ssDNA coated by RPA protein (Jackson & Bartek, 2009). Since ATR is required for cell viability and is also involved in normal cellular processes such as progression of DNA replication forks (Shechter *et al.*, 2004; Brown & Baltimore, 2003), its kinase activity does not alter significantly in response to DNA damage. Instead, its activity is controlled by its localisation and its interacting partner ATRIP (ATR-interacting protein) which is responsible for ATR localisation to RPA coated ssDNA (Zou & Elledge, 2003; Abraham, 2001). On the other hand, ATM is activated by autophosphorylation in response to DNA strand breaks, in particular DSBs. In undamaged cells, ATM exists as an inactive homodimer and upon DDR signalling ATM becomes phosphorylated at S1981 resulting in a conformational change and an activated monomeric protein (Bakkenist & Kastan, 2003).

At the site of DNA damage, activation of both ATM and ATR trigger immediate events to promote recruitment of more DDR proteins. For example, the histone variant H2AX becomes phosphorylated at S139 of the C-terminal tail (the phosphorylated form being known as γ -H2AX), resulting in the assembly of large DDR complexes at DNA damage sites (Celeste *et al.*, 2002; Fernandez-

Capetillo *et al.*, 2002). This results in the recruitment of proteins involved in amplification and transduction of the DDR signal as well as chromatin remodelling and DNA repair proteins (Huen & Chen, 2008). Such components include the heterodimer Ku70/Ku80, DNA ligases, 53BP1 and BRCA1. In the case of DSBs, this causes more ATM recruitment and as a result the spread of γ H2AX along the chromatin (d'Adda di Fagagna, 2008). This results in the formation of detectable DDR foci which disassemble upon repair of the lesion.

In addition to local DNA damage site activity, ATM and ATR phosphorylate a whole host of downstream targets that function away from the lesion, with ATM being reported to phosphorylate over 700 proteins once activated (Matsuoka *et al.*, 2007b). The most important and well-studied of which is the phosphorylation of the tumour suppressor protein, p53, and the serine/threonine protein kinases, checkpoint kinase 1 (Chk1) and checkpoint kinase 2 (Chk2) (Matsuoka *et al.*, 1998; Ahn *et al.*, 2000). Although, Chk1 and Chk2 are unrelated proteins, they show overlapping function and substrate preferences (Zhou & Elledge, 2000). Chk2 can be activated throughout the cell cycle by dimerization and autophosphorylation mainly in response to DSB through ATM signalling (Bartek & Lukas, 2003). Chk1, on the other hand, functions mainly during S and G2 and also plays key roles in normal cell cycle processes such as DNA replication and cell cycle progression (Bartek & Lukas, 2003). In response to stalled replication and DNA damage, it becomes activated further mainly by ATR. Importantly, both Chk1 and Chk2 can be activated through crosstalk between the pathways, for example Chk1 is activated by ATM in response to DNA damage induced by IR (Sorensen *et al.*, 2003; Gatei *et al.*, 2003).

In order to initiate a cellular response pathway, mediators then transduce DDR signals to downstream effector proteins (Reinhardt & Yaffe, 2009). These essentially act to execute the DDR and include proteins such as BRCA1, p53 and Cdc25 phosphatases (cell-division cycle 25) (Zhou & Elledge, 2000). In the following sections some of the key cellular response pathways activated in response to the DDR are described.

1.3.3.1 Transcription

In yeast and mammals, DNA damage detection leads to upregulation of the transcription of genes involved in DNA damage surveillance, repair and apoptosis (Zhou & Elledge, 2000; Ljungman, 2010). This occurs through activation of transcription factors in response to DDR signalling by ATM and ATR kinases and their binding to a target promoter. This stimulates the binding of RNA polymerase II and the assembly of transcription factors for mRNA synthesis (Christmann & Kaina, 2013).

The most important transcription factors activated by the DDR are the p53, BRCA1 (breast cancer-associated protein 1), NF- κ B (nuclear factor kappa B) and AP-1 (activator protein 1) proteins (Christmann & Kaina, 2013). p53 is activated in response to DSBs and DNA replication arrest playing multiple roles in DDR pathways including cell cycle regulation, apoptosis and DNA repair. In response to DNA damage, ATM and ATR phosphorylate the ubiquitin ligase, MDM2, a negative regulator of p53, thereby causing its proteasomal degradation and as a result stabilisation of p53 protein. Furthermore, ATM and ATR also activate Chk1 and Chk2 which phosphorylate S20 of p53, activating it. These events result in the enhanced transcription of p53 targets and the increased response to DNA damage (Christmann & Kaina, 2013). BRCA1 is also activated by ATM and ATR and is able to stimulate p53 activity through binding to it. In addition, BRCA1 promotes transcription of DNA repair genes with overlapping targets with p53 (Christmann & Kaina, 2013). NF- κ B is a dimeric transcription factor comprised of proteins RelA, RelB, c-Rel, NF- κ B1, or NF- κ B2 and is activated through degradation of its inhibitor proteins belonging to the I κ B family, and its subsequent relocalisation to the nucleus (Christmann & Kaina, 2013). Finally, AP-1, is a heterodimeric protein which consists of proteins from the Jun, Fos or CREB/ATF families. It functions to regulate gene expression in response to different stimuli and transcriptional targets depend on the composition of AP-1 complexes (Christmann & Kaina, 2013).

Gene expression is also controlled at the post-transcriptional level, through alternative splicing, mRNA stabilisation and translation of specific mRNA products (Ljungman, 2010). This again is mainly mediated through ATM and ATR kinases and interestingly, proteins directly phosphorylated by ATM also reveal that a vast number of them are involved in RNA metabolism, and include proteins with roles in transcription, splicing, mRNA stability and translation (Ljungman, 2010).

1.3.3.2 Cell cycle arrest at DNA damage checkpoints

Propagation of damaged genetic material is deleterious to the organism and therefore, in response to the presence of DNA damage, the cell becomes quickly arrested in the cell cycle to allow time for DNA repair processes and as a result maintain genome integrity. Cell cycle arrest occurs through activation of DNA damage checkpoints which involve a vast network of proteins that ultimately control the activation of Cdks. The key DDR checkpoints are the G1/S and G2/M checkpoints, and in response to stalled DNA replication the intra-S phase checkpoint. These are discussed in more detail in section 1.4. Upon satisfactory DNA repair the cell will then continue to progress to the next phase of the cell cycle and complete cell division.

1.3.3.3 DNA Repair

Cell cycle arrest allows time for cells to begin repairing their DNA before progressing to the next stage. The late 20th century saw the identification of multiple DNA repair pathways including the nucleotide excision repair (NER), base excision repair (BER), mismatch repair (MMR) and non-homologous end joining (NHEJ) repair pathways (Ljungman, 2010). Like with most other DDR pathways, activation is initiated by the ATM and ATR kinases with ATM signalling DSBs, and ATR preferentially signalling SSBs and resected DSBs (Jackson & Bartek, 2009). Therefore, activation of specific repair pathways are dependent on the severity and type of damage incurred (Figure 1.5). In common with most DNA repair pathways however, are the enzymatic activities

required for repair, including the removal of the affected nucleotides by a nuclease, polymerisation of DNA and then ligation of the phosphodiester backbone by DNA ligases (Lieber, 2008).

In response to DNA lesions induced by endogenous sources, by oxidative damage or depurination events, the BER pathway is activated (Ljungman, 2010). This involves the recognition of a damaged base by DNA glycosylase, its excision to generate an AP site, followed by repair by DNA polymerase and ligase (David *et al.*, 2007). NER is the major pathway activated upon recognition of bulky helix-distorting lesions such as pyrimidine dimers, and can be subdivided into two pathways depending on how the lesion is recognised: transcription-coupled NER (TC-NER) and global-genome NER (GG-NER) (Jackson & Bartek, 2009). In both pathways, a region of 22-30 nucleotides are excised before DNA polymerases and ligases repair the now single-stranded region of DNA (Hoeijmakers, 2001). The final repair pathway that acts on a single DNA strand, is mismatch repair (MMR), which corrects mispaired bases that arise during DNA replication.

Repair of the more deleterious DSB occurs mainly through either homologous recombination (HR) or non-homologous end-joining (NHEJ). HR requires the presence of a template in the form of the sister chromatid, and so therefore occurs after DNA replication. During this process a single-strand is generated through signalling by the MRN complex. This ssDNA then invades the undamaged template of the sister chromatid and polymerases use this to repair the DNA. NHEJ, on the other hand is more error-prone, with introduction of mutations and loss of nucleotides a common occurrence at the break site. However, it is the major pathway for DSB repair given that it can occur throughout the cell cycle and without the presence of a DNA template (Lieber, 2008). NHEJ involves the alignment between two DNA segments and joining of the ends by DNA ligase IV, but since the joining is not informed by the wild-type stand, this unsurprisingly is imprecise and often generates mutations. Recognition of DSBs occurs by binding of the Ku heterodimer (Ku70/Ku80) to

sites of the break, which then acts to recruit DNA-PKcs, a serine/threonine kinase belonging to the PIKK family (Lieber, 2008). Ku then recruits and interacts with the nuclease, polymerase and ligase enzymes to elicit DNA repair.

1.3.3.4 Senescence and apoptosis induction

If DNA repair processes are inefficient or if DNA damage becomes chronic or is too severe, cells undergo programmed cell death via apoptosis. Alternatively, they may survive but irreversibly exit from the cell cycle and this is known as cellular senescence (Campisi & d'Adda di Fagagna, 2007). The deciding factors for the induction of either apoptosis or senescence are not entirely clear; however, some determinants could be the severity of damage incurred, the duration of damage and the cell type (d'Adda di Fagagna, 2008).

Activation of senescence is crucial in suppression of cancer cell development; however the accumulation of senescent cells in living organisms also contributes to the ageing process. Senescence was first described upon the observation that fibroblasts in culture eventually stopped proliferating even when growth conditions were met. Cells that remained viable but not able to divide were described to have entered replicative senescence (Hayflick, 1965). This occurs when normal cells reach their Hayflick limit, or the maximum number of times that a cell will divide before entering senescence (Hayflick, 1965). This is due to the fact that after each cellular division, telomeres exhibit shortening (loss of 50-200 base pairs), which eventually triggers the DDR when they reach a critical length, in a p53-dependent manner (Harley *et al.*, 1990). Senescence is also activated by exposure to exogenous and endogenous DNA damaging sources and especially in the presence of DSBs (Di Leonardo *et al.*, 1994). In common with telomere-initiated senescence, senescence induced by DNA damage depends on the p53-p21 and p16-pRb pathways (Di Leonardo *et al.*, 1994; Herbig *et al.*, 2004). Prolonged DDR signalling causes alternative-reading frame protein (ARF) to inhibit the ubiquitin ligase HDM2 which normally

functions to degrade p53. Upon p53 stabilisation, p53 causes the upregulation of the CKI, p21, resulting in the induction of senescence through inhibition of Cdks. Although senescence induction is predominantly dependent on p53 function, a second barrier to prevent proliferation is provided by the activation of the p16-pRb pathway. (Jacobs & de Lange, 2004). Activation of p16, inhibits Cdks and keeps pRb in a hypophosphorylated and active state thus preventing function of E2F in promoting transcription of cell proliferation genes.

On the other hand, apoptosis, or programmed cell death, is induced as a last resort if DNA damage is too severe or if DNA repair is too slow or incomplete, in order to eliminate the damaged cells (Ljungman, 2010). This process is essential for multicellular organisms not only in development but in the prevention of cancers. Common agents that induce apoptosis include IR, methylating agents and anticancer drugs, identified through the use of cells carrying defective repair genes and therefore unable to repair damaged DNA leading to hypersensitivity to these agents and subsequent cell death (Roos & Kaina, 2013). Again, induction of this pathway in most cell types relies heavily on p53 function (Clarke *et al.*, 1993; Lowe *et al.*, 1993). In the presence of low levels of DNA damage, p53 signals the transcription of p21 to induce cell cycle arrest, however high levels results in the accumulation of p53 protein above a certain level. This results instead in p53 upregulating the transcription of pro-apoptotic genes, the most important of which are BAX (BCL2-associated X protein), PUMA (p53 upregulated modulator of apoptosis) and Fas (Lane, 1992).

1.4 DNA damage induced cell cycle checkpoints

In mammals, the first indication that transition between cell cycle phases in response to DNA damage is controlled was through the examination of ataxia telangiectasia (AT) cells which carry a defective *atm* gene (Zhou & Elledge, 2000; Painter & Young, 1980). In this study, AT cells showed hypersensitivity to radiation and were observed to progress from G2 to M phase without DNA

repair (Painter & Young, 1980). In addition, A-T individuals suffer from high frequencies of cancer, immune deficiencies and loss of motor control (Zhou & Elledge, 2000). The term 'checkpoints' was first described in 1988 through studies carried out in yeast (Weinert & Hartwell, 1988). In these studies, yeast carrying mutant Rad9 protein were observed to continue to divide and eventually die instead of arresting at G2/M in response to DNA damage (Weinert & Hartwell, 1988).

As already discussed, in the presence of DNA damage, activation of cell cycle checkpoints arrests cells at various points within the cell cycle to allow for DNA repair, or induction of apoptosis if damage is too severe. This is crucial in order to maintain genomic integrity and to prevent the accumulation of mutations and formation of harmful diseases, such as cancer. Checkpoints activated in response to the DNA damage response can be divided broadly into p53-dependent and p53-independent pathways, and are discussed in more detail below.

1.4.1 The G1/S checkpoint

The arrest of cells at the G1 to S-phase transition is mostly dependent on the p53-p21 pathway, and prevents the initiation of DNA replication in the presence of DNA damage. In response to genotoxic insult, activated ATM/ATR and Chk1/Chk2 kinases, directly phosphorylate p53 at multiple serine and threonine residues within its transactivation domain, as well as also phosphorylating HDM2, a ubiquitin ligase responsible for degrading p53 in undamaged cells (Maya *et al.*, 2001). These events lead to the stabilisation and transcriptional activation of p53 protein (Abraham, 2001). As a result, p53 upregulates the transcription of p21, a CKI, which inhibits the activity of Cdk2/cyclin E complexes thus leading to cell cycle arrest (Figure 1.6) (el-Deiry *et al.*, 1993). The activation of this checkpoint however, in response to IR for example, is not fully achieved until 2-3 hours post DNA damage induction (Deckbar *et al.*, 2010; Cann & Hicks, 2006).

In early to mid G1, the main mediators of G1 arrest are through ATM and Chk2 signalling. At this time, activation of the DDR also functions to keep the Rb-E2F complex intact, thus acting as a second blockade to cell cycle progression. In late G1, after the R-point, ATR and Chk1 protein levels increase, as well as Cdc25 phosphatase protein levels. In undamaged cells, Cdc25A activates Cdk2/cyclinE(A) complexes to promote entry and progression through S-phase. However, in response to DNA damage, Chk1 and Chk2 activity increases and promotes rapid degradation of Cdc25A, leaving Cdk complexes in an inactive state, thus arresting the cell (Donzelli & Draetta, 2003). This p53-independent mechanism of cell cycle arrest occurs in a more rapid manner, with activation observed within the hour (Deckbar *et al.*, 2011).

1.4.2 Intra-S

Initiation of the intra-S DNA damage checkpoint, in response to abnormal DNA structures, ensures accurate copying of the genome by preventing firing from origins of replication that have not been initiated (Kastan & Bartek, 2004). Activation occurs through detection of stalled replication forks and misincorporation of DNA bases during replication, as well as exogenous sources of DNA damage (Abraham, 2001). Again, this occurs in response to ATM/ATR signalling, which leads to the phosphorylation and activation of Chk1 and proteolysis of Cdc25A, leaving Cdk2/cyclin A inactive (Lobrich & Jeggo, 2007). The result being prevention of new replication origin firing and a slowing down of replication. An additional intra-S pathway involving MRN, BRCA1, FANCD2 and SMC1 has also been described (Kastan & Bartek, 2004).

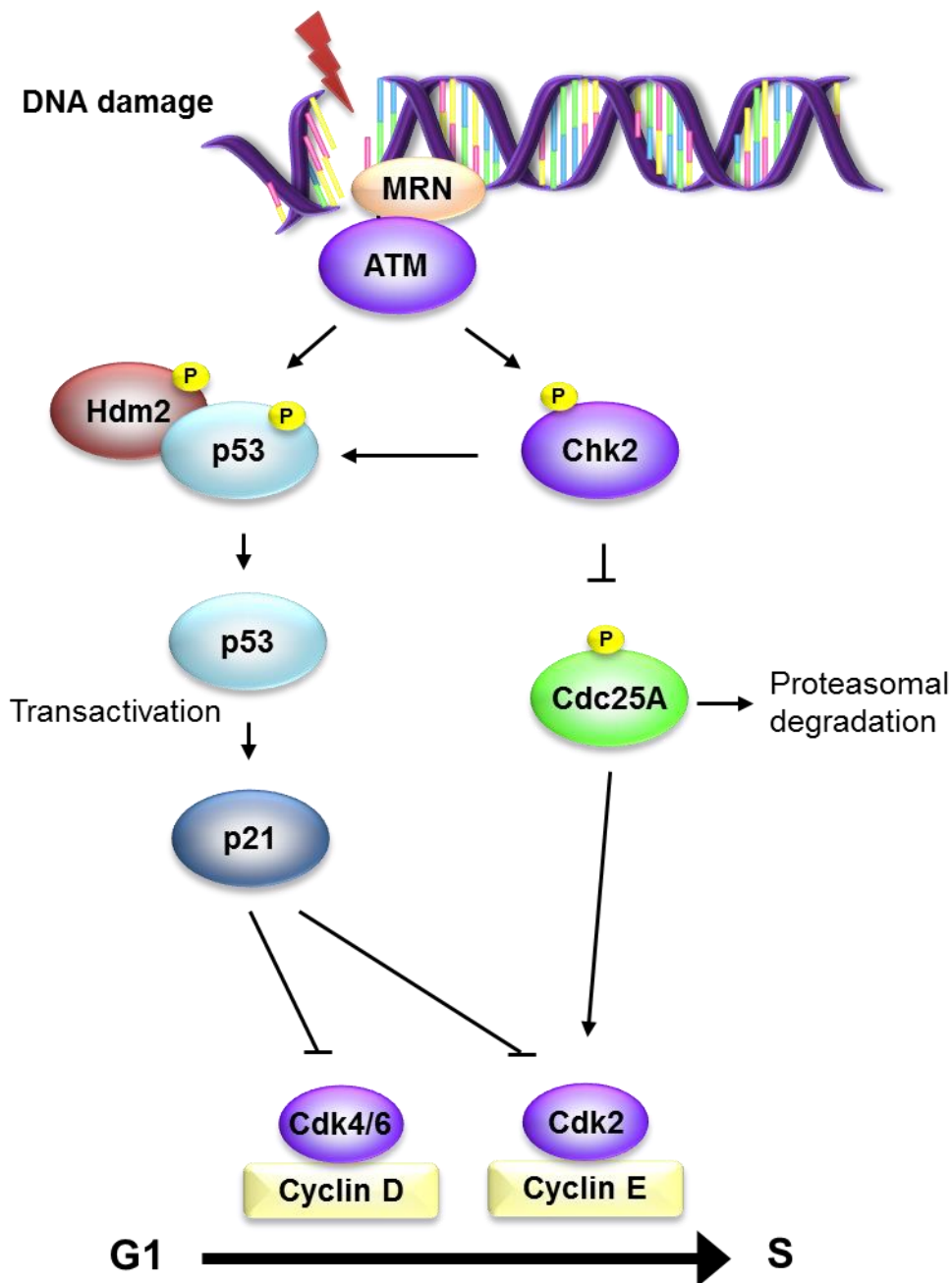


Figure 1.6 The G1/S DNA damage checkpoint

Induction of DNA damage during G1 results in the stabilisation and phosphorylation of p53 tumour suppressor protein through nuclear export of Hdm2 and phosphorylation of p53. This results in upregulation of p21 transcription and subsequent inhibition of Cdk complexes. This pathway is slow and takes around 2-3 hours. A second, faster, pathway involving the activation of Chk2 results in the phosphorylation and degradation of Cdc25A resulting in an inactive Cdk2/cylin E complex and arrest at the G1/S boundary. With reference to Deckbar et al., 2011.

1.4.3 G2/M

Initiation of the G2/M checkpoint arrest mainly occurs in a p53-independent manner and unlike the p53-dependent G1/S checkpoint, it is quickly initiated. Arrest at this boundary prevents the segregation of damaged chromosomes during mitosis, which can lead to tumorigenesis or cell death from failed mitosis and genomic instability (O'Connell & Cimprich, 2005). Progression of cells into mitosis requires the activation of the MPF, the Cdk1/cyclin B heterodimer. This as discussed, occurs through phosphorylation and dephosphorylation events. Of most importance here, is the removal of inhibitory phosphate groups, Thr14 and Tyr15, on Cdk1, by the action of the Cdc25 phosphatase family, including Cdc25A, Cdc25B and Cdc25C. In response to DNA damage however, upstream signalling by ATM and ATR activates Chk proteins, with the main target being activation of Chk1 through phosphorylation of S317 and S345 residues (Zhao & Piwnica-Worms, 2001; Liu *et al.*, 2000). Chk1 then phosphorylates Cdc25 proteins at sites which contribute to its proteasomal degradation through binding of the ubiquitin ligase, SCF- β -TrCP, or through binding of 14-3-3 proteins resulting in their inhibition and sequestration in the cytoplasm. As a result, Cdc25 is not present in the nucleus to promote activation of Cdk1 and therefore cells remain in G2 (Figure 1.7). A further pathway activated in response to stress stimuli is through the p38 mitogen-activated protein kinase and this also regulates the sequestration and degradation of Cdc25 phosphatases.

Until DNA damage is repaired, p53 and BRCA1-mediate upregulation of CKIs to ensure the maintenance of the checkpoint. p53 also promotes transcriptional activation and regulation of GADD45 and 14-3-3 proteins (Hermeking *et al.*, 1997; Wang *et al.*, 1999). The first indication that p53 also functions at G2 was through overexpression of p53 in undamaged cells, which led to arrest of cells at the G2/M boundary (Agarwal *et al.*, 1995). However, p53 function for G2/M arrest is not essential, since cells lacking the tumour suppressor protein are still able to arrest at G2 after bypassing G1 and S-phase checkpoints

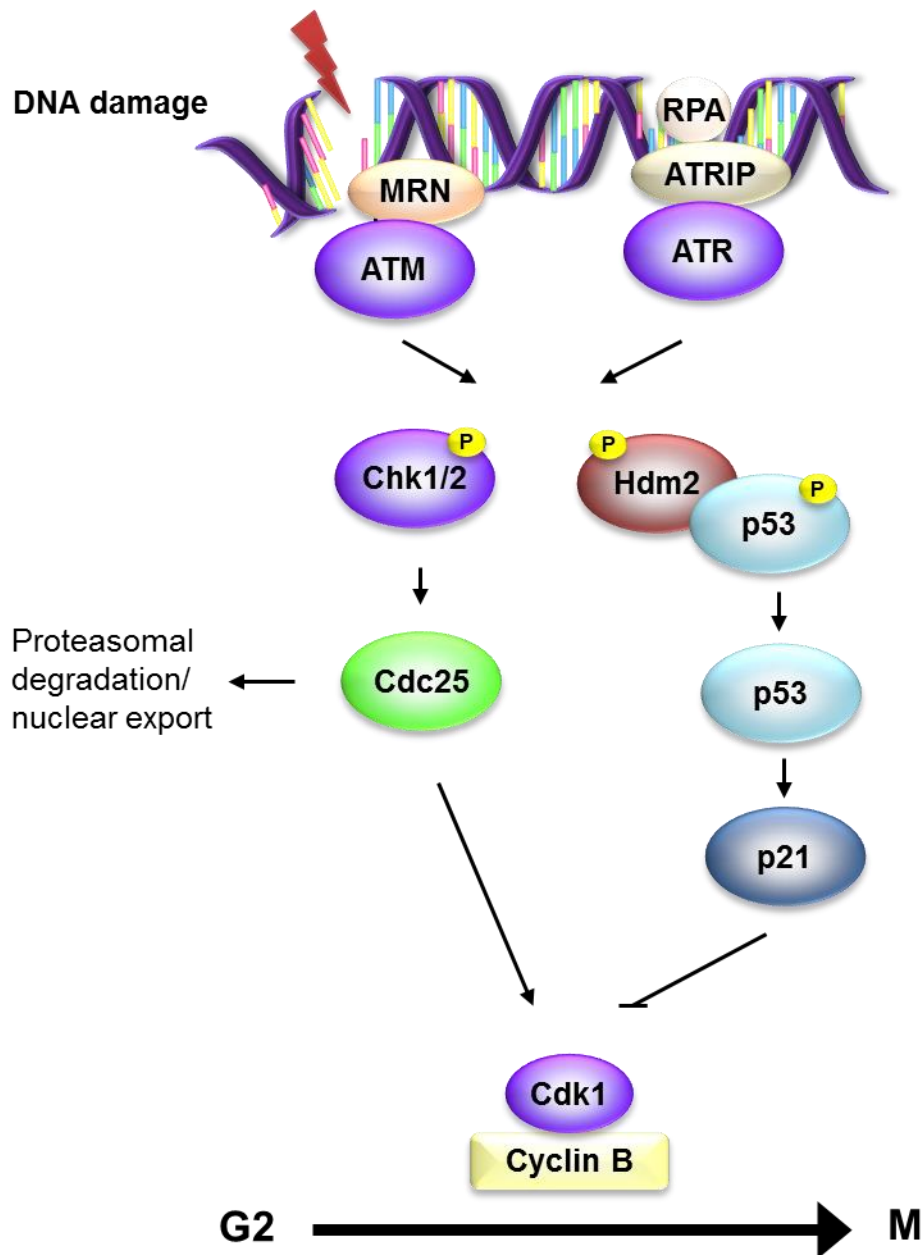


Figure 1.7 The G2/M DNA damage checkpoint

DNA damage sensed by MRN and RPA recruit and activate ATM and ATR, respectively. These both phosphorylate and activate Chk1 and Chk2 resulting in phosphorylation of Cdc25 phosphatases consequently Cdk1/cyclin B inactivation resulting in cell cycle arrest. Maintenance of the checkpoint occurs through activation of p53 and subsequent inhibition of the Cdk1/cyclin B complex by p21. With reference to Deckbar et al., 2011.

(Kastan *et al.*, 1991). Upon repair of DNA damage, Cdc25 becomes stabilised and cells progress into mitosis through activation of Cdk1/cyclin B. Interestingly however, observations show that cells released from G2 may still harbour a significant number of DSBs (10-20 unrepaired DSBs), suggesting that although the arrest is quickly activated, this pathway shows more insensitivity compared to the G1/S pathway (Deckbar *et al.*, 2011).

1.4.4 The DDR, cell cycle checkpoints and relevance to cancer

Cancer is closely associated with genomic instability which is both a characteristic of many cancers but can also act to drive cancer cell development. In recent years, the DDR has become a major focus in the understanding and treatment of cancer. Firstly, activation of the DDR functions to maintain genomic stability through cell cycle arrest, DNA repair and promotion of cell death (Kastan & Bartek, 2004). In this manner, DDR pathways act to prevent tumorigenesis (Bartkova *et al.*, 2005). Following on from this, mutations of proteins involved in DDR pathways often predispose individuals to many forms of cancer through proliferation in the presence of mutations and through the selective pressure of cells that can proliferate in an uncontrolled manner (Jackson & Bartek, 2009; Ljungman, 2010). For example, homozygous ATM mutations resulting in AT, predisposes patients to the formation of leukaemia and lymphomas. Other commonly mutated DDR genes that lead to familial predisposition to cancer include that of p53, Chk2, BRCA1/2 and MMR genes (Kastan & Bartek, 2004). A third link to cancer is that along with surgery, cancer is most commonly treated through chemotherapeutic DNA damaging agents or radiotherapy (Jackson & Bartek, 2009). These treatments are efficient at targeting cancer cells since they are actively proliferating cells and are therefore more susceptible to the toxic and mutagenic effects of cytotoxic agents (Ljungman, 2010). Furthermore, defective DDR pathways in cancer cells have more recently been exploited in order to specifically sensitise cancer cells to treatment with DNA damaging agents.

As mentioned, mutations or mis-regulation of proteins involved in the checkpoint control pathways can have significant effects on a cell. The result can be cell death through premature entry into mitosis, or formation of cancer cells due to favoured rates of proliferation. For example, mutation or loss of p53, a key protein in G1/S checkpoint control, is observed in around 50% of cancers. As a result, cells lose the checkpoint and cannot respond to DNA damage. Whilst this may be detrimental to the organism, in recent years this difference between normal and cancer cells has allowed the development of new drugs to specifically target cancer cells. This is based on the principle of synthetic lethality whereby lack of G1/S activation in cancer cells, combined with inhibition of G2/M checkpoint activation through drugs against a key checkpoint player, sensitises cells to DNA damaging agents.

1.5 NIMA-related protein kinases

1.5.1 NIMA

Never in mitosis A (NIMA) is a serine/threonine protein kinase expressed in the fungus, *Aspergillus nidulans* (Osmani *et al.*, 1988). Identification of NIMA came through genetic screening of conditional cell cycle mutants (Morris, 1975). The screen identified two types of cell cycle mutants: those that were blocked in mitosis (bim), or those that were never in mitosis (nim) and were instead blocked in G2, when cells were incubated at the restrictive temperature (Morris, 1975; Oakley & Morris, 1983). Upon returning to the permissive temperature, nim cells would enter mitosis with disassembly of cytoplasmic microtubules, mitotic spindle formation and condensation of chromosomes (Osmani & Ye, 1996).

In 1987, the *nimA* gene was isolated by complementation of the mutant phenotype (Osmani *et al.*, 1987). The gene encodes NIMA, a 79 kDa nuclear protein (De Souza *et al.*, 2000) with an N-terminal catalytic domain and a C-

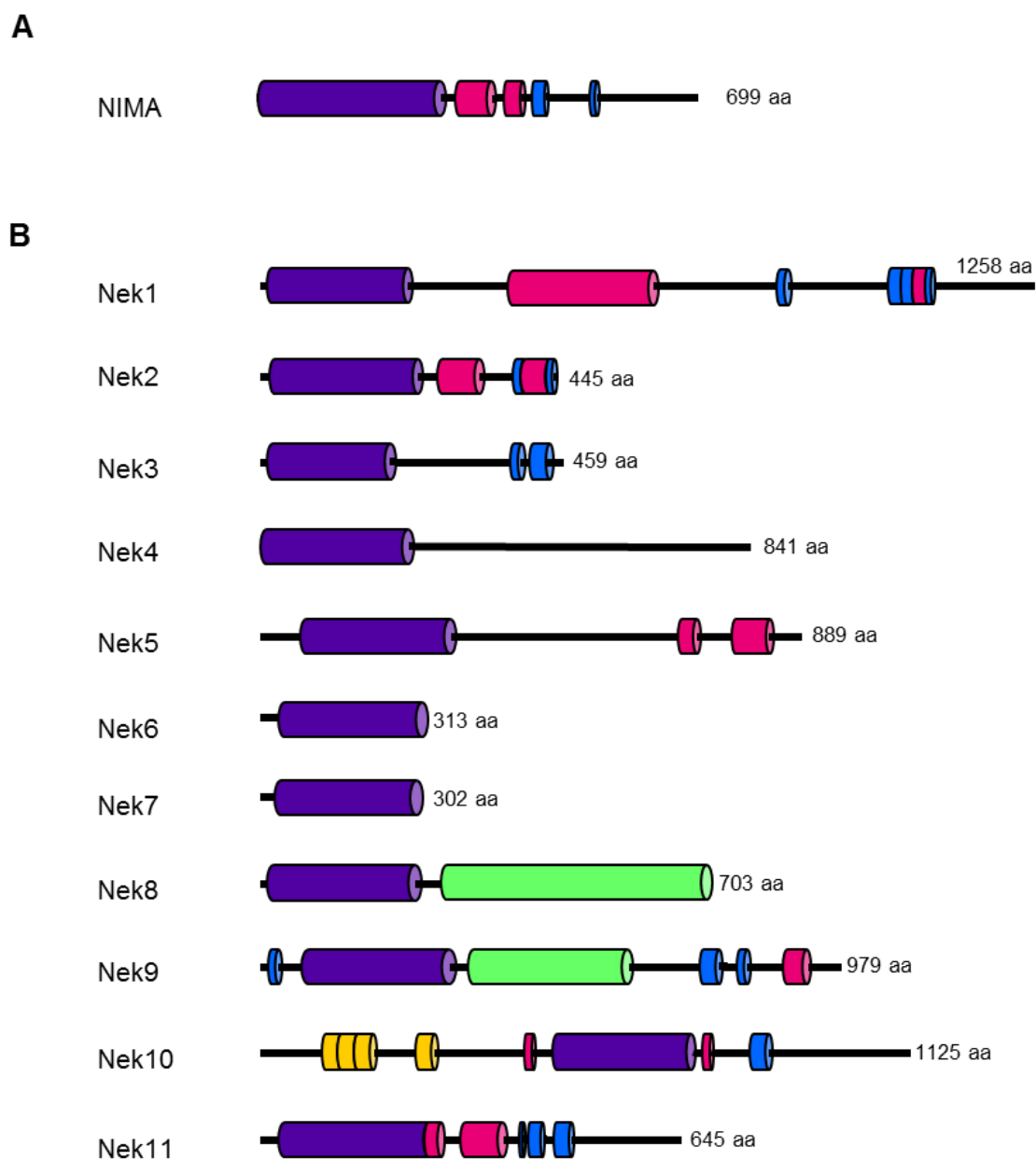


Figure 1.8 *Aspergillus* NIMA and the human NIMA-related protein kinase family

Schematic representation of **(A)** *Aspergillus nidulans* NIMA and **(B)** the human Nek protein kinase family. Domains shown include the kinase domain (purple), coiled-coil domains (pink), PEST-like degradation motifs (blue), RCC1-like domains (green), and armadillo repeats (yellow). Amino acid lengths are indicated. Adapted from Fry et al., 2012.

terminal regulatory domain containing two coiled-coil motifs followed by two PEST-like motifs (Figure 1.8A). The coiled-coils mediate the formation of NIMA oligomers (Lu *et al.*, 1994), whilst the PEST sequences have been shown to direct ubiquitin-dependent proteolysis (O'Connell *et al.*, 2003a; Pu & Osmani, 1995a).

NIMA mRNA and protein levels are cell cycle regulated with levels peaking as cells enter mitosis (Osmani *et al.*, 1987; Osmani *et al.*, 1991a). Similarly, NIMA kinase activity increases throughout interphase, peaking at the G2/M transition, before dropping again as cells exit mitosis (Osmani *et al.*, 1988; Osmani *et al.*, 1991b). Overexpression of wild-type NIMA results in cells prematurely entering mitosis from any stage of the cell cycle (Osmani *et al.*, 1988). Collectively, these findings indicate that NIMA is required for the transition of cells into mitosis (Oakley & Morris, 1983; Osmani *et al.*, 1987; Bergen *et al.*, 1984). More specifically, NIMA controls the initiation of mitosis by regulating the transport of active Cdc2/cyclin B complex into the nucleus and to the spindle pole body (SPB) (Wu *et al.*, 1998). Furthermore, during mitosis NIMA associates with chromatin and has been shown to phosphorylate Histone 3 at serine 10, thereby promoting chromosome condensation (De Souza *et al.*, 2000; Davies *et al.*, 2004). Conversely, exit from mitosis requires both degradation and inactivation of NIMA. This was demonstrated by expressing the kinase domain lacking the C-terminal regulatory region in cells. This resulted in a more stable protein product that continued to promote mitosis and was therefore toxic to cells (Pu & Osmani, 1995b; O'Connell *et al.*, 1994).

Given the importance of NIMA in cell cycle control it seemed likely that it would be conserved across evolution as has been observed for many key cell cycle regulators. Indeed, the first indication that NIMA-like kinases may exist in other organisms was through overexpression studies of NIMA in fission yeast, *Xenopus* oocytes and human HeLa cells (O'Connell *et al.*, 1994; Lu & Hunter, 1995b). NIMA overexpression in these systems resulted in the induction of pseudomitotic events including chromatin condensation, nuclear membrane

breakdown, and spindle assembly regardless of cell cycle stage (O'Connell *et al.*, 1994; Lu & Hunter, 1995b). Furthermore, expression of dominant-negative mutants of *nimA* in HeLa cells resulted in G2-arrest (Lu & Hunter, 1995b). In subsequent years, a NIMA homologue, Nim-1, was identified in another filamentous fungus, *Neurospora crassa* (Pu *et al.*, 1995). NIMA-related kinases have also been identified in various species, including the Nrks in trypanosomes (Gale & Parsons, 1993), Fa2 in *Chlamydomonas* (Mahjoub *et al.*, 2002), Fin1 in fission yeast (Krien *et al.*, 1998; Jones & Rosamond, 1990), Kin3 in budding yeast (Jones {{330 Jones,D.G. 1990}}) and the Neks in multicellular eukaryotes such as *Drosophila*, *C. elegans*, *Xenopus*, mice and humans (Fry *et al.*, 2012a) (Figure 1.8).

1.5.2 NIMA homologues in lower eukaryotes

To date, the only known functional homologue that can complement the *nimA* temperature sensitive mutant is Nim-1, isolated from another filamentous fungus, *Neosporra crassa* (Pu *et al.*, 1995). This protein shares 75% sequence identity within the catalytic domain to that of NIMA making it more closely related to NIMA than any of the other NIMA-related kinases. Single NIMA-related genes were also isolated in both budding (Kin3) and fission yeast (Fin1); however, despite roles in cell cycle events they are not required for viability. Like NIMA though, activity of Fin1 is cell-cycle regulated. Moreover, it shows localisation to SPBs in G2 and mitosis, and overexpression results in premature chromosome condensation (Krien *et al.*, 1998; Krien *et al.*, 2002). Furthermore, Fin1 is required for the localisation of Plo1 (the fission yeast polo-like kinase) to the SPB, where it activates Cdc25 leading to *cdc2* activation and mitotic entry (Grallert and Hagan, 2002). During mitosis, it also exhibits roles in the formation of robust mitotic spindles and Fin1 mutation leads to monopolar spindle formation (Krien *et al.*, 2002; Grallert & Hagan, 2002; Grallert *et al.*, 2004).

Overexpression or depletion of Kin3, on the other hand, resulted in no observable phenotype (O'Connell *et al.*, 2003a). However, interestingly *kin3Δ*

cells are defective in their DNA damage response and fail to arrest at G2/M in response to a number of DNA damaging agents, including MMS, cisplatin, doxorubicin and nitrogen mustard (Moura et al., 2010). This is intriguing given what we are now learning about the role of some mammalian Neks in the DDR (see section 1.5.3.4).

1.5.3 The Mammalian NIMA-related kinase family

The presence of NIMA-like kinases in vertebrates was first revealed in 1992 with the identification and characterisation of mouse Nek1 (Letwin *et al.*, 1992). Subsequent degenerate PCR studies revealed the presence of additional NIMA-related sequences in humans (Schultz & Nigg, 1993). And complete genome sequencing indicated the existence of a family of eleven NIMA-related kinases (Neks), termed Nek1 to Nek11 in mammals (Figure 1.8B). Various biochemical and functional studies have now been undertaken on these enzymes, although compared to many other kinases, they remain relatively poorly characterised (Letwin *et al.*, 1992; Schultz & Nigg, 1993; Lu & Hunter, 1995a; Chen *et al.*, 1999; Tanaka & Nigg, 1999; Kandli *et al.*, 2000; Holland *et al.*, 2002; Noguchi *et al.*, 2002; Forrest *et al.*, 2003). Structurally, apart from Nek10, which has a central kinase domain, the human Nek proteins contain an N-terminal catalytic domain which shares approximately 40-45% sequence similarity to that of NIMA and 40-85% to each other (O'Connell *et al.*, 2003b). In contrast, the C-terminal regions are highly variable in length, amino acid sequence and domain organisation. The consequence of this is reflected in differences in protein function, activity, localisation and regulation within cells (Table 1.1). Nevertheless, just as NIMA is required for mitotic entry and progression many of the human Nek members are also implicated in a number of aspects of cell cycle progression and differentiation, including mitotic progression, checkpoint control, proliferation and ciliogenesis.

Nek	Activity	Localisation	Function
Nek1	Genotoxic insults (IR, UV, crosslinking agents, oxidative injury)	Cytoplasm...nucleus?, centrosomes, cilia, sites of DNA damage	Ciliogenesis/DDR
Nek2	S, G2/M phases	Centrosomes	Mitosis
Nek3	Prolactin receptor	Cytoplasmic	Prolactin signalling
Nek4	?	Basal bodies	Ciliogenesis, DDR
Nek5	?	?	?
Nek6	Activated by Nek9, mitosis	Mitotic spindle	Mitosis
Nek7	Activated by Nek9, mitosis	Weakly to spindle poles	Mitosis
Nek8	Serum starvation	Nucleus, centrosomes, cilia	Ciliogenesis, DDR
Nek9	Mitosis	Mainly cytoplasmic, nuclear, spindle poles	Mitosis
Nek10	UV, G2/M	?	DDR
Nek11	DNA replication inhibitors and genotoxic insults, S to the G2/M phase	Nucleus/ Nucleoli, spindle microtubules	DDR

Table 1.1 Activation, localisation and function of human Neks

Summary of what is known so far about the activation, localisation and function of the eleven NIMA-related kinase members. Adapted from Fry et al., 2012.

1.5.3.1 Mitotic Neks

One of the most studied functions of the human Neks is their involvement in mitosis. Unlike NIMA, no single Nek has been found to be necessary for mitotic entry. However, so far, four human Neks have been implicated in mitotic events: these are Nek2, Nek6, Nek7 and Nek9. Between them, roles include centrosome separation, assembly of the mitotic spindle and nuclear envelope breakdown (Fry *et al.*, 2012a). Of these, Nek2 is the most well characterised of the Nek family and it is also the most similar to NIMA sharing 47% sequence similarity in the N-terminal catalytic domain (Schultz *et al.*, 1994b). Furthermore, like NIMA it contains two coiled-coil motifs in the C-terminal domain which facilitates homodimerization causing both autophosphorylation and activation. In addition, its expression is cell cycle regulated and exhibits biochemical properties that implicate it in mitosis (Fry *et al.*, 1995). Despite this however, Nek2 is unable to rescue the *nimA* mutant phenotypes indicating that it is not a functional homologue of NIMA (O'Connell *et al.*, 2003b).

Whilst expression and activity of NIMA is maximal in late G2 and early mitosis, Nek2 expression and activity increases from S through to G2 suggesting a role earlier in the cell cycle. It is expressed as at least three isoforms: Nek2A, Nek2B and Nek2C, derived by alternative splicing. Nek2 localises to centrosomes throughout interphase and all stages of mitosis where it plays an important role in the initiation of mitotic spindle formation (Fry *et al.*, 1998b). Overexpression of active Nek2 leads to premature centrosome separation (Fry *et al.*, 1998b; Faragher & Fry, 2003), whilst depletion of Nek2 inhibits it but without affecting mitotic entry (Fletcher *et al.*, 2005). Functionally therefore, Nek2 plays a direct role in centrosome disjunction. This occurs through phosphorylation of intercentriolar linkage proteins, C-Nap1, Rootletin and β -catenin, by Nek2, resulting in their dissociation from the centrosomes, loss of centrosome cohesion and centrosome separation at G2/M (Fry *et al.*, 1998a; Bahe *et al.*, 2005). In addition, other cell division roles for Nek2 have been proposed; for example, Nek2 interacts with the kinetochore protein, Hec1/Ndc80 whilst Nek2 depletion results in displacement of Mad2 from the kinetochores resulting in

impaired chromosome segregation (Lou *et al.*, 2004; Moniz *et al.*, 2011). These data implicate Nek2 in the spindle assembly checkpoint.

The remaining mitotic kinases, Nek6, Nek7 and Nek9, all show elevated kinase activity during mitosis, and act within a cascade to regulate mitotic progression (Belham *et al.*, 2003). In the pathway, Nek6 and Nek7 are activated by the upstream kinase, Nek9. In part this may be through either direct phosphorylation or indirect autophosphorylation of Ser206 and Ser195 residues, in their respective activation loops (Belham *et al.*, 2003; Roig *et al.*, 2002). However, structural studies have revealed that interaction of Nek9 with Nek6 and Nek7 also leads to disruption of their auto-inhibitory conformations as an additional mechanism of activation (Richards *et al.*, 2009).

In terms of their organisation, Nek6 and Nek7 consist of a short N-terminal extension followed by a catalytic domain which between them share 87% sequence similarity (Kandli *et al.*, 2000). Unlike other members of the Nek family, they lack a C-terminal regulatory region but have short, distinct extensions N-terminal to the catalytic domain. Functionally, both kinases contribute to the formation of mitotic spindles, as well as having roles in cytokinesis (O'Regan & Fry, 2009; Yin *et al.*, 2003; Yissachar *et al.*, 2006). Nek9, on the other hand, has a large C-terminal non-catalytic domain containing an RCC1 homology region followed by two PEST sequences and a coiled-coil domain. It is through this C-terminal domain that Nek9 is able to both oligomerise and to interact with Nek6 and Nek7 (Roig *et al.*, 2002; Richards *et al.*, 2009).

The first indication that these three Neks contribute to spindle formation came through overexpression and antibody microinjection studies (Roig *et al.*, 2002; Yissachar *et al.*, 2006). Overexpression of kinase-dead Nek6 or Nek7 results in mitotic arrest, nuclear abnormalities, apoptosis and importantly, spindle defects (O'Regan & Fry, 2009; Yin *et al.*, 2003; Yissachar *et al.*, 2006). Whilst,

expression of inactive Nek9 or truncated mutants leads to missegregation of chromosomes, and upon injection of Nek9 antibodies, aberrant spindle formation (Roig *et al.*, 2002; O'Regan & Fry, 2009). Roles in organisation of the mitotic spindle was confirmed through RNAi depletion studies of Nek6, Nek7, and Nek9 which resulted in fragile spindle formation and activation of the spindle assembly checkpoint (SAC) (O'Regan & Fry, 2009; Roig *et al.*, 2005). In addition, upon entry into mitosis both Nek7 and Nek9 show localisation to the centrosomes where they play roles in nucleation and organisation of spindle microtubules (O'regan *et al.*, 2007a). Indeed, studies have shown that Nek7 is required to recruit γ -tubulin to spindle poles since its depletion leads to decreased levels of γ -tubulin at the centrosome (Yissachar *et al.*, 2006; Kim *et al.*, 2007). Nek9 is also able to interact with components of the γ -tubulin ring complex (γ -TuRC), which initiates nucleation of microtubules, and phosphorylate NEDD1/GFP-WD, a γ -TuRC adaptor protein (Roig *et al.*, 2005; Fry *et al.*, 2012b).

1.5.3.2 Ciliary Neks

As discussed in section 1.5.3.1, several Neks exhibit roles in mitosis. However, it has now emerged that other members have key roles in ciliogenesis, revealing a more general role for Neks in the organisation of microtubules (O'regan *et al.*, 2007b). Nek1 and Nek8 were both implicated in ciliogenesis through mapping of mutations found in mouse models of polycystic kidney disease (PKD) (Liu *et al.*, 2002; Upadhyya *et al.*, 2000; Mahjoub *et al.*, 2005). Research into the molecular processes underlying cyst formation in PKD, has revealed that a major cause is through dysfunctional ciliary signalling with many of the proteins implicated in PKD showing localisation to the cilium (Yoder, 2007; Pazour *et al.*, 2005).

Nek1 was the first mammalian Nek to be identified through screening of mouse cDNA expression libraries (Letwin *et al.*, 1992). Nek1 is the longest of the Neks consisting of an N-terminal catalytic domain that shares 42% identity with that of

NIMA, followed by two coiled-coil motifs and a number of PEST-like sequences. Although having been first characterised in 1992, its role in ciliogenesis was not revealed until 2000. Studies on the *kat* and *kat^{2J}* mice that exhibit a slow progressive form of PKD as well as male sterility, facial dysmorphisms and dwarfing, revealed mutations in the Nek1 gene (Upadhyaya *et al.*, 2000; Vogler *et al.*, 1999; Janaswami *et al.*, 1997). Yeast two-hybrid studies confirmed that Nek1 interacts with proteins involved in the development of PKD, as well as microtubule dependent proteins, and interestingly, proteins involved in the G2/M DNA damage checkpoint (discussed in more detail in section 1.5.3.4) (Surpili *et al.*, 2003). In addition, Nek1 localised to centrosomes throughout interphase and mitosis as well as to primary cilia and basal bodies in quiescent cells (Mahjoub *et al.*, 2005; Shalom *et al.*, 2008). Finally, overexpression of mutated Nek1 in MEF cells resulted in abnormal cilia formation, whilst expression of a kinase-dead form resulted in disruption of centrosome organisation (Mahjoub *et al.*, 2005; Shalom *et al.*, 2008; White & Quarmby, 2008).

In a similar way, implication of Nek8 in ciliopathies came from analysis of juvenile cystic kidney (*jck*) mutant mouse strain, which exhibits characteristics of the autosomal recessive form of PKD (ARPKD) (Liu *et al.*, 2002). Furthermore, injection of morpholino antisense oligonucleotides against Nek8 into zebrafish resulted in the formation of pronephric cysts (Liu *et al.*, 2002). Nek8 consists of an N-terminal catalytic domain, but unlike NIMA or many of the other Neks, it does not contain any PEST or coiled-coil motifs. Instead, analogous to Nek9, it has an RCC1-like domain. It is within this domain that the missense mutation, G446V, is found in *jck* mice, causing mislocalisation of Nek8 protein (Liu *et al.*, 2002; Mahjoub *et al.*, 2005). As with Nek1, Nek8 shows localisation to primary cilia in WT kidney epithelial cells however, this is lost in cells derived from *jck* mice, with the added observation of increased cilia length (Mahjoub *et al.*, 2005; Smith *et al.*, 2006). More specifically in mouse kidney tubules, Nek8 localises to the proximal portion of primary cilia and has been found to associate with Polycystin-2 (PC2), a protein that is mutated in the autosomal dominant form of PKD (ADPKD) (Sohara *et al.*, 2008). Furthermore, it was observed that both

increased expression of polycystin-1 (PC1) and PC2, and abnormal phosphorylation of PC2, was present in *jck* mouse kidney, suggesting that Nek8 acts to regulate these proteins (Sohara *et al.*, 2008). In addition to human PKD, mutated Nek8 protein has now also been implicated in the progression of the renal ciliopathy, nephronophthisis (NPHP) (Otto *et al.*, 2008).

1.5.3.3 Signal transducing Neks

Functional characterisation of Nek3 has not revealed any obvious roles for it in mitosis or cell cycle regulation. In fact, Nek3 expression and activity remains relatively unchanged throughout the cell cycle, and no changes in cell cycle progression have been observed upon overexpression of wild-type or inactive Nek3, or upon microinjection of Nek3 antibodies (Tanaka & Nigg, 1999). More recently, Nek3 has been implicated in the regulation of prolactin (PRL)-mediated cytoskeleton rearrangement and motility of breast cancer cells, through phosphorylation of Vav2, a RhoGEF and component within the PRL signalling pathway (Moniz *et al.*, 2011; Miller *et al.*, 2007). In addition, Nek3 overexpression in CHO (Chinese hamster ovary) cells resulted in reorganisation of the cytoskeleton when treated with PRL, whilst depletion reduces it (Miller *et al.*, 2007). Nek3 also regulates cytoskeletal dynamics in neurons through microtubule deacetylation (Chang *et al.*, 2009).

1.5.3.4 Neks implicated in the DNA damage response (DDR)

Roles for Nek family members in the regulation of cell cycle progression in response to DNA damage have emerged in recent years. While some members, such as Nek2 and Nek6, are DNA damage checkpoint targets and are inhibited by DNA damage (Fletcher *et al.*, 2004; Lee *et al.*, 2008), others such as Nek1, Nek4, Nek8, Nek10 and Nek11 have been directly implicated in the DDR pathways (Polci *et al.*, 2004; Nguyen *et al.*, 2012; Choi *et al.*, 2013; Moniz & Stambolic, 2011; Melixetian *et al.*, 2009).

Nek1 is implicated in sensing and repair of DNA strand breaks and in DNA damage checkpoint control (Polci *et al.*, 2004; Chen *et al.*, 2011; Chen *et al.*, 2008a; Pelegrini *et al.*, 2010). In response to a number of genotoxic insults including IR, UV, cross-linking agents, and oxidative injury, both expression and kinase activity of Nek1 are quickly elevated (Polci *et al.*, 2004; Chen *et al.*, 2008a), with activity increasing as early as 4 minutes post-IR in primary and transformed cells (Polci *et al.*, 2004). Meanwhile, depletion of Nek1 results in defective activation of G1/S and G2/M checkpoints as well as inefficient repair, with DSBs persisting long after low dose IR (Polci *et al.*, 2004; Chen *et al.*, 2008b). In addition, cells lacking Nek1 fail to activate Chk1 and Chk2 in response to DNA damage, thereby placing it upstream of these kinases, although how it acts remains an important question (Chen *et al.*, 2008b). It was suggested that Nek1 may be required for transport of Chk1 or Chk2 from the cytoplasm to nucleus to enable their activation by ATM and ATR. Alternatively, it may directly phosphorylate a priming site or another protein required for interaction between ATM/ATR and Chk1/Chk2 (Chen *et al.*, 2008b). Activation of Nek1 is not ATM or ATR dependent though, suggesting that it may act as an independent transducer of the DDR (Chen *et al.*, 2011). As mentioned previously, a yeast two-hybrid screen identified interaction of Nek1 with a number of proteins involved in DNA repair and cell cycle arrest, such as ATRX, MRE11 and p53BP1 (Surpili *et al.*, 2003). Consistent with this and a role in the sensing of DSBs, a proportion of Nek1 protein shows rapid relocalisation from the cytoplasm in untreated cells to γ -H2AX and NFB1/MDC1 nuclear foci in response to genotoxic insult (Polci *et al.*, 2004; Chen *et al.*, 2008b).

Nek10 diverges structurally from the other Neks in that it has a central kinase domain and is the only Nek to contain armadillo repeat sequences (Moniz & Stambolic, 2011). A role for Nek10 in the G2/M DNA damage checkpoint in response to UV irradiation was established in 2011 (Moniz & Stambolic, 2011). Exposure to UV, but not mitogens, results in formation of a trimeric complex, mediated by Raf-1, and consisting of Nek10, MEK1 and Raf-1. This results in MEK1 activation followed by phosphorylation and activation of ERK1/2

(extracellular signal-related kinase 1/2) and cell cycle arrest at the G2/M checkpoint (Moniz & Stambolic, 2011). Activation of MEK1/2 and/or ERK1/2 in response to UV is impaired upon Nek10 depletion, resulting in G2/M checkpoint abrogation.

The most recent Neks to be implicated in the DDR are Nek4 and Nek8. Suppression of Nek4 results in defective checkpoint activation in response to DSBs (Nguyen *et al.*, 2012). Furthermore, proteomic analysis has provided evidence for interaction of Nek4 with Ku70, Ku80 and DNA-PKcs which together make up DNA-PK, a complex involved in NHEJ after DNA damage. Interestingly, depletion of Nek4 results in reduced DNA-PKcs recruitment to DNA breaks. This causes decreased γ -H2AX, a phosphorylation target of DNA-PK and reduced p53 activation (Nguyen *et al.*, 2012).

Nek8 was identified in a siRNA screen as a protein involved in DNA repair and the replication stress response, mediated by ATR and Chk1 (Choi *et al.*, 2013). Defects in Nek8 protein had been previously established to cause ciliopathies linked to disorders such as PKD and NPHP. Recently, a number of other proteins involved in NPHP have been implicated in DNA repair pathways, including NF423, CEP164 and NPHP10 (Jackson, 2013; Chaki *et al.*, 2012). Specifically, depletion of Nek8 results in enhanced detection of DNA DSBs during aphidicolin-induced replication stress, as well as increased kinase activity of Cyclin A/Cdk2, a complex responsible for regulating S-phase progression (Choi *et al.*, 2013). Furthermore, Nek8 is able to interact with the Cyclin A/Cdk2 complex, as well as other DNA damage checkpoint components, including ATR, ATRIP and Chk1 (Choi *et al.*, 2013). With Nek1, Nek8 and increasingly more proteins being involved in both ciliogenesis and DDR pathways, it suggests a causal link between these pathways, and the possibility that defective DDR pathways have roles in the pathogenesis of renal ciliopathies. Indeed, kidneys with mutant Nek8 in *jck* mice exhibit increased DDR signalling, while Nek8 depletion not only induces replication stress but also reduces the frequency of cilia in renal epithelia (Choi *et al.*, 2013).

1.5.4 Nek11

Nek11 was first identified in 2002, by Noguchi *et al.*, through screening of an EST database (Noguchi *et al.*, 2002). It consists of an N-terminal kinase domain that shares 33% amino acid identity with that of NIMA, and phylogenetic analysis of catalytic domains revealed that it is most closely related to Nek1, Nek3 and Nek4 (Noguchi *et al.*, 2002). The C-terminal regulatory region contains 2 coiled-coil motifs followed by 3 PEST-like sequences. It has been reported to be expressed as at least 3 alternatively spliced isoforms: Nek11 Long (Nek11L, ~74 kDa), Nek11 Short (Nek11S, ~54 kDa) and Nek11C (~56 kDa) (Noguchi *et al.*, 2002; Sahota, 2010), and further expression database analysis revealed a fourth isoform, Nek11D (~69 kDa) (this study). These isoforms differ in length and amino acid sequence at the end of the C-terminal non-catalytic domain (Figure 1.9). All isoforms are identical in sequence up to residue 466, after which Nek11S continues for 4 amino acids and Nek11C for a further 16 amino acids. Nek11L and Nek11D share sequence identity up to amino acid 541, and extend to 645 and 599 amino acids, respectively.

1.5.4.1 Nek11 and the DNA damage response

Expression analysis indicated that like NIMA and other Nek family members, Nek11 is cell-cycle regulated with expression increasing from S phase and peaking at G2/M (Noguchi *et al.*, 2002). The activity on the other hand is specifically increased in response to genotoxic stress by IR, etoposide and adriamycin, or replication inhibitors, such as aphidicolin, thymidine and hydroxyurea (Noguchi *et al.*, 2002; Melixetian *et al.*, 2009). In addition, this activity is inhibited when cells are treated with caffeine, an inhibitor of ATM and ATR, indicating that Nek11 acts downstream of these kinases in response to DNA damage (Noguchi *et al.*, 2002; Melixetian *et al.*, 2009). Indeed, more recently, an shRNA screen by Melixetian *et al.* (2009), provided mechanistic evidence for how Nek11 acts in the G2/M DNA damage response checkpoint. U2OS cells transfected with an shRNA library were irradiated and cells that failed to arrest at the G2/M DNA damage checkpoint were collected and shRNA constructs in those cells isolated to identify the genes involved. As well as

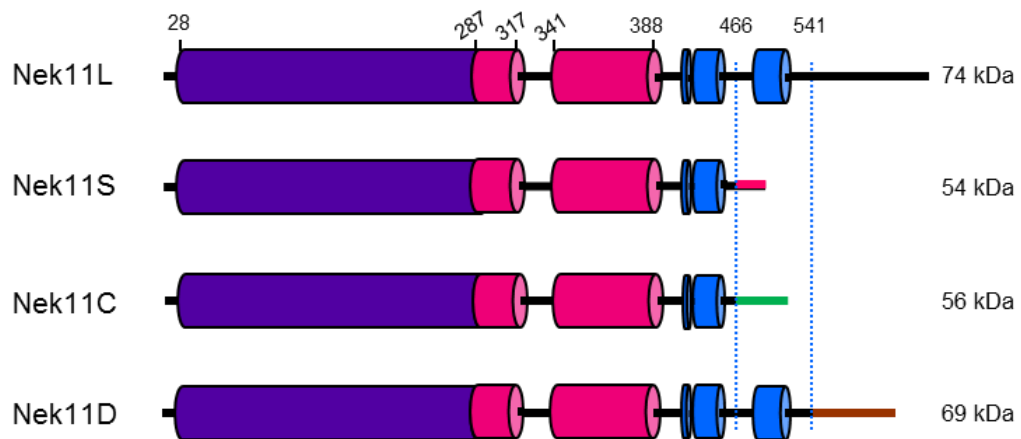


Figure 1.9 Nek11 exists as at least four alternatively spliced isoforms

Schematic representation of the four Nek11 isoforms, Nek11L (Long), Nek11S (Short), Nek11C and Nek11D. Kinase domains (purple), coiled-coil (pink) and degradation motifs (blue) are indicated. Coloured lines at C-terminal ends represent regions where amino acid identity differs between isoforms. All are identical up to aa 466 and Nek11L and Nek11D are identical up to aa 541. Molecular weights are indicated (kDa).

recovering shRNAs against well-known components of the DDR pathways, such as Chk1 and ATR, the screen also identified Nek11 (Melixetian *et al.*, 2009).

In normal cycling cells, progression from G2 in to mitosis requires activation of the Cdk1/Cyclin B complex. This is achieved through dephosphorylation of the Tyr15 and Thr14 residues on Cdk1 by the Cdc25 phosphatase family (Stark & Taylor, 2006). In response to DNA damage, Cdc25 proteins are degraded or sequestered in the cytoplasm resulting in cell cycle arrest (Stark & Taylor, 2006). Interestingly, upon Nek11 depletion, Cdc25A protein levels remain stable in response to DNA damage by IR (Melixetian *et al.*, 2009). In addition, Nek11 was found to phosphorylate Cdc25A at S82 and S88, sites that lie within DSG motifs known to be important for degradation, which until recently was phosphorylated by an unknown kinase. Intriguingly, depletion or inhibition of Chk1 resulted in reduced Nek11 activity and subsequently a consensus Chk1 phosphorylation site was identified in Nek11 (Melixetian *et al.*, 2009). Further experiments confirmed that in response to DNA damage Chk1 is able to phosphorylate S273 of Nek11 stimulating its activity. Mutation of this site to alanine resulted in a reduction in its kinase activity in response to IR and as a consequence Cdc25A was not properly targeted for proteolysis (Melixetian *et al.*, 2009). Overall then, the proposed pathway is that in response to IR, ATM and ATR kinases activate Chk1. Chk1 then phosphorylates Cdc25A at residue S76, priming it for further phosphorylation at the DSG motifs, whilst also activating Nek11 through phosphorylation of S273. Nek11 then phosphorylates Cdc25A at the phosphodegron DSG sequences, thereby creating a docking site for the ubiquitin ligase SCF^{β-TrCP}. Ultimately, this results in proteasomal degradation of Cdc25A and cell cycle arrest (Figure 1.10).

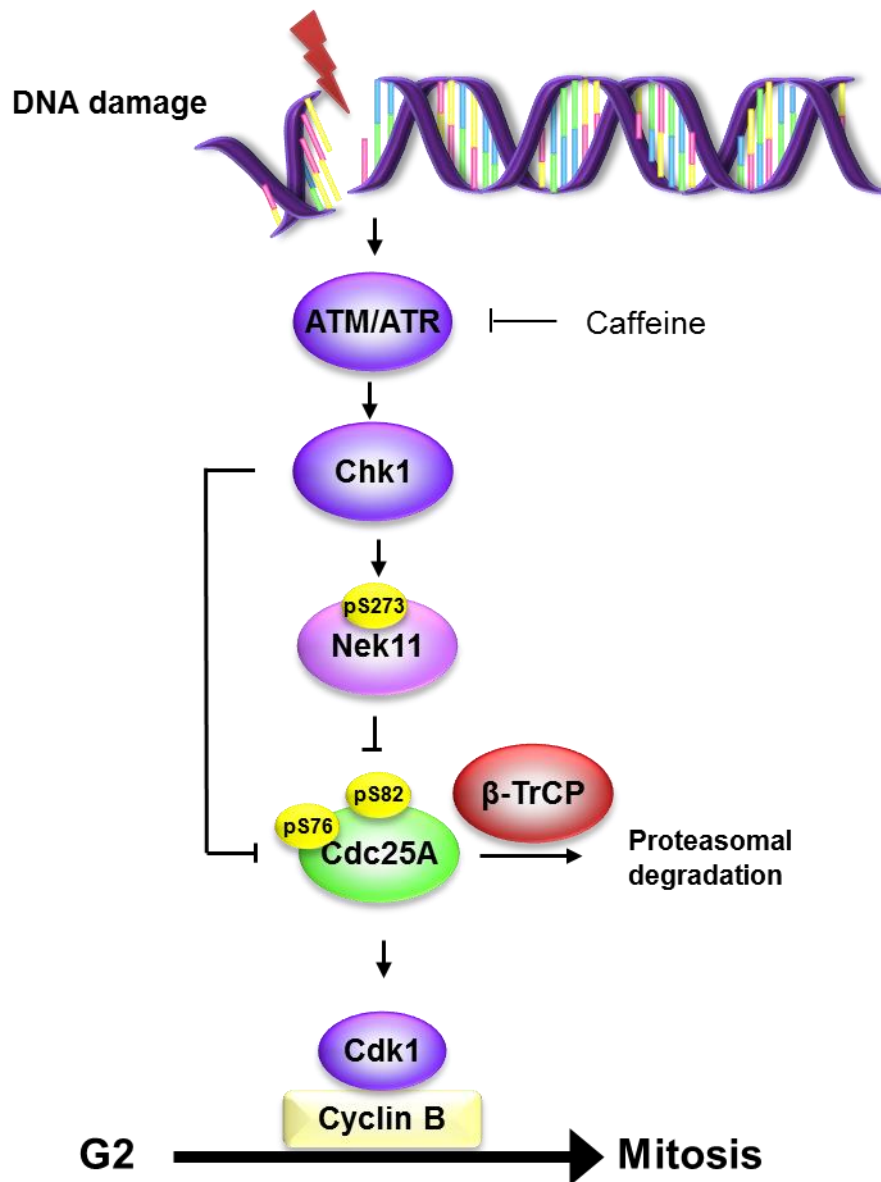


Figure 1.10 Proposed role for Nek11 at the G2/M DNA damage checkpoint

In response to DNA damage, ATM and ATR kinases activate Chk1 through phosphorylation. Chk1 phosphorylates Cdc25A at S76 as well as S273 of Nek11 thereby activating it. Nek11 phosphorylates Cdc25A at S82, targeting it for degradation through binding of the ubiquitin ligase SCF^{β-TrCP}. As a result Cdk1/cyclin B remains inactive and cells arrest at the G2/M transition. Adapted from Fry et al., 2012.

However, since this study other proteins, and not Nek11, have been suggested to be responsible for the phosphorylation and degradation of Cdc25A in response to DNA damage. In particular, casein kinase 1 α (CK1 α) was shown to target Cdc25A for degradation through phosphorylation of S79 and S82 in response to IR in HeLa cells (Honaker & Piwnica-Worms, 2010; Piao *et al.*, 2011). Furthermore, kinase assays carried out with Nek11 and full-length Cdc25A failed to detect phosphorylation of S82 under conditions where MBP was phosphorylated by Nek11 (Honaker & Piwnica-Worms, 2010).

An alternative role for Nek11 in the DDR has recently been proposed with the finding that Nek11 can phosphorylate the Bloom syndrome helicase (BLM). BLM which binds to TopBP1, a key mediator protein involved in DNA replication checkpoint control (Wang *et al.*, 2013). Hence, much still remains to be learnt about the pathways in which Nek11 might contribute to the DDR.

1.5.4.2 Nek11 localisation and interaction with Nek2

Examination of Nek11 localisation in HeLa cells revealed cell-cycle stage specific behaviour. Although overall protein expression is low during interphase, Nek11 was detected at nuclei and as cells progress into mitosis localisation shifted to polar microtubules (Noguchi *et al.*, 2002). A further study by the same group with the same antibody, but in U2OS cells localised Nek11 to nucleoli during interphase, as well as perichromosomal regions during mitosis (Noguchi *et al.*, 2004). Interestingly, during these localisation experiments, the authors also found that Nek11 co-localised with Nek2A at nucleoli (Noguchi *et al.*, 2004). Furthermore, Nek11 co-immunoprecipitates with active Nek2A, and Nek2A is able to phosphorylate residues in the C-terminal domain of Nek11, with increased interaction and phosphorylation observed in G1/S arrested cells (Noguchi *et al.*, 2004). The authors proposed a model in which phosphorylation by Nek2A releases an autoinhibitory conformation of Nek11, thereby activating it (Noguchi *et al.*, 2004). However, whether this is required for activation of Nek11 in the presence of DNA damage is not clear.

1.5.4.3 Nek11 as a potential cancer drug target

The DNA damage checkpoint pathways are essential in order to maintain genome stability. However, mutation or loss of proteins in these pathways can lead to cell death in the presence of elevated DNA damage. As a result, proteins involved in the DNA damage response have recently become attractive targets for drug development. Around 50% of cancer cells carry either mutated or inactive p53, a key factor required in the G1/S checkpoint. These cells are therefore solely reliant on the G2/M checkpoint to arrest the cell cycle and allow time to repair damaged DNA. Therefore, inhibition of the G2/M checkpoint combined with exposure to DNA damage, would result in normal proliferating cells arresting at the G1/S checkpoint, but cancer cells with mutated p53 protein being incapable of arresting cell cycle progression (Jackson & Bartek, 2009; Xiao *et al.*, 2003). The cancer cells would be forced to go through mitosis with significant damage leading to mitotic catastrophe, thereby specifically killing cancer cells through synthetic lethality (Figure 1.11) (Melixetian *et al.*, 2009).

Inhibitors against Chk1 have already been developed and are in clinical trials. However, Chk1 is also involved in repair pathways and needed for proliferation of normal cells, so inhibiting its action may not necessarily be detrimental solely to cancer cells (Melixetian *et al.*, 2009; Sorensen *et al.*, 2010). With its reported roles in the replication and G2/M checkpoints, Nek11 is therefore a potentially exciting new drug candidate. Furthermore, immunohistochemistry analysis with a commercial Nek11 antibody against tissue microarrays of human primary tumours, showed that Nek11 expression was increased in 35% of the colon adenomas and carcinomas tested compared to normal tissue (Sorensen *et al.*, 2010). In addition, expression was higher in colorectal adenomas compared to carcinomas suggesting a role for Nek11 in the prevention of tumorigenesis. This specifically raises the prospect that a therapeutic window may exist for targeting Nek11 in colorectal cancer.

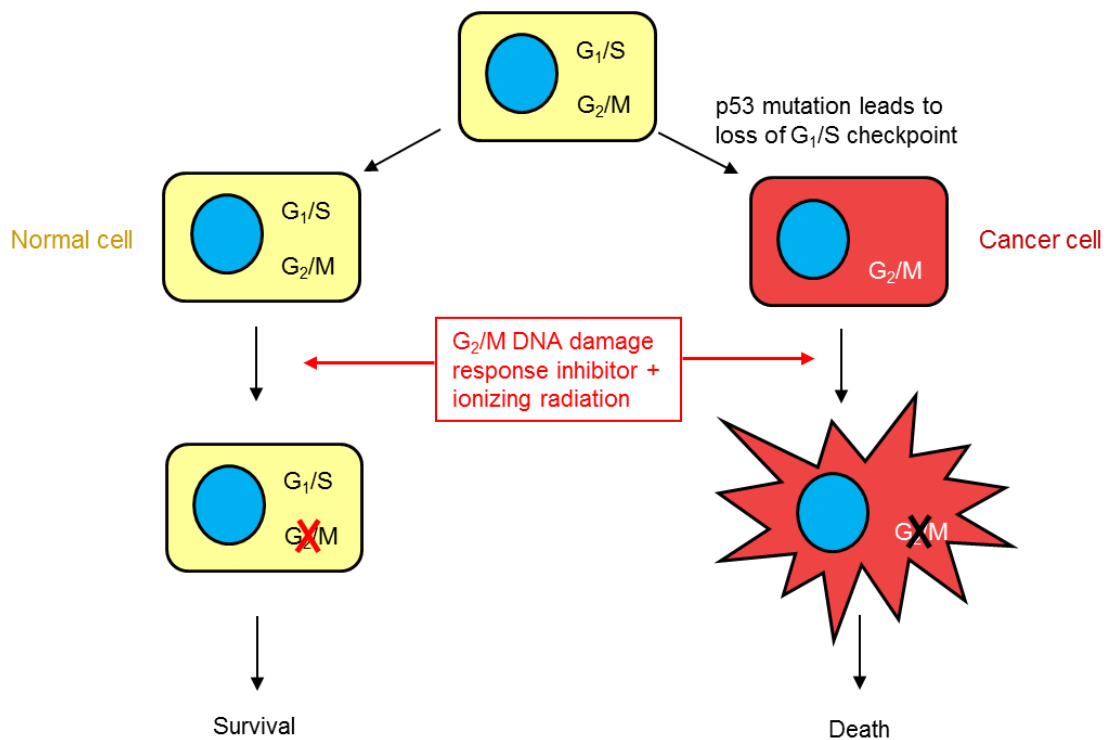


Figure 1.11 Exploiting DNA damage checkpoints for cancer treatment

50% of cancer cells harbour mutated or loss of p53 and thus have weakened G₁/S checkpoints. Treatment with a drug that targets a G₂/M component followed by a DNA damaging agent results in normal cells arresting at their intact G₁/S checkpoint, repairing their DNA and progressing in the cell cycle. However, cancer cells continue proliferating with unrepaired DNA and thus die from excessive damage or mitotic catastrophe. Adapted from Jackson et al., 2009

1.6 Colorectal cancer

1.6.1 Colorectal cancer incidence

Colorectal cancer is the third most common cancer and the fourth most common cancer cause of death globally (Ferlay *et al.*, 2010). Whilst 35% of colorectal cancer risk might be attributable to hereditary components (Lichtenstein *et al.*, 2000), most colorectal cancers occur sporadically and develop slowly over time, hence as a result is more prevalent in the older population (Brenner *et al.*, 2014). In addition, development of the disease is linked to lifestyle since it is more common in Europe, North American and Oceania (Center *et al.*, 2009). Some lifestyle risk factors linked to the development of colorectal cancer include consumption of red and processed meat, smoking, excessive alcohol consumption, obesity, diabetes and lack of exercise (Brenner *et al.*, 2014).

1.6.2 Development of colorectal cancer

Colorectal cancer development is a multi-step process and arises from the accumulation of both genetic and epigenetic changes in epithelial cells (Lao & Grady, 2011). Like many cancers, genetic mutations often inactivate tumour suppressor and DNA repair genes, and activate oncogenes (Arnold *et al.*, 2005). Most common in early colorectal cancer development is mutation of the tumour suppressor, adenomatous polyposis coli (APC), in normal epithelium resulting in the development of adenomatous polyps (Ballinger & Anggiansah, 2007). Mutation of APC is observed in around 70-80% of colorectal carcinomas and is often regarded as the initiating event in the pathway to tumorigenesis (Fearon, 2011). Another common tumour suppressor mutation is that of p53 during the late adenoma stage promoting carcinoma formation. Also common during early adenoma stage is the activation of the proto-oncogene, v-Ki-ras2 Kirsten rat sarcoma viral oncogene homologue (KRAS), to an oncogene. KRAS signalling occurs through BRAF to activate MAPK pathways. Therefore mutations of both KRAS and BRAF, found in 55-60% of colorectal cancers, results in the promotion of proliferation and inhibition of apoptosis (Lao & Grady,

2011). Overall, accumulation of these mutations results in normal epithelial cells obtaining a selective growth advantage and as a result drives transformation of cells into adenomas followed by the formation of invasive carcinomas.

1.6.3 Current treatments

Treatment for colorectal cancers depends on the location and grade of the tumour, but treatments are mainly through surgery, radiotherapy and chemotherapy. In early stage cancers where there is invasion but not through the bowel wall, then surgery is the most common treatment. First-line or neo-adjuvant therapy is used before surgery when invasion occurs through the muscle wall or has spread to lymph nodes. This is often in the form of chemotherapy and acts to reduce the tumour size to improve surgery success rates. After surgery, patients can receive further chemotherapy, known as adjuvant chemotherapy. Finally, metastatic colorectal cancers which have spread to other organs often have a poor prognosis but are normally controlled with a combination of surgery, radiotherapy and chemotherapy.

In terms of chemotherapy the only available agent available for colorectal cancer treatment up until 1985 was the anti-metabolite 5-fluorouracil (5-FU) (Wilke & Van Cutsem, 2003). 5-FU is a pyrimidine analogue and therefore acts to block DNA synthesis through inhibition of DNA polymerase. In later years, the combination with folinic acid (FA, or leucovorin) increased the efficacy of this treatment. In the present day, 5-FU/FA is commonly used in combination with irinotecan and oxaliplatin – FOLFIRI and FOLFOX, respectively. Irinotecan, first licensed in the UK in 1998, is a topoisomerase I inhibitor. Treatment with irinotecan leads to the formation of SSBs through prevention of the religation step, this later leads to the formation of a DSB through replication fork collapse. Oxaliplatin, on the other hand, is a platinum based compound and covalently binds to DNA thus generating DNA adducts that lead to the formation in inter- and intrastrand platinum-DNA crosslinks. This prevents DNA replication and transcription and leads to DNA damage, culminating in cell death.

1.7 Aims and objectives

The aims of this project were to (1) determine the importance of Nek11 in the DNA damage response, (2) to characterize individual Nek11 isoforms and (3) to investigate whether Nek11 is a potentially valid target for cancer therapy. Specifically, this was done by using a variety of biochemical and cell biology based assays in cultured cells to examine the function, localisation and expression of the four Nek11 splice variants in the presence and absence of DNA damage.

The experimental objectives for which the results chapters are based on are as outlined below:

1. To determine the importance of Nek11 in the G2/M checkpoint arrest in colorectal cancer cells in response to different DNA damaging agents. These functional studies will be carried out using siRNA-mediated depletion of Nek11 in combination with DNA damage induction and analysed via flow cytometry.
2. Generate stable cell lines expressing each of the four Nek11 isoforms to examine whether Nek11 splice variants exhibit an isoform specific localization pattern and to analyse whether the localisation of Nek11 changes in response to ionizing radiation.
3. To optimise immunoprecipitation of Nek11 from stable cell lines for the purpose of identifying potential interacting partners.
4. To examine the relative expression of the four Nek11 splice variants using qRT-PCR in a panel of colorectal cancer cell lines.

5. To assess the roles of individual Nek11 isoforms at the G2/M DNA damage checkpoint using isoform specific siRNA oligonucleotides followed by flow cytometry. In addition, use of flow cytometry analysis of stable cell lines to determine the effects of overexpression of Nek11 isoforms on cell cycle progression.

6. To optimise Nek11 antibodies for detection of Nek11 protein in colorectal tumour tissue samples via immunohistochemistry.

CHAPTER 2 MATERIALS AND METHODS

2.1 Materials

2.1.1 Chemical suppliers

All chemicals were of analytical grade purity or higher and supplied by Sigma (Poole, UK), Roche (Lewis, UK), or as indicated below. All cell culture solutions were supplied by Gibco Invitrogen (Paisley, UK). Other reagents are stated in the text with their relevant supplier.

Reagent	Supplier
Isopropanol	Acros organics (Geel, Belgium)
Precision Plus all blue protein standards	Bio-Rad (Hemel Hempstead, UK)
G418 sulfate Hoechst 33258	Calbiochem (Nottingham, UK)
GeneRuler 1 kb DNA ladder	Fermentas (York, UK)
Boric acid Bovine serum albumin (fraction V) EDTA; EGTA; KCl; KH_2PO_4 ; MgCl_2 ; MnCl_2 ; NaCl; Na_2HPO_4 Ethanol Glacial acetic acid Glycerol Methanol Tween-20	Fisher Scientific (Loughborough, UK)
ProtoFLOWgel (30% w/v acrylamide)	Flowgen Bioscience (Nottingham, UK)
PMSF	Fluka (Gillingham, UK)
Super RX X-Ray film	Fuji photo film (Tokyo, Japan)
Deoxyribonucleotides (dATP, dCTP, dGTP, dTTP) Ethidium bromide Lipofectamine 2000 reagent Oligonucleotide primers RNase A Superscript III reverse transcriptase <i>Taq</i> DNA polymerase	Invitrogen/Gibco – Part of Life Sciences (Paisley, UK)

Hepes SDS	Melford (Suffolk, UK)
Bacto-agar Bacto-tryptone Yeast extract	Oxoid (Basingstoke, UK)
BCA protein assay reagent ECL Western blotting reagent	Pierce (Rockford, USA)
Skimmed milk powder (Marvel)	Premiere Beverages (Stafford, UK)
GelPilot LE Agarose QIAfilter plasmid maxiprep kit QIAfilter plasmid miniprep spin kit QIAquick PCR purification kit	Qiagen (Hilden, Germany)
Nitrocellulose transfer membrane	Schleicher and Schuell (Dassel, Germany)
His ₆ Nek11	Upstate (Millipore) (Dundee, UK)
3 MM chromatography paper	Whatman International (Maidstone, UK)

2.1.2 Vectors

Vector	Application	Supplier
pGEM-T Easy	Cloning	Promega (Southampton, UK)
pLEICS-21	Mammalian protein expression	PROTEX (University of Leicester, UK)

2.1.3 Antibodies

2.1.3.1 Primary antibodies

Primary antibodies for Western blotting were diluted in PBS supplemented with 0.1% v/v Tween-20 and 5% w/v non-fat milk powder unless otherwise stated.

Antibody (species)	Dilution ([ab])	Supplier
Anti- α tubulin (Mouse)	1:1000 (0.6 μ g/ml)	Sigma
Anti- α tubulin (Rabbit)	1:2000 (0.1 μ g/ml)	Abcam
Anti-Chk1 (Mouse)	1:1000 in 3% BSA w/v in TBST (0.2 μ g/ml)	Santa Cruz
Anti-CK18	IHC: 1:100	Novus Biologicals
Anti- γ -H2AX (pSer139) (Mouse)	1:1000 (0.5 μ g/ml)	Abcam
Anti- γ -H2AX (pSer139) (Rabbit)	1:1000	Cell Signaling Technology
Anti- γ -tubulin (Mouse)	1:500	Sigma
Anti-GAPDH (14C10) (Rabbit)	1:1500	Cell Signaling Technology
Anti-GFP (Rabbit)	WB: 1:2500 (0.2 μ g/ml) IF: 1:1000 (0.5 μ g/ml) IP: 1:500 (1 μ g/ml)	Abcam
Anti-Ki-67 (clone MIB-1) (Mouse)	IHC:1:1000	Dako
Anti-Ku70 (E-5) (Mouse)	1:1000 (0.2 μ g/ml)	Santa Cruz
Anti-Nek11 (Mouse)	WB: 1:2000 (0.25 μ g/ml) IHC: 1:100 (5 μ g/ml)	Origene
Anti-Nek11 (3216) (Rabbit)	1:1000 (0.5 μ g/ml)	N.K. Sahota and A.M. Fry
Anti-phospho Chk1 (Ser345) (Rabbit)	1:500 in 3% w/v BSA in TBST	Cell Signaling Technology

* Where known, final antibody concentrations are stated in brackets after the working dilution

2.1.3.2 Secondary antibodies

Antibody	Dilution ([ab])	Supplier
Goat anti-mouse Alexa 488	1:200 (10 µg/ml)	Molecular Probes – Part of Life technologies (Paisley, UK)
Goat anti-mouse Alexa 594	1:200 (10 µg/ml)	
Goat anti-rabbit Alexa 488	1:200 (10 µg/ml)	
Goat anti-rabbit Alexa 594	1:200 (10 µg/ml)	
Goat anti-mouse horseradish peroxidase conjugate	1:1000	Sigma (Poole, UK)
Goat anti-rabbit horseradish peroxidase conjugate	1:1000	

*Where known, final antibody concentrations are stated in brackets after the working dilution

2.1.4 Drugs

The following drugs were used to treat cells at the indicated final concentrations. All stocks were made by dissolving in ddH₂O unless otherwise stated below.

Drug	[Stock]	[Final]	Supplier
G418	100 mg/ml	1 mg/ml	Calbiochem (Darmstadt, Germany)
Irinotecan hydrochloride	5 mM in DMSO	5 µM	Sigma-Aldrich (Dorset, UK)
Leptomycin B (LMB)	37 µM in EtOH	20 nM	Calbiochem (Darmstadt, Germany)
MG132	20 mM	20 µM	Calbiochem (Darmstadt, Germany)
Oxaliplatin	2.5 mM	5 µM	Sigma-Aldrich (Dorset, UK)
UCN-01	2 mM in DMSO	250 nM	Sigma-Aldrich (Dorset, UK)

2.1.5 siRNAs

siRNA	Target sequence (5' to 3')	Supplier
siNek11 oligo 1	GAACAAGAAUCCUUCAUUAUU	Dharmacon (Lafayette, USA)
siNek11 oligo 2	GAAGGAGGCUGCUCAUUAUU	
siNek11 oligo 3	GAACCUBAAUGUGUAGAUUUU	
siNek11 oligo 5	GCCGAGAUCUGGACGAUAAUU	
siNek11L/D oligo 6	CTGCCTATGCTTGGAGTCATA	Qiagen (Hilden, Germany)
siNek11L/D oligo 7	TGAGATAAGCTTATAGATCAA	
siNek11S oligo 14	CTGGAATAGCCTGAGACTCTA	
siNek11S oligo 15	CTGGGTCTACAAGGAGCATGA	
Silencer GAPDH	Not available	Ambion - Part of Life technologies (Paisley, UK)
Luciferase GL2	AACGTACGCGGAATACTTCGA	Qiagen (Hilden, Germany)

2.1.6 qRT-PCR primers

Target	Product size (bp)	Forward primer sequence	Reverse primer sequence
Nek11L	275	AGAGGATGCCACATCTGACC	CATGGTGGTGATGGTCTTTG
Nek11S	141	AGAGGATGCCACATCTGACC	CATCTGAATGGTGGGGTAGG
Nek11C	108	ATGGACCTCCACGAACTTGA	TTTTTCATTTTTCCAGTATTCGTC
Nek11D	271	AGAGGATGCCACATCTGACC	TTCTGCATGGCTGATCTAGA
GAPDH	238	GAGTCAACGGATTTGGTCGT	TTGATTTTGGAGGGATCTCG
HPRT1	132	GACCAGTCAACAGGGGACAT	CCTGACCAAGGAAAGCAAAG

2.2 Molecular biology techniques

2.2.1 Cloning

To generate plasmid DNA containing full length Nek11S and Nek11D DNA, a basic cloning procedure was followed involving amplification of insert DNA by polymerase chain reaction (PCR) from cDNA generated from extracted RNA, purification of PCR products and ligation into the destination vector. This was then transformed into bacteria after which individual colonies were picked to verify that the plasmid contained the appropriate insert DNA. The specific details of each stage are described below.

2.2.1.1 Oligonucleotide design

Oligonucleotides for PCR were designed to be 18-24 nucleotides in length with a GC:AT ratio of ~50%, thus ensuring a practical annealing temperature of around 55-60°C. In this case, oligonucleotides were designed against the 5' and 3' ends of the coding sequences for Nek11S and Nek11D in order to generate full length sequences for cloning.

2.2.1.2 Polymerase chain reaction

To obtain insert DNA for cloning, PCR amplification was carried out using Platinum *Taq* DNA polymerase High Fidelity (Invitrogen). Required DNA was synthesised from cDNA that had been generated from 5 µg RNA extracted from U2OS cells as described in section 2.3.1 and 2.3.2. A standard reaction mixture was 25 µl in volume and typically contained 1x high fidelity PCR buffer, 0.2 mM dNTPs, 2 mM MgSO₄, 1 µl cDNA, 200 nM forward primer, 200 nM reverse primer, 1 U DNA polymerase and the appropriate volume of nuclease-free water to complete the reaction volume. The reaction was carried out by a DNA Engine DYAD thermal cycler and a basic PCR reaction consisted of one cycle of denaturation at 94°C for 2 minutes, followed by 30 cycles of denaturation at 94°C for 30 seconds, annealing at the appropriate temperature for the primer pair for 30 seconds, and extension at 68°C for 1 minute per kb of

PCR product, followed by one cycle of extension at 68°C for 10 minutes. PCR products were then analysed by agarose gel electrophoresis to assess yield.

2.2.1.3 Agarose gel electrophoresis

DNA was combined with loading dye (50% v/v Glycerol, 0.1 M EDTA, 0.3% w/v bromophenol blue) in a 5:1 ratio and resolved alongside an appropriate DNA ladder by electrophoresis on a 1-2% (w/v) agarose gel made by dissolving agarose in TBE (89 mM Tris, 89 mM Boric acid, 2 mM EDTA pH 8.0) supplemented with ethidium bromide (0.5 µg/ml). Electrophoresis was carried out at 80 V for 45 minutes after which resolved DNA was analysed by UV transillumination (302 nm) and images captured using a GeneGenius gel imaging system (Syngene).

2.2.1.4 Purification of PCR products

Upon verification that the PCR reaction had produced DNA product of predicted size (bp) and of sufficient yields, PCR products were purified for cloning using a QIAquick PCR purification kit (QIAGEN) according to the manufacturer's instructions. Purified DNA was eluted in 50 µl of sterile water and product yield assessed by agarose gel electrophoresis.

2.2.1.5 DNA ligation into pGEM-T Easy vector

Purified DNA was ligated into pGEM-T Easy vectors (Promega) according to the manufacturer's instructions. Briefly, a vector: insert ratio of 1:1 was employed in a standard reaction mix of 50 ng vector DNA, the appropriate amount of insert DNA calculated using the equation below and 3 U T4 DNA ligase diluted in rapid ligation buffer. Reactions were mixed and incubated for 1 hour at room temperature.

$$\text{ng of insert} = \frac{\text{ng of vector} \times \text{kb size of insert}}{\text{kb size of vector}} \times \text{insert: vector molar ratio}$$

2.2.1.6 Bacterial transformation

2 μ l of ligation reaction was added to competent DH5 α E. coli cells (containing the mutation *lacZ* Δ M15 to allow for β -galactosidase selection), which had been thawed on ice. The two were gently mixed by tapping the side of the tube and incubated on ice for 25 minutes before being heat shocked at 42°C for 45 seconds to induce plasmid DNA uptake, and then returned to ice for a further 2 minutes. 450 μ l of Luria Broth (LB) media (17 mM NaCl, 0.5% w/v yeast extract, 1% w/v tryptone, 10 mM Tris pH 7.5) was added to the cells and incubated for 1 hour at 37°C, 225 rpm. Following incubation, 200 μ l of the cell suspension was spread onto LB agar plates (LB plus 2% w/v agar) containing the appropriate antibiotic for selection (ampicillin at 100 μ g/ml or kanamycin at 50 μ g/ml). For cloning, plates were also supplemented with 0.5 mM IPTG and 80 μ g/ml X-Gal to verify transformation of recombinant DNA. Plates were incubated for 16 hours at 37°C, and then colonies picked for either insert screening by PCR or plasmid preparation.

2.2.1.7 Colony PCR

PCR screening of colony DNA was used to verify the presence of appropriate DNA insert using Taq DNA polymerase (Invitrogen). A standard reaction mixture was 25 μ l in volume and typically contained PCR amplification buffer, 1.5 mM MgCl₂, 0.2 mM dNTPs, 200 nM forward primer, 200 nM reverse primer, 1 U DNA polymerase and nuclease-free water to complete the reaction volume. White colonies containing recombinant DNA to be screened were picked using a pipette tip and streaked onto a gridded LB-agar plate where individual squares had been numbered for future reference; the plate was incubated at 37°C for 16 hours. The tip was then used to inoculate a PCR reaction mix of which the tube had been labelled with the corresponding number. PCR reaction cycles consisted of one cycle of denaturation at 94°C for 2 minutes, followed by 30 cycles of denaturation at 94°C for 1 minute 30 seconds, annealing at the appropriate temperature for the primer pair for 2 minutes, and extension at 68°C for 1 minute per kb of PCR product, followed by one cycle of extension at 68°C

for 10 minutes. Colonies which proved positive by PCR screen were then grown up for DNA isolation and further insert verification by DNA sequencing.

2.2.1.8 Isolation of plasmid DNA by miniprep purification

5 ml LB supplemented with the appropriate antibiotic was inoculated with an individual bacterial colony picked off a transformation plate. The mixture was incubated for 16 hours at 37°C, 225 rpm. Following incubation, cells were collected by centrifugation (2000 rpm, 10 minutes), supernatant discarded, and DNA isolated from the cell pellet using the QIAprep Spin Miniprep kit (QIAGEN) according to the manufacturer's instructions. DNA was eluted into 50 µl of sterile water and stored at -20°C.

2.2.1.9 DNA quantification

Plasmid concentration was determined by measuring the absorbance at 260 nm using a BioPhotometer Plus (Eppendorf).

2.2.1.10 DNA sequencing

Plasmid DNA along with appropriate sequencing primers were sent to the Protein Nucleic Acid Chemistry Laboratory (PNAACL) at the University of Leicester for automated sequencing. Data received from PNAACL was analysed using CLC sequence viewer 6 (CLCbio).

2.2.2 Generation of eGFP tagged Nek11 constructs

To generate N-terminal eGFP tagged constructs for expression in mammalian cells appropriate PCR primers and vector containing target DNA were submitted to Protein Expression laboratory (PROTEX) at the University of Leicester. Forward and reverse primers were designed with 5' vector homology regions followed by a 15-25 bp insert homology region to amplify the required region of

target DNA from its original vector for insertion into pLeics-21 (family D homology vector). Vectors were then sent for sequencing to verify insert sequence as in section 2.2.1.10.

2.2.3 Site-directed mutagenesis

2.2.3.1 Oligonucleotide design

Primers for site-directed mutagenesis were approximately 30-35 nucleotides in length. The forward and reverse primers contained the desired mutation in the middle of the sequence with 10-15 bases of correct sequence on both sides.

2.2.3.2 Site-directed mutagenesis reaction

To induce nucleotide changes in plasmid DNA, the Quickchange® II XL Site-Directed Mutagenesis Kit (Stratagene) was used according to the manufacturer's instructions. In brief, 10 ng of target plasmid was amplified by PCR with appropriate mutagenesis primers in a reaction mix containing 338 nM forward primer, 338 nM reverse primer, 0.2 mM dNTPs, 6% v/v QuickSolution, 1x reaction buffer, 2.5 U *PfuUltra* HF DNA polymerase and sterile water to a final volume of 50 µl. The PCR amplification cycle consisted of denaturation at 95°C for 1 minute, followed by 18 cycles of denaturation at 95°C for 50 seconds, annealing at 60°C for 50 seconds and elongation at 68°C for 1 minute/kb of plasmid length, and a final elongation step at 68°C for 7 minutes. Amplification was confirmed by agarose gel electrophoresis (section 2.2.1.3), following which 10 U *Dpn* I restriction enzyme was mixed with the amplification reaction and incubated at 37°C for 1 hour to digest the parental methylated and hemimethylated plasmid DNA, leaving plasmid containing the mutation only. The *Dpn* I treated DNA was then transformed into XL10-Gold Ultracompetent cells (Agilent technologies). 45 µl cells were thawed and incubated with 2 µl β-Mercaptoethanol for 10 minutes on ice with gentle swirling. 2 µl of DNA was then added and gently mixed before incubating on ice for a further 30 minutes. Cells were heat shocked at 42°C for 30 seconds and returned to ice for 2

minutes before 0.5 ml preheated S.O.C. medium (Invitrogen) was added. The mixture was incubated at 37°C for 1 hour, 225 rpm. Transformants containing plasmid DNA was selected for on appropriate selective media and DNA from individual colonies was isolated and mutation verified by DNA sequencing.

2.2.4 Isolation of plasmid DNA by maxiprep purification

For isolation of large quantities of ultrapure transfection grade plasmid DNA, DNA plasmid maxipreps were used. A single transformation colony was used to inoculate a 5 ml LB starter culture containing the appropriate antibiotic and incubated for 8 hours at 37°C, 225 rpm. 1 ml of this was then used to inoculate 100 ml LB containing antibiotic which was subsequently incubated at 37°C, 225 rpm for 16 hours. Cells were collected by centrifugation at 6000x g for 15 minutes at 4°C before plasmid DNA was isolated using a QIAfilter Plasmid Maxi kit (QIAGEN) according to the manufacturer's instructions. Isolated plasmid DNA was resuspended in 150 µl water and DNA concentration was determined as in section 2.2.1.9. 1 µg/µl plasmid stocks were made and stored at -20°C for use in transfections.

2.3 Real-time quantitative RT-PCR

2.3.1 RNA extraction

To prepare RNA for RT-PCR, culture media was removed from adherent cells in a 10 cm² cell culture dish, cells were washed with PBS before addition of 1 ml of Tri reagent (Sigma). The resulting cell lysate was then collected and passed through a pipette tip several times to form a homogenous lysate. RNA isolation was performed according to the manufacturer's instructions. Briefly, the homogenate was separated into aqueous and organic phases by addition of chloroform and centrifugation. RNA, partitioned to the aqueous phase, was then precipitated with isopropanol before washing with ethanol and solubilising in 50 µl RNase-free water. Total RNA concentration was calculated by measuring A₂₆₀ and purity by A₂₆₀/A₂₈₀ (≥1.7). Samples were stored at -80°C.

2.3.2 First strand cDNA synthesis

Isolated RNA was used for first strand cDNA synthesis with Superscript III reverse transcriptase (Invitrogen) according to the manufacturer's instructions. Briefly, 5 µg of RNA was used in a reaction containing 500 ng oligo(DT)₁₂₋₁₈, 0.5 mM dNTPs, 1x first strand buffer, 5 mM DTT, 40 U RNaseOUT, 200 U Superscript III reverse transcriptase. Secondary RNA structures were denatured by incubation at 65°C for 5 minutes after which the reaction mix was rapidly cooled on ice for 1 minute to prevent reannealing. First strand synthesis was then carried out by incubation at 50°C for 1 hour and the reaction was inactivated by incubation at 70°C for 15 minutes. 1 µl cDNA was then used in RT-PCR reactions with *Taq* DNA polymerase using reaction components and set-up as described in section 2.2.1.7. PCR products were analysed by agarose gel electrophoresis.

2.3.3 qRT-PCR

In order to quantitatively assess the expression of selected genes real-time quantitative reverse-transcription PCR was employed as described below.

2.3.3.1 Oligonucleotide design

Gene specific primers were designed using the selected targets cDNA sequence and Primer 3 software (freely available at: http://biotools.umassmed.edu/bioapps/primer3_www.cgi) (Rozen and Skaletsky, 1998). Forward and reverse primers were designed to be 20-25 nucleotides in length, contain a GC content of ~50% and produce a DNA product of 100-300 base pairs. Primer specificity was tested against the human genome and EST databases using the BLAT alignment tool (Kent, 2002). The forward and reverse oligonucleotide sequences, along with the expected product length are listed in section 2.1.6.

2.3.3.2 qRT-PCR amplification conditions

Real time qRT-PCR was performed on the LightCycler 480 (Roche) using the Maxima SYBR Green/ROX qPCR master mix (Fermentas) according to the manufacturer's instructions. Briefly, cDNA was diluted 1 in 5 and 1 µl of this was mixed with 300 nM forward primer, 300 nM reverse primer, and 1x Maxima SYBR Green master mix in a total reaction volume of 10 µl. Samples were pipetted into white 96-well LightCycler 480 multiwell plates (Roche) in triplicate and, after sealing with plastic film, centrifuged (1000 rpm, 4 minutes) to collect samples to the bottom of wells. Reactions consisted of 1 cycle of initial denaturation at 95°C for 10 minutes, followed by 40 cycles of denaturation at 95°C for 15 seconds, annealing at 60°C for 30 seconds, and extension at 72°C for 30 seconds. Data acquisition was performed after each extension step. Finally, primer specificity was further validated by performing a melt curve analysis at the end of the reaction to ensure amplification of a single product. For this, a dissociation curve was generated by gradually increasing the temperature 1°C at a time (from 55°C to 95°C) and by measuring the fluorescence at the end of each temperature increase.

2.3.3.3 Data analysis

qRT-PCR data and melt curve analysis was carried out using LightCycler 480 software, version 1.5 (Roche). The average threshold cycle (Ct) value was determined for each sample and normalised against that of a reference gene. Finally, the change in gene expression between the samples and a calibrator sample was calculated by normalising against the calibrator, in this case a normal colorectal cancer cell line. The change in gene expression was calculated using the following equation:

$$\text{Change in gene expression} = 2^{-\Delta\Delta Ct} = \text{Relative quantity (RQ)}$$

2.4 Cell culture techniques

2.4.1 Human cell line maintenance

U2OS, HCT116, HT29, SW480, SW620 and HCEC cells were cultured in Dulbecco's Modified Eagle's Medium (DMEM) with GlutaMAXTM-I (Invitrogen). U2OS cells stably expressing GFP-Nek11 constructs and GFP only were cultured in DMEM with GlutaMAXTM-I supplemented with 1 mg/ml G418 Sulfate (Calbiochem). All cells were supplemented with 10% v/v heat inactivated foetal bovine serum (FBS) (Invitrogen) and penicillin-streptomycin (100 U/ml and 100 µg/ml, respectively) (Invitrogen). Cell lines were maintained at 37°C in a humidified 5% CO₂ atmosphere and passaged before reaching confluency. To passage, growth media was aspirated and adherent cells were washed with phosphate buffered saline (PBS) (137 mM NaCl, 2.7 mM KCl, 8.1 mM Na₂HPO₄, 1.5 mM KH₂PO₄, pH 7.4). Cells were detached by either incubation in PBS containing 0.5 mM EDTA or 0.05% Trypsin/EDTA (Invitrogen). Cells were then seeded into appropriate dishes containing fresh, pre-warmed media at the required density. In the case of HCEC cells, plasticware required pre-coating before cells were seeded. Briefly, sterile filtered pre-coating media (0.01% w/v BSA, 2.5 µg/ml fibronectin, 1 µg/ml collagen) was incubated on plates for 30 minutes at 37°C before this was removed and cells were seeded at appropriate density.

2.4.2 Cell line storage and recovery

For long term storage, cell lines were cryopreserved in liquid nitrogen. Briefly, cells were resuspended as described in section 2.4.1 and collected by centrifugation (1100 rpm, 5 minutes). The supernatant was aspirated and the cell pellet resuspended in FBS supplemented with 10% v/v DMSO and transferred to cryotubes (TPP Helena Biosciences). The cryotubes were then placed in an isopropanol filled cryo 1°C freezing container (Nalgene) and stored at -80°C for at least 16 hours before tubes were transferred to liquid nitrogen.

To recover cells, a cryotube was removed from liquid nitrogen and rapidly thawed in a 37°C waterbath. Cells were then washed with pre-warmed media,

pelleted at 1100 rpm for 5 minutes, and resuspended in fresh growth media and transferred to a culture dish.

2.4.3 Cell counting

Cells seeded for experimental set-up were counted using the Sceptor™ 2.0 Cell Counter (Merck Millipore). Briefly, cells were resuspended to generate a single-cell suspension and 50 µl of this was drawn up through the sensor. The cell population required was gated and the concentration of cells/ml obtained. Appropriate numbers of cells were seeded into culture vessels.

2.4.4 Transient transfections

Transient transfection of cultured mammalian cells to induce expression of appropriate recombinant proteins was achieved using Lipofectamine 2000 (Invitrogen) or FuGENE HD (Roche), as described below.

2.4.4.1 Lipofectamine transfection

Cells were seeded in appropriate culture vessels 24 hrs prior to transfection to reach 70-80% confluency on the day of transfection. Plasmid DNA and lipofectamine were mixed together in optimal ratios for each construct (typically 1 µg: 4 µl) in Opti-MEM™ reduced serum medium (Invitrogen), according to the manufacturer's instructions. Transfection mix was then added drop-wise to cells on which the growth media had been replaced with Opti-MEM media. The dishes were returned to the incubator for 4 hours after which the media was replaced with pre-warmed growth media and incubated for a further 24 hours before being processed as required.

2.4.4.2 FuGENE HD transfection

Cells were either seeded in culture vessels 24 hours prior to transfection to reach at least 60% confluency on the day of transfection or freshly seeded in complete growth media just before addition of transfection reaction. Briefly, plasmid DNA and FuGENE HD were mixed at a ratio of 1 µg: 3 µl in Opti-MEM, according to the manufacturer's instructions. The mixture was then added drop-wise to cells and then incubated for at least 24 hours to allow for protein expression.

2.4.5 Generation of U2OS:GFP-Nek11 and U2OS:GFP stable cell lines

2.4.5.1 G418 kill curve

To determine the minimal concentration of G418 required to kill cells, complete growth media supplemented with different concentrations of G418 (0.2- 1.2 mg/ml) was added to cells at 70% confluency in 6-well plates and incubated (37°C, 5% CO₂). Media in each well was replaced with fresh media containing the appropriate amount of G418 every 2 days. The number of days taken for cells to die was recorded for each concentration of G418.

2.4.5.2 Stable cell line generation

Stable cell lines were generated by transfection of U2OS cells seeded in 10 cm plates with DNA vectors containing neomycin resistance as described in 2.4.4.2. After 24 hours, growth media was removed from transfected cells and replaced with pre-warmed growth media supplemented with 1 mg/ml G418. Cells were allowed to proliferate in selection media until foci containing 50-100 cells could be detected (3-4 weeks). All cells were then pooled together to generate a mixed cell population and passaged as normal. Expression of the plasmid was determined by SDS-PAGE and Western blotting of whole cell lysates and indirect immunofluorescence microscopy of fixed cells.

2.4.6 RNA interference

7×10^4 or 1.4×10^5 cells were seeded in either 6-well plates or 6 cm dishes, respectively, in growth media containing no antibiotics the day before transfection. 100 nM siRNA oligonucleotides and Oligofectamine™ transfection reagent (Invitrogen) were mixed in Opti-MEM according to manufacturer's instructions. The mixture was added drop-wise to the cells whose media had been replaced with Opti-MEM. Cells were incubated for 4 hours (37°C, 5% CO₂), after which antibiotic free media containing 30% v/v FBS was added to cells and incubated for a 72 hours before being processed as required.

2.4.7 Irradiation treatment

Cells were irradiated with X-rays delivered at 1 Gy/min until final dosage required had been achieved (250 kV constant potential, Pantak industrial X-ray machine, Connecticut, USA).

2.4.8 Clonogenic assay

Cells were irradiated as in section 2.4.7 and incubated for 16 hours (37°C, 5% CO₂). Growth media was aspirated from adherent cells and cells were resuspended in PBS-EDTA and counted, as previously described (sections 2.4.1 and 2.4.3). To accurately seed such low numbers of cells, serial dilutions were performed so that 200-1000 µl of cell suspension was used in order to obtain the required number of cells per well of a 6-well plate. The final volume of media was made up to 3ml and each sample was seeded in triplicate. Cells were incubated until visible colonies could be seen under the microscope (12-14 days). Growth media was removed and cells fixed in 100% methanol for 2 minutes, washed with dH₂O and left to air dry. Colonies were stained with 0.5% Crystal violet solution (Sigma) for 1 minute, washed with dH₂O, dried and then counted. The mean plating efficiency (PE) of cells from each treatment was calculated using the following equation:

$$PE = \frac{\text{Average number of colonies counted}}{\text{Number of cells plated}} \times 100$$

The surviving fraction (SF) for each treatment was then calculated using the following equation:

$$\text{SF} = \frac{\text{PE of treated sample}}{\text{PE of control}} \times 100$$

2.5 Flow cytometry

2.5.1 Cell cycle analysis

To determine cell cycle distribution, cell populations for analysis were harvested and collected by centrifugation (1100 rpm, 5 minutes), washed in PBS and resuspended in 200 µl PBS before being fixed in 2 ml 70% ice-cold ethanol whilst gently vortexing to disperse cell clumps. Fixed cells were then stored at -20°C for at least 30 minutes before being stained with propidium iodide (PI, Sigma). Briefly, cells were collected by centrifugation (3000 rpm, 5 minutes, 4°C) and washed twice with PBS to remove all traces of ethanol, before being resuspended in staining solution (50 µg/ml PI, 100 µg/ml RNase A in PBS) and transferred to FACS tubes. Cells were stained at 4°C overnight, in the dark. DNA content of 10,000 events was recorded for each sample using a BD FACSCanto™ II flow cytometer and analysed using FACSDiva™ 6.0 software (Becton Dickinson).

2.5.2 Annexin V assay

To determine the percentage of cells in apoptosis, 2×10^5 cells/ml in a final volume of 100 µl was mixed with 100 µl of Annexin V and Dead cell reagent (Merck Millipore) and incubated for 20 minutes at room temperature in the dark. Cells were analysed using a Muse Cell Analyzer and Muse 1.3 Analysis software (Merck Millipore).

2.6 Protein analysis

2.6.1 Preparation of cell lysates

Whole cell lysates were prepared for separation by SDS-PAGE or for immunoprecipitation in either RIPA lysis buffer (50 mM Tris-HCl pH 8, 150 mM NaCl, 1% v/v Nonidet P-40, 0.1% w/v SDS, 0.5% w/v sodium deoxycholate, 5 mM NaF, 5 mM β -glycerophosphate, 30 μ g/ml RNase, 30 μ g/ml DNase I, 1x Protease Inhibitor cocktail (PIC), 1 mM PMSF) or NEB lysis buffer (50 mM HEPES-KOH pH 7.4, 5 mM $MnCl_2$, 10 mM $MgCl_2$, 5 mM EGTA, 2 mM EDTA, 100 mM NaCl, 5 mM KCl, 0.1% v/v Nonidet P-40, 5 mM NaF, 5 mM β -glycerophosphate, 30 μ g/ml RNase, 30 μ g/ml DNase I, 1x PIC, 1 mM PMSF). Briefly, cells were washed with PBS, harvested, and collected by centrifugation (1,200 rpm, 5 minutes). The cell pellet was then resuspended in an appropriate volume of ice-cold lysis buffer and cell lysis was carried out on ice for 30 minutes after which lysates were passed 10 times through a 27G needle and then centrifuged (13,000 rpm, 10 minutes, 4°C) to remove insoluble material. Supernatants were either used directly as required or snap frozen and stored at -80°C.

2.6.2 BCA protein assay

Protein concentration of cell lysates was determined using the BCA protein assay. BCA working reagent was prepared according to the manufacturer's instructions and 1 ml added to 5 μ l of cell lysate diluted to a final volume of 50 μ l in dH_2O . Samples were incubated for 30 minutes at 37°C, allowed to cool to room temperature and the absorbance at 550 nm measured. A serial dilution of BSA standards (50 μ l) was prepared and assayed alongside the protein samples to allow construction of a standard curve from which the protein concentration of the samples could be read.

2.6.3 SDS polyacrylamide gels

Protein samples were resolved on 8, 10 or 12 % polyacrylamide gels according to the size of the protein to be studied. Gels were cast and resolved using the Mini-PROTEAN 3 polyacrylamide gel electrophoresis (PAGE) system (Bio-Rad). Resolving gel (26.7 – 40% ProtoFlowgel (30% w/v acrylamide), 375 mM Tris-HCl pH 8.8, 0.1% w/v SDS, 0.13% w/v APS, 0.08% v/v TEMED) was overlaid with stacking gel (13% ProtoFlowgel (30% w/v acrylamide), 126 mM Tris-HCl pH 6.8, 0.1% w/v SDS, 0.15% w/v APS, 0.1% v/v TEMED). Samples to be resolved were mixed with an appropriate volume of 3x Laemmli buffer (62.5 mM Tris-HCl pH 6.8, 10% v/v glycerol, 2% w/v SDS, 5% v/v β -mercaptoethanol, 0.01% w/v bromophenol blue) and denatured at 95°C for 5 minutes. Precision Plus all blue protein standards (Biorad) were loaded alongside all samples as an indication of protein size. Electrophoresis was carried out at 180 V for ~1 hour using an SDS-running buffer (0.1% w/v SDS, 25 mM Tris, 192 mM Glycine).

2.6.4 Staining of protein gels

2.6.4.1 Standard Coomassie Blue staining

To directly visualise proteins after electrophoretic separation, resolving gels were submerged in Coomassie Blue solution (0.25% w/v Brilliant Blue R, 40% v/v IMS, 10% acetic acid) and then gently agitated for at least 30 minutes at room temperature. The Coomassie Blue solution was then replaced with destain solution (7.5% v/v acetic acid, 25% IMS) and repeated washes were carried out until protein bands could be distinguished and the background was clear. Gels were dried onto Whatman 3 MM chromatography paper under a vacuum at 80°C for 2 hours. Radiolabelled proteins were visualised by autoradiography where necessary.

2.6.4.2 Brilliant blue colloidal stain for mass spectrometry (MS)

For more sensitive protein detection SDS-PAGE gels were placed in fixing solution (7% v/v glacial acetic acid, 40% v/v methanol) for 1 hour. Immediately before staining 4 parts of 1X Brilliant Blue G-Colloidal coomassie (Sigma) was combined with 1 part methanol and vortexed. Gels were placed in staining solution and incubated for 2 hours with gentle agitation before destaining by placing in destain solution 1 (10% v/v acetic acid, 25% v/v methanol) for 1 minute followed by destain solution 2 (25% methanol) until bands could be visualised clearly. Gels were submitted to PNAACL for mass spectrometry analysis.

2.6.5 Western blotting

Resolved proteins were transferred to nitrocellulose membrane for immunodetection using semi-dry electrophoretic blotting. Briefly, the resolving gel, 0.45 µm pore size nitrocellulose membrane (Schleicher and Schuell) and 6 pieces of Whatman 3 MM chromatography paper were soaked in blotting buffer (25 mM Tris, 192 mM glycine, 10 % v/v methanol) before the gel was placed on the membrane and sandwiched between 3 pieces of blotting paper on either side. Transfer was carried out in a TE 77 semi-dry transfer unit (Amersham) for 1 hour at 1 mA/cm² membrane. Successful transfer was visualised by ponceau red stain solution (0.1% w/v Ponceau S, 5% v/v acetic acid) and the position of lanes marked in pencil. Blots were then blocked in 5% w/v non-fat milk powder in 0.1% v/v Tween-20 in PBS for 30 minutes with agitation to block non-specific antibody binding. The membrane was then incubated with primary antibody at the appropriate dilution in 5% non-fat milk powder/PBST for 1 hour at room temperature or overnight at 4°C depending on the antibody used. Membranes were then washed 3 times in PBST to remove unbound primary antibody, before being incubated with the horseradish peroxidase-conjugated secondary antibody in 5% non-fat milk powder/PBST for a further 1 hour at room temperature. Membranes were washed a further 3 times in PBST to remove unbound secondary antibody and then developed in enhanced chemiluminescence (ECL) Western blotting detection solution (Pierce)

according to the manufacturer's instructions, and the proteins visualised by autoradiography on X-ray film developed using a compact X4 X-ray film processor (Xograph imaging system).

2.6.6 Immunoprecipitation

Immunoprecipitation experiments were carried out on whole cell lysates (see section 2.6.1) using the rabbit GFP polyclonal antibody bound to Protein A-Agarose beads (Sigma). Briefly, 50 μ l of protein A beads were washed 3 times with PBS and resuspended in 50 μ l NEB buffer. Cell lysate was diluted to a final volume of 500 μ l and incubated with 20 μ l washed bead slurry for 30 minutes rotating at 4°C to pre-clear the lysate of any proteins that non-specifically bind to beads. Supernatant was transferred to fresh tubes and incubated with GFP antibody at the appropriate dilution on ice for 1 hour before adding 30 μ l beads and incubating for 3 hours or overnight at 4°C with rotating agitation. Beads were washed 3 times with NEB buffer and either boiled in Laemmli buffer for SDS-PAGE analysis or used in *in vitro* kinase assays.

2.6.7 Indirect immunofluorescence microscopy

Cells grown on acid-etched coverslips were rinsed once in 1x PBS and fixed with ice-cold 100% methanol and incubated for a minimum of 20 minutes at -20°C. Cells were rehydrated by three 5 minute washes in PBS. Non-specific antibody binding was blocked by incubation for 10 minutes in PBS supplemented with 1% w/v BSA. Blocking solution was then replaced with primary antibody diluted to a suitable concentration in 3% w/v BSA in PBS and incubated on coverslips for 1 hour at room temperature. Unbound antibody was removed by 3 washes with PBS for 5 minutes each before incubation with appropriate secondary antibodies diluted in PBS supplemented with 3% w/v BSA and 0.8 μ g/ml Hoechst 33258 in the dark for 1 hour at room temperature. Again, coverslips were washed 3 times with PBS for 5 minutes each to remove unbound antibody and then inverted onto a drop of mounting solution (80% v/v glycerol, 3% w/v n-propyl gallate in PBS) on glass microscope slides and sealed

with clear nail varnish. Fluorescence microscopy was performed using a Nikon TE300 inverted microscope using a Plan Apo 60x or 100x DIC oil immersion objective (NA 1.4). Fluorescence images were obtained using an ORCA-R² camera (Hamamatsu) using Velocity software, version 6.0.1 (PerkinElmer), and images were processed using Adobe Photoshop 7. Alternatively, where high resolution images were needed, microscopy was performed on a Leica TCS SP5 laser scanning confocal microscope equipped with a Leica DMI 6000B inverted microscope using a Plan Apo 63x oil objective (NA 1.4). Images were captured and processed using Leica LAS AF software.

2.7 Immunohistochemistry

2.7.1 Generation of cytoblocks from cell suspensions

U2OS:GFP-Nek11L and U2OS parental cells were formalin-fixed and paraffin-embedded to generate cytoblocks to be used in optimisation of immunohistochemistry technique. For this purpose, cells were grown to confluency in a 150 cm² flask, resuspended and collected by centrifugation (1000 rpm, 5 minutes). Cytoblocks were then produced by the Histology facility (Core Biotechnology Services (CBS), University of Leicester). Briefly, cells were fixed in 10% formal saline for 30 minutes at room temperature before the cytoblock was made using the Shandon Cytoblock Cell Block Preparation System (Thermoscientific) according to the manufacturer's instructions. The resulting cell buttons were embedded in paraffin wax and stored at room temperature.

2.7.2 Immunohistochemical analysis

Formalin-fixed paraffin-embedded cytoblocks or tissue blocks were sectioned and mounted on Vectabond slides by the Histology facility (CBS). Immunohistochemistry was carried out using the NovoLink Polymer Detection System (Leica microsystems) according to the manufacturer's instructions. Briefly, wax was melted by heating slides at 65°C for 10 minutes, sections were then deparaffinised by two incubations in xylene for 3 minutes each, followed by rehydration through graded alcohols (99%, 99%, 95% v/v IMS) for 1 minute each, before finally washing in water for 5 minutes. Antigen retrieval was performed by microwaving slides (750 W, 15 minutes; Tecnolec Superwave) in 10 mM sodium citrate buffer (pH 6) and left to cool for 30 minutes. Slides were washed once in dH₂O and incubated with peroxidase block for 5 minutes in a humidified chamber to neutralise endogenous peroxidase, slides were then washed twice in TBS for 3 minutes each before protein block was added for a further 5 minutes and slides washed again twice in TBS for 3 minutes each. Primary antibody was diluted in TBS at the appropriate concentration and incubated on tissue sections for 18-20 hours at 4°C. Slides were washed twice in TBS (5 minutes each) to remove unbound antibody and then incubated with post primary block for 30 minutes, before washing twice with TBS and incubating with Novolink polymer for a further 30 minutes and washing again with TBS. Freshly prepared DAB working solution (Dab Chromogen and NovoLink DAB substrate buffer at 1:20, respectively) was incubated on slides for 5 minutes and then rinsed in water. Samples were counterstained with Mayer's Haematoxylin for 30 seconds and washed for 5 minutes in running water before being dehydrated in graded alcohols, incubated in xylene for 10 minutes and mounted onto coverslips using Dpx mounting medium (Sigma).

2.7.3 Ethical approval

Ethics entitled 'Cell signalling in gastrointestinal tumours' (REC 7176) was obtained from NRES committee Leicestershire, Rutland and Northamptonshire, in May 2004. No clinical information was available for patient tissue samples.

2.8 Statistical analysis

Results are presented as the mean of three independent experiments, unless otherwise stated. Error bars represent standard deviation of the mean (S.D., $n=3$). p values were calculated using a one-tailed unpaired Student's t -test assuming unequal variance.

CHAPTER 3 **NEK11 IS REQUIRED FOR G2/M CHECKPOINT ACTIVATION IN COLORECTAL CANCER CELLS**

3.1 Introduction

Of the mammalian NIMA-related kinase (NEK) family, so far, Nek1, Nek4, Nek8, Nek10 and Nek11 have been implicated in DNA damage response pathways (Noguchi *et al.*, 2002; Polci *et al.*, 2004; Nguyen *et al.*, 2012; Moniz & Stambolic, 2011; Melixetian *et al.*, 2009). Whilst Nek11 remains poorly characterised there is growing evidence that it is a key player of the G2/M DNA damage checkpoint. The first study into Nek11 function by Noguchi *et al.* (2002) found that Nek11 activity is increased by around 2-fold in response to DNA replication inhibitors such as aphidicolin, thymidine and hydroxyurea, and in response to the DNA damaging agents, etoposide, adriamycin, camptothecin and cisplatin. Interestingly, the time taken for Nek11 to be activated after the various types of treatment varies. The topoisomerase inhibitors, etoposide, adriamycin and camptothecin, which introduce DNA strand breaks activate Nek11 as early as 30 minutes after treatment, whereas cisplatin, which induces formation of DNA adducts, activates Nek11 more gradually. This suggests that multiple DDR pathways can activate Nek11 (Noguchi *et al.*, 2002). Furthermore, Nek11 activation is suppressed upon treatment with caffeine, an inhibitor of the ATM and ATR kinases, suggesting a role downstream of these (Noguchi *et al.*, 2002).

In 2009, a screen for novel components of the G2/M checkpoint was published. U2OS cells were transfected with a shRNA library before being irradiated and stained for the mitotic marker histone H3 pS10. shRNA inserts were isolated from those cells that had lost the DNA damage checkpoint and entered mitosis in the presence of DNA damage. This led to the identification of Nek11 as an important G2/M checkpoint regulator (Melixetian *et al.*, 2009). In order for a cell to progress into mitosis activation of the Cdk1/cyclin B complex is required. This occurs through removal of inhibitory phosphate groups on Cdk1 by Cdc25A. However, in response to DNA damage, Cdc25A is targeted for proteasomal

degradation. It has long been established that ATM and ATR activate Chk1 in response to DNA damage which in turn phosphorylates Cdc25A at S76, priming it for further phosphorylation by another kinase, whose identity remained unknown. Melixetian *et al.* (2009) identified that Nek11 contains a conserved consensus Chk1 phosphorylation site, S273, which is phosphorylated in response to DNA damage leading to Nek11 activation. In addition, depletion of Nek11 in the presence of DNA damage resulted in the stabilisation of Cdc25A. Furthermore, *in vitro* kinase assays revealed that Nek11 was able to phosphorylate Cdc25A on S82 and S88 residues, resulting in the binding of the ubiquitin ligase, β -TrCP and the subsequent degradation of Cdc25A and cell cycle arrest. This led to the proposal that Nek11 acts downstream of Chk1 and upstream of Cdc25A to control G2/M checkpoint activation in response to damage by IR. However, the medium for Cdc25A degradation remains controversial. Another study reported that in HeLa cells exposed to IR it was casein kinase 1 α (CK1 α) that phosphorylates Cdc25A and targets it for degradation (Honaker & Piwnica-Worms, 2010). Therefore, clearly, further studies are required to determine whether Nek11 is essential for the G2/M DNA damage checkpoint.

In this chapter, using RNAi-mediated depletion, we have investigated the role of Nek11 at the G2/M DNA damage checkpoint in colorectal cancer cells exposed to chemotherapeutically relevant agents. We chose to perform the studies in colorectal cancer cells as expression of Nek11 was reported to be increased in colorectal adenomas and carcinomas as compared to normal tissue (Sorensen *et al.*, 2010).

3.2 Results

3.2.1 Optimisation of RNAi-mediated depletion of Nek11

To assess the effect of Nek11 depletion on the DNA damage response of colorectal cancer cells, a set of four individual siRNA oligonucleotides specific to the coding region were obtained from Dharmacon. To initially test the efficiency of each of these oligos, U2OS cells were transfected with the individual oligonucleotides (siNek11-1, siNek11-2, siNek11-3, and siNek11-5) or with GAPDH oligonucleotides, as a control. After 48 hours, cells were transiently transfected with GFP-Nek11L and after a further 24 hours, lysates were prepared and analysed by Western blot (Figure 3.1). GFP-Nek11L protein was expressed in both mock and siGAPDH transfected cells. In comparison, all samples where Nek11 siRNA oligos were co-transfected, GFP-Nek11L expression was much reduced. In addition, a more efficient knockdown was observed with siNek11-1, siNek11-2 and siNek11-5 duplexes (Figure 3.1). Upon repeating this experiment, siNek11-1 and siNek11-2 showed the most consistently robust depletion of Nek11. Therefore, we used these oligonucleotides to next confirm depletion of endogenous Nek11 by qRT-PCR and Western blot analysis.

Using a polyclonal antibody (3216) generated in-house to detect Nek11 protein (Sahota, 2010), we identified two bands that were present in siGL2 (luciferase) and siGAPDH transfected cells that were significantly reduced in cells transfected with siNek11-1 and 2 (Figure 3.2A, indicated by arrows). The upper band corresponds to the predicted molecular weights of the Nek11L or Nek11D isoform, whilst the lower band matches the predicted molecular weight of the Nek11S or Nek11C isoforms. Next, using qRT-PCR analysis with primers capable of detecting all isoforms, we found that these oligonucleotides are able to deplete the mRNA of all Nek11 isoforms (Figure 3.2B). Moreover, consistent with Figure 3.2A, siNek11-2 was more efficient at depleting Nek11 than siNek11-1.

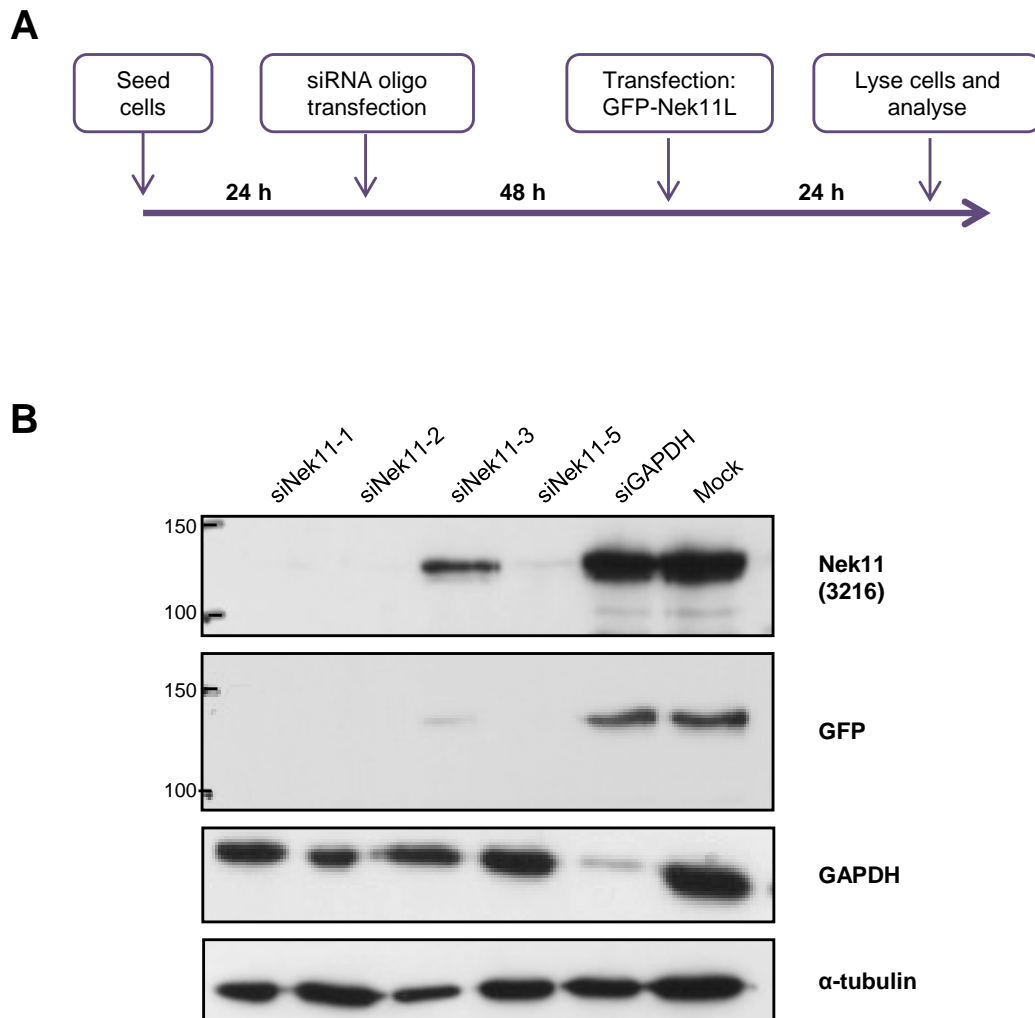


Figure 3.1 siRNA-mediated depletion of recombinant GFP-Nek11L

A. Schematic represents the methodology employed for GFP-Nek11L depletion. Time in hours (h) indicate time between individual steps. **B.** U2OS cells were transfected with siRNA oligonucleotides to deplete Nek11 (siNek11-1, 2, 3 or 5) or GAPDH, as indicated. After 48 hours, cells were transfected with GFP-Nek11L, before being lysed after a further 24 hours. Lysates were analysed by SDS-PAGE and Western blotting with the antibodies stated. Molecular weights are indicated (kDa).

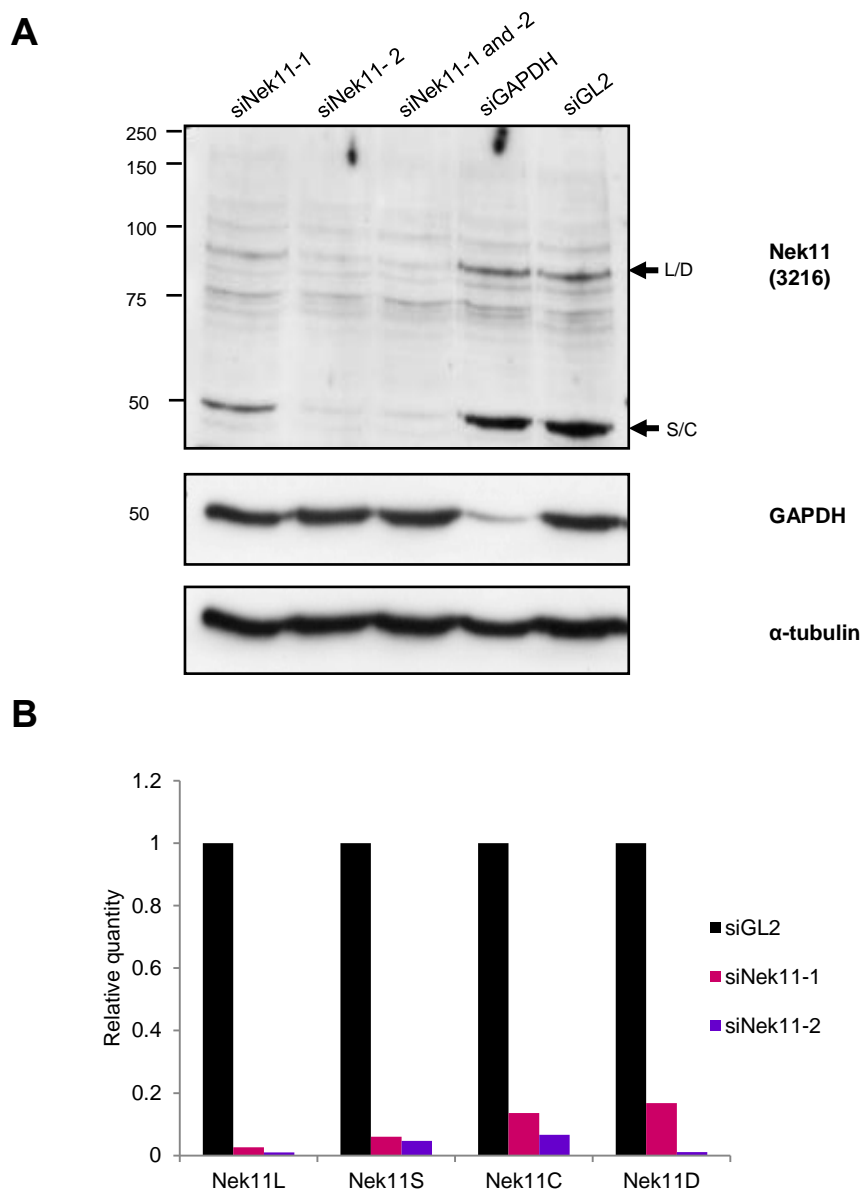


Figure 3.2 siRNA mediated depletion of endogenous Nek11

A. U2OS cells were transfected with siRNAs indicated, lysed 72 hours post-transfection and analysed by Western blotting with antibodies indicated. Molecular weights are shown (kDa), as are the positions of the Nek11L and D (L/D) isoforms and Nek11S and C (S/C) isoforms. **B.** HCT116 WT cells were transfected with siRNAs indicated, RNA was extracted 72 hours post-transfection and qPCR analysis carried out using isoform specific primers. The amount of mRNA detected is shown for each isoform relative to the amount detected following depletion with the luciferase control siGL2.

3.2.2 Nek11 depletion has no effect on cell cycle progression in HCT116 cells

Compared to normal colorectal tissue, Nek11 has been reported to be highly expressed in colon adenomas and carcinomas (Sorensen *et al.*, 2010). We therefore wanted to investigate the role of Nek11 in colorectal cancer cells. In addition, we wanted to examine whether p53 status affected the sensitivity of these cells to Nek11 depletion. The main cell line used in this study was HCT116 cells, derived from a colorectal carcinoma and an isogenic HCT116 p53-null cell line. These cell lines were kindly provided by Prof. B. Vogelstein (Johns Hopkins University, USA).

To first examine the effect of Nek11 depletion on normal cell cycle progression, Nek11 siRNA oligonucleotides were transfected into HCT116 cells along with siGL2 control oligos and cell cycle profiles analysed after 72 hours by flow cytometry (Figure 3.3). Results showed that depletion of Nek11 had no significant effect on normal cell cycle progression since the profiles and percentage of cells in G1, S and G2/M were comparable to the siGL2 control.

3.2.3 G2/M checkpoint activation in HCT116 cells is Chk1 dependent

Due to conflicting data on the role of Nek11 at the G2/M checkpoint, we first wanted to validate its role in response to IR, and examine whether it is required for G2/M checkpoint arrest in colorectal cancer cells. Firstly, to confirm that DNA damage induced by ionising radiation (IR) leads to G2/M arrest in HCT116 cells, cells were irradiated with increasing doses of IR before fixation after 16 hours. In response to 10 Gy, approximately 60% of HCT116 WT cells arrested at G2/M, in comparison to 21.5% in untreated cells (Figure 3.4). This arrest was dose-dependent as increased doses led to more cells arresting at G2/M. p53-null cells exhibit an increased percentage of cells arresting at G2/M, with 80.7% at G2/M in response to 10 Gy IR. This is consistent with the loss of p53 resulting in a lack of an intact G1/S checkpoint and a greater reliance of the G2/M checkpoint (Figure 3.5A and B).

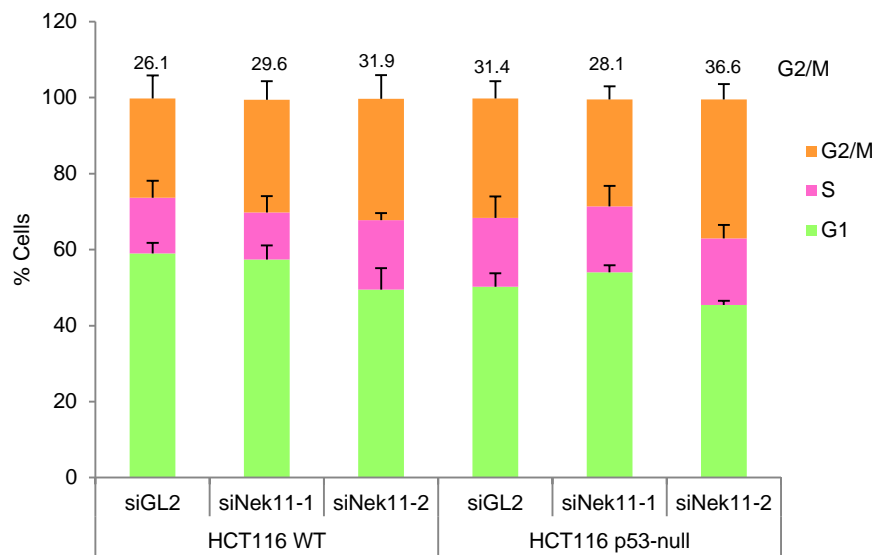


Figure 3.3 Depletion of Nek11 does not affect normal cell cycle progression

HCT116 WT and p53-null cells were transfected with siRNAs against Nek11 (siNek11-1 or siNek11-2) or luciferase (siGL2) and cell cycle profiles analysed by flow cytometry after 72 hours. The percentage of cells at G2/M is indicated above each sample and the data represents means (\pm S.D.) of 3 separate experiments.

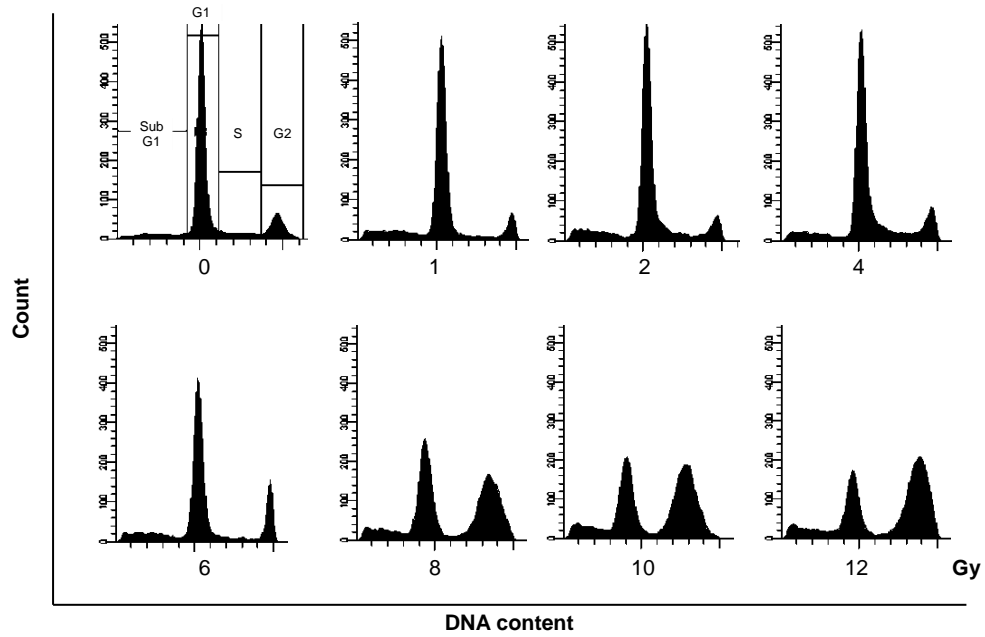
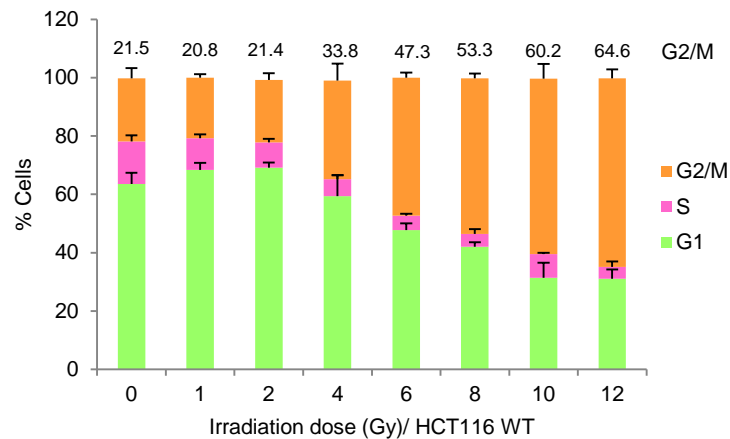
A**B**

Figure 3.4 Optimisation of G2/M checkpoint activation in HCT116 WT cells

A. HCT116 WT cells were irradiated with the doses indicated and cell cycle profiles analysed by flow cytometry after 16 hours. The first profile represents how gates were set to measure percentage of cells at each cell cycle stage. **B.** Histogram represents the percentage of cycling cells at each stage of the cell cycle. The percentage of G2/M cells are indicated above each sample and the data represents means (\pm S.D.) of 3 separate experiments.

Next, we confirmed that this G2/M checkpoint arrest in response to IR is Chk1-dependent by treating cells with UCN-01, an inhibitor of Chk1, a kinase that is well established to play a key role in the G2/M checkpoint. Combination of 10 Gy and UCN-01 treatment led to a marked abrogation of the checkpoint, with a reduction in G2/M arrest from 60% to 18.7% in WT cells and from 80.7 to 29.4% in p53-null cells when compared to treatment with IR alone. This indicates that induction of the G2/M arrest by IR in HCT116 cells occurs in a Chk1-dependent manner (Figure 3.5).

3.2.4 Nek11 is required for IR-induced DNA damage response in HCT116 WT and p53 null

Having set up an assay to successfully detect abrogation of the G2/M checkpoint, we next investigated the effect of Nek11 depletion in HCT116 cells in response to IR. Cells were transfected with GL2 or Nek11 siRNA oligonucleotides for 72 hours and 16 hours before collection were either irradiated or left untreated. In response to 10 Gy, the percentage of HCT116 WT cells arresting at G2/M dropped from 61.8% in siGL2 treated cells, to 44.9% and 29.7%, for cells transfected with siNek11-1 and siNek11-2, respectively (Figure 3.6A and B). A stronger effect was observed with siNek11-2 and this is consistent with previous findings that siNek11-2 is more efficient at depleting Nek11 (Figure 3.2). We next looked at the effect of Nek11 depletion in cells lacking p53. Like the WT cells, depletion of Nek11 in HCT116 p53-null cells in combination with IR led to a significant reduction in the percentage of cells exhibiting a G2/M arrest (Figure 3.6C and D), indicating that Nek11 is required for G2/M checkpoint activation independent of p53.

3.2.5 Nek11 depletion enhances cell death in HCT116 cells

Due to the observation of dead cells by microscopy before sample collection and detection of sub-G1 peaks in Nek11 depleted cells by flow cytometry (Figure 3.6A and C), we next investigated the effect of Nek11 depletion on cell survival. We first assessed the effect of Nek11 depletion on cell death via

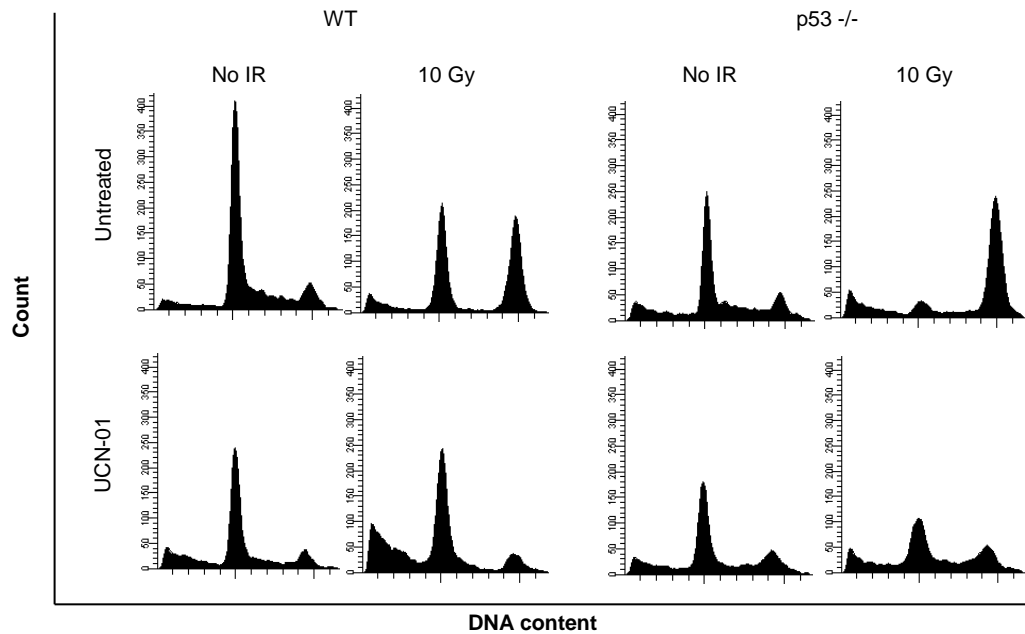
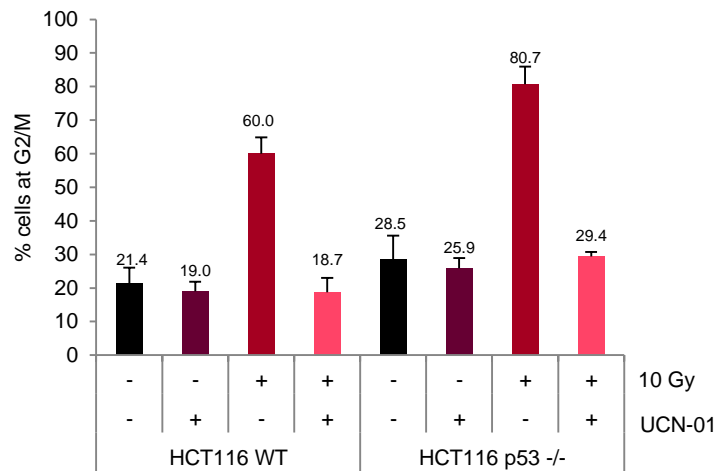
A**B**

Figure 3.5 G2/M arrest in response to IR in HCT116 cells is Chk1 dependent

A. HCT116 WT and p53-null cells were either untreated or treated with 250 nM UCN-01 30 minutes before being irradiated (10 Gy) or left untreated. Cells were fixed and processed for cell cycle analysis 16 hours post-IR. **B.** Histogram shows the percentage of cells at G2/M and data represents means (\pm S.D.) of 2 separate experiments.

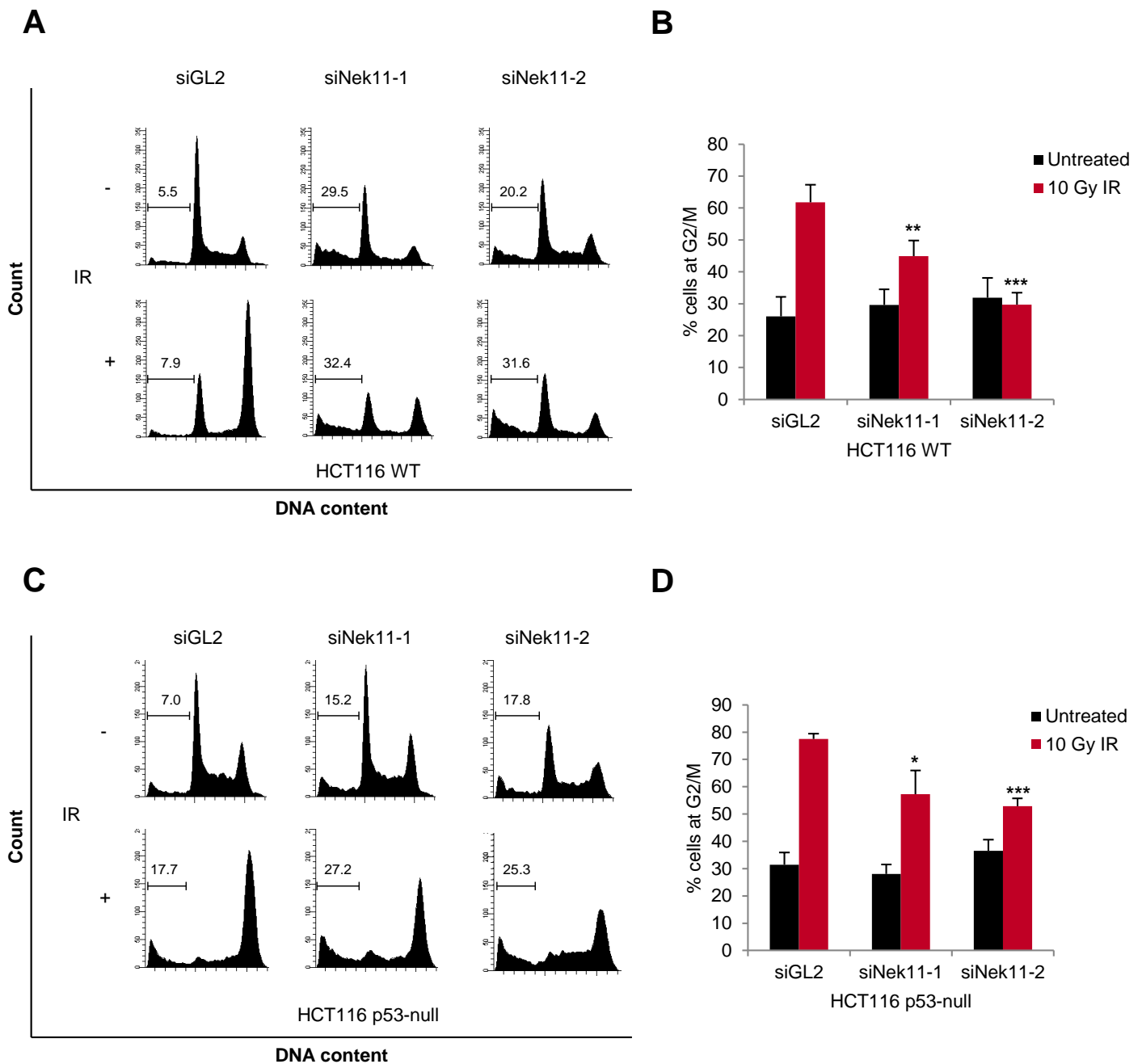


Figure 3.6 Nek11 is required for G2/M arrest in response to IR in HCT116 WT and p53-null cells

A. HCT116 WT cells were transfected with the siRNAs indicated and, after 56 hours, were either untreated or irradiated with 10 Gy. Cells were collected 72 hours post-transfection and processed for cell cycle analysis by flow cytometry. Also indicated is the percentage of cells in SubG1 phase for the experiment shown. **B.** Histogram represents the percentage of cycling cells at G2/M from the experiment in A. **C. & D.** HCT116 p53-null cells were treated and analysed as in A & B, respectively. Data represent means (\pm S.D.) of 3 separate experiments. *, $p < 0.05$; **, $p < 0.01$, and ***, $p < 0.001$ in comparison to siGL2 depletion by unpaired t-test.

apoptotic assays using Annexin V staining. In viable cells, phosphatidylserine is located on the inner surface of the cell membrane, however upon apoptotic induction these phospholipids are translocated to the outer membrane thereby making cells attractive targets to macrophages (Vermes *et al.*, 1995). Fluorochrome-conjugated Annexin V can be utilised to detect apoptotic cells via flow cytometry, since Annexin V binds with high affinity to the exposed phosphatidylserines. In untreated HCT116 WT cells, 15% of siGL2 transfected cells exhibited apoptotic induction and this was more than doubled to 35-40% in cells that were depleted of Nek11. Nek11 depletion was then combined with DNA damage induced by 10 Gy IR and this revealed that the percentage of apoptotic cell population was enhanced further still to 50% (Figure 3.7A and B). Analysis by Annexin V/7-AAD staining exhibited the same trend as cell death measured by analysis of the SubG1 population via PI staining. We propose that this is an effect of the combination of treatments since irradiation alone did not produce a significant increase in apoptosis in siGL2 cells. In comparison, the HCT116 p53-null cells transfected with siGL2 oligonucleotides, exhibited more cell death upon exposure to IR compared to the WT cells, most likely due to inefficient arrest at G1/S. However, although depletion of Nek11 alone and in combination with IR resulted in an increase in apoptotic cell population compared to the siGL2 control, the percentage observed was lower compared to that in WT cells.

Next, we examined long-term cell survival following Nek11 depletion using a colony formation or “clonogenic” assay. The assay assesses the sensitivity of cells to various treatments on the basis that a single viable cell will proliferate and form a colony (Franken *et al.*, 2006). Clonogenic assays were set up using HCT116 cells transfected with either siGL2 or siNek11-2 duplex and left untreated or irradiated with a low dose of 2 Gy (Figure 3.8A). Following growth for around 2 weeks, cells were fixed and stained with crystal violet. Colonies were counted across triplicate plates and percentage cell survival calculated by comparing the plating efficiency of the treated sample with control samples

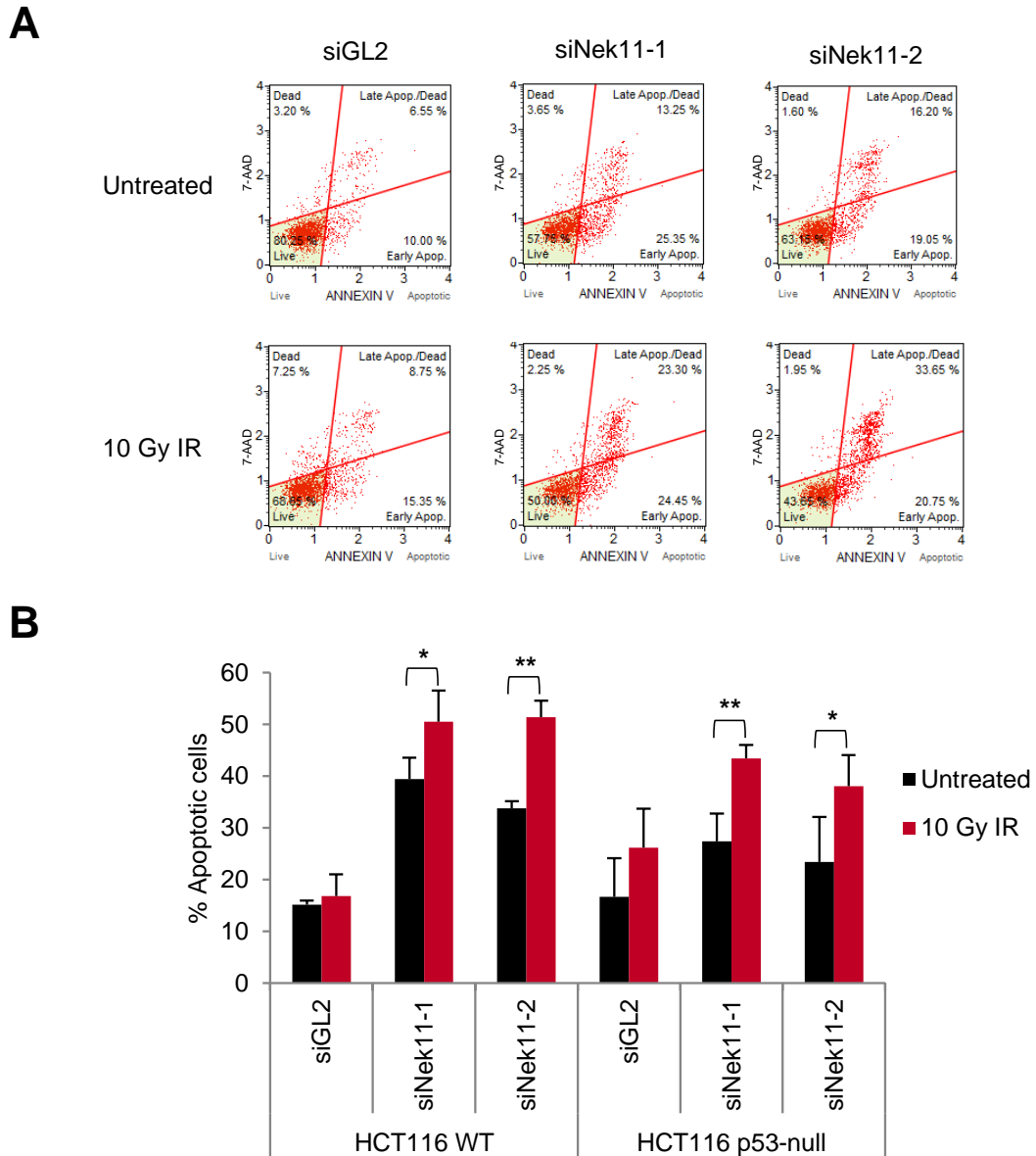


Figure 3.7 Loss of Nek11 induces apoptosis and this is enhanced in combination with IR in HCT116 cells

A. HCT116 WT cells were transfected with the siRNAs indicated and, after 56 hours, either untreated or irradiated with 10 Gy. Cells were then collected 72 hours post transfection and assayed for apoptosis using Annexin V/7-AAD staining followed by flow cytometry. Plots show percentage of cells in live, early apoptotic and late apoptotic stages. **B.** Histogram represents the percentage of cells in apoptosis in HCT116 WT and p53-null cells (early and late apoptosis combined), following the treatment protocol in A. Data represents the mean (\pm S.D.) of 3 separate experiments. *, $p < 0.05$; **, $p < 0.01$ in comparison to untreated cells by unpaired t-test.

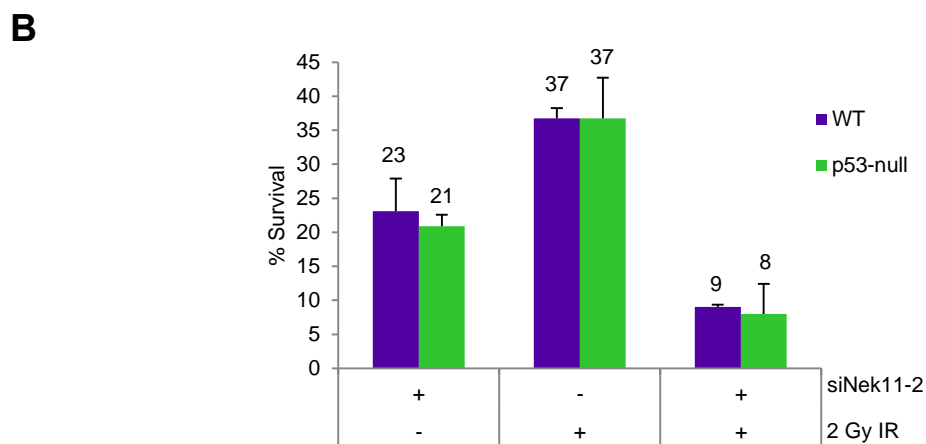
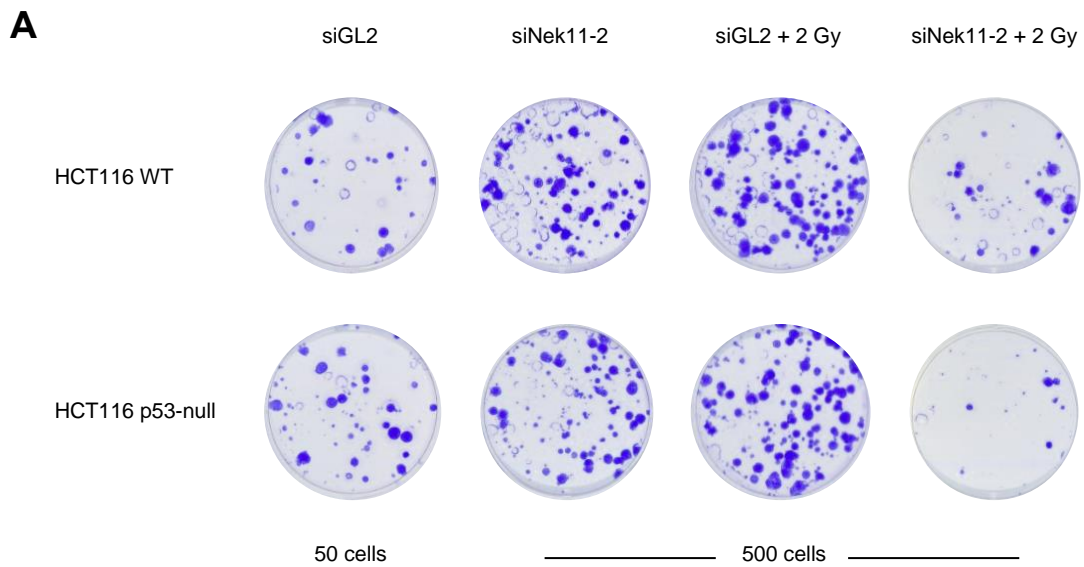


Figure 3.8 Nek11 depletion in combination with IR affects cell proliferation

A. HCT116 WT and p53-null cells were transfected with either siGL2 or siNek11-2 and after 56 hours either untreated or irradiated with 2 Gy. Cells were collected 72 hours post-transfection and plated for clonogenic assays. After 2 weeks colonies were detected by crystal violet staining. Note that only 50 cells were plated for the siGL2 controls, whereas 500 cells were plated for the other samples. This was to achieve a suitable number of colonies that could be counted for each condition. **B.** Colonies from experiment in A were set-up in triplicate and counted to determine the percentage survival, as described in the Materials and Methods. Data represents the mean (\pm S.D.) of 2 separate experiments.

(Figure 3.8B). Results showed that Nek11 depletion alone resulted in around 21-23% cell survival compared to 100% for the siGL2 control. Exposure to 2 Gy IR led to only 37% of cells surviving, however, when Nek11 was depleted in combination with 2 Gy less than 10% of cells survived to form colonies. This confirms that Nek11 depletion alone has deleterious effects on normal cell cycle progression, but that this is exacerbated in the presence of DNA damage induced by IR.

3.2.6 Nek11 is required for G2/M arrest induced by chemotherapeutic agents

For over 40 years the antimetabolite 5-fluorouracil (5-FU) has been used to treat colorectal cancers. To improve response rates to 40-50% and prolong survival, 5-FU is currently used in combination with newer cytotoxic drugs, oxaliplatin and irinotecan (Giacchetti *et al.*, 2000; Douillard *et al.*, 2000). Oxaliplatin, is a platinum based compound, and works by generating covalent inter- and intrastrand platinum-DNA adducts. This results in prevention of DNA replication and transcription and ultimately leads to double strand breaks and activation of DNA response pathways as well as apoptosis (Grothey & Goldberg, 2004; Cao *et al.*, 2006). Irinotecan is a topoisomerase I inhibitor, and acts by preventing ligation of the nicked DNA strand during DNA unwinding and relaxation in DNA replication. Formation of a stable single-strand break (SSB) results, and collision with a replication fork creates a double-strand break (Fuchs *et al.*, 2006). Consequently, this leads to cell cycle arrest and induction of apoptosis (Rothenberg, 1997).

3.2.6.1 Oxaliplatin-induced G2/M arrest is Nek11 dependent in HCT116 WT but not p53-null cells

HCT116 WT cells were treated with increasing doses (up to 20 μ M) of oxaliplatin for 24 hours to determine the cell cycle response and minimum dose required to achieve a significant G2/M arrest (Figure 3.9A and B). A maximum of 52.8% of cells arresting at G2/M was achieved with a dose of 5 μ M; therefore

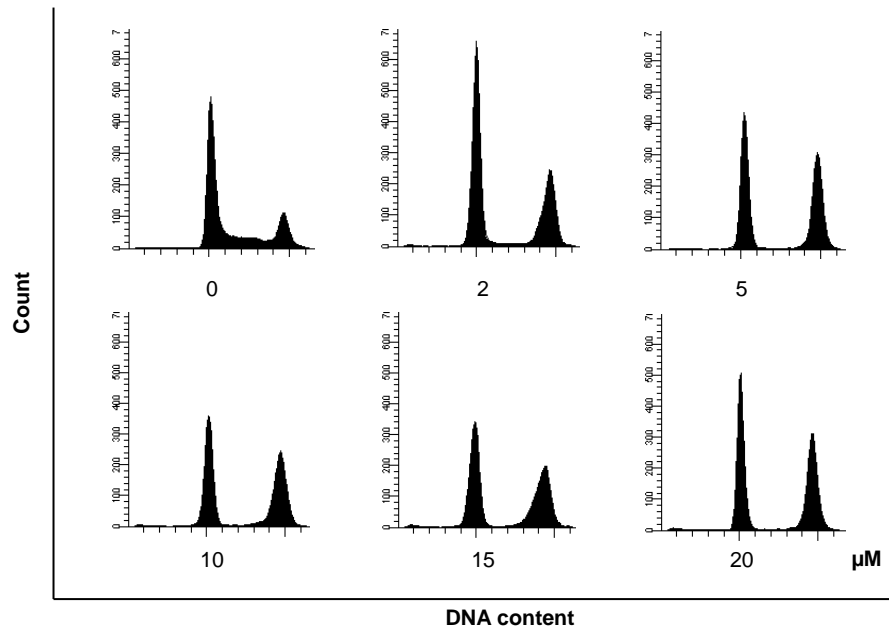
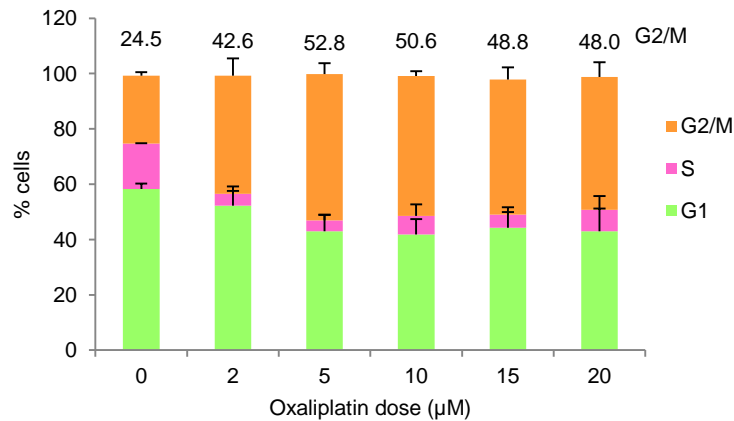
A**B**

Figure 3.9 Oxaliplatin induces a dose-dependent G2/M arrest in HCT116 WT cells

A. HCT116 WT cells were treated with the indicated concentrations of oxaliplatin for 24 hours. Cells were fixed and cell cycle profiles analysed by flow cytometry. **B.** Histogram represents the percentage of cycling cells at G1, S and G2/M phases for each concentration of oxaliplatin. Percentage of cells at G2/M are indicated for each sample. Data represents means (\pm S.D.) of 3 separate experiments

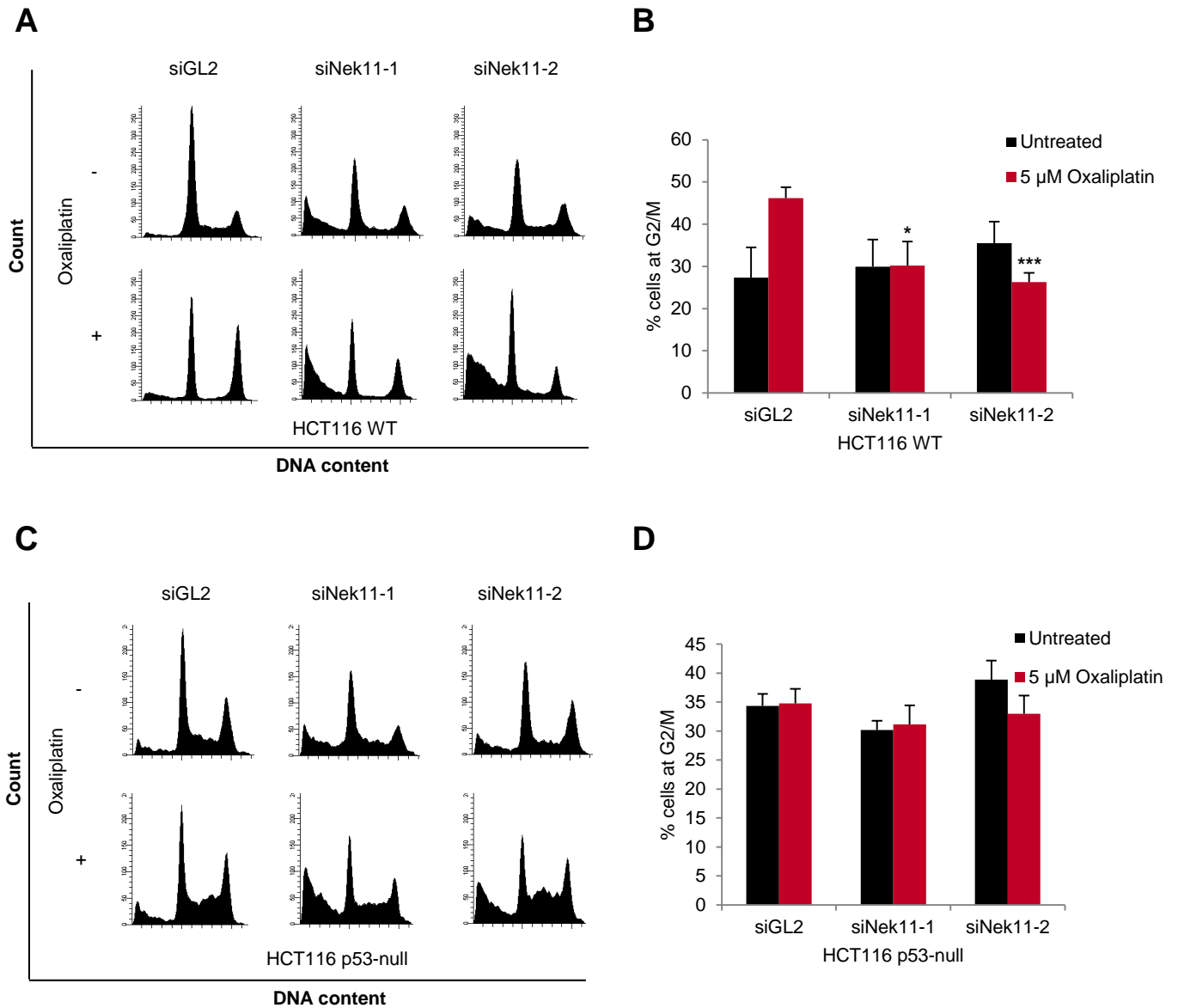


Figure 3.10 Oxaliplatin induced G2/M arrest is Nek11 dependent in HCT116 WT but not p53-null cells

A. HCT116 WT cells were transfected with the siRNAs indicated and, after 52 hours, either untreated or treated with 5 μ M oxaliplatin. Cells were collected 72 hours post-transfection and processed for cell cycle analysis by flow cytometry. **B.** Histogram represents the percentage of cycling cells at G2/M from the experiment in A. **C.** & **D.** HCT116 p53-null cells were treated and analysed as in A & B, respectively. Data represents means (\pm S.D.) of 3 separate experiments. *, $p < 0.05$; ***, $p < 0.001$, in comparison to siGL2 oxaliplatin-treated cells by unpaired t-test.

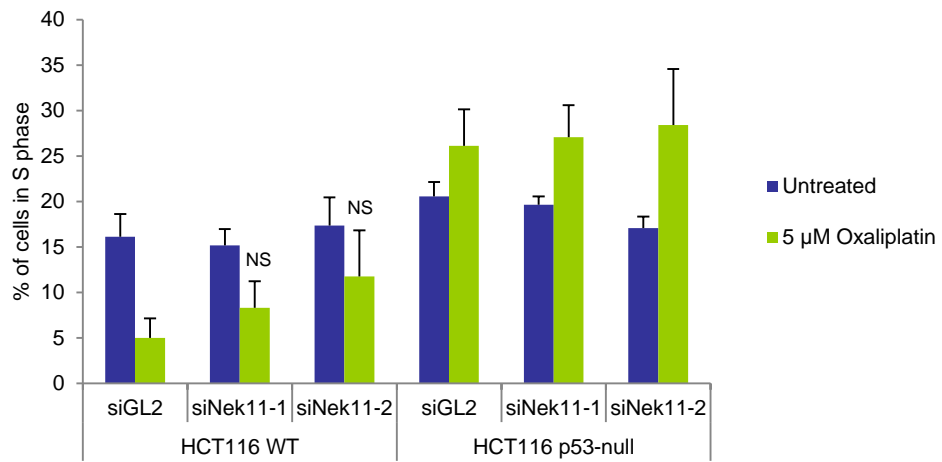


Figure 3.11 Oxaliplatin treatment results in a reduction of S-phase cells in HCT116 WT but an increase in HCT116 p53-null cells

Histogram compares percentage of cycling cells in S-phase for experiments performed as in Figure 3.10. NS represents no statistical significance between indicated sample and siGL2/oxaliplatin-treated cells.

this concentration was used in subsequent experiments in combination with Nek11 depletion. In HCT116 WT cells, depletion of Nek11 in combination with oxaliplatin treatment led to abrogation of the G2/M arrest with a reduction from 46.2% in siGL2 cells to 30 and 26% in siNek11-1 and siNek11-2 treated cells, respectively (Figure 3.10A and B). In contrast, treatment of HCT116 p53-null cells with 5 μ M oxaliplatin did not lead to a G2/M arrest, with the percentage of cells at G2/M in both untreated and treated siGL2 samples being not significantly different (Figure 3.10C and D). Furthermore, depleting Nek11 in these cells did not significantly alter the percentage of cells at G2/M. It was observed however, that instead of exhibiting a G2/M arrest the HCT116 p53-null cells showed an accumulation of cells in S-phase upon treatment with oxaliplatin (Figure 3.10C). Comparing WT and p53-null siGL2 transfected cells we see that upon treatment with oxaliplatin there is a reduction in the S-phase fraction in WT cells but an increase in p53-null cells (Figure 3.11). In addition, we also noticed that Nek11 depletion in WT cells in combination with oxaliplatin led to a slight recovery of S-phase cells when compared to the siGL2 control, indicating a potential role for Nek11 at the G1/S transition; however, the increase did not reach a level of significance (Figure 3.11).

3.2.6.2 Irinotecan-induced G2/M arrest is Nek11-dependent in HCT116 cells

To assess the effects of irinotecan on the cell cycle of HCT116 cells, HCT116 WT cells were treated with 1 to 20 μ M of drug for 24 hours before cell cycle profiles were analysed by flow cytometry (Figure 3.12A and B). A dose of only 1 μ M was able to cause 52.1% of cells to arrest at G2/M as compared to 29% in untreated cells. 5 μ M irinotecan caused a maximal arrest with 79.6% at G2/M. Nek11 was then depleted for 72 hours in both HCT116 WT and p53-null cells and treated for the last 20 hours with 5 μ M irinotecan to determine whether Nek11 was required for this G2/M arrest. Figure 3.13 shows that that in both cell lines Nek11 depletion with both siRNA oligonucleotides led to abrogation of the irinotecan-induced G2/M arrest (Figure 3.13A-D).

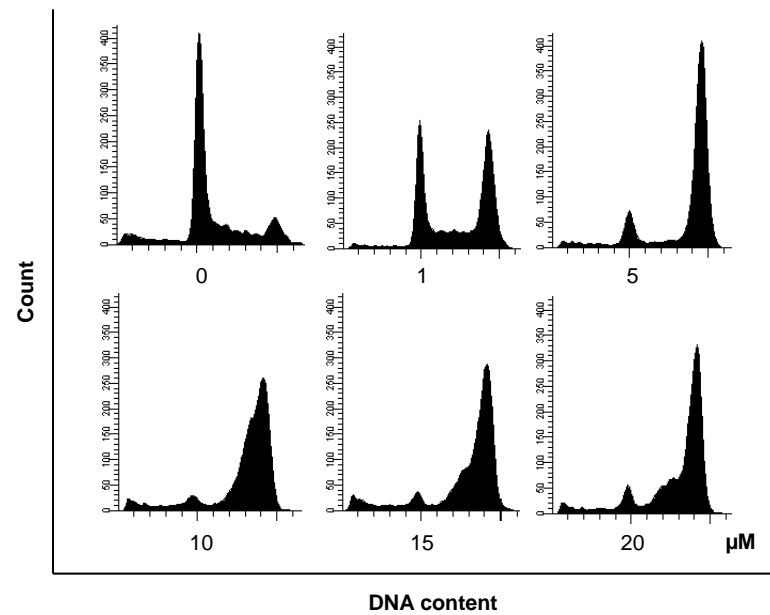
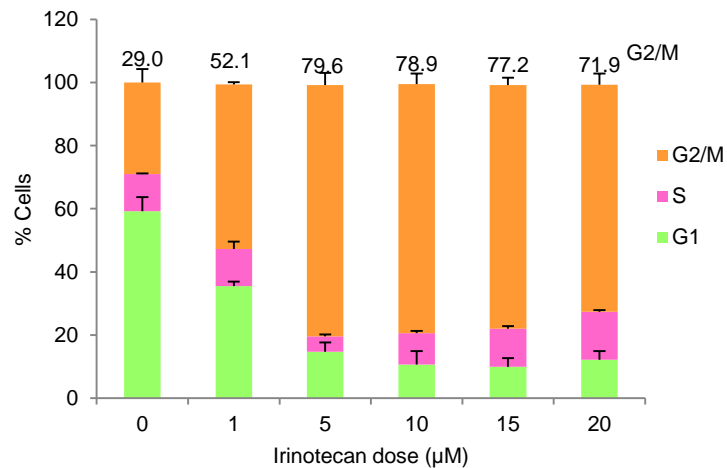
A**B**

Figure 3.12 Irinotecan induces a dose-dependent G2/M arrest in HCT116 WT cells

A. HCT116 WT cells were treated with the indicated concentrations of irinotecan for 24 hours. Cells were collected and fixed before being processed for cell cycle analysis. **B.** Histogram represents the percentage of cycling cells at G1, S and G2/M phases for each irinotecan dose. Percentage of cells at G2/M are indicated above each sample. Data represents means (\pm S.D.) of 2 separate experiments.

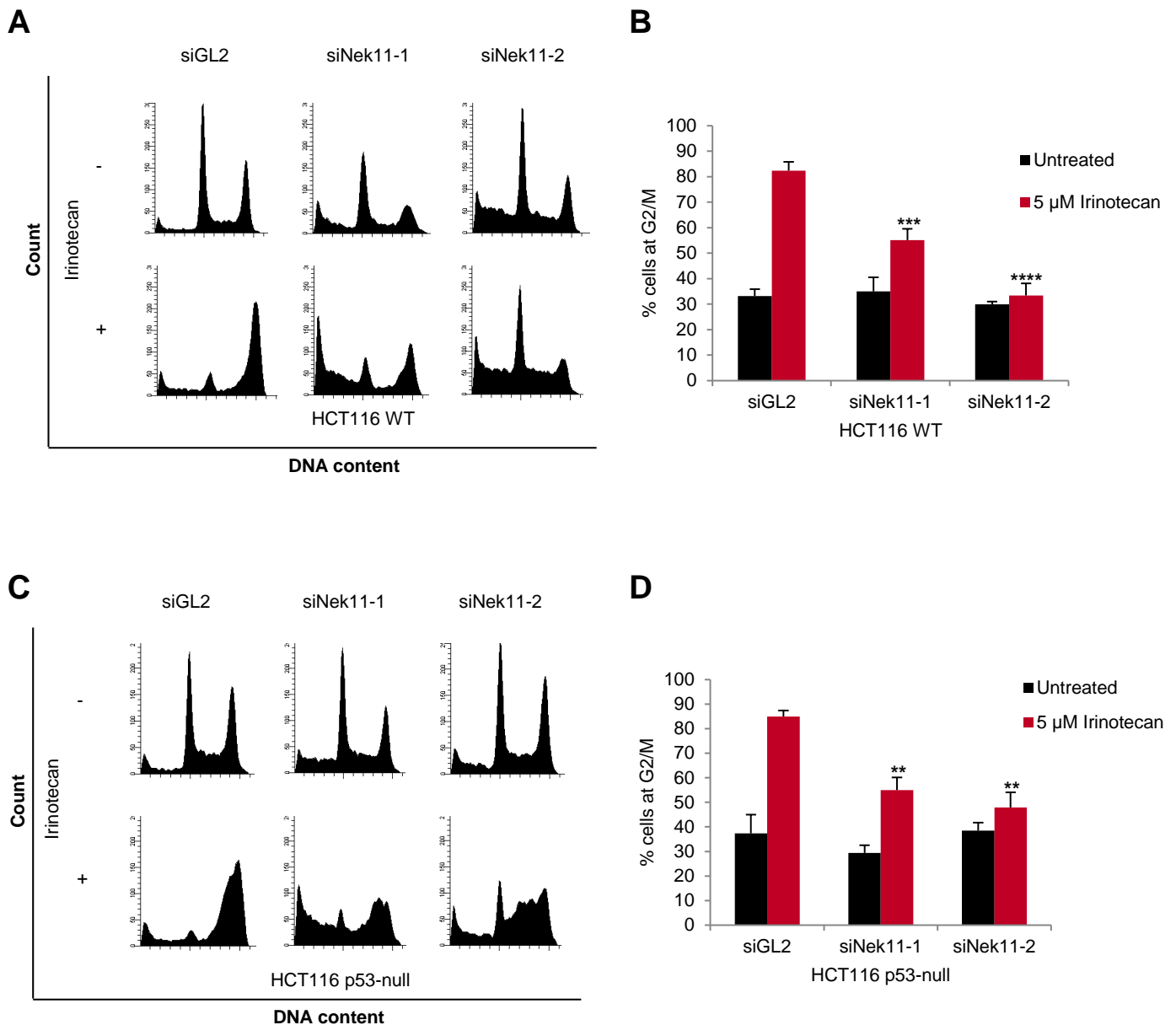


Figure 3.13 Irinotecan-induced G2/M arrest is Nek11-dependent in HCT116 WT and p53-null cells

A. HCT116 WT cells were transfected with siRNAs indicated and, after 52 hours, either untreated or treated with 5 μ M irinotecan. Cells were collected 72 hours post-transfection and processed for cell cycle analysis by flow cytometry. **B.** Histogram represents the percentage of cycling cells at G2/M from the experiment in A. **C.** & **D.** HCT116 p53-null cells were treated and analysed as in B & C, respectively. Data represents means (\pm S.D.) of 3 separate experiments. **, $p < 0.01$; ***, $p < 0.001$; ****, $p < 0.0001$, in comparison to siGL2 irinotecan-treated cells by unpaired t-test.

3.2.7 Depletion of Nek11S results in a greater checkpoint abrogation

To assess the importance of individual Nek11 isoforms at the G2/M checkpoint in colorectal cancer cells, we employed the use of siRNA oligonucleotides specific to each of the Nek11 variants (Figure 3.14A). Two oligonucleotides that recognised either Nek11L and D or two that recognised Nek11S were used. To confirm specific depletion of Nek11 isoforms, HCT116 cells were transfected with oligonucleotides against Nek11L/D, Nek11S or GL2 for 72 hours. Extracted mRNA was then used in qRT-PCR experiments with isoform specific primers. mRNA expression of Nek11 isoforms was compared to expression in siGL2 treated cells (Figure 3.14B). Depletion of Nek11L and Nek11D isoforms, and not Nek11S, was confirmed with siNek11L/D oligonucleotides. Similarly, depletion of Nek11S, and not Nek11L or Nek11D, was confirmed with siNek11S oligonucleotides, although depletion efficiency was lower compared to Nek11L depletion with siNek11L/D oligos. Interestingly, there was an increase in Nek11L and Nek11D expression seen upon depletion of Nek11S, suggesting compensatory upregulation.

Next, we examined the effect on G2/M checkpoint activation upon specific isoform depletion. HCT116 cells were transfected with isoform specific oligos and either left untreated or treated with 10 Gy IR, 5 μ M irinotecan or 5 μ M oxaliplatin. All cells were collected 72 hours post-transfection and cell cycle profiles analysed (Figure 3.15A). Depletion of Nek11L/D variants led to a significant abrogation of the G2/M checkpoint in response to IR, but not upon treatment with irinotecan or oxaliplatin. However, depletion of Nek11S led to a significant abrogation of the G2/M checkpoint in response to all DNA damaging agents. The effect of specific isoform depletion was then also examined in HCT116 p53-null cells (Figure 3.15B). In this case, depletion of Nek11L/D led to significant abrogation of the G2/M checkpoint in response to irinotecan. Depletion of Nek11S led to a more substantial and significant abrogation of the G2/M checkpoint in response to IR and irinotecan treatment. As previously seen, oxaliplatin treatment of p53-null cells has no effect on G2/M population so the effect of depletion of Nek11 could not be detected. Overall, these results reveal an important role for the Nek11S isoform at the G2/M checkpoint in response to DNA damage in HCT116 cells.

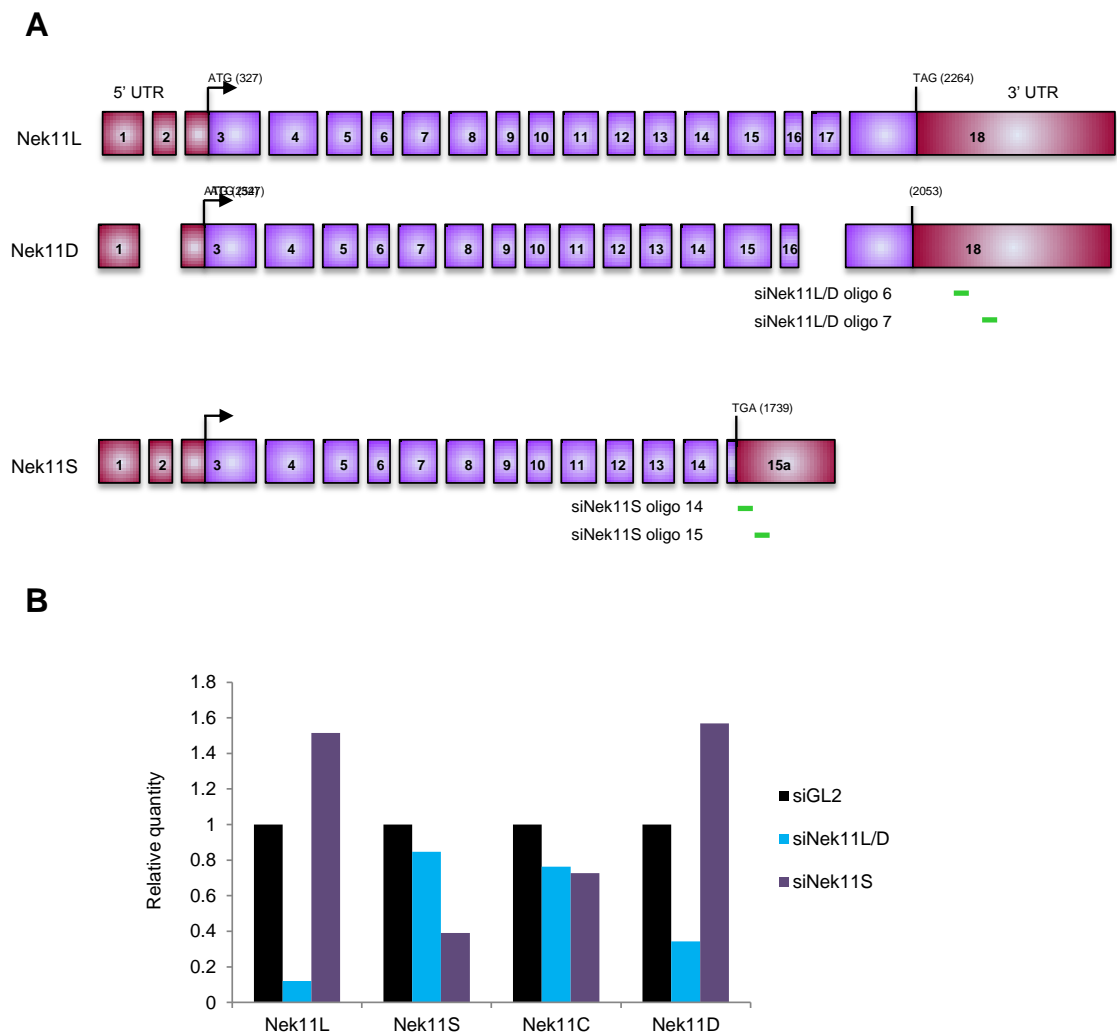


Figure 3.14 Validation of isoform specific RNAi using qRT-PCR

A. Schematic diagram indicates regions to which Nek11L/D or Nek11S oligonucleotides (green) recognise. **B.** HCT116 WT cells were transfected with siRNAs against luciferase (siGL2) or the Nek11L and D isoforms, (siNek11L/D) or Nek11S (siNek11S), and mRNA abundance determined by qPCR analysis with isoform-specific primers. Histogram represents the expression of each isoform relative to siGL2 control. These results represent one experiment.

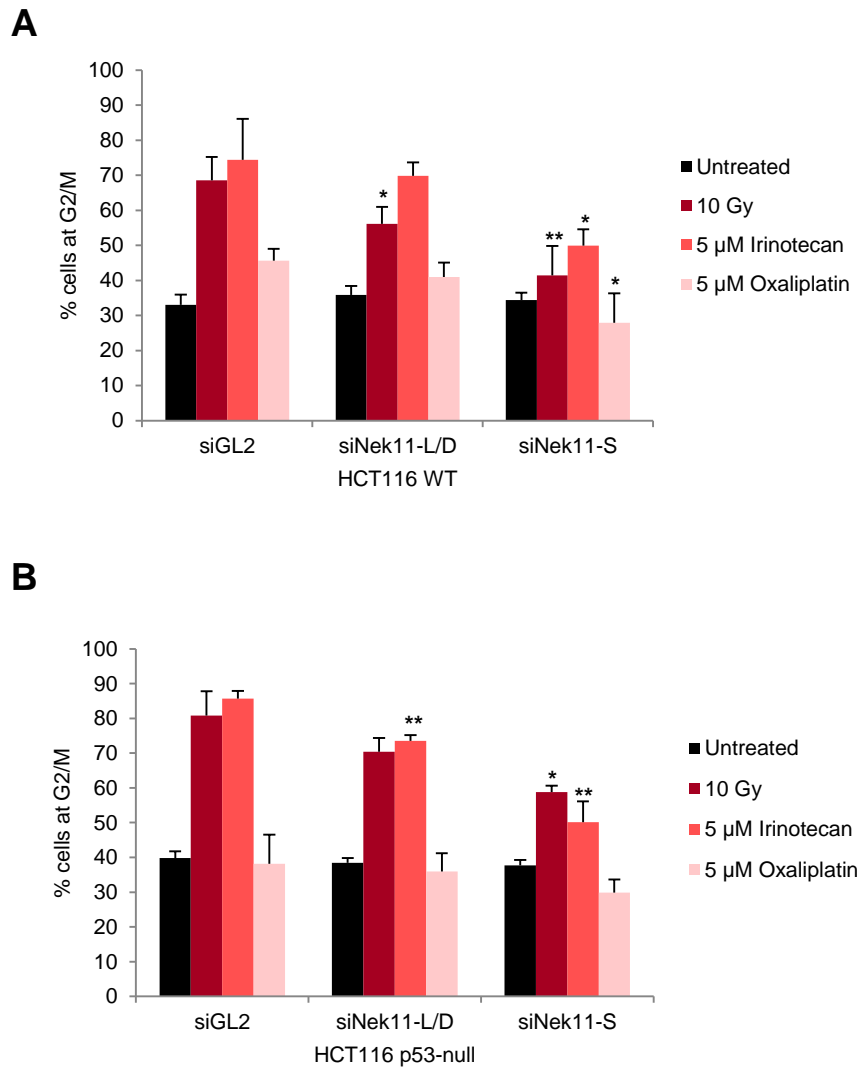


Figure 3.15 Cell cycle response to Nek11 isoform specific depletions in combination with DNA damaging agents in HCT116 WT and p53-null cells

HCT116 WT (**A**) and p53-null (**B**) cells were transfected with siRNAs to deplete Nek11L and Nek11D (L/D), Nek11S or luciferase (siGL2), as indicated. Subsequently, cells were either untreated or irradiated with 10 Gy after 56 hours, or treated with 5 μM irinotecan or 5 μM oxaliplatin after 52 hours. Cells were collected 72 hours post-transfection, processed for cell cycle analysis by flow cytometry and the percentage of cycling cells at G2/M determined. Data represents means (\pm S.D.) of 3 separate experiments. *, $p < 0.05$; **, $p < 0.01$ in comparison to siGL2 cells for each treatment by unpaired t-test.

3.3 Discussion

One of the many cellular responses to DNA damage is the activation of cell cycle checkpoints (Ciccia & Elledge, 2010). This allows time for DNA repair and therefore acts to maintain genomic stability and prevent cancer cell formation. Many cancer cells carry defects in key checkpoint machinery and consequently rely on the remaining functional checkpoints. As a result, components of these pathways have become increasingly attractive targets for cancer drug development in order to sensitise cancer cells with a particular genetic background to DNA damaging agents. Studies are ongoing to better understand players within checkpoint control in response to DNA damage and recently Nek11 was identified as being required for the G2/M arrest through controlling Cdc25A protein levels (Melixetian *et al.*, 2009). However, the role of Nek11 at the checkpoint has been a matter of debate and CK1 α was suggested to be responsible for Cdc25A degradation at G2/M (Honaker & Piwnica-Worms, 2010). In this chapter, we show evidence that Nek11 plays a key and important role for successful induction of the G2/M DNA damage checkpoint in response to different types of DNA damage induced by IR, oxaliplatin and irinotecan. This is consistent with observations that Nek11 is activated in response to various DNA damaging agents including camptothecin, of which SN-38, the metabolite of irinotecan, is an analogue (Noguchi *et al.*, 2002).

Since immunohistochemistry data suggested that Nek11 is highly expressed in colorectal cancers, specifically in adenomas and carcinomas (Sorensen *et al.*, 2010), experiments in this chapter were carried out in HCT116 cells, derived from a colorectal carcinoma. Using two independent oligonucleotides to deplete Nek11, we show that Nek11 gene silencing leads to significant abrogation of the G2/M checkpoint in response to IR and the clinically relevant agents, oxaliplatin and irinotecan. siNek11-2 generally showed a stronger abrogation of the G2/M arrest and this is consistent with a more efficient knockdown of endogenous Nek11 as examined by Western blot and qRT-PCR analysis in U2OS and HCT116 cells, respectively. This is also good evidence that the abrogation seen upon RNAi depletion of Nek11 is not an off-target effect. Hence, we conclude

that HCT116 cells rely on Nek11 for G2/M arrest upon exposure to various DNA damaging agents. This could be fully validated through the use of p-H3 Ser10 to determine the percentage of mitotic cells as previously demonstrated in U2OS cells (Melixetian *et al.*, 2009).

It would be interesting to now determine the effects of Nek11 depletion in cells with varying levels of Nek11 expression. In particular, it would be interesting to examine cell lines derived from different stages of colorectal cancer progression since Nek11 expression was shown to be highest in early stage colorectal tumours (Sorensen *et al.*, 2010). This would reveal whether specific tumour stages are more sensitive to Nek11 inhibition in combination with DNA damage. Extending this further still, the effect of Nek11 depletion in primary tumour derived material could also be examined. However, these studies may require the development of a small molecule inhibitor of Nek11.

Analysis of sensitivity to Nek11 depletion via apoptotic assays show that depletion of Nek11 alone resulted in a 2-3 fold increase in cell death. This suggests that Nek11 plays an important role in maintaining cell viability in HCT116 cells even in the absence of DNA damage. Melixetian *et al.* (2009) showed that T98G glioblastoma cells that were depleted of Nek11 progressed slower through the cell cycle suggesting a role in normal cell proliferation (Melixetian *et al.*, 2009). One possibility might be that Nek11 is required to monitor S-phase progression since its activity was increased in response to agents that block DNA replication (Noguchi *et al.*, 2002). Combining Nek11 depletion with IR resulted in an enhanced induction of apoptosis. Additionally, clonogenic assays revealed that Nek11 depleted cells that did survive initial treatment showed a reduced capacity of cell proliferation upon DNA damage with survival falling from 23 to 9% upon combination with 2 Gy IR. It would be interesting to perform similar studies with the chemotherapeutic agents, oxaliplatin and irinotecan. Nevertheless, these data show that Nek11 is required for DNA damage induced G2/M checkpoint activation and inhibition of expression promotes cell death, indicating that Nek11 would make a potentially

good drug target. However, further studies would need to be carried out to examine the effects of Nek11 depletion in normal colorectal cells, such as HCECs, to determine whether targeting Nek11 in colorectal tumours would specifically target cancer cells.

Approximately, 50% of colorectal tumours exhibit p53 mutation or loss (Baker *et al.*, 1990), resulting in a weakened G1/S checkpoint. Therefore, using an isogenic p53-null cell line, we also examined the effect of Nek11 depletion on HCT116 cells lacking p53 to see whether these cells would be sensitised to treatment with DNA damaging agents. Importantly, initiation of the G2/M checkpoint is p53-independent but in order to maintain the arrest the p53-p21 pathway plays a role at later stages (Fei & El-Deiry, 2003; Taylor & Stark, 2001). So whether Nek11 acts downstream of p53 could also be examined in these cells. Results indicated that in response to IR and irinotecan, p53-null cells showed abrogation of the G2/M checkpoint upon Nek11 gene silencing in a similar manner to WT cells. This indicates that Nek11 is required for G2/M checkpoint activation regardless of p53 status.

However, p53-null HCT116 cells did not exhibit a G2/M arrest in response to oxaliplatin treatment. Instead we observed an increase in the S-phase cell population. Other studies have found that inactivation of p53 in HCT116 cells results in an increased resistance to oxaliplatin, reduction of cell cycle arrest at G2/M and induction of apoptosis. This was also seen in a panel of colorectal cancer-derived cell lines harbouring inactive p53 (Arango *et al.*, 2004; Toscano *et al.*, 2007). Therefore, wild-type p53 is required for effective sensitivity to oxaliplatin treatment. As a result, Nek11 inhibition in combination with oxaliplatin in p53 mutated or null cells may not make an effective combination for treatment. Interestingly, in HCT116 WT cells depletion of Nek11 led to an increase in the percentage of S-phase cells upon treatment with oxaliplatin. This effect correlated with the efficiency of the oligo, with the more effective siNek11-2 showing a greater percentage of cells in S-phase. This suggests a potential role for Nek11 during the S-phase stress response as suggested in previous

studies (Noguchi *et al.*, 2002). However, the effect did not reach a level of significance. It may still be possible that Nek11 is playing some role in this phase given its activation in response to replication inhibitors, but it could be that other DNA replication stress proteins are able to complement the role of Nek11 in its absence (Noguchi *et al.*, 2002).

In terms of apoptosis and cell survival, we did not observe an increase upon treatment with IR in the p53-null cells when compared to HCT116 WT cells. It may be possible that because p53 is also a key player in the induction of apoptosis, the loss of Nek11 does not lead to an increase in apoptotic cell death. Alternatively, it may be that Nek11 depletion in combination with IR is sufficient to induce such substantial cell death in the HCT116 WT cells that any additional effects of p53 loss would be difficult to observe. Furthermore, other studies have also indicated that the mutational status of p53 can increase or decrease tumour sensitivity to chemotherapeutic agents (Arango *et al.*, 2004). So it may be possible that p53 status is not an indicator of potential sensitivity to Nek11 loss. Whether the presence of other common colorectal tumour mutations, such as KRAS or APC, sensitises cells to Nek11 depletion remains to be investigated. In addition it will be interesting to examine the role of Nek11 in other tumour types. For example, an analysis of online expression databases show an increase in Nek11 expression in lung cancers (Joon Wee and Andrew Fry, unpublished data). Hence, similar experiments to those performed here should be undertaken in panels of lung cancer cell lines which is also currently treated with radiotherapy.

Finally, we assessed the role of individual Nek11 variants at the G2/M checkpoint using oligonucleotides that specifically deplete either Nek11L/D or Nek11S. During validation of the isoform-specific oligonucleotides by qRT-PCR analysis, we saw that depletion of Nek11S resulted in an increase in the expression of Nek11L and Nek11D mRNA. This could indicate that the absence of Nek11S leads to a switch in expression to other isoforms to compensate. However, repeat experiments would need to be done before further

investigation. Interestingly, cell cycle analysis showed that whilst depletion of Nek11L/D produced a moderate abrogation of the checkpoint in response to some treatments, depletion of Nek11S resulted in a more significant abrogation in response to all of the DNA damaging agents tested, namely IR, irinotecan and oxaliplatin. The role of Nek11C at the G2/M checkpoint remains to be specifically examined and oligonucleotides specific to its mRNA sequence would need to be designed.

Based on these results, we propose that Nek11S plays a key role at the G2/M checkpoint. However, whether Nek11S is more important compared to other isoforms remains to be determined. As discussed in Chapter 6, Nek11L mRNA is more highly expressed however, this may not directly relate to protein levels. It may well be that Nek11S protein is more abundant resulting in a more substantial loss of the checkpoint upon depletion. Western blot analysis in U2OS cells suggests that this might be the case, since Nek11S/C protein was more abundant than the Nek11L/D protein. One way to examine which proteins contribute to the checkpoint would be to deplete cell isoforms and then add back RNAi resistant individual isoforms. Indeed, the Nek11 variant-specific oligonucleotides used here recognise sequences within the 3'UTR non-coding regions of Nek11 mRNA, and therefore would not deplete mRNA expressed from Nek11 vectors. This means that it would be possible to deplete endogenous Nek11 protein and overexpress each of the Nek11 isoforms to examine which isoforms are able to rescue the checkpoint and importantly how effectively.

CHAPTER 4 LOCALISATION AND FUNCTION OF NEK11 ISOFORMS

4.1 Introduction

Localisation studies of mammalian NIMA-related kinases have provided key insights into their roles in many cellular processes, including mitosis, the DNA damage response and ciliogenesis. Localisation of Nek2 to centrosomes has shown that not only does it play a key role in centrosome disjunction at G2/M but it does so through phosphorylation and subsequent displacement of the inter-centriolar linker proteins, C-Nap1 and Rootletin (Fry *et al.*, 1998b; Faragher & Fry, 2003; Fry *et al.*, 1998a). Nek7 localises to centrosomes throughout the cell cycle and shows temporal localisation to the midbody during cytokinesis. Centrosomal localisation is required for microtubule nucleation and therefore required for organised spindle assembly (Yissachar *et al.*, 2006; Kim *et al.*, 2007). As well as localising to centrosomes, both Nek1 and Nek8 localise to primary cilia and multiple studies have implicated them in ciliogenesis (Mahjoub *et al.*, 2005; Shalom *et al.*, 2008; White & Quarmby, 2008). In addition, Nek1 has also been found to play a role in the DNA damage response. In unstimulated cells, Nek1 is predominantly cytoplasmic however, upon treatment with genotoxic agents it quickly redistributes to sites of DNA damage in the nucleus (Polci *et al.*, 2004; Chen *et al.*, 2008a). Overall, these studies not only contribute to our knowledge of how proteins are regulated in the cell but also help to determine their functional roles, and so, here I summarise what is currently known on the expression and subcellular localisation of Nek11.

Initial studies on Nek11 identified the expression of two alternatively spliced variants, Nek11 Long (Nek11L) and Nek11 Short (Nek11S) (Noguchi *et al.*, 2002). Both isoforms are identical in amino acid sequence up to residue 466; this includes an N-terminal catalytic domain, two predicted coiled-coil domains and two putative PEST-like motifs. After this the sequences diverge; Nek11S continues for a further 4 aa and Nek11L for a further 179 aa to also include an additional PEST-like motif. Although the functions of these domains have not

been studied in detail in Nek11, previous studies on NIMA and human NEK family members have shown that coiled-coil domains are important to mediate oligomerisation thereby promoting autophosphorylation and activation, and PEST-sequences play a role in proteasome-dependent proteolysis (Pu & Osmani, 1995a; Fry *et al.*, 2012a; Surpili *et al.*, 2003; Hames *et al.*, 2001). In 2004, Noguchi *et al.* proposed that Nek11 is activated by Nek2A through direct phosphorylation of serine residues in the C-terminal domain (within regions 287-337 and 468-573). Additionally, they proposed that the PEST-like elements are responsible for complex formation with Nek2B (Noguchi *et al.*, 2004). Western blot analysis using an antibody raised against residues 327-470 of the C-terminal domain, and therefore able to recognise both isoforms, showed that the Nek11L variant was more abundant in U2OS, HeLa, HEK293T and A431 cell lines, as compared to the Nek11S isoform (Noguchi *et al.*, 2002). Using the same antibody, indirect immunofluorescence studies in HeLa cells showed that endogenous Nek11 is nuclear during interphase and shifts to polar microtubules during early mitosis, after which it becomes difficult to detect. In 2004, the same group then identified Nek11 at nucleoli of U2OS and HeLa cells; it is here they propose that Nek2A activates Nek11 in G1/S due to their co-localisation (Noguchi *et al.*, 2004). Finally, overexpression of exogenous Nek11 exhibited cytoplasmic localisation, although, the isoform overexpressed here was not stated (Noguchi *et al.*, 2004). Studies carried out on Nek11 localisation are therefore limited and somewhat unclear, with no focus so far on individual variants.

Analysis of gene expression databases at the start of this study revealed the expression of two additional Nek11 splice variants, which we termed Nek11C and Nek11D. Like Nek11S, Nek11C is identical to Nek11L up to amino acid 466, after which it continues for a further 16 residues. On the other hand, Nek11D is identical to Nek11L up to residue 541, which includes the third PEST-like sequence, before terminating at amino acid 599. In this chapter, the main objective was to study the individual localisation behaviours of each of the

Nek11 isoforms to gain insight into the importance and potential mechanisms of action of Nek11 in the cell.

4.2 Results

4.2.1 Isolation of Nek11S and Nek11D cDNA from U2OS cells

To start to assess the role of each alternatively spliced Nek11 isoform, we firstly isolated full-length cDNAs for each variant. These could then be used to clone into expression vectors with molecular tags for biochemical characterisation of proteins. Nek11L and Nek11C coding DNAs were previously obtained from Genscript and GeneCopoeia, respectively. To obtain Nek11S and Nek11D cDNAs mRNA was extracted from U2OS cells. Specific primers were designed to amplify full-length coding sequences and used in RT-PCR reactions to generate Nek11S or Nek11D cDNAs (Figure 4.1A and Figure 4.2A). To ensure the specificity of the primers by the amplification of a single DNA product, and to check that the predicted product size was obtained, samples were separated on an agarose gel and bands visualised by ethidium bromide staining. For Nek11S the expected size of 1413 bp was obtained (Figure 4.1B). DNA from the RT-PCR reactions was then purified and ligated into pGEM-T easy vectors before being transformed and screened for recombinant DNA. Since primers designed for Nek11D also amplified the Nek11L isoform, colonies screened positive for recombinant DNA were then subjected to a colony PCR to determine which isoform had been cloned. Primers were designed to amplify DNA from exon 16 through to exon 18 (Figure 4.2A). The presence of Nek11L DNA resulted in a product of 442 bp in size, and conversely, the insertion of Nek11D DNA resulted in a shorter product of 345 bp as it lacks exon 17 due to alternative splicing (Figure 4.2B). Colonies confirmed to be expressing Nek11D were then picked, and purified DNA plasmids sequenced.

4.2.2 Generation of GFP Nek11 stable cell lines

At the time of this study there were no commercial antibodies available to distinguish individual Nek11 isoforms. Therefore, localisation studies would not be able to reveal information about the roles of each of the Nek11 variants in the cell. A common way to get around this is through the use of tagged proteins introduced into cells through transient transfection.

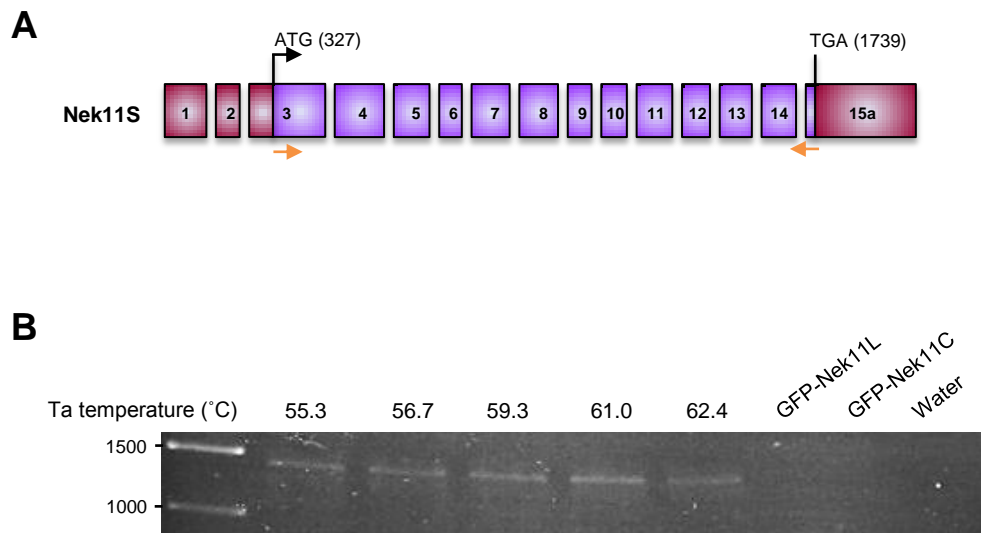


Figure 4.1 Isolation of Nek11S cDNA

A. Schematic representation of Nek11S exon organisation. Red and purple boxes indicate untranslated and coding regions, respectively. Orange arrows indicate regions to which primers were designed. **B.** RNA was extracted from U2OS cells and used in RT-PCR reactions using Nek11S primers and an annealing temperature gradient (T_a), as indicated. Products were separated on an agarose gel to determine presence of Nek11S insert (1413 bp). GFP-Nek11L, GFP-Nek11C plasmids and water were used as negative controls. Size markers (bp) are indicated.

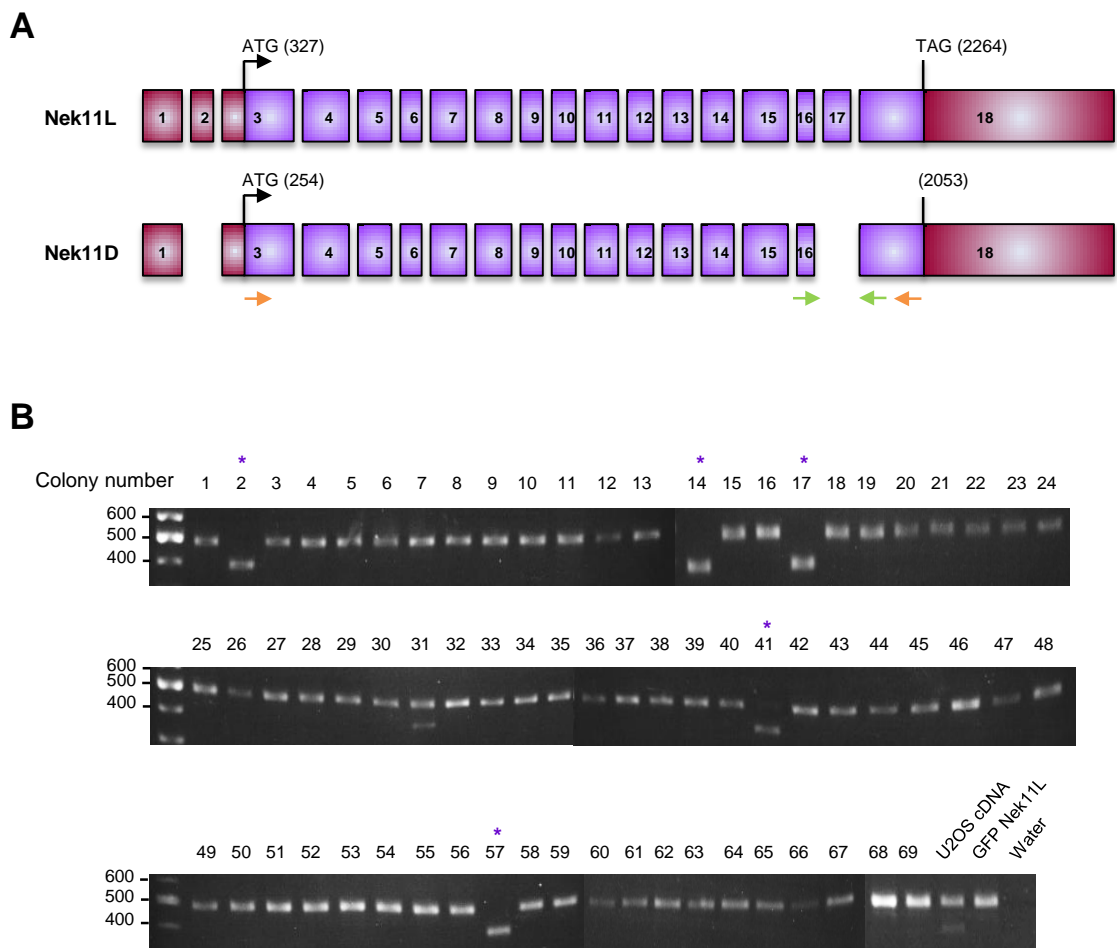


Figure 4.2 Isolation of Nek11D cDNA

A. Schematic representation of Nek11L and Nek11D exon organisation. Red and purple boxes indicate untranslated and coding regions, respectively. Orange arrows indicate region to which primers were designed to generate full length Nek11D. Green arrows indicate primers designed for colony PCR. **B.** Colony PCR reactions were carried out using primers (green) indicated in A, and white colonies expressing vector containing insert. Products were separated on a 1.5% agarose gel and presence of Nek11L (442bp) or Nek11D (345 bp) insert determined. Colony numbers marked with an asterisk (*) contained Nek11D insert. Size markers (bp) are indicated.

However, multiple transfections can be expensive and overexpression of recombinant protein may lead to behaviour not seen with lower endogenous levels of protein. A useful tool in cell biology is the use of stable cell lines as it allows large-scale biochemical analyses and protein levels are generally more similar to that of endogenous protein. We therefore decided to generate stable cell lines expressing each of the Nek11 isoforms in U2OS cells. As well as having considerable experience with these cells in the lab, Nek11 has previously been shown to be expressed in U2OS cells and, these cells are proficient in the G2/M checkpoint (Noguchi *et al.*, 2002; Melixetian *et al.*, 2009).

Firstly, the optimal antibiotic concentration for selecting stable cells was determined. To do this, a dose-response experiment was carried out where U2OS cells were treated with increasing amounts of G418-containing media and toxicity examined under a microscope (Figure 4.3). Ideally, the optimal dose of antibiotic to use would result in cell death after 6-7 days of antibiotic selection, therefore, we decided to use a selection dose of 1 µg/ml G418 to generate the cell lines. Having isolated human cDNA for each of the Nek11 isoforms we next cloned these into mammalian expression vectors to generate recombinant proteins with an N-terminal eGFP-tag (Figure 4.4A). In addition to the four Nek11 variants, a catalytically inactive version of Nek11L (Nek11L-KD) was generated which harboured mutations to key residues in the catalytic site (K61R/D158A). U2OS cells were transfected with each of these constructs as well as an eGFP-only control vector, and 24 hours post-transfection selection media was added to cells until colonies expressing the eGFP-tagged constructs remained due to the presence of a neomycin resistance marker in the vector. For our studies we decided to generate a mixed population of cells to rule out potential anomalies observed from a single clonal population, and to examine possible effects of differential expression levels of Nek11 protein.

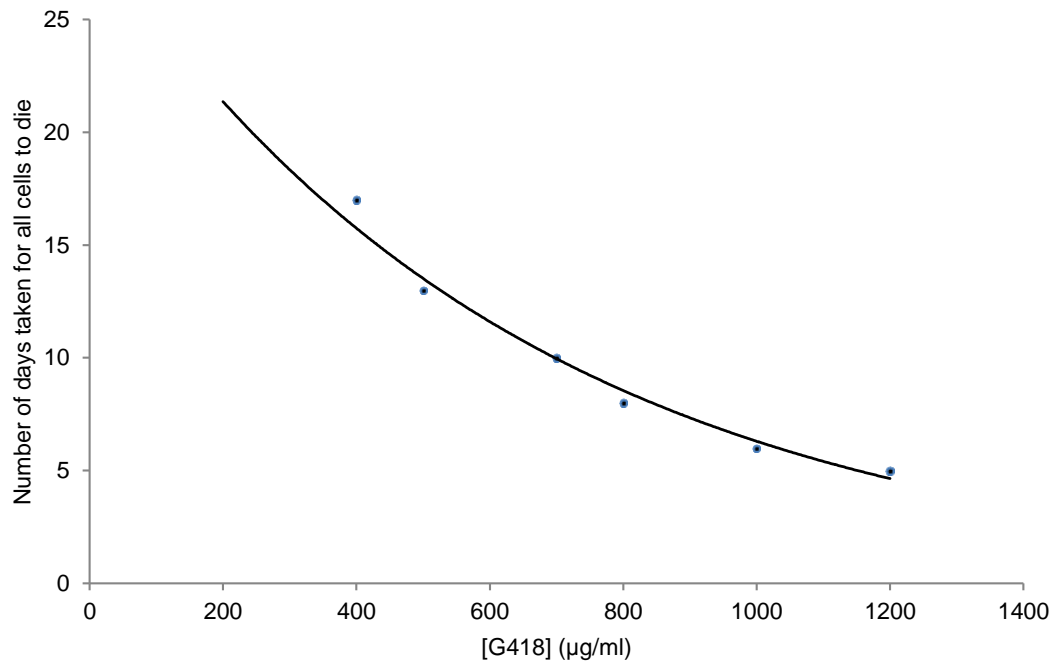


Figure 4.3 G418 dose response curve

U2OS cells were seeded in 6 well-plates and media was replaced with G418 containing media at the concentrations indicated every 2 days. Curve indicates the number of days taken for cells to die at a given dose of G418.

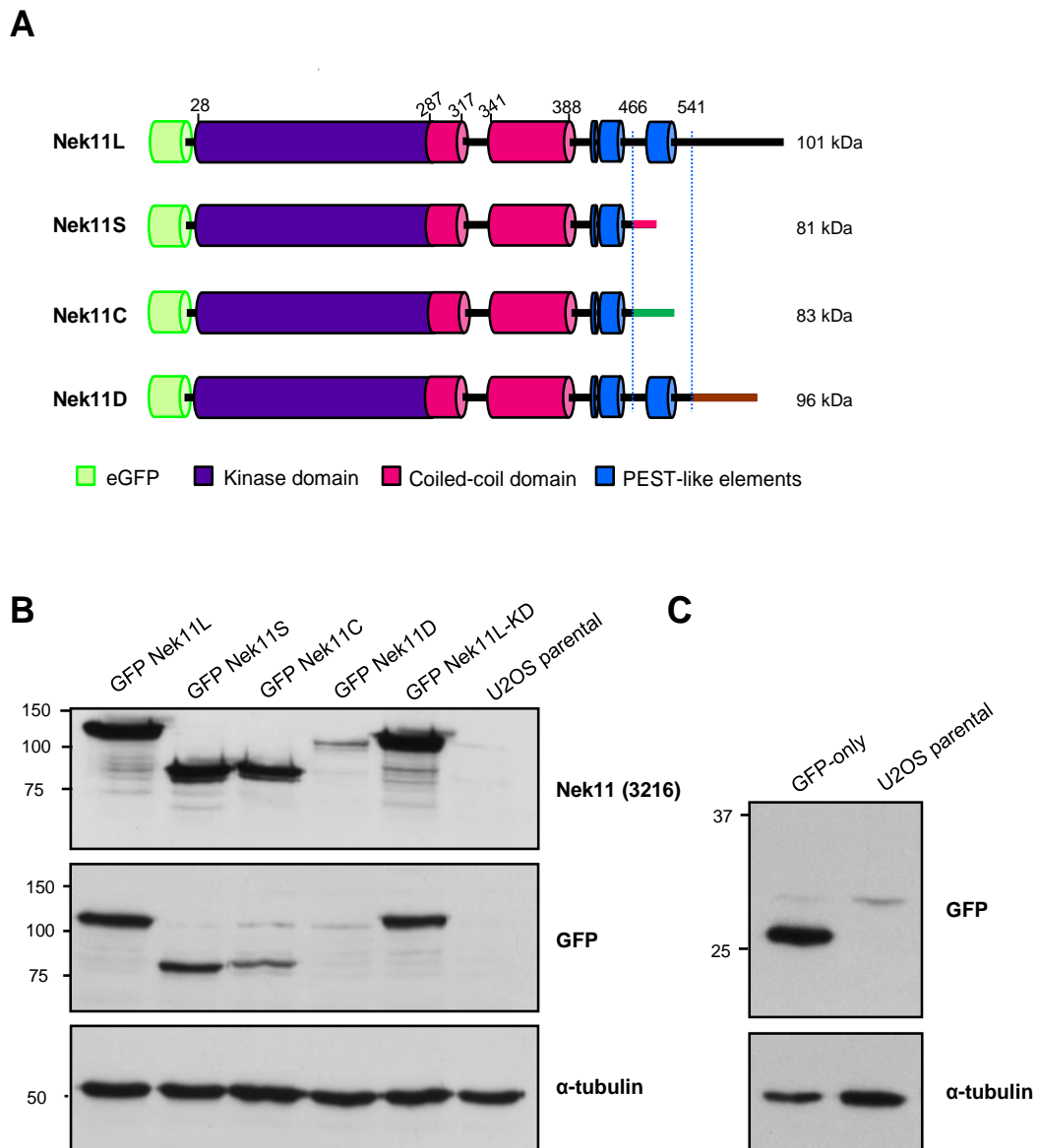


Figure 4.4 Generation of U2OS:GFP-Nek11 and GFP-only stable cell lines

A. Schematic representation of the four N-terminal eGFP-tagged Nek11 splice variants used to generate the stable cell lines. Kinase domain (purple), putative coiled-coils (pink), and predicted PEST-like elements (blue) are indicated. The different C-termini are indicated in different colours and dotted lines indicate the positions at which the isoforms diverge. Residue numbers and predicted molecular weights are indicated. **B** and **C.** Lysates from U2OS:GFP-Nek11 (**B**) and U2OS:GFP-only (**C**) stable cell lines or U2OS parental cells were analysed by SDS-PAGE and Western blotting with antibodies against Nek11 (3216), GFP and α -tubulin. Molecular weights are indicated (kDa).

4.2.3 Nek11D is degraded by the proteasome

To confirm the expression of tagged protein of predicted molecular weight in each stable cell line, lysates were analysed by SDS-PAGE and Western blotted with GFP antibodies (Figure 4.4B and C). It was observed that Nek11D expression in the stable cell line was consistently reduced compared to protein expression in the other stable lines (Figure 4.4B). To determine why this might be, U2OS cells were transiently transfected with each Nek11 isoform and cells were either left untreated or treated with a proteasome inhibitor, MG132, before lysing cells and analysing protein expression by Western blot (Figure 4.5). This revealed that upon treatment with MG132, Nek11D expression was upregulated, whereas expression of the other isoforms remained relatively equal in comparison to untreated samples. Hence, the Nek11D isoform is specifically subject to proteasomal degradation in U2OS cells.

4.2.4 Subcellular localisation of recombinant Nek11 isoforms

To gain further insight into the individual roles that the Nek11 isoforms may be playing we next used the stable cell lines to examine subcellular localisation. Interestingly, the two longer isoforms, Nek11L and Nek11D were predominantly cytoplasmic whereas Nek11S and Nek11C showed localisation to both the cytoplasm and nucleus, suggesting that these isoforms may indeed have distinct roles (Figure 4.6). In addition, this localisation was not dependent on catalytic activity since Nek11L-KD was also cytoplasmic.

Some of the localisation patterns observed were reminiscent to that of the microtubule network therefore fixed cells were stained with anti-GFP to detect recombinant protein and co-stained with anti- α -tubulin to detect microtubules (Figure 4.7). High resolution imaging was carried out on the confocal microscope, however, there did not seem to be any obvious co-localisation with the microtubules. It was noted though that there did seem to be a population of protein at the sites of microtubule nucleation indicating potential localisation to the centrosomes.

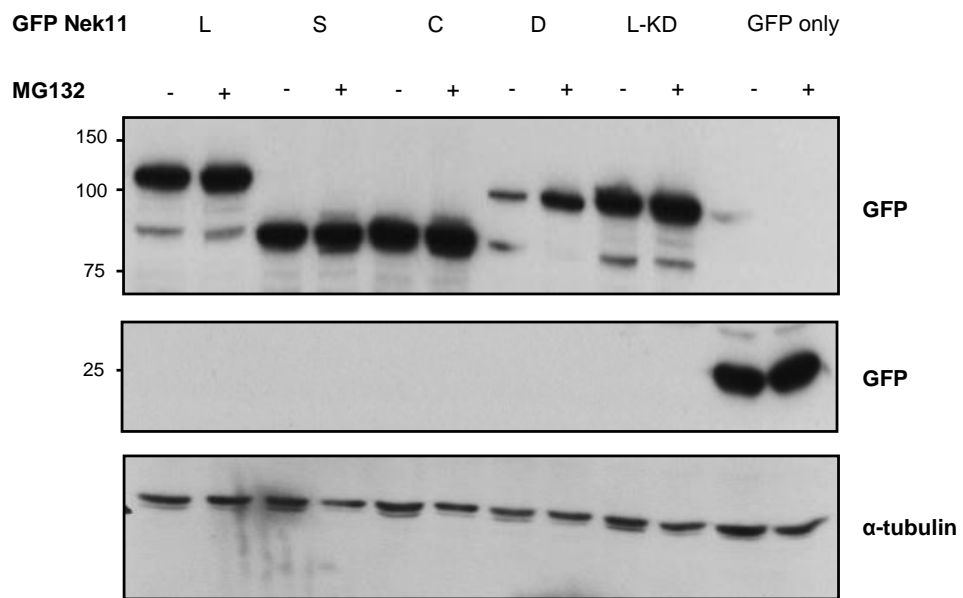


Figure 4.5 Nek11D is subject to proteasomal degradation

U2OS cells were transiently transfected with constructs indicated and, after 20 hours, treated \pm MG132 for 4 hours. Lysates were analysed by Western blot with antibodies indicated. Molecular weights (kDa) are indicated.

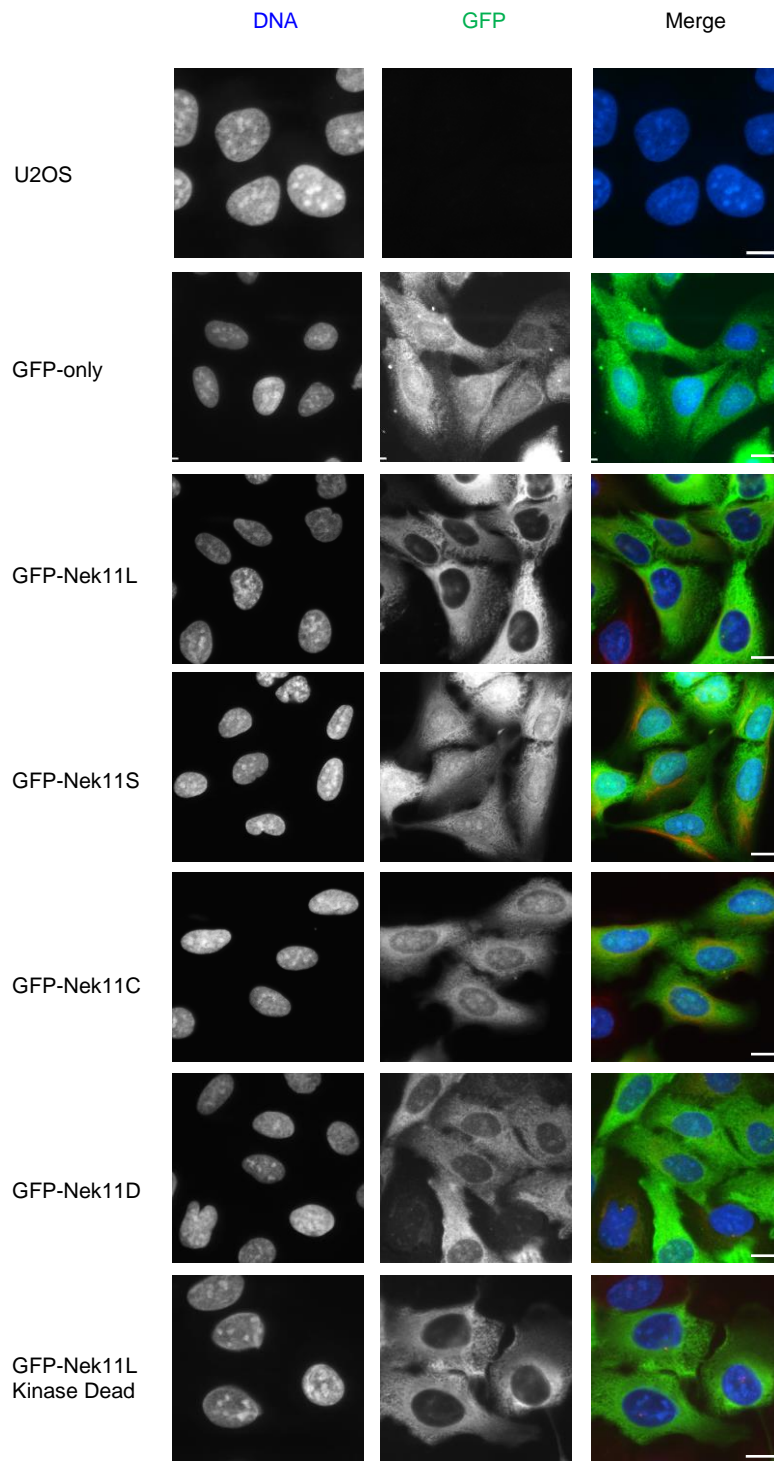


Figure 4.6 Nek11 isoforms exhibit distinct localisation patterns

GFP-Nek11, GFP only and parental U2OS cell lines were fixed and stained with GFP (green) antibody. DNA was stained with Hoechst 33258 (blue). Scale bars, 10 μm .

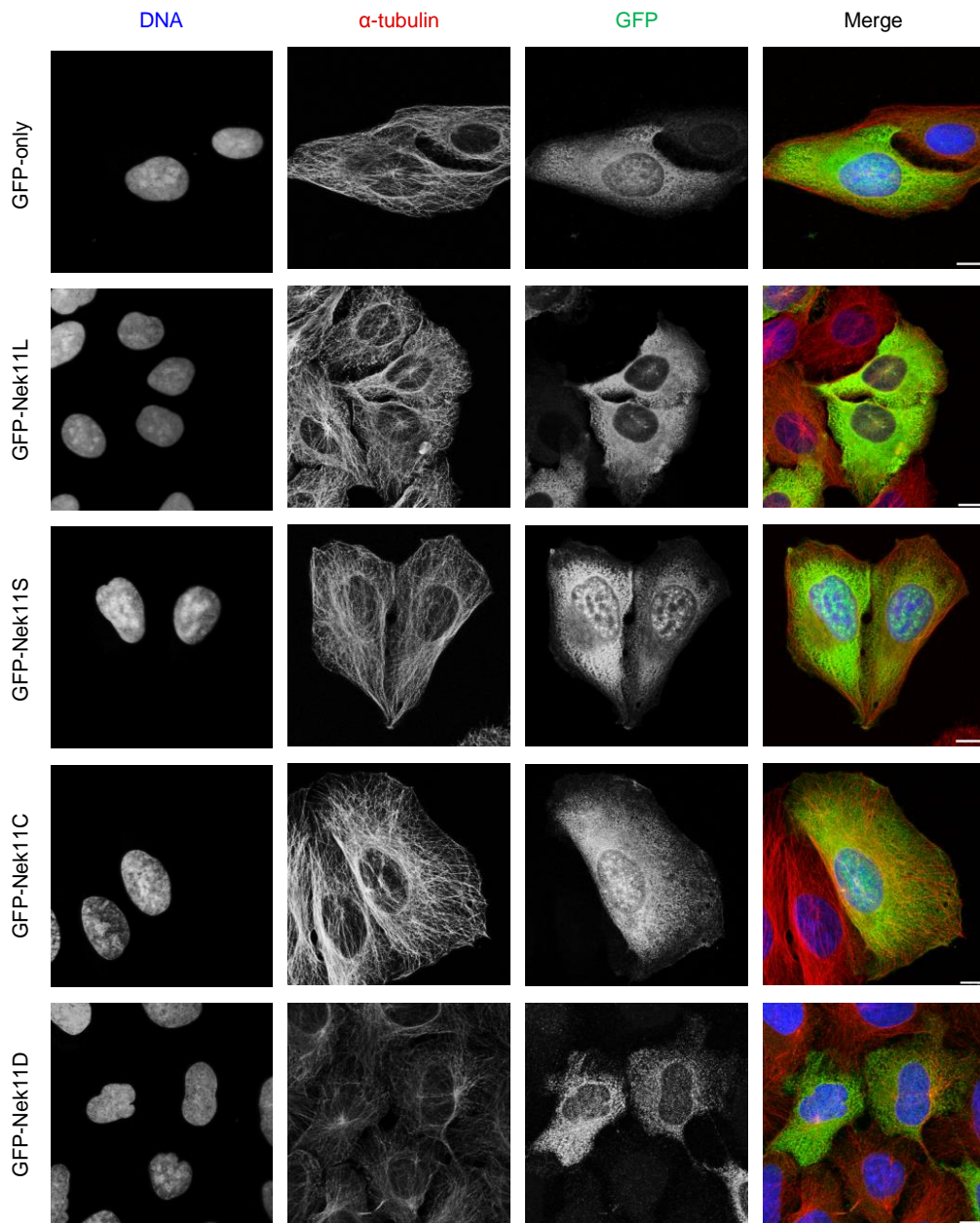


Figure 4.7 Nek11 isoforms do not show localisation to the microtubule network

GFP-Nek11 and GFP-only stable cell lines were fixed and stained with anti- α tubulin (red) to reveal the microtubule network, and anti-GFP (green) antibodies. DNA was stained with Hoechst 33258 (blue). Scale bars, 10 μ m.

Nek11 cell lines were therefore processed for indirect immunofluorescence microscopy and co-stained with anti- γ -tubulin antibody to detect centrosomes (Figure 4.8). This revealed that a small fraction of all the Nek11 isoforms exhibited localisation to the centrosomes. A polyclonal antibody (referred to as 3216) generated in-house by Dr. Navdeep Sahota was then employed to examine endogenous Nek11 protein localisation (Sahota, 2010). Due to the sequence similarity between kinase domains of the human Neks, this antibody was raised against the C-terminal non-catalytic region of Nek11C (aa 287-450): it should therefore be able to recognise all Nek11 isoforms (Figure 4.9A). Indeed, as previously shown in Figure 3.2, this antibody is able to detect endogenous Nek11 proteins by Western blot analysis. Examination of Nek11 protein localisation in U2OS cells by immunofluorescence microscopy with the 3216 antibody revealed localisation of Nek11 to nuclei and strong localisation to centrosomes during interphase and on spindle poles throughout mitosis, as determined by γ -tubulin staining to detect centrosomes (Figure 4.9B). Closer examination of the localisation to centrosomes and spindle poles revealed detection of Nek11 as two dots per centrosome indicating more specific localisation to the centrioles.

Finally, analysis of Z-stacks taken during confocal imaging of GFP-Nek11L stable cells revealed a proportion of GFP signal coming from denser regions of chromatin staining (Figure 4.10A). Therefore, cells were costained with nucleophosmin (NPM), a nucleolar marker (Figure 4.10B). This revealed that a fraction of Nek11L also showed localisation to nucleoli. This is consistent with previous studies by Noguchi et al. (2004).

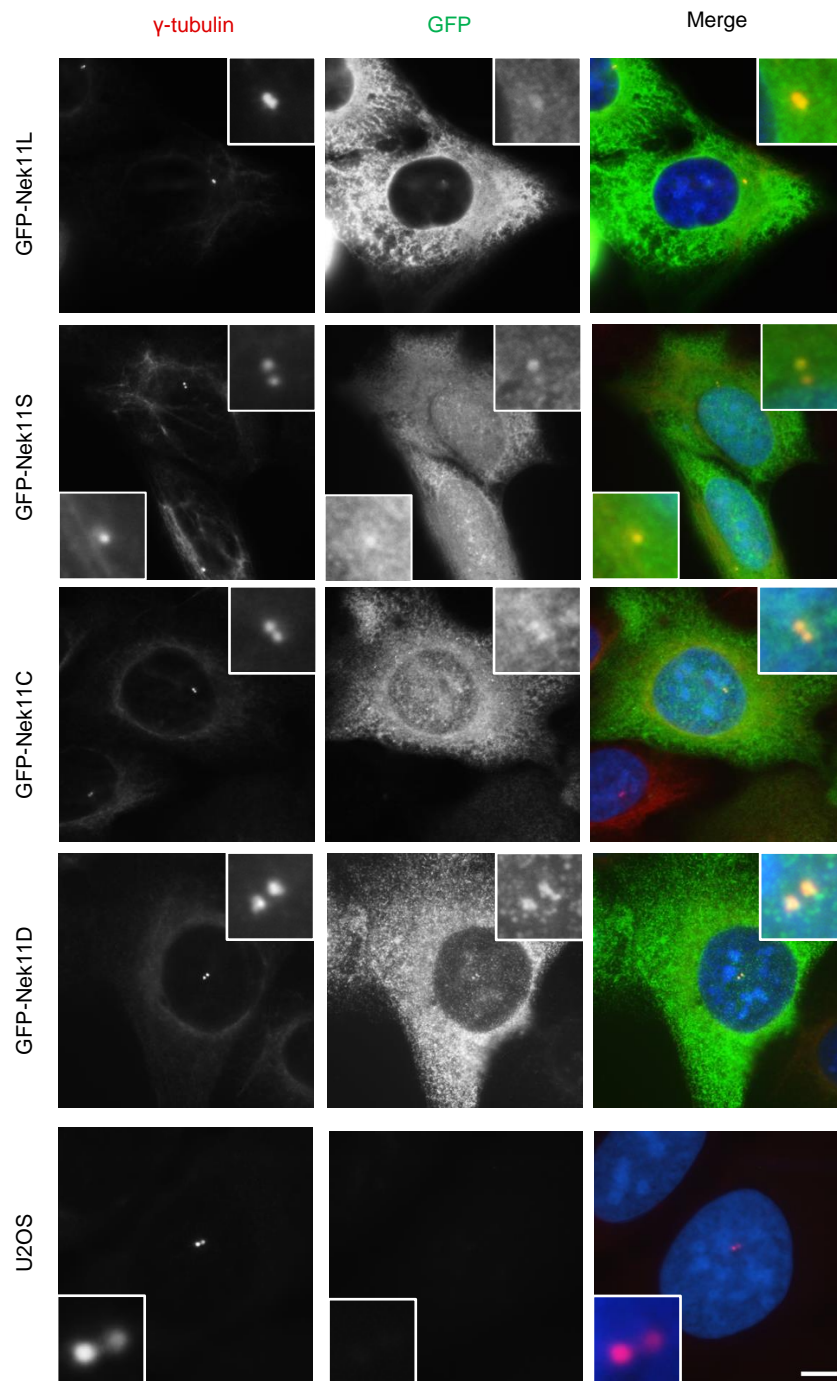


Figure 4.8 Nek11 isoforms show weak localisation to centrosomes during interphase

Parental U2OS and GFP-Nek11 stable cell lines were fixed with methanol and stained with GFP (green) and γ -tubulin (red) to reveal centrosomes. DNA was stained with Hoechst 33258 (blue). Scale bars, 10 μ m.

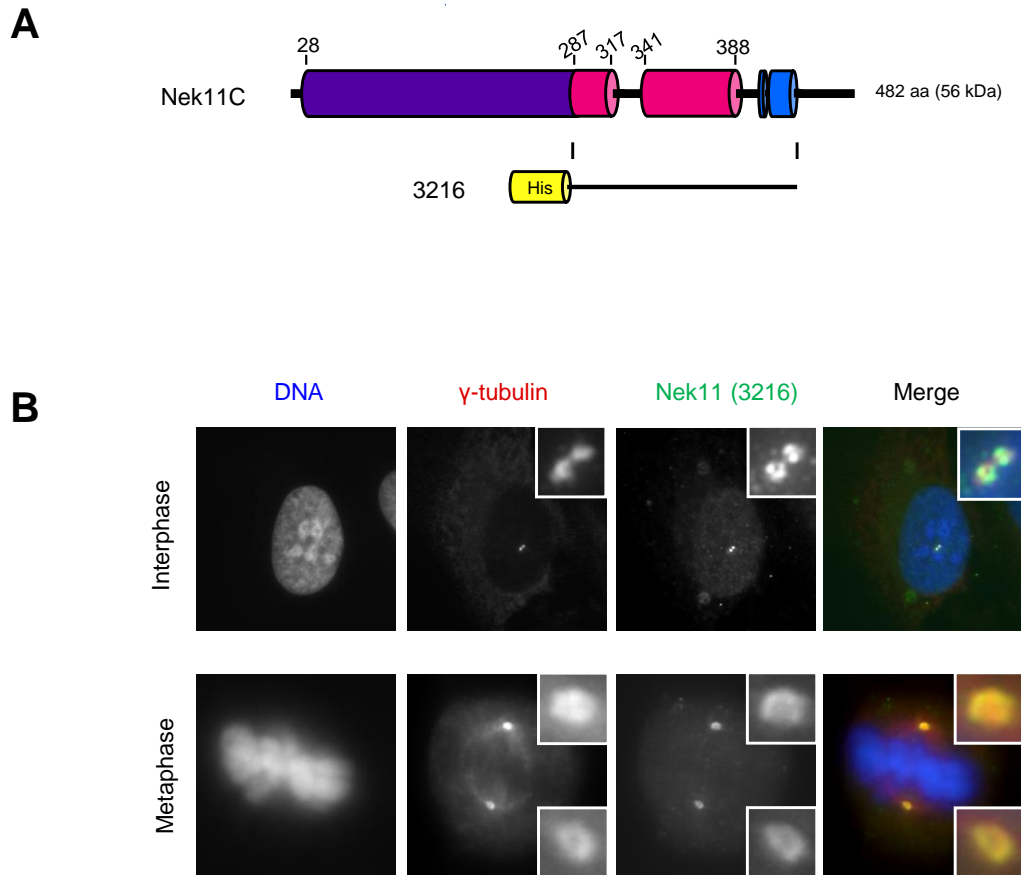


Figure 4.9 Endogenous Nek11 localises to centrosomes in interphase and spindle poles during mitosis

A. Schematic representation of the Nek11C isoform and the His tagged Nek11 (amino acids 288-446) protein used for antibody generation. **B.** U2OS cells were fixed with methanol and immunostained with Nek11 antibody (3216, green) and co-stained with γ -tubulin (red) to detect centrosomes. DNA was stained with Hoechst 33258 (blue).

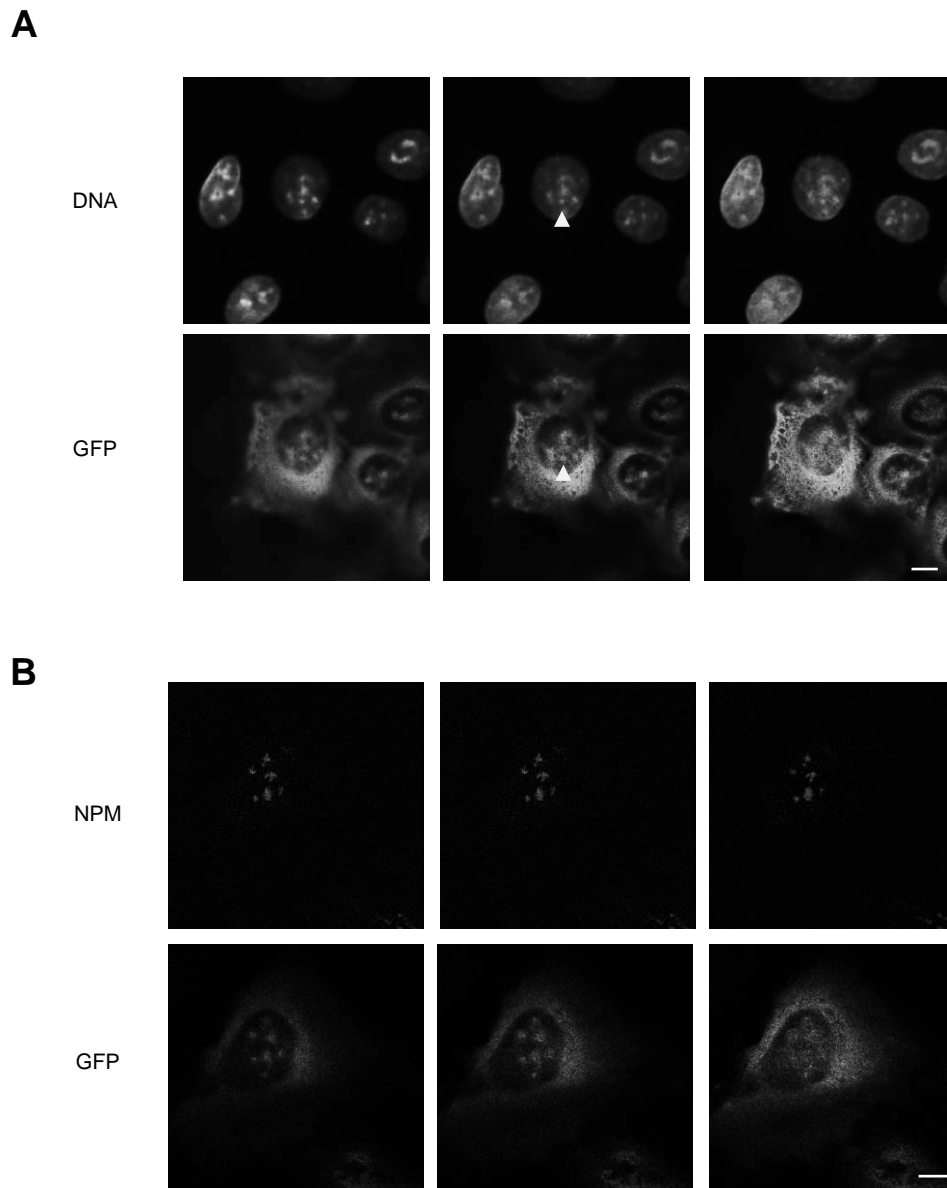


Figure 4.10 GFP-Nek11L localises to nucleoli

GFP-Nek11L stable cells were fixed and processed for analysis by confocal microscopy. **A.** Cells were probed with GFP antibodies and DNA was stained with Hoechst 33258. **B.** Cells were probed with GFP antibodies to detect GFP-Nek11L protein and anti-NPM to visualise nucleoli. In A and B, images show three individual Z-stacks through a cell. Scale bars, 10 μm .

4.2.5 Nek11 isoforms exhibit nucleocytoplasmic shuttling

We next investigated how dynamic these localisation patterns are in order to determine how the isoforms may be regulated. GFP-Nek11 and GFP-only cell lines were treated with the fungicide, Leptomycin B (LMB), which interacts with CRM1, a receptor responsible for nuclear export of proteins with a Leucine-rich NES, and therefore inhibits CRM1-mediated nuclear export. Cells were treated with LMB for 3 hours before fixation and staining with anti-GFP antibodies (Figure 4.11A). Microscope analysis showed that all Nek11 isoforms accumulate in the nucleus upon export inhibition indicating that all isoforms undergo nucleocytoplasmic shuttling. Furthermore, nucleocytoplasmic shuttling of Nek11 is not dependent on kinase activity since Nek11L-KD behaves in a similar manner to wild-type Nek11L. Interestingly, LMB treatment of the GFP-Nek11L, S and C cell lines resulted in close to 100% of cells showing mainly nuclear localisation however only 59.3% of Nek11D expressing cells show predominantly nuclear localisation (Figure 4.11B).

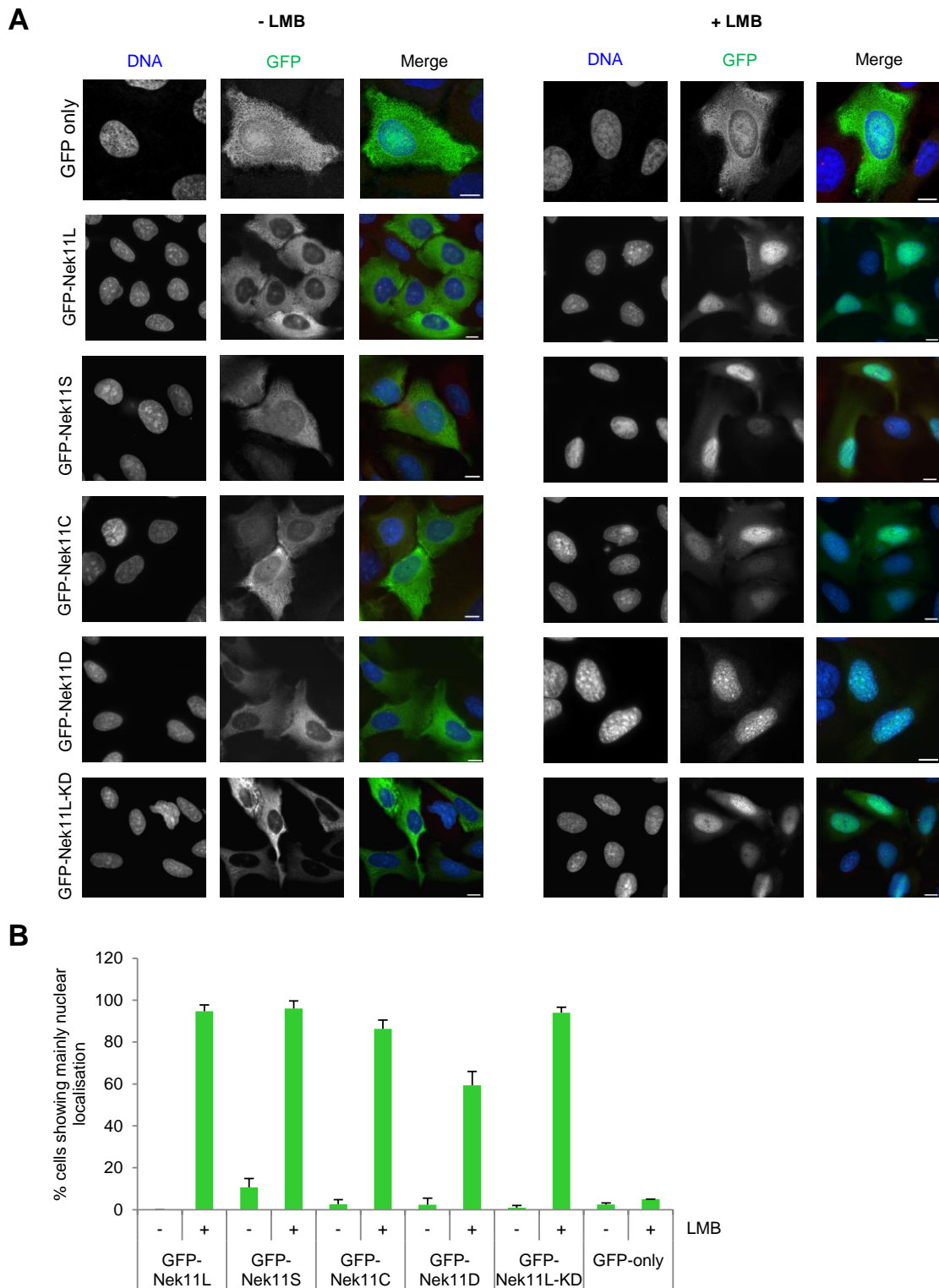


Figure 4.11 Nek11 splice variants exhibit nucleocytoplasmic shuttling

A. GFP-only and GFP-Nek11 stable cell lines were either treated or untreated with LMB (20 ng/ml) for 3 hours before fixation and staining with GFP antibodies (green). DNA was stained with Hoechst 33258 (blue). Scale bars, 10 μ m. **B.** Histogram indicates percentage of cells showing predominantly nuclear localisation. At least 100 cells were counted and data represent means (\pm S.D.) of 3 separate experiments.

To identify the region of Nek11 responsible for the nucleocytoplasmic shuttling, Nek11 protein sequence was scanned for putative nuclear export sequences using the online tool, NetNES 1.1 (<http://www.cbs.dtu.dk/services/NetNES/>) (la Cour *et al.*, 2004). The program identified a strong NES in the Nek11L isoform from residues 624 to 633 (Figure 4.12A). Typically, NES sequences consist of 4-5 hydrophobic residues (especially leucines) (la Cour *et al.*, 2003; Wen *et al.*, 1995). Therefore, leucine residues at 631 and 633 positions of Nek11L were both individually mutated, and mutated in combination, to alanine. The resulting constructs were transiently transfected into U2OS cells and localisation patterns examined. However, mutation of these sites did not affect Nek11L localisation and it remained predominantly cytoplasmic (Figure 4.12B).

We therefore decided to carry out mapping studies using truncated proteins to map regions of the protein required for shuttling. Using the Nek11L isoform, eGFP-tagged constructs of the kinase domain (aa 1-287) and C-terminal domain (aa 288-645) were generated (Figure 4.13A). Transient transfections confirmed the presence of each protein at the predicted molecular weight (Figure 4.13B), and these were then used for indirect immunofluorescence microscopy studies with cells treated with and without LMB. Upon LMB treatment, the kinase domain remained cytoplasmic whereas the C-terminal domain accumulated in the nucleus, thus indicating that nucleocytoplasmic shuttling is dependent on the C-terminal domain (Figure 4.13C and D).

To elucidate the regions responsible, further constructs were generated where the kinase domain and varying lengths of the C-terminal domain were tagged with eGFP. The addition of the kinase domain acted to prevent the smaller C-terminal fragments from passively diffusing through the nuclear pore (Figure 4.14A). After validating the expression of protein with the correct molecular weight by Western blot analysis (Figure 4.14B), U2OS cells were transfected with each construct and treated with LMB as before (Figure 4.14C). GFP-Nek11L 1-341 which includes the first coiled-coil, showed even distribution throughout the cell with and without LMB. This indicates that it must encompass

A

Consensus NES:

L-x(2,3)-[LIVFM]-x(2,3)-L-x-[LI]

Nek11L NES:

L624-L-Y-F-E-E-Q-L-L-I633

B

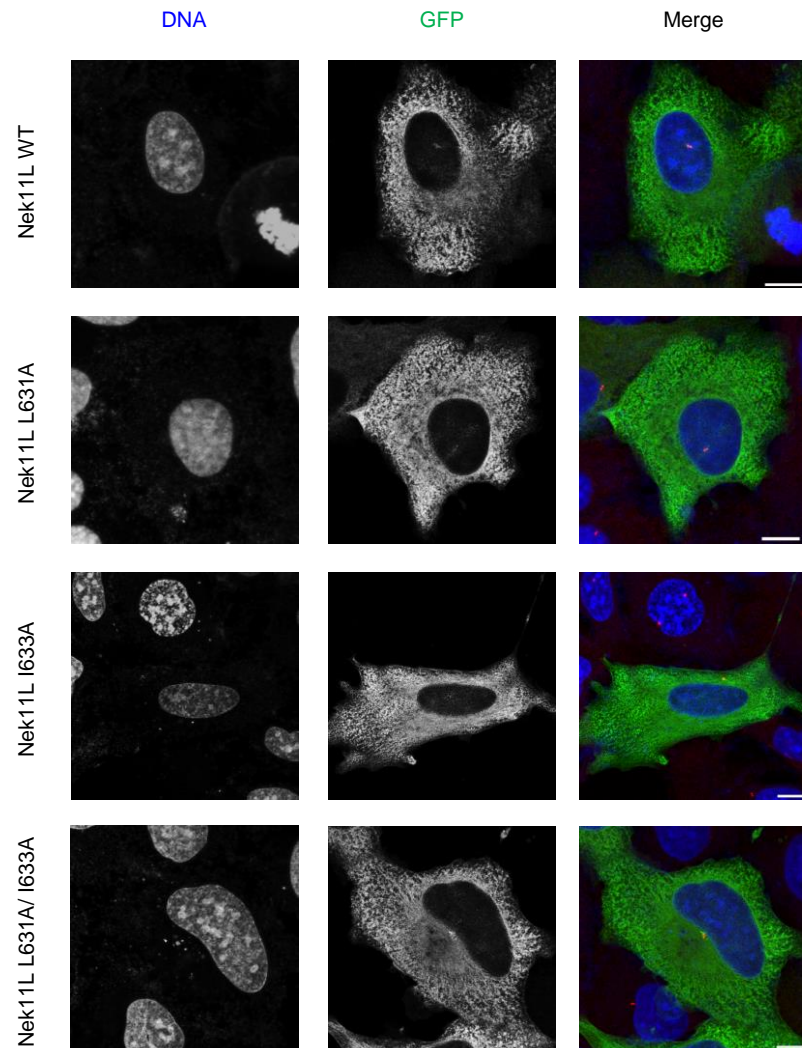


Figure 4.12 Cytoplasmic localisation of Nek11L is not affected by mutation of a putative nuclear export sequence

A. Putative NES sequence in Nek11L isoform predicted using NetNES 1.1. **B.** U2OS cells were transiently transfected with GFP-Nek11L constructs indicated and fixed after 24 hours before being processed for immunofluorescence microscopy. GFP-tagged proteins were stained with anti-GFP antibodies (green). DNA was stained with Hoechst 33258. Scale bars, 10 μ m.

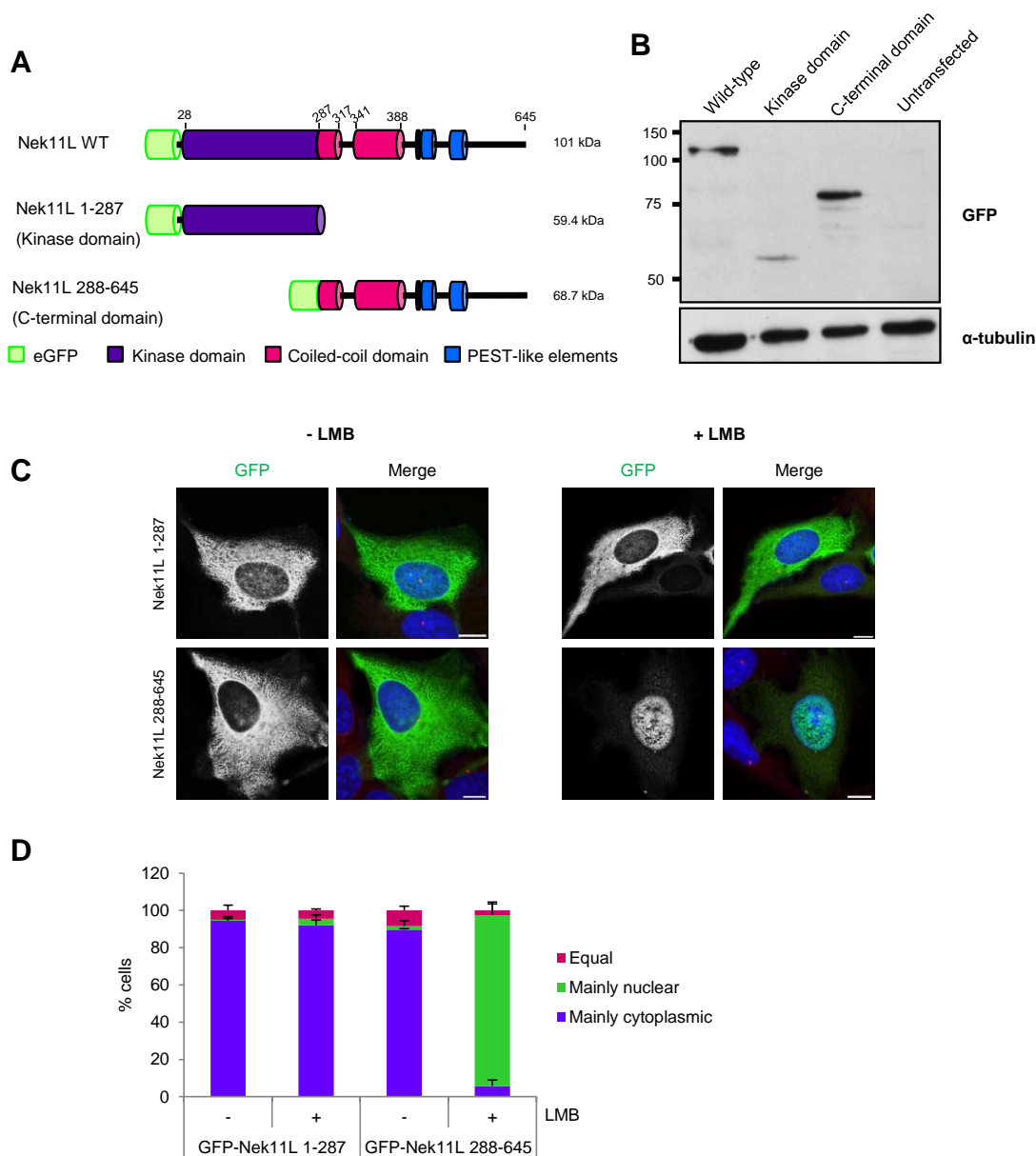


Figure 4.13 The non-catalytic domain of Nek11L is responsible for nuclear localisation

A. Schematic of GFP-Nek11L constructs generated to examine subcellular localisation. Predicted molecular weights are indicated. U2OS cells were transiently transfected with indicated GFP-tagged constructs. After 24 hours, cells were either **(B)** lysed and analysed by SDS-PAGE and Western blotting using antibodies indicated (molecular weights are shown, kDa), **(C)** left untreated or treated with LMB for 3 hours before fixation and staining with GFP antibodies (green). DNA was stained with Hoechst 33258 (blue). Scale bars, 10 μ m. **D.** Histogram indicates percentage of cells showing mainly nuclear, cytoplasmic or equal distribution for experiment in C. At least 100 cells were counted and data represent means (\pm S.D.) of 2 separate experiments.

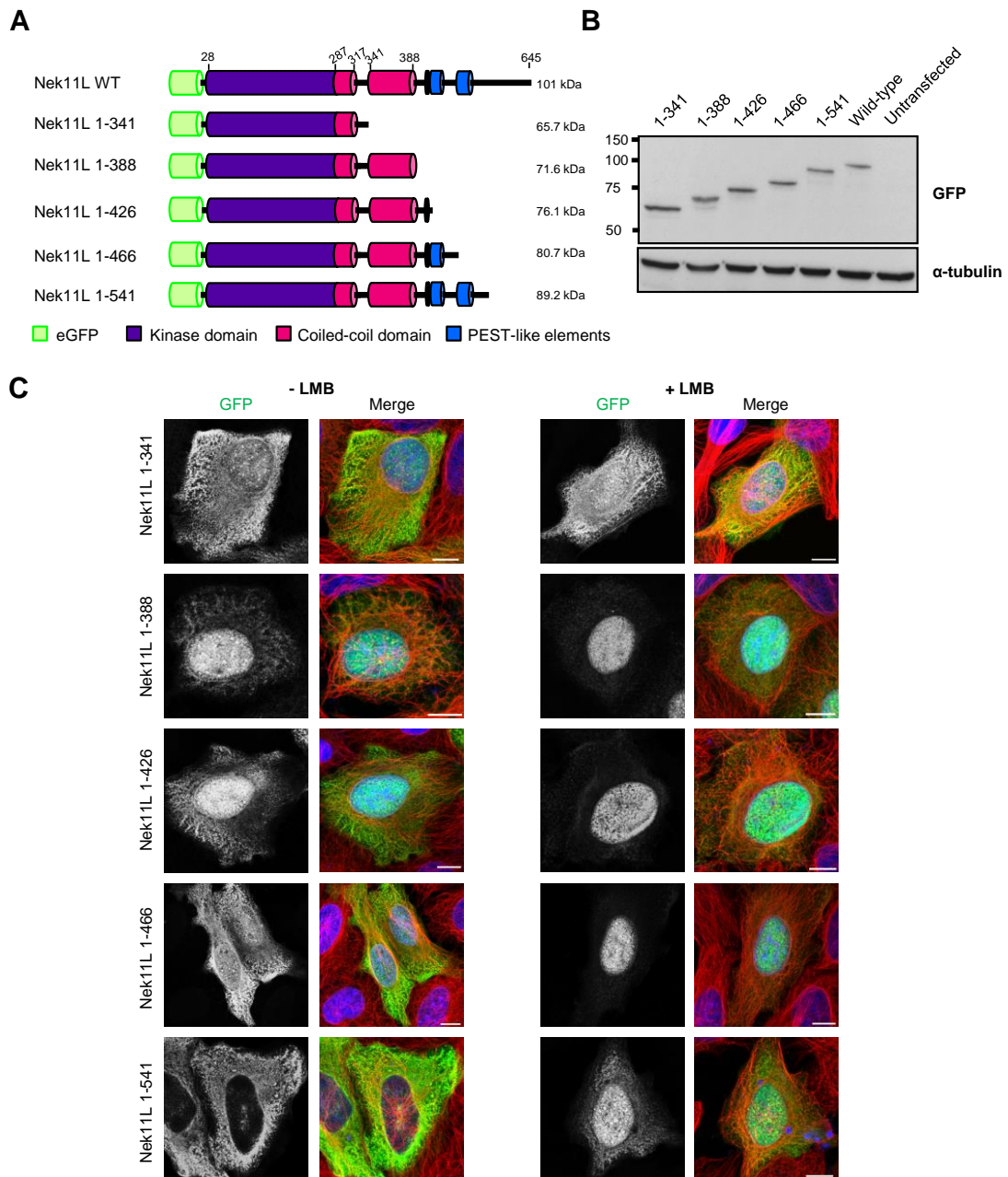


Figure 4.14 Non-catalytic domain constructs reveal nuclear targeting and export sequences

A. Schematic of GFP-Nek11L constructs generated to examine subcellular localisation. Predicted molecular weights are indicated. U2OS cells were transiently transfected with indicated GFP-tagged constructs. After 24 hours, cells were either **(B)** lysed and analysed by SDS-PAGE and Western blotting using antibodies indicated (molecular weights are shown, kDa), or, **(C)** left untreated or treated with LMB for 3 hours before fixation and staining with GFP antibodies (green). DNA was stained with Hoechst 33258 (blue). Scale bars, 10 μm .

a weak or part of a nuclear localisation signal, since the kinase domain alone showed only cytoplasmic localisation. Extending this to include the second coiled-coil domain resulted in protein localising to the nucleus in the absence of LMB treatment indicating the presence of a strong nuclear targeting signal and the absence of a nuclear export signal since this protein is unable to enter the cytoplasm. Extended further up to amino acid 466, the residue after which the Nek11 isoforms differ in amino acid sequence, revealed localisation to the nucleus and cytoplasm indicating the additional presence of a weak export sequence. Extending this yet again to residue 541, where Nek11L and Nek11D sequences diverge, results in full restoration of cytoplasmic localisation (Figure 4.14C).

4.2.6 IR exposure leads to Nek11 recruitment to sites of DNA damage

Due to the role of Nek11 at the G2/M checkpoint after DNA damage and the fact that we see dynamic movements of Nek11, we next examined whether Nek11 localisation changes after DNA damage. Using GFP-Nek11L and GFP-only stable cell lines, cells were irradiated with 10 Gy and fixed through a time-course of 24 hours. Cells were then stained with anti-GFP antibodies to detect recombinant protein and anti- γ -H2AX antibodies, a marker of DNA damage (Figure 4.15). At first glance, the majority of Nek11L protein remained cytoplasmic throughout the time-course, even though DNA damage was present throughout as indicated by γ -H2AX foci. Looking more closely, however, at the 7 hour time-point Nek11L, and not GFP-only, could be seen to co-localise with γ -H2AX foci (Figure 4.15A). Furthermore, quantitative analysis across a number of foci confirmed a correlation in relative intensities between γ -H2AX and Nek11L protein (Figure 4.15B).

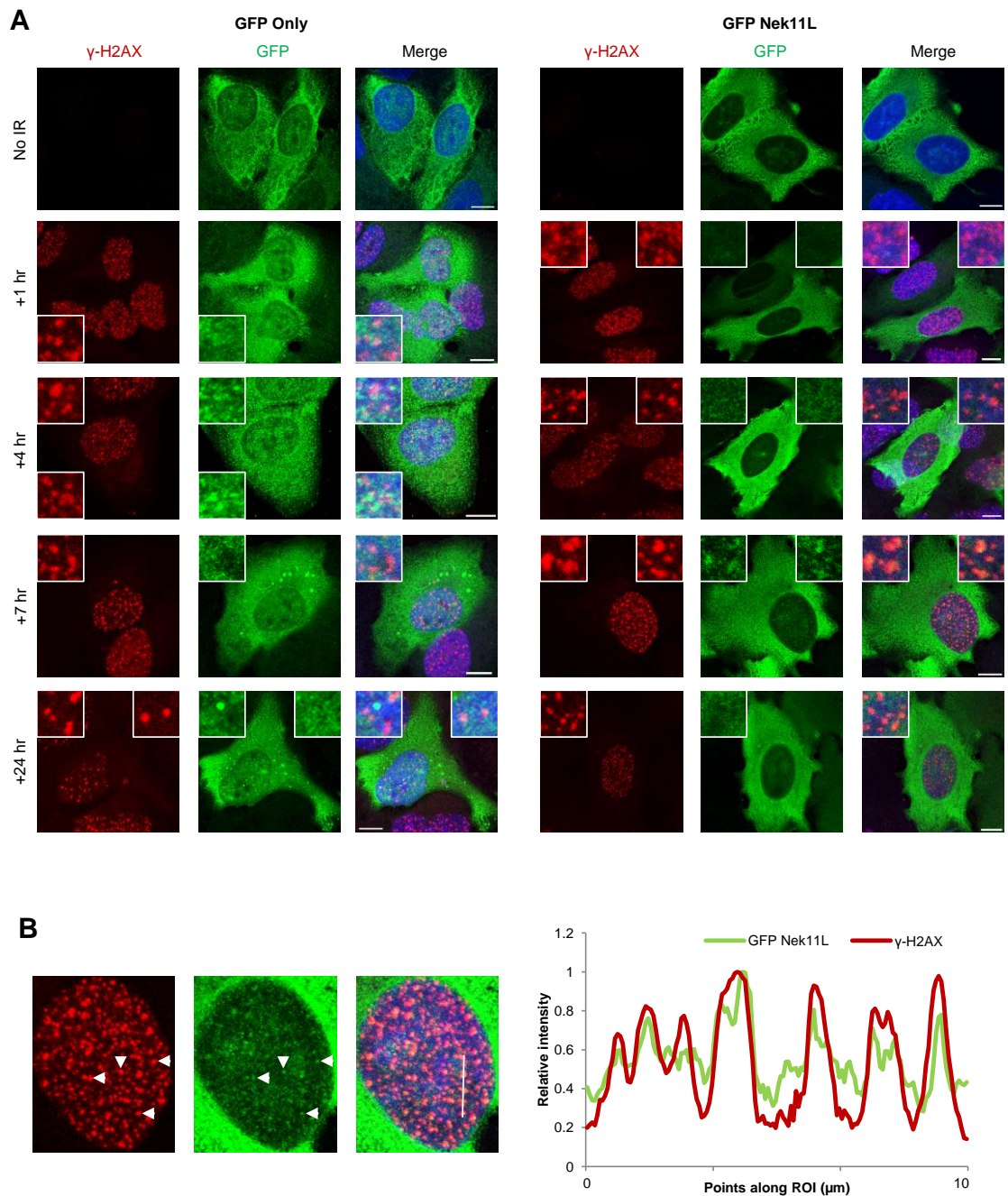


Figure 4.15 Nek11 is recruited to DNA damage foci upon IR treatment

A. U2OS:GFP-Nek11L stable cells were either untreated (No IR) or irradiated with 10 Gy and fixed at times indicated post-IR. Cells were immunostained stained with GFP (green) and γ -H2AX (red) antibodies. Merged images include DNA stain (blue). Insets show magnified views of γ -H2AX foci. Scale bars, 10 μ m. B. Left panel is a magnification of GFP-Nek11L cells at 7 hr timepoint in A. White arrowheads indicate specific γ -H2AX foci. Right panel shows intensity measurements for γ -H2AX (red) and GFP (green). These were determined along a 10 μ m linear region of interest and normalised for each channel. ROI used is indicated by white line on merge image in left panel.

4.2.7 Overexpression of Nek11L causes G2/M arrest and polyploidy

We next asked what effect overexpression of Nek11 isoforms would have on the G2/M checkpoint or the cell cycle in general. For this we used the stable U2OS cell lines expressing GFP-Nek11L, GFP-Nek11S or GFP-Nek11L-KD. Cells were fixed and processed for cell cycle analysis before also sorting into GFP high-expressing and GFP low-expressing cells (Figure 4.16A). Comparison with parental U2OS cells reveal that cells expressing low levels of GFP-Nek11L exhibited a marked increase in the percentage of cells at G2/M from 21.3 to 36.9%. A significant change in the G2/M population was not observed in cells expressing low levels of GFP-Nek11S. In addition, there was no change in cells expressing the catalytically inactive Nek11L, meaning that this delay was dependent on Nek11L kinase activity. Examination of high expressing cells showed a more substantial G2/M arrest with the wild-type Nek11L (42.5%), but still no change in cells expressing Nek11S or catalytically-inactive Nek11L (Figure 4.16B).

Unexpectedly, we also observed the presence of a polyploid population in the active Nek11L cell line (Figure 4.16A, indicated by arrow). Low expressing GFP-Nek11L cells exhibited around 3-fold increase in percentage of polyploid cells compared to the parental cell line, while highly-expressing GFP-Nek11L cells exhibiting DNA content greater than 4N, showed a 12-fold increase over the parental cells (Figure 4.16C). Cells expressing high, but not low, levels of Nek11S or catalytically-inactive Nek11L also begin to reveal a polyploid population showing ~4-5 fold increase over the parental cells.

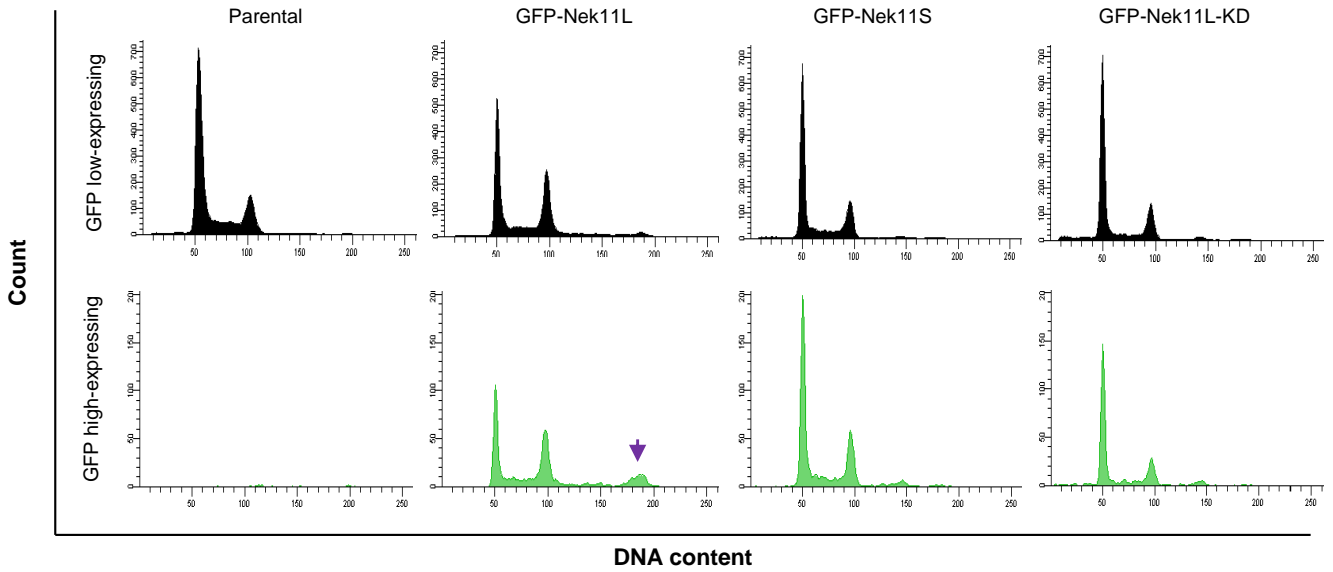
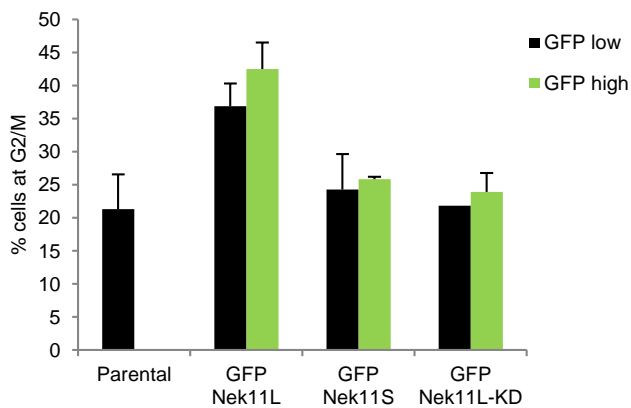
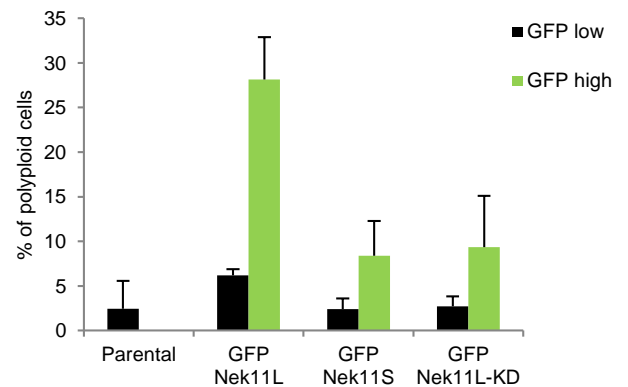
A**B****C**

Figure 4.16 Nek11L overexpression induces G2/M arrest and polyploidy

A. Parental U2OS cells or GFP-Nek11L, GFP-Nek11S or GFP-Nek11L-KD stable U2OS cell lines were analysed by flow cytometry. Cells were sorted for low and high GFP expression with a gate set such that 5% of parental U2OS cells scored positive. Arrow indicates polyploid population. **B.** Histogram represents % G2/M cells from A. **C.** Histogram represents % cells exhibiting $>4n$ DNA from A. Data from B and C represents means (\pm S.D.) of 3 separate experiments.

4.3 Discussion

Through generating stable cell lines that express each of the Nek11 variants we have examined the subcellular localisation of the four different isoforms as well as the effect of Nek11 overexpression on the cell cycle. We show that the Nek11 variants exhibit distinct localisation patterns and although no clear localisation is seen to microtubules, all of the isoforms are able to localise to centrosomes. In addition, all variants are able to undergo nucleocytoplasmic shuttling and this is regulated by the C-terminal domain. Interestingly, we reveal the exciting finding that, upon ionising radiation treatment, Nek11L relocates to sites of DNA damage.

Nek11 is expressed as at least four alternatively spliced variants, Nek11L, Nek11S, Nek11C and Nek11D ((Noguchi *et al.*, 2002), and this study). These differ only in amino acid sequence in the C-terminal regions and, interestingly, this difference is sufficient for the Nek11 isoforms to exhibit distinct localisation patterns. The longer isoforms, Nek11L and Nek11D, are predominantly cytoplasmic, whilst Nek11S and Nek11C exhibit a more even distribution across the cell showing localisation to both the nucleus and cytoplasm. Our data indicate that the C-terminal regulatory domain is responsible for these differential patterns and suggest that there may be potential differences in the roles, regulation and interacting partners of the Nek11 isoforms in the cell. Additionally, these patterns are dynamic since inhibition of nuclear export increased the amount of recombinant Nek11 isoforms in the nucleus. Quantitative analysis revealed that Nek11D was less efficient at this accumulation and this may be due to the fact that we see proteasomal degradation of this variant in cells.

It is interesting that we see degradation of Nek11D and not Nek11L since these proteins are identical in sequence up to amino acid 541, after which Nek11D continues for 58 aa and Nek11L for 104 aa. They both contain three PEST-like elements, and searches for additional degradation motifs, such as D-box or

KEN boxes, specific to Nek11D only revealed the presence of two putative D-box sequences in regions that are identical in both isoforms. It may be possible that the longer C-terminal stretch of the Long isoform is able to mask potential degradation motifs where the D isoform cannot and this would fit with the model introduced by Noguchi *et al.* suggesting that the C-terminal domain makes an intramolecular interaction with the N-terminal catalytic domain to inhibit kinase activity (Noguchi *et al.*, 2004).

Regions required for nucleocytoplasmic shuttling were identified by mapping studies using truncated Nek11 recombinant proteins. Our data indicates that there is a nuclear import signal present in the coiled-coil regions and a nuclear export signal present from residues 427-466 (Figure 4.17A). These regions are present in all Nek11 isoforms and explains why they all exhibit shuttling. After examining these regions further we identified a weak putative NES sequence present from residues 447 to 455 (Figure 4.17B). Next, using a cNLS mapper tool online (http://nls-mapper.iab.keio.ac.jp/cgi-bin/NLS_Mapper_form.cgi) (Kosugi *et al.*, 2009) residues 321 to 363 were identified to contain a potential bipartite nuclear localisation sequence. Closer examination of the residues in this region confirmed that approximately 33% of the residues here are basic and, although a canonical NLS [(K/R)(K/R)X₁₀₋₁₂(K/R)_{3/5}] was not identified, the residues in the C-terminal region of this area closely matches one (Figure 4.17C). Sequence logos generated by a collective study on proteins containing NES signals, found that for residues in the sequence that were not hydrophobic, the most common residues identified were either glutamate, aspartate and serine (la Cour *et al.*, 2004); this seems to fit with the weak NES identified here. To confirm whether this is true, mutagenesis of key residues would need to be carried out. On the other hand, these regions may be required for interaction with other proteins that shuttle in and out of nuclei. Furthermore, homo-oligomer formation of Nek11L in nocodazole-arrested cells was detected via co-immunoprecipitation assays, suggesting that Nek11 is able to dimerize and this could hint at a possible method for nuclear shuttling (Noguchi *et al.*, 2004).

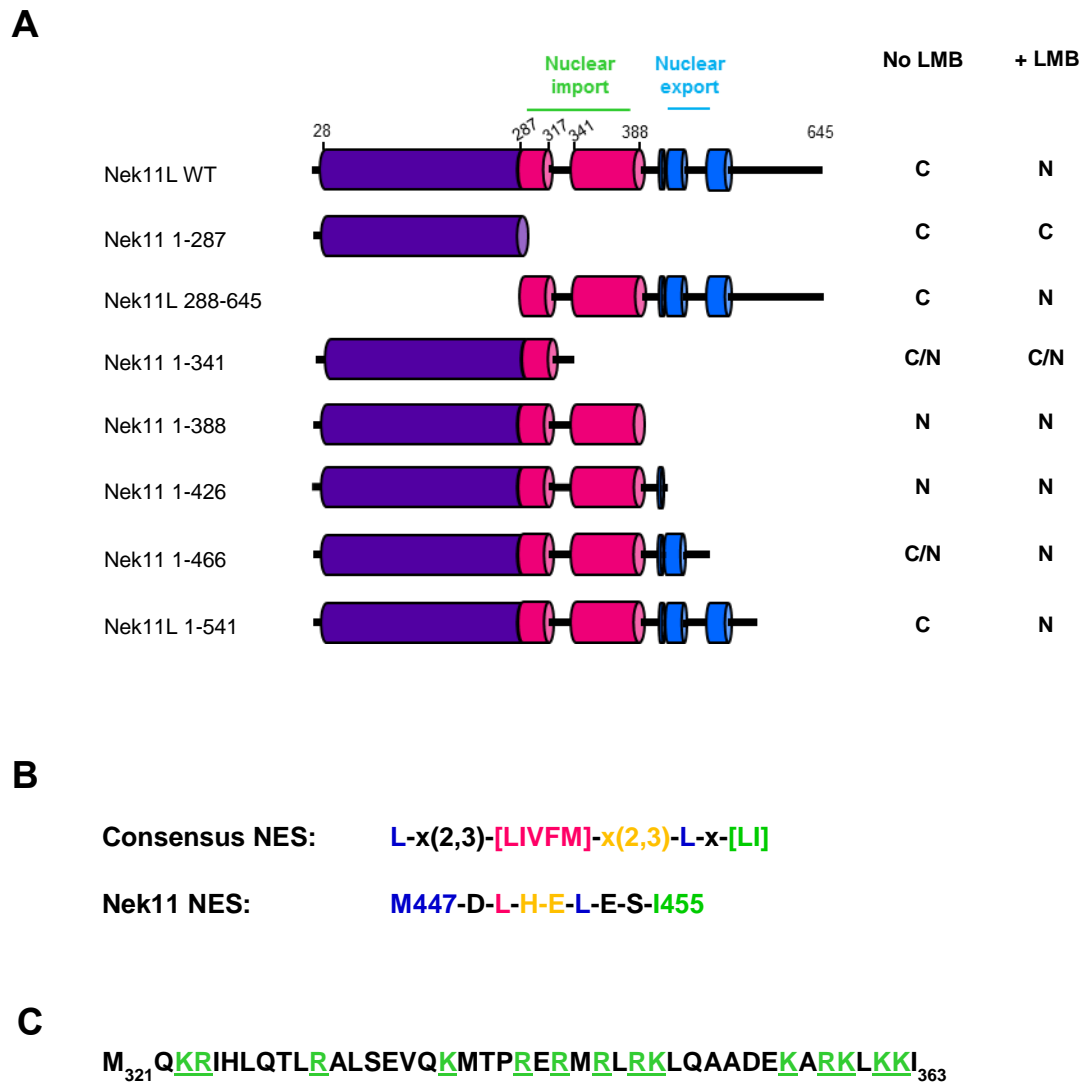


Figure 4.17 The non-catalytic domain of Nek11 contains both nuclear import and export sequences

A. Schematic representation of GFP-Nek11L constructs used to examine subcellular localisation. Predominant localisation to cytoplasm (C), nucleus (N) or equal distribution (C/N) \pm LMB treatment are indicated. **B.** Putative weak NES sequence in Nek11 predicted using NetNES 1.1. **C.** Putative nuclear localisation sequence predicted using cNLS mapper.

The regions identified for nuclear targeting and protein export are present in all four isoforms, therefore the question remains as to why the isoforms exhibit differential localisation patterns in untreated cells. One reason may be due to the different amino acid sequences at the C-terminal ends of each isoform and the possibility that additional localisation signals may be present. In the case of Nek11L, we identified another, NES signal between residues 624 and 633. However, subsequent mutation of key hydrophobic leucines did not affect its localisation. It was concluded, therefore, that mutation of this site alone is not sufficient to affect its nuclear export. Another possibility for different localisation patterns could be due to the length of the C-terminal tails. Evidence suggests that the export sequence in the shorter variants is less efficient since experiments with a construct of similar size (GFP-Nek11 1-466) exhibited equal distribution throughout the cytoplasm and nucleus much like the full-length Nek11S and Nek11C protein. When this was extended by 75 amino acids, the localisation then became cytoplasmic, much like the Nek11L and Nek11D isoforms. One explanation may be that the longer C-terminal domain found in Nek11L and Nek11D isoforms creates a structure that is more easily recognisable by export partners, and therefore allows for more efficient export.

Looking more closely at localisation patterns, the Nek11L isoform also showed localisation to nucleoli, this is consistent with the study by Noguchi *et al.* (2004), who found Nek2A to colocalise with Nek11 at nucleoli. It could also suggest that Nek11 plays additional roles here, as the yeast homologue, Kin3, was found to interact with the nucleolar protein, Nog1, involved in ribosome biogenesis (Uetz *et al.*, 2000; Kallstrom *et al.*, 2003). In addition, recombinant Nek11 isoforms show localisation to centrosomes during interphase. This is not an uncommon feature of the mammalian Neks with a number of them playing key roles in centrosome separation and spindle assembly (Fry *et al.*, 1998b; O'Regan & Fry, 2009; Roig *et al.*, 2005; Kim *et al.*, 2007; Mahjoub *et al.*, 2005; Otto *et al.*, 2008). It is possible therefore, that Nek11 may play a role here in similar processes. Utilisation of the 3216 antibody to detect endogenous Nek11 revealed a predominantly nuclear localisation of Nek11 consistent with previous

studies by Noguchi *et al.* (2002). This localisation is also similar to that of Nek11S and Nek11C exogenous protein, suggesting that the shorter isoforms may be more abundant in U2OS cells. Consistent with recombinant protein localisation Nek11 was also detected at the centrosomes but more specifically Nek11 was observed at a 2 to 1 ratio to γ -tubulin dots indicating potential localisation to the centrioles. This should be confirmed by co-staining with centriolar markers, such as centrin.

To date, Nek1, Nek8, Nek10 and Nek11 have been implicated in the DNA damage response (Noguchi *et al.*, 2002; Polci *et al.*, 2004; Choi *et al.*, 2013; Moniz & Stambolic, 2011; Melixetian *et al.*, 2009). Out of these, only the localisation effects of Nek1 in response to DNA damage has been studied. In response to IR, UV, etoposide and cisplatin treatments, Nek1 shifts from being cytoplasmic to localising to sites of DNA damage within minutes, with the intensity of Nek1 at nuclear foci increasing over time after insult (Polci *et al.*, 2004; Chen *et al.*, 2008a). Due to the observation that Nek11 isoforms exhibit nucleocytoplasmic shuttling we examined whether the presence of DNA damage would cause re-localisation of Nek11. Interestingly, whilst the majority of Nek11L protein remains cytoplasmic up to 24 hours post DNA damage induction with IR, a small amount of protein localises to sites of DNA damage identified by co-staining with the DNA damage marker, γ -H2AX. This re-localisation is first observed at the 7 hour time-point and seems to have dissipated after 24 hours. In contrast to Nek1 being involved early in the DNA damage sensing pathway, this suggests that Nek11 may play an additional role in the later stage of the DDR, hence concluding that Nek11 is not part of the initial recognition machinery. It may possibly be involved in the late recognition of DSBs to maintain the DNA damage checkpoint or be involved in DNA repair. To discriminate between localisation to SSBs or DSBs, p-RPA and 53BP1, respectively could be employed. On the other hand, it is possible that it is present at sites of DNA damage at earlier times but at lower undetectable levels. What is still unclear though, and would be interesting to follow up, is whether this localisation to foci is required for Nek11's role in the DNA damage

checkpoint. This could be investigated through expression of mutants that affect its localisation to DNA damage foci. In addition, future studies would need to examine whether all isoforms exhibit similar localisation to foci and whether Nek11 kinase activity is required for this localisation. It is also important to assess lower doses of IR that are clinically relevant to allow analysis in the context of DNA repair. Finally, to determine the functional role for Nek11 at DNA damage foci the identification of potential binding partners would be a useful next step.

Finally, using the stable cell lines generated we examined the effect of Nek11 overexpression on the cell cycle. Consistent with results of depletion, overexpression in U2OS cells showed that Nek11 is involved in progression of cells past the G2/M checkpoint. This is based on observing an increased fraction of cells expressing active Nek11L at this stage. However, this was not seen for cells expressing Nek11S, even though in the depletion studies it appeared to have a strong role at the G2/M checkpoint in HCT116 cells. One possible reason for this difference may be the differences in cell types used as isoform expression may vary dependent on cell type. In addition, overexpression studies were carried out in the absence of DNA damage so it may be possible that Nek11S only plays an active role at the G2/M in the presence of DNA damage. Unexpectedly though, overexpression of the active Nek11L variant also resulted in a high percentage of polyploid cells. Cells become polyploid through a number of means including viral-induced cell fusion, cytokinesis failure and endoreduplication (Ganem *et al.*, 2007). These data therefore suggest that the presence of too much Nek11 protein could play a role in contributing to polyploidy and could potentially be a cause for cancer cell transformation. The delayed G2/M progression and induction of polyploid cells in response to Nek11L overexpression occurs in an activity dependent manner, since overexpression of the inactive version of Nek11L did not reveal the same effects. Therefore, this suggests that in undamaged cells Nek11 has a level of basal activity that is required for cell cycle progression and cell division.

CHAPTER 5 IDENTIFICATION OF NOVEL NEK11 BINDING PARTNERS USING IP-MS ANALYSIS

5.1 Introduction

The human genome encodes 518 protein kinases representing approximately 1.7% of all human proteins. These play roles in multiple cellular processes including cell cycle progression, apoptosis, cell signalling, metabolism and cellular differentiation (Manning *et al.*, 2002). As a result, mutation or deregulation of kinases can cause pathological changes within a cell thus leading to disease (Cohen, 2002). It is estimated that kinases modify at least 50% of all cellular proteins (Kornev & Taylor, 2010). However, many of the protein phosphorylation networks remain to be elucidated, and this in part is due to the difficulty in studying such events in a physiological setting. For example, regulation of proteins through phosphorylation may occur at specific cell cycle stages or in response to specific stimuli, and this serves to increase or decrease the affinity for their target proteins. In many cases such as in signalling cascades, this interaction is weak or transient (Berggard *et al.*, 2007). Thus, the ability to successfully isolate such an interaction relies in part on cell cycle stage, protein modification, and affinity of the interaction.

Protein function of single proteins is commonly determined through RNAi depletion studies. However, it is estimated that more than 80% of proteins operate as part of a complex (Berggard *et al.*, 2007). Therefore, combining functional studies with the identification of potential interacting partners is particularly helpful in elucidating a protein's role in the cell and determining how it may be regulated within a specific pathway. Numerous methodologies to examine protein interactions have been developed, and increasingly, a commonly used tool is mass spectrometry after affinity purification of a protein of interest from cells or tissue (Gingras *et al.*, 2005).

At the time of this study, Nek11 interaction studies were limited and so far no such large-scale interaction studies had been carried out. Interaction of Nek11 with another human NIMA-related kinase member, Nek2A, was proposed due to the observation that both proteins localised at nucleoli. Co-immunoprecipitation studies confirmed complex formation, with strongest interaction detected in G1/S-arrested cells (Noguchi *et al.*, 2004). Truncation studies identified that interaction occurred through the non-catalytic domains of Nek2 and Nek11. Furthermore, active Nek2 was found to directly phosphorylate Nek11 on multiple serine residues as determined by phosphoamino acid analysis, thereby activating it (Noguchi *et al.*, 2004). The significance of the interaction at nucleoli was not determined; however, it was noted that the yeast NIMA-related kinase, Kin3, is able to interact with nucleolar Nog1, which plays a role in ribosome biogenesis (Uetz *et al.*, 2000; Park *et al.*, 2001). Additionally, Kin3 can also interact with Tem1, a mitotic GTP-binding protein, and both Tem1 and Nog1 can interact with Fob1, a nucleolar protein involved in blocking DNA replication fork progression (Kobayashi & Horiuchi, 1996). Interestingly, Fob1 can interact with Rad53, a DNA damage checkpoint kinase (Uetz *et al.*, 2000). It was suggested that Kin3 may be involved in a signalling pathway that links ribosome biogenesis and the DNA replication checkpoint and a conserved role may exist for nucleolar Nek11 in mammalian cells given its activation in G1/S arrested cells (Noguchi *et al.*, 2004).

As discussed earlier, in 2009, a shRNA library screen for novel G2/M checkpoint components identified Nek11 as a protein required for cell cycle arrest after IR (Melixetian *et al.*, 2009). Transition from G2 to M phase of the cell cycle requires the activation of the Cdk1-Cyclin B complex and this is carried out through removal of inhibitory phosphate groups on Cdk1 by Cdc25 phosphatases. Upon DNA damage, Chk1 is phosphorylated and activated by the ATM/ATR kinases, and this then phosphorylates Cdc25A at S76. Chk1 also phosphorylates Nek11 at S273 thereby activating it and Nek11 then phosphorylates Cdc25A on S82 targeting it for degradation (Melixetian *et al.*, 2009). Furthermore, depletion of Nek11 leads to Cdc25A protein stabilisation

upon DNA damage. Therefore, Nek11 was placed in the G2/M DNA damage checkpoint response pathway downstream of Chk1 and upstream of Cdc25A. Evidence for complex formation between Nek11 and either Chk1 or Cdc25A has thus far not been provided. However, given the rapid turn-over rate of Cdc25A and the multiple roles of Chk1, complex formation may be short-lived. More recently, Nek11 was found to phosphorylate the Bloom syndrome helicase, BLM and promote its interaction with TopBP1, a protein required for the replication stress response (Wang *et al.*, 2013).

Together, the pathways and interactions identified so far reveal important insights into Nek11 function. However, the data are limited and there is plenty of potential for more interactions to be discovered. In this chapter, we use IP-mass spectrometry (IP-MS) analysis with the aim to identify novel interacting partners of Nek11 and thereby learn more about Nek11 functions in the DDR or within other cellular pathways.

5.2 Results

5.2.1 Small-scale optimisation of Nek11 immunoprecipitation

In order to identify novel Nek11 binding partners, we utilised immunoprecipitation to purify Nek11 protein and interacting partners through co-immunoprecipitation. Ideally, to reduce non-specific interactions from overexpression of protein, endogenous Nek11 should be isolated. An in-house generated antibody against Nek11 (3216), was used to examine immunoprecipitation of endogenous Nek11. U2OS cells were either untreated or transiently transfected with GFP-Nek11L before soluble lysates were subjected to immunoprecipitation with the Nek11 antibody. Western blot analysis with anti-GFP and anti-Nek11 antibodies showed that GFP-Nek11L protein was successfully immunoprecipitated from lysates with the Nek11 antibody. Endogenous Nek11 was also detected in bound samples but the protein level was very low (Figure 5.1, blue arrow). In order to observe sufficient protein for mass spectrometry analysis as judged by Coomassie Blue staining, a large amount of cells and antibody would be needed. Therefore, we decided to utilise the U2OS:Nek11 stable cell lines instead in order to bulk up protein more easily and act as a starting point for identification of potential partners. These could be later validated by Western blot following immunoprecipitation of the endogenous protein. Immunoprecipitation was therefore carried out with soluble lysates prepared from U2OS:GFP-Nek11L stable cell lines using a polyclonal GFP antibody. Small-scale immunoprecipitation resulted in most of the GFP-Nek11L protein binding to the beads as observed by Western blot analysis with the anti-GFP antibody (Figure 5.2).

5.2.2 Large-scale immunoprecipitation of GFP-Nek11L for LC-MS/MS analysis

Having optimised immunoprecipitation conditions for GFP-tagged protein we next scaled up the experiment in order to have sufficient protein to detect by Coomassie Blue staining. As we wanted to identify novel binding partners that may associate with Nek11 before or after DNA damage, GFP-Nek11L stable

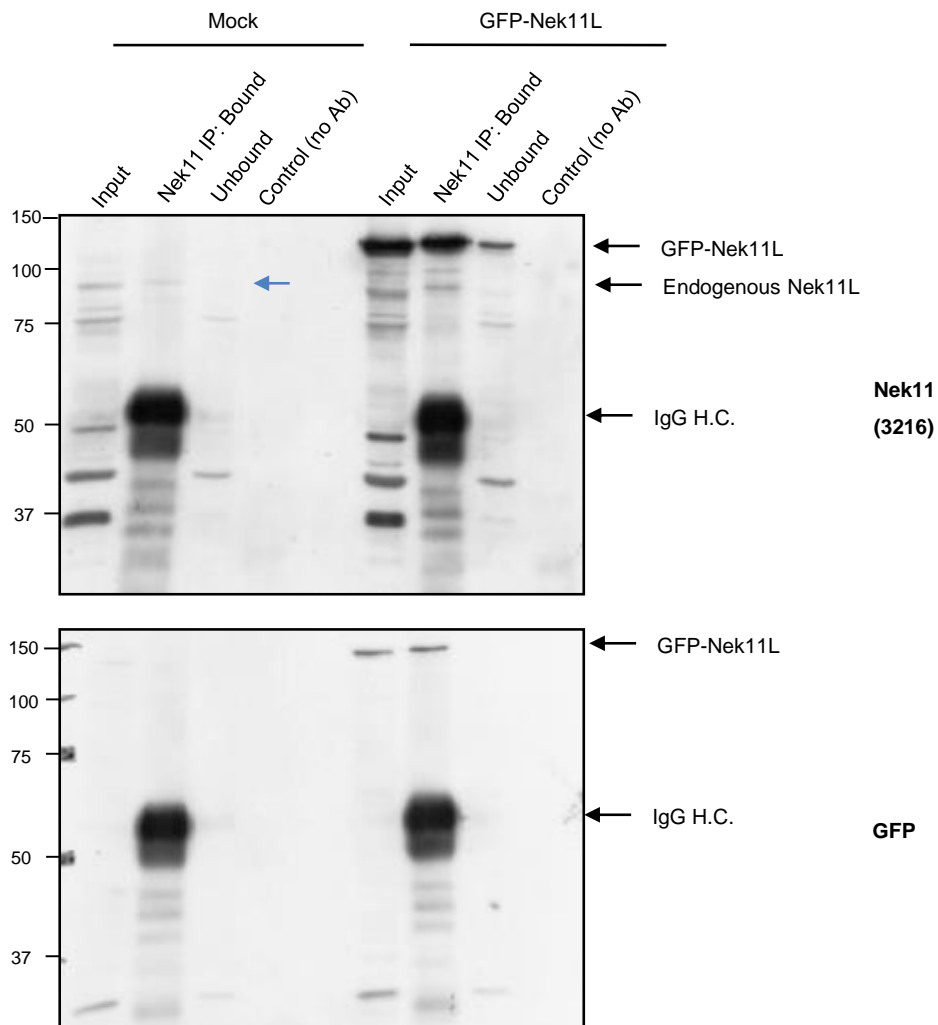


Figure 5.1 Immunoprecipitation of endogenous Nek11 protein with Nek11 (3216) antibody

U2OS cells were either mock-transfected or transiently transfected with GFP-Nek11L for 24 hours before cells were lysed and soluble lysate subjected to immunoprecipitation with Nek11 antibody (3216). Input, bound and unbound fractions were resolved by SDS-PAGE and analysed by Western blot with the antibodies indicated. Blue arrow, indicates endogenous Nek11 protein. The presence of the IgG heavy chains (H.C.) is also indicated. Molecular weights are shown (kDa).

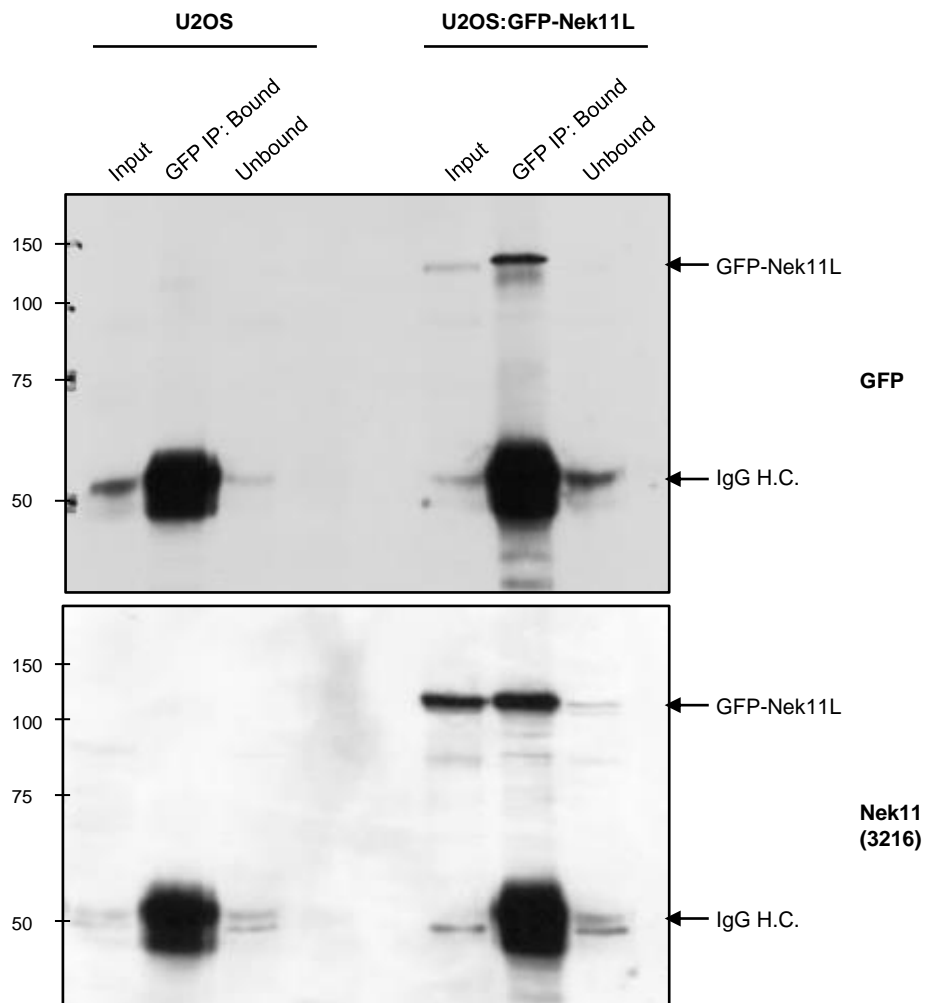


Figure 5.2 Small-scale optimisation of GFP-Nek11 immunoprecipitation

U2OS and U2OS:GFP-Nek11L cells were lysed and soluble lysate subjected to immunoprecipitation with GFP antibodies (1 $\mu\text{g/ml}$) bound to Protein A beads. Input, bound and unbound fractions were resolved by SDS-PAGE and analysed by Western blot with antibodies indicated. The presence of the IgG heavy chains (H.C.) is also indicated. Molecular weights are shown (kDa).

cells were either left untreated or irradiated with 10 Gy and collected 3 hours post-DNA damage induction. U2OS cells stably expressing GFP alone were used as a negative control to account for proteins that may bind non-specifically to the GFP-tag or protein A beads. Immunoprecipitation was carried out using cells collected from two 15 cm² cell culture dishes containing $\sim 3.5 \times 10^7$ cells. Successful precipitate of GFP-tagged proteins from each sample was confirmed by Western blot analysis with GFP antibodies (Figure 5.3A). Proteins to be analysed by mass spectrometry were resolved on a 1.5 mm SDS-PAGE gel to allow 50 μ l of sample to be loaded. The protein gel was then stained with Colloidal Coomassie Blue (G-250) to visualise protein bands. Briefly, Colloidal Coomassie Blue allows the detection of as little as 10 ng of protein rather than 100 ng with classical Coomassie Blue (R-250), since it uses a modified version of the dye. Furthermore, Colloidal Coomassie Blue provides minimal background staining of the gel allowing clear detection of bands (Weiss *et al.*, 2009; Candiano *et al.*, 2004).

Colloidal Coomassie Blue staining enabled visualisation of immunoprecipitated GFP-Nek11L and GFP protein and also revealed the presence of bands specific to the GFP-Nek11L precipitates (Figure 5.3B).

Gels were then provided to PNAACL (University of Leicester) and gel sections excised as shown in Figure 5.3B. Slices representing the IgG heavy chains (50 kDa) were omitted from MS analysis. The other gel slices were subjected to digestion by trypsin before being analysed by liquid chromatography-tandem mass spectrometry (LC-MS/MS). The LC-MS/MS method first separates the digested sample mixture by liquid chromatography (HPLC), before individual peptides are ionised and sorted by mass-to-charge ratio (m/z) and relative abundance. Fragments of each m/z ratio then undergo a further round of MS to determine the peptide sequence which is then used to search protein databases. A list of identified proteins was produced using Mascot protein identification software (Matrix Science) and the human UniProt database. Individual results were then analysed using Scaffold3 proteomics software.

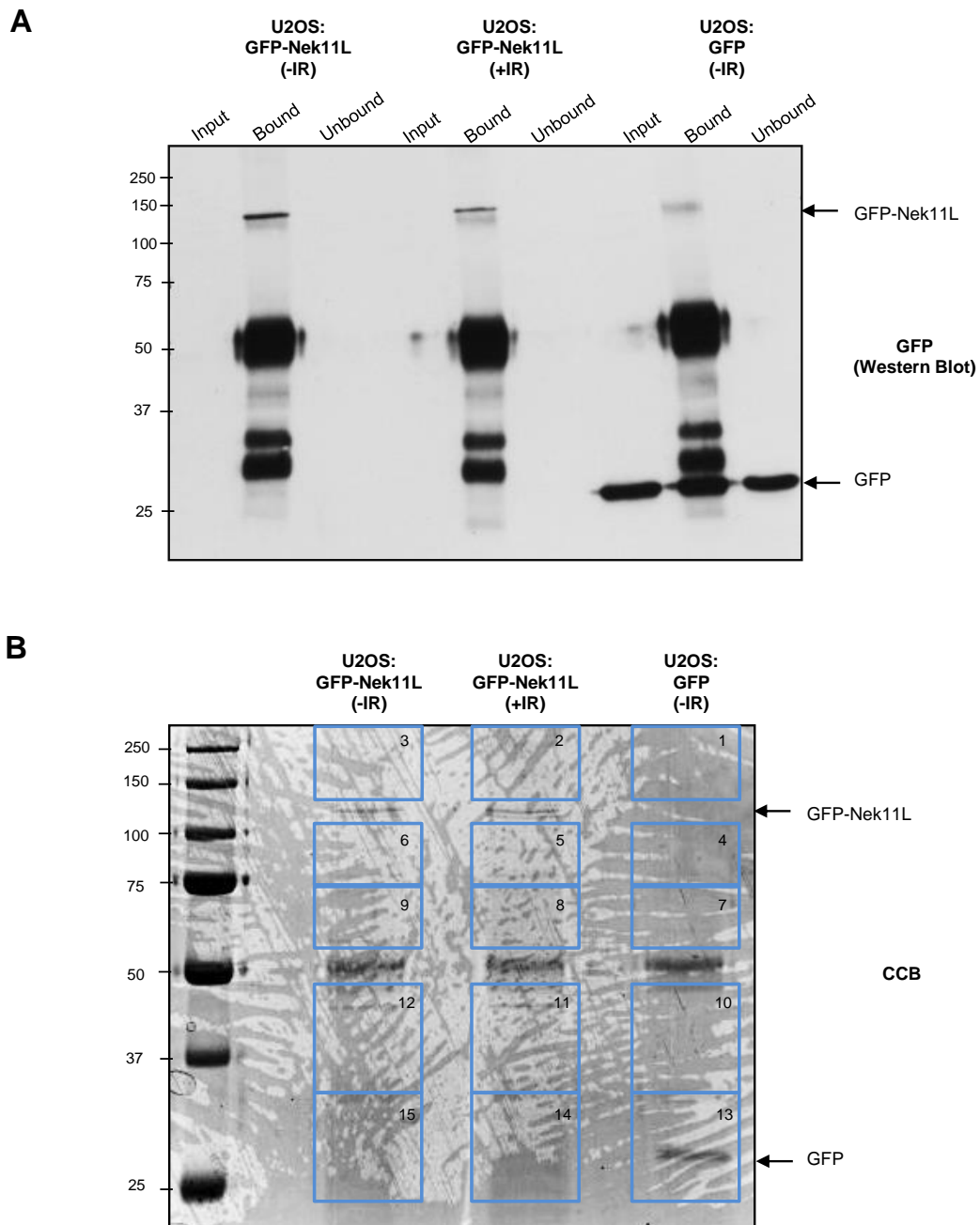


Figure 5.3 Large-scale GFP IP for the identification of novel binding partners by mass spectrometry analysis

U2OS:GFP-Nek11L and U2OS:GFP-only stable cell lines were either left untreated or irradiated (10 Gy), as indicated. 3 hours post-IR cell lysates were collected and soluble fractions were incubated overnight with GFP antibody bound to Protein A beads. **A.** Soluble lysate, bound and unbound samples were separated by SDS-PAGE to check immunoprecipitation. Blots were probed with GFP antibody. Molecular weights are indicated (kDa). **B.** Bound samples were resolved on a 1.5 mm SDS-PAGE gel and stained with Colloidal Coomassie Blue (CCB) to observe protein bands. Boxes indicate sections that were trypsin digested and analysed by LC-MS/MS. Molecular weights are indicated (kDa).

Since mass spectrometry is a highly sensitive technique inclusion parameters were set to minimise the number of false-positives. Firstly, proteins for which less than 3 different peptides were detected were discarded along with proteins with a statistical confidence level less than 95%. Secondly, common protein contaminant families such as keratins were removed (Trinkle-Mulcahy *et al.*, 2008; Mellacheruvu *et al.*, 2013), before finally discarding proteins that were identified in the GFP-only control sample. This left us with 48 potential interacting partners, which were grouped according to their presence in the GFP-Nek11L irradiated or untreated samples, their function, and for their localisation within the cell. Proteins identified varied vastly in protein function with proteins being involved in the DNA damage response and repair pathways, mRNA processing, splicing, transcription and protein biosynthesis. In addition, proteins also show localisation to the cytoplasm and/or nucleus with a number showing more specific localisation to nucleoli (Table 5.1).

5.2.3 GFP-Nek11L co-immunoprecipitates with Ku70

An interesting potential binding partner that emerged from the proteomic study was Ku70. Upon double-strand break (DSB) induction, Ku70 forms a heterodimer with Ku80, and this complex binds to DNA ends where it recruits the catalytic subunit of the DNA-dependent protein kinase (DNA-PK). Upon assembly, the serine/threonine kinase domain of DNA-PK is activated resulting in phosphorylation and recruitment of downstream targets for DSB repair by non-homologous end joining (NHEJ) (Lee & Kim, 2002). In addition DNA-PK is involved in DNA damage checkpoint pathways where it is required for G1/S-phase arrest, and exit from a DNA damage induced G2 checkpoint arrest (Lee *et al.*, 1997). Additional roles for Ku70 and Ku80 include telomere maintenance, regulation of gene transcription and apoptosis (Gullo *et al.*, 2006).

	Accession Number	Molecular Weight	Localisation	Sample
DDR and DNA repair factors				
ATP-dependent RNA helicase DDX1 *	Q92499	82 kDa	Nucleus	+IR, -IR
FACT complex subunit SPT16	Q9Y5B9	120 kDa	Nucleus	+IR, -IR
Splicing factor, proline- and glutamine-rich *	P23246	76 kDa	Cytoplasm/nucleus	-IR
Transitional endoplasmic reticulum ATPase	P55072	89 kDa	Cytoplasm/nucleus/ER	+IR, -IR
X-ray repair complementing defective repair in Chinese hamster cells 6 (Ku autoantigen, 70kDa)*	B1AHC7	64 kDa	Nucleus	+IR, -IR
RNA biogenesis/splicing/processing factors				
Nucleolar RNA helicase 2	Q9NR30	87 kDa	Nucleolus	+IR, -IR
Pre-mRNA-processing factor 6	O94906	107 kDa	Nucleus	-IR
Pre-mRNA-processing-splicing factor 8	Q6P2Q9	274 kDa	Nucleus	+IR
Putative pre-mRNA-splicing factor ATP-dependent RNA helicase DHX15	F5H6K0	90 kDa	Nucleus/nucleolus	-IR
Serine/arginine-rich splicing factor 1	Q07955	28 kDa	Nucleus	+IR, -IR
Serine/arginine-rich splicing factor 2	Q01130	25 kDa	Nucleus	+IR, -IR
Splicing factor 3B subunit 1	O75533	146 kDa	Nucleus	+IR
Splicing factor 3B subunit 2	E9PPJ0	98 kDa	Nucleus	+IR
Splicing factor U2AF 65 kDa subunit	P26368	54 kDa	Nucleus	+IR, -IR
tRNA-splicing ligase RtcB homolog	Q9Y3I0	55 kDa	Cytoplasm	+IR, -IR
U5 small nuclear ribonucleoprotein 200 kDa helicase	O75643	245 kDa	Nucleus	+IR, -IR
Transcriptional activators/transcription factors				
DBIRD complex subunit ZNF326	Q5BKZ1	66 kDa	Nucleus	+IR, -IR
Nucleolar transcription factor 1	E9PKP7	87 kDa	Nucleolus	+IR, -IR
Poly(U)-binding-splicing factor PUF60	Q9UHX1	60 kDa	Cytoplasm/nucleus	+IR
RNA-binding motif protein, X chromosome	P38159	42 kDa	Nucleus	+IR, -IR
TATA-binding protein-associated factor 2N	F5GWQ7	40 kDa	Cytoplasm/nucleus	-IR
UPF0568 protein C14orf166	Q9Y224	28 kDa	Cytoplasm/nucleus	+IR, -IR
Protein biosynthesis				
Elongation factor 2	P13639	95 kDa	Cytoplasm/nucleus	+IR, -IR
Eukaryotic translation initiation factor 3 subunit A	F5H335	163 kDa	Cytoplasm	+IR
Eukaryotic translation initiation factor 3 subunit L	B0QY89	71 kDa	Cytoplasm	+IR
Other				
Fragile X mental retardation syndrome-related protein 1	B4DXZ6	68 kDa	Cytoplasm	+IR, -IR
Nucleolin	E7EX81	66 kDa	Nucleolus	-IR

Table 5.1 Proteins identified in Nek11L immunoprecipitates by LC-MS/MS analysis

Listed are 27 proteins out of 48 identified in the IP-MS analysis together with the accession number and predicted molecular weight. Proteins are categorized according to function. The proposed subcellular localisation as well as whether the proteins were detected in the +IR, -IR or both samples is also indicated. Proteins under the DDR and DNA repair factors heading that are marked with an asterisk (*), also play roles in mRNA biogenesis and splicing processes.

In order to confirm whether Nek11L is able to interact with Ku70 and to test binding of Ku70 to other Nek11 isoforms, we performed co-immunoprecipitation experiments. GFP-Nek11L, GFP-Nek11S and GFP-only stable cell lines were lysed and subjected to immunoprecipitation with a GFP antibody (Figure 5.4A). Ku70 was highly abundant in the input lysate sample. Co-immunoprecipitation of Ku70 with GFP-Nek11L was observed, albeit with weak coprecipitate detected in the control GFP-only immunoprecipitate. Interestingly, Ku70 did not co-immunoprecipitate with GFP-Nek11S any more than with the control, and notably less than with GFP-Nek11L (Figure 5.4A). We next investigated whether kinase activity was required for this interaction and so the experiment was repeated with cells expressing GFP-Nek11L and the GFP-Nek11L kinase-inactive (KD) protein. This also revealed that Ku70 is able to co-immunoprecipitate with GFP-Nek11L but the inactive form shows only weak coprecipitate (Figure 5.4B). However, this was similar to that seen with GFP IP control therefore any potential interaction between Nek11 and Ku70 will require further validation.

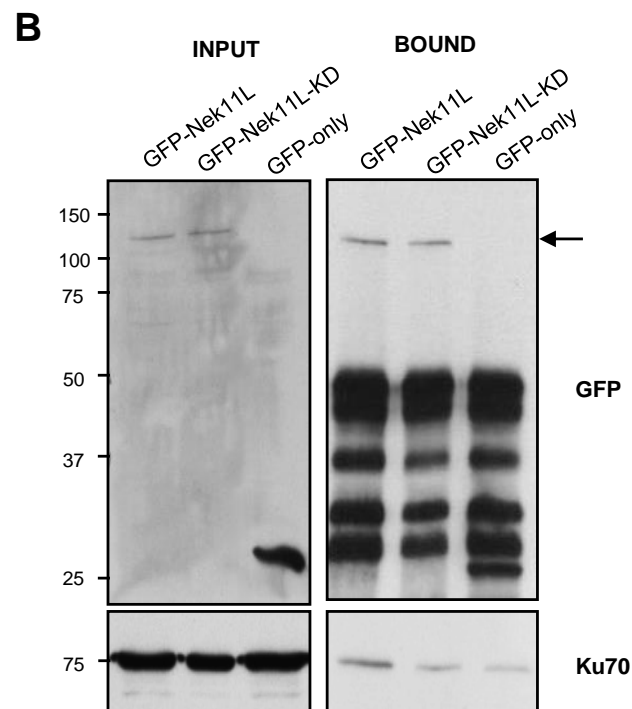
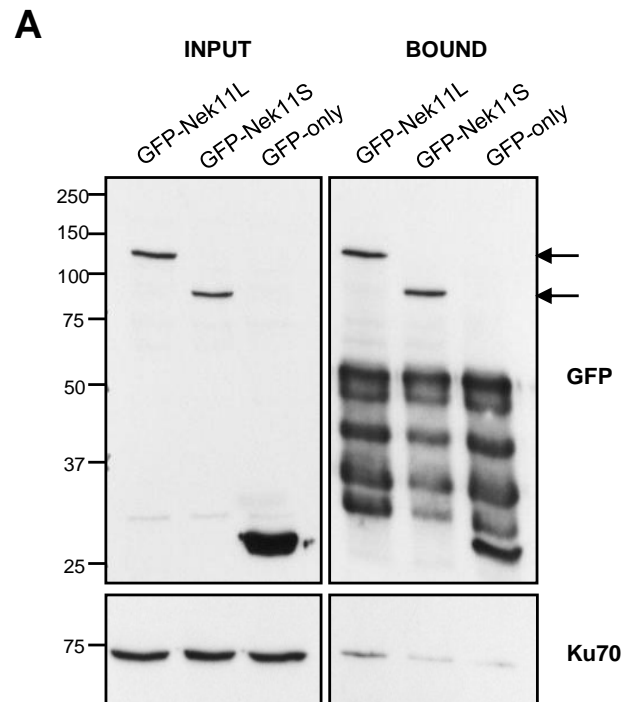


Figure 5.4 Ku70 co-immunoprecipitates with Nek11L but not Nek11S or inactive Nek11L

A. GFP-Nek11L, GFP-Nek11S and GFP-only, or **B.** GFP-Nek11L, GFP-Nek11L-KD and GFP-only stable U2OS cell lines, were lysed and lysates subjected to immunoprecipitation with GFP antibody. Input and bound samples were separated by SDS-PAGE and analysed by Western blotting with antibodies indicated. GFP-Nek11 proteins are indicated with arrows. Molecular weights are indicated in kDa.

5.3 Discussion

Identification of protein kinase substrates is an invaluable tool in cancer research. It allows us to understand protein function and to learn more about molecular pathways within the cell, which could potentially lead to novel ways of targeting cancer cells. Interacting partners of the mammalian Nek family is still a relatively unexplored field with many family members, including Nek11, having limited data (Meirelles *et al.*, 2014). Using IP-MS analysis, we took an unbiased approach to identify novel binding partners of Nek11 to gain further insight into pathways and processes in which it may be involved.

To identify interacting partners of Nek11, we isolated GFP-tagged Nek11 protein from cells via immunoprecipitation. Isolation of endogenous Nek11 protein would reduce false-positive results which may occur through overexpression of protein. However, pilot experiments with endogenous Nek11 protein indicated that a large number of cells would be required to obtain enough protein to be detectable by mass spectrometry. We therefore opted to use GFP-Nek11L stable cell lines with the hope that any potential interacting partner that was identified could then be confirmed with endogenous Nek11 protein at a later stage through co-immunoprecipitation studies. To reduce identification of false-positives, lysates prepared from cells expressing GFP only were used as a control to cross-reference against the GFP-Nek11L samples. This would account for any proteins that bind non-specifically to the affinity matrix or the GFP-tag. Finally, to minimise masking effects from common contaminants or more highly abundant proteins, the gel was cut into sections to be analysed separately thereby increasing the chances of detecting low abundance proteins.

Overall, our study identified 48 unique proteins involved in a number of cellular processes including the DNA damage response, DNA repair, mRNA biogenesis, splicing, transcription and translation. Some of the protein groups

that were selectively immunoprecipitated with GFP-Nek11L are discussed in more detail below.

5.3.1 DNA damage response and repair proteins

The first group are proteins involved in the DNA damage response and repair of double strand breaks. Given the fact that Nek11 plays a key role at the G2/M checkpoint in response to DNA damage this is potentially very exciting. The previously identified upstream and downstream partners of Nek11 in the G2/M checkpoint, Chk1 and Cdc25A (Melixetian *et al.*, 2009), were not identified by this screen. However, this may be due to these interactions being very weak or too transient to allow detection. Chk1, for example, is involved in multiple signalling pathways and, upon phosphorylation Cdc25A is quickly degraded to ensure rapid activation of the cell cycle checkpoint, therefore isolation of a stable complex is probably unlikely. This type of interaction may not be uncommon for Nek11 and future studies for interacting partners could include an additional protein crosslinking step to capture more transient or low affinity interactions (Berggard *et al.*, 2007). Furthermore, in this study we used an asynchronous cell population to identify interacting partners. However, Nek11 is described to be activated in G1/S-arrested and G2/M cells (Melixetian *et al.*, 2009; Noguchi *et al.*, 2004). Therefore, synchronisation of cells could reveal these more transient partners.

Nevertheless, the proteomic study revealed a number of interesting potential interacting partners involved in both the DDR and DNA repair pathways. Amongst these, identification of the FACT complex subunit SPT16 was particularly interesting. FACT (Facilitating Chromatin Transcription) is a heterodimer consisting of SPT16 and SSRP1 and is a general chromatin remodelling factor involved in the reorganisation of nucleosomes. Arrested transcription caused by UV-light induced DNA damage, results in the recruitment of SPT16 to these sites where it is also required for efficient restart of transcription upon DNA damage repair (Dinant *et al.*, 2013; Mandemaker *et*

et al., 2014). Furthermore, FACT associates with a number of DNA damage response proteins including H2AX, DNA-PK, PARP1, and in response to UV, Casein Kinase 2 (CK2), which then phosphorylates S392 of p53 (Heo *et al.*, 2008; Keller *et al.*, 2001). Interestingly, FACT forms a stable complex with Nek9, another member of the human Nek family (Tan & Lee, 2004). While this complex has not been implicated in specific DDR roles, it has been shown to regulate progression from G1 to S phases (Tan & Lee, 2004).

Another potential interacting partner was the identification of Transitional endoplasmic reticulum ATPase (or Valosin-containing protein, VCP). VCP is a member of the AAA (ATPase associated with a variety of activities) ATPase family (Wang *et al.*, 2004) and is a ubiquitin-selective chaperone (Mosbech *et al.*, 2012). VCP associates with the Werner syndrome protein, BRCA1 and is a substrate for DNA-PK and other PIKK family members, therefore implicating it in DNA damage response pathways (Partridge *et al.*, 2003; Zhang *et al.*, 2000; Livingstone *et al.*, 2005). Furthermore, phosphorylated VCP accumulates at sites of DSBs and cooperates with the ubiquitin ligases, RNF8 and RNF168, for the assembly of signalling complexes and DSB repair factors, such as 53BP1 at DNA damage sites (Livingstone *et al.*, 2005; Meerang *et al.*, 2011; Acs *et al.*, 2011).

Interestingly, a number of the DDR factors identified also play key roles in mRNA biogenesis (Asterisked proteins in table 5.1), and over the years several proteins have been identified to play dual roles in the DDR and mRNA biogenesis, discussed in further detail in section 5.3.2 (Ha *et al.*, 2011). One such protein identified in this study is the polypyrimidine tract-binding protein-associated splicing factor (PSF) (or DNA-binding p52/p100 complex, or splicing factor proline and glutamate-rich, SFPQ). PSF was first identified as a component of spliceosomes and is also involved in transcription and RNA processing (Patton *et al.*, 1993; Morozumi *et al.*, 2009). PSF is recruited to sites of DNA damage, where it stabilises paired DNA DSB ends and cooperates with Ku protein (Salton *et al.*, 2010; Bladen *et al.*, 2005). In addition, it is implicated

in homology-directed DNA repair through association with RAD51 proteins and XRCC2 (Morozumi *et al.*, 2009; Rajesh *et al.*, 2011).

Finally, ATP-dependent RNA helicase DDX1 was also identified. This modifies RNA secondary structure and in response to IR redistributes to γ -H2AX and phosphorylated ATM foci. Interestingly, this occurs in an ATM-dependent fashion but only to foci containing RNA-DNA structures (Li *et al.*, 2008), suggesting a role for DDX1 in RNA clearance at DSB sites to allow for template-guided repair of transcriptionally active regions (Li *et al.*, 2008).

5.3.1.1 *Nek11L interacts with Ku70*

The only binding protein from the mass spectrometry analysis which we validated was Ku70. Ku70 is a protein which together with Ku80 is involved in NHEJ. Interestingly, Nek4, another member of the human Nek family, has been shown to interact with DNA-PK (which is together constituted by Ku70, Ku80 and DNA-PKcs) (Nguyen *et al.*, 2012). Nek4 depletion led to impaired cell cycle arrest in response to DNA damage and inefficient localisation of DNA-PKcs to DSBs (Nguyen *et al.*, 2012). Given that the catalytic domain of Nek11 shows 43% identity with Nek4 (Noguchi *et al.*, 2002), it would be interesting to know whether Nek11 also regulates the localisation of Ku70 or other DNA-PK subunits.

Western blots of immunoprecipitation experiments confirmed interaction of Ku70 with GFP-Nek11L. The amount of Ku70 protein that co-immunoprecipitated with Nek11L however, was notably lower in comparison to the input. This suggests that in the absence of DNA damage there is a low basal level of Nek11-Ku70 complex formation. It will be interesting to determine how this changes at different points after DNA damage. It would also be interesting to examine whether Nek11 is able to associate with Ku80 or DNA-PKcs at DSBs and therefore potentially play a role in the NHEJ pathway.

Finally, it will be important to perform the reverse immunoprecipitation experiment by immunoprecipitating Ku70 and blotting for Nek11L; this was attempted however a suitable antibody for Ku70 IP was not found during the study.

Interestingly, Ku70 did not show co-immunoprecipitation with inactive Nek11L, suggesting that kinase activity is required for this interaction. One possibility may be that the conformation of kinase-inactive Nek11L does not allow cooperation with other proteins. This would fit with the proposed model by Noguchi *et al.* (2004) whereby inactive Nek11 is kept in a closed conformation. Furthermore, Ku70 did not interact with Nek11S. A possible explanation might be that it lacks part of the C-terminal domain required for proper binding. This suggests that residues 467-645 of Nek11L are necessary for this interaction. This could be further investigated through truncation studies to map binding regions required.

5.3.2 mRNA processing factors

A large proportion of proteins identified in our screen play key roles at different stages of the mRNA biogenesis pathway. In 2007, a large-scale screen for ATM and ATR substrates identified that a number of proteins that were phosphorylated in response to DDR activation were RNA splicing and RNA metabolic factors (Matsuoka *et al.*, 2007a). Furthermore, later in 2009, a genome-wide siRNA screen carried out to identify novel genome stabilisation genes through phosphorylation of γ -H2AX, identified mRNA processing factors to play roles in preventing DNA damage (Paulsen *et al.*, 2009). In fact, this was the most enriched group of genes identified by this study. Since then, the DNA damage response pathway has been increasingly associated with RNA metabolism, indicating that these pathways are linked.

A recent study identified that BRCA1 forms a protein complex with key components of the mRNA splicing machinery, such as Prp8, U2AF65, U2AF35 and SF3B1, mediated through BCLAF1, in response to DNA damage, and this was found to regulate splicing of a number of genes involved in DNA repair and DNA damage signalling (Savage *et al.*, 2014). Interestingly, our study also identified Prp8, U2AF65 and SF3B1, amongst many other spliceosomal subunits, to co-immunoprecipitate with Nek11. Furthermore, most of these interactions were identified in both non-irradiated and irradiated samples, which could indicate that Nek11, like BCLAF1, may form a complex with the spliceosome machinery and upon DNA damage associate with another DDR protein to play a role in the regulation of splicing of genes. Of course, further studies would be required to test this hypothesis and to identify the mechanisms and purpose of these interactions. In addition, it has been found that depletion of spliceosomal proteins such as U2AF65 has been shown to result in sensitivity to DNA damage and defective DNA repair (Savage *et al.*, 2014), so it would also be interesting to determine whether depletion of Nek11 alone also results in DNA repair defects to see whether it plays a role in the DNA repair pathway potentially through regulation of splicing factors.

In addition to the mRNA processing factors already mentioned, our study also identified potential interaction of Nek11 with serine/arginine-rich splicing factors 1 and 2 (SRSF1 (ASF/SF2) and SRSF2 (SC35)). Both play key roles in spliceosome assembly and during constitutive and alternative pre-mRNA splicing (Long & Caceres, 2009). They are regulated through phosphorylation and dephosphorylation events and have both been implicated in DDR pathways (Lenzken *et al.*, 2013). SRSF1 is hyperphosphorylated in response to chronic replication-dependent DNA damage thus affecting its subcellular distribution and AS pattern of target genes (Leva *et al.*, 2012). SRSF2, on the other hand, is upregulated in response to DNA damaging agents (Edmond *et al.*, 2011).

5.3.3 Nucleolar proteins

Our proteomic analysis revealed interaction of Nek11 with a number of nucleolar proteins. The nucleolus is a structure within the nucleus that has been well established as the centre of ribosomal RNA (rRNA) transcription, rRNA processing, ribosome assembly and maturation. However, in recent years other processes such as regulation of the cell cycle, stress response and telomerase activity have also been identified (Shaw & Brown, 2012). The localisation of Nek11 to nucleoli was previously described by Noguchi *et al.* (2004). It was here that they suggested that Nek2A was able to interact with and activate Nek11 in G1/S arrested cells (Noguchi *et al.*, 2004). It was also proposed that the Nek11-Nek2A complex might link ribosome biogenesis and the DNA replication checkpoint mechanism through an unidentified pathway (Noguchi *et al.*, 2004). Possibly because our study did not utilise G1/S-arrested cells we were unable to detect interaction with Nek2. However, we did identify a number of nucleolar proteins and multiple factors involved in RNA biogenesis (such as DDX1 (Bleoo *et al.*, 2001)), transcription and protein biosynthesis which could be in agreement with proposed roles of Nek11 by Noguchi *et al.* (2004).

Genotoxic insult results in the change of both nucleolar structure and protein content (Golomb *et al.*, 2014; Boulon *et al.*, 2010). For example, stabilisation of p53 occurs by sequestration of Mdm2 by ARF at nucleoli, therefore resulting in activation of the DNA damage response pathways (Zimber *et al.*, 2004). Milder stresses, such as those caused by hypoxia or growth factor deprivation, results in blocking of ribosome biogenesis thereby also resulting in activation of the tumour suppressor, p53 (Golomb *et al.*, 2014). Aside from p53, other proteins with roles in DNA repair or tumour suppression, such as Rb, Bloom and Werner syndrome proteins, RAD17 and RAD52 have been shown to associate with nucleoli, either through being recruited to these sites or relocating to new sites from nucleoli (Dellaire & Bazett-Jones, 2007). Furthermore, nucleolin, an abundant nucleolar protein that plays roles in ribosome biogenesis and regulation of transcription (Mongelard & Bouvet, 2007) and found to interact with Nek11 in this study, has been shown to play roles in regulation of p53

protein levels in response to DNA damage, through binding with Mdm2 resulting in its proteasomal degradation and stabilisation of p53 (Daniely *et al.*, 2002; Saxena *et al.*, 2006). In addition, nucleolin has also been implicated in DNA repair processes by its interaction with replication protein A (RPA) (Kim *et al.*, 2005). After confirming interaction with nucleolin, further studies should examine how Nek11 might be implicated in these pathways.

5.3.4 Comparison of partners identified in the presence or absence of DNA damage

We also compared differences in peptides detected in samples with and without DNA damage. Overall, the majority of proteins detected were identified in both samples however; to quantitatively assess whether there is a difference between the samples, future experiments could use stable isotope labelling by amino acids in culture (SILAC) followed by mass-spectrometry. This will give a more accurate picture of the differences between the samples.

In summary, we have identified a number of potential novel Nek11 binding partners in this study. Intriguingly, results provide evidence for Nek11 in previously unidentified pathways such as the DNA repair and mRNA processing pathways, although the exact mechanism and role remains to be determined. It would be interesting to also assess Nek11 interactors in foci evident following 7 hrs post-IR. In addition, performing IPs in more stringent salt conditions would enable the identification of true interactors of Nek11.

CHAPTER 6 ASSESSMENT OF NEK11 EXPRESSION IN COLORECTAL CANCER CELLS AND TISSUE

6.1 Introduction

Gene expression studies are widely used to predict the role of individual proteins in developmental, physiological and pathological processes (Murphy, 2002). They can provide key insights into how a particular gene is regulated under normal conditions or how it changes in response to disease progression or treatment. Hence, they provide important information on protein function and can be used for diagnostic and prognostic purposes. The initial study into Nek11 function identified expression of two different cDNAs encoding Nek11 isoforms with distinct C-terminal tails (Noguchi *et al.*, 2002). The mRNA expression of these isoforms, named Nek11L and Nek11S, was studied via Northern blot analysis. This showed that whilst overall expression of *nek11* mRNA was low, the abundance of the *nek11L* isoform was higher in a number of cell lines as compared to *nek11S* (Noguchi *et al.*, 2002). Furthermore, *nek11L* mRNA expression levels are cell cycle regulated, with expression increasing from S to G2/M phases of the cell cycle before returning to basal levels upon re-entry into G1 (Osmani *et al.*, 1987; Noguchi *et al.*, 2002; Schultz *et al.*, 1994a).

Using a tissue microarray, Noguchi *et al.* (2002) found that *nek11L* mRNA was weakly detected in tissues such as the cerebellum, trachea, lung, appendix, and uterus. In addition, semi-quantitative RT-PCR analysis using primers that do not discriminate between Nek11 isoforms, showed that *nek11* is expressed in a number of cancer cell lines including colorectal, breast and pancreatic cancer cell lines (Sahota, 2010). Whilst these studies show that a range of cancer cells express Nek11 mRNA, they are not fully quantitative and detailed comparisons between normal and cancer cells have not yet been undertaken. Furthermore, we have identified an additional two isoforms, Nek11C and Nek11D, and their expression remains to be determined.

Protein expression analysis by immunohistochemistry is also a useful tool in comparing expression of proteins between normal and diseased samples (Matos *et al.*, 2010). It can be used to examine protein expression and localisation in intact tissue sections. Data obtained can be used to validate new drug targets, understand progression of diseases, such as cancer, and help to determine treatment options. It has been reported that in early, pre-invasive stages of tumourigenesis there is constitutive activation of DNA damage signalling (Bartek *et al.*, 2007). Examination of Nek11 protein expression, using tissue microarrays of primary tumours, found that expression is increased in 35% of colon adenomas and carcinomas compared to normal tissue. (Sorensen *et al.*, 2010). Furthermore, expression was highest in pre-cancerous lesions, suggesting that Nek11 may play a protective role at early stages of tumour development (Sorensen *et al.*, 2010).

So far, we have examined the role of Nek11 at the G2/M DNA damage checkpoint in colorectal cancer cells, and have studied in detail the localisation of individual Nek11 isoforms. Here, we move on to examine the expression of Nek11 isoforms in a panel of colorectal cancer cells and colorectal cancer tissue using qRT-PCR and immunohistochemistry.

6.2 Results

6.2.1 Nek11 isoforms are expressed in colorectal cancer cell lines

As previously discussed in Chapter 4, database analysis revealed that Nek11 is expressed as at least four variants: Nek11L, Nek11S, Nek11C and Nek11D. All isoforms are transcribed from the same gene on chromosome 3 and are alternatively spliced to generate proteins with different C-terminal tails. The exon structure of each isoform was determined by aligning the Nek11 isoform cDNA to genomic DNA (Accession: NT_005612) using Basic Local Alignment Search Tool (BLAST; <http://blast.ncbi.nlm.nih.gov/Blast.cgi>) (Figure 6.1). The coding region for all isoforms begins from the same start codon; however, differences between the isoforms are apparent in the 3' end, after exon 14. Nek11L contains 18 exons in total and Nek11D, whilst very similar, skips exon 17, resulting in an early stop codon. Compared to Nek11L, the Nek11S and Nek11C coding regions differ only by the very 3' exon (exon 15) which results in an earlier stop codon and therefore translation of a shorter protein.

Given that Nek11 expression is increased in colorectal cancer tissue (Sorensen *et al.*, 2010), we investigated the relative mRNA expression of each of the Nek11 isoforms in a panel of colorectal cancer cells compared to immortalised Human Colonic Epithelial Cells (HCEC). To accurately quantify variations in gene expression we utilised real-time quantitative RT-PCR (qRT-PCR). Briefly, like RT-PCR this method requires the generation of cDNA from mRNA and subsequent amplification of the target gene by PCR. However, it specifically allows the measurement of DNA product generated after each PCR cycle. There are a number of methods that allow detection of DNA product; in this study we utilised SYBR Green, a dye which intercalates into dsDNA thereby emitting a fluorescent signal. The cycle number at which the fluorescence detected crosses a background level is known as the cycle threshold (Ct) and this is directly proportionate to the amount of starting template (Ginzinger, 2002). The lower the cycle number at which this happens signifies more starting template and therefore a higher mRNA abundance in that sample.

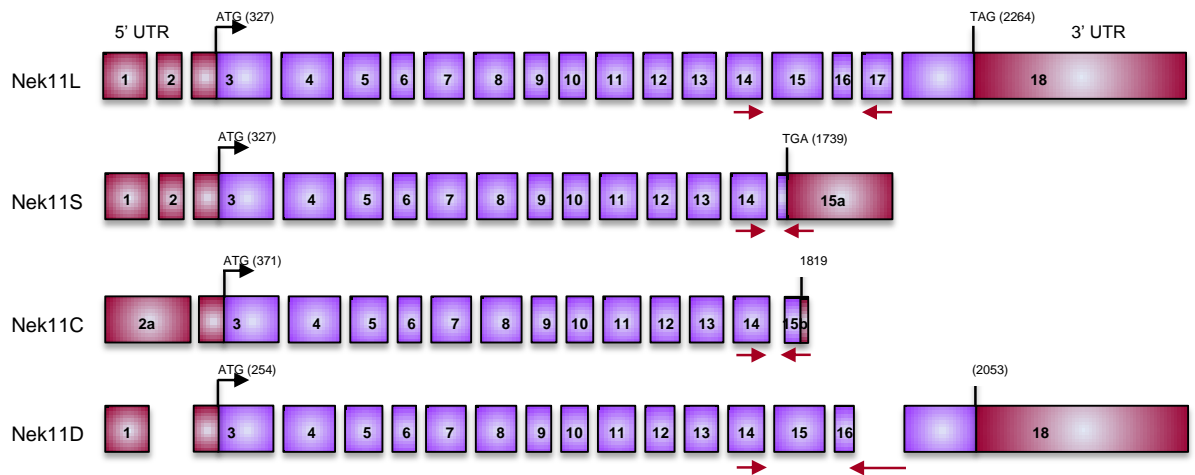


Figure 6.1 Exon organisation of Nek11 isoforms

Schematic diagram showing exon organisation of Nek11 isoforms, determined by BLAST analysis. Red boxes indicate untranslated regions and purple boxes indicate coding region. Numbers indicate nucleotide position based on exon 1 starting at 1. Red arrows indicate regions to which isoform specific primers were designed for qPCR analysis.

Firstly, using the exon information and the online primer design program, Primer3 (<http://bioinfo.ut.ee/primer3/>), primer pairs were designed to specifically anneal and amplify DNA from specific isoforms (Figure 6.1, red arrows), and specificity of primer sequences were confirmed by a BLAT search. The primers were then used in qRT-PCR reactions using cDNA generated from U2OS lysates. Specificity of the primers was verified experimentally by performing a melt curve analysis at the end of the reaction. PCR products were exposed to a temperature gradient from 65 to 95°C and fluorescence recorded throughout. The temperature at which the dsDNA dissociates (melting temperature) results in a drop in fluorescence and a single PCR product is confirmed by the presence of a single peak when the rate of change of fluorescence is plotted against temperature. Melt curve analyses with the PCR products generated with Nek11 isoform specific primers revealed the presence of single dissociation peaks that are absent in the 'no template' control (Figure 6.2A). Furthermore, separation of the end products of the reactions on an agarose gel resulted in detection of single bands of the expected size for each of the reactions (Figure 6.2B). Together, both sequence comparison to human DNA and experimental analysis confirmed the specificity of the Nek11 primers.

cDNA was then generated from a panel of colorectal cancer cell lines, including HCT116, SW480, SW620 and HT29 cells and, for comparison, the HCEC cell line. Comparing the relative expression of each isoform to that of Nek11C within each cell line, revealed that across all cell lines tested, Nek11L mRNA is the most abundant. Conversely, Nek11C is the least highly expressed isoform (Figure 6.3).

To directly compare gene expression levels between different cell lines, data should be normalised to correct for variation between the samples (Wong & Medrano, 2005). Normally, housekeeping or ribosomal RNA (rRNA) genes are used for this purpose, since they are constitutively expressed. In this study, we designed and tested primers against a number of commonly used normalisation genes including hypoxanthine phosphoribosyltransferase 1 (HPRT1),

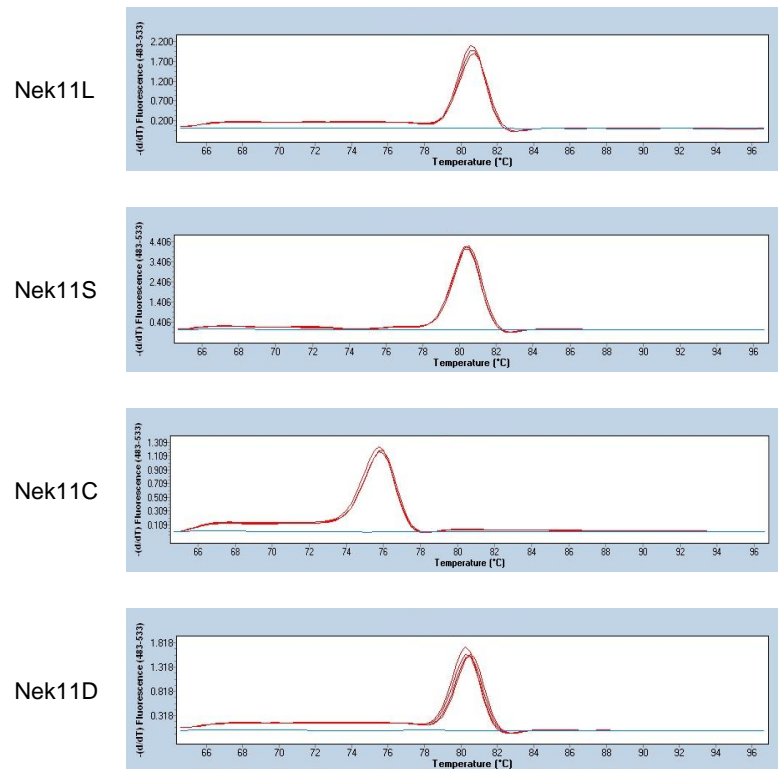
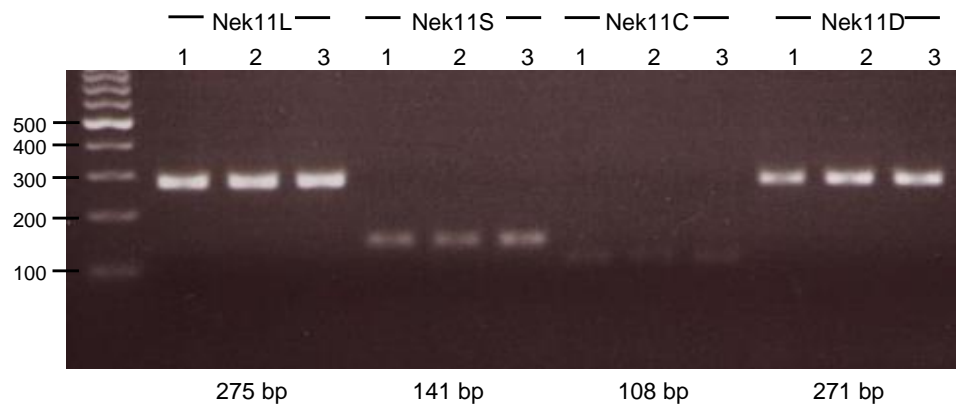
A**B**

Figure 6.2 Presence of a single amplification product with Nek11 isoform-specific primers was determined by melt curve and agarose gel analysis

cDNA was reverse transcribed from mRNA extracted from U2OS cells and used in qRT-PCR reactions with Nek11 isoform-specific primers. **A.** Melting temperatures of DNA products were determined by subjecting DNA to increasing temperatures up to 95°C. Dissociation curves (red) represent the change in fluorescence as a function of time. For each curve, reactions were performed in triplicate. Blue lines indicate the no template control (NTC). **B.** Three representative samples of RT-PCR products (1, 2 & 3) were separated on an agarose gel and visualised. Product size (bp) for each reaction is indicated, as well as DNA ladder markers (bp).

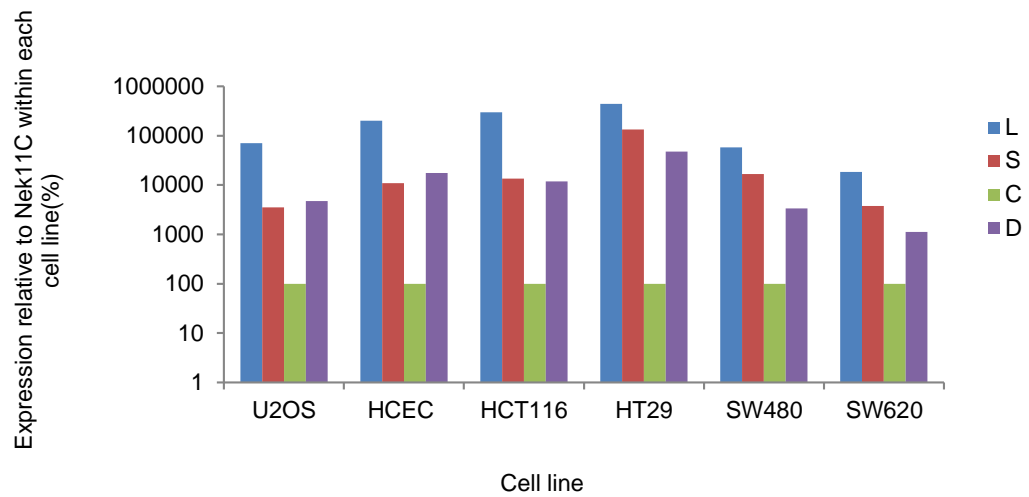


Figure 6.3 Nek11L is the most highly expressed isoform across a panel of cell lines

mRNA was extracted from the cell lines indicated and used for qPCR with Nek11 isoform-specific primers. Reactions were set up in triplicate and resulting Ct values were averaged. Histogram shows expression of each isoform relative to Nek11C within each cell line. These results represent one experiment.

glyceraldehyde-3-phosphate dehydrogenase (GAPDH) and 18S ribosomal RNA (18S rRNA). Production of a single PCR product of expected size for each primer set was first confirmed by agarose gel analysis (Figure 6.4A). Next, melt curve analysis identified single peaks for each of the amplification reactions and this was absent from the no template control (Figure 6.4B). The peak observed for 18S rRNA had a slight shoulder which could indicate the presence of primer dimers, or may be due to some regions of the dsDNA melting more quickly than more GC rich areas resulting in two melting phases. We therefore further analysed reactions with GAPDH and HPRT1 primers by comparing the gene expression across all the colorectal cancer cell lines and HCEC cells. Box plot analysis where the average Ct values for each cell line were plotted found that GAPDH expression was more consistent across the cell lines with a standard deviation of 0.65, compared to 0.96 with HPRT1 (Figure 6.4C). Data obtained for Nek11 expression across the cell lines was then normalised to GAPDH expression and then the normal colorectal cell line HCEC was used as a calibrator to compare Nek11 isoform expression (Figure 6.5). Results indicate that, the expression of Nek11 isoforms was in most cases either similar or reduced in cancer cell lines compared to the HCEC line. Expression of all Nek11 isoforms was reduced in HCT116 and SW480 cells. However, expression of Nek11S was increased 7-fold in HT29 cells and Nek11C was elevated 4-fold in SW620 cells as compared to HCEC cells. It should be noted however that this data are from only one experiment.

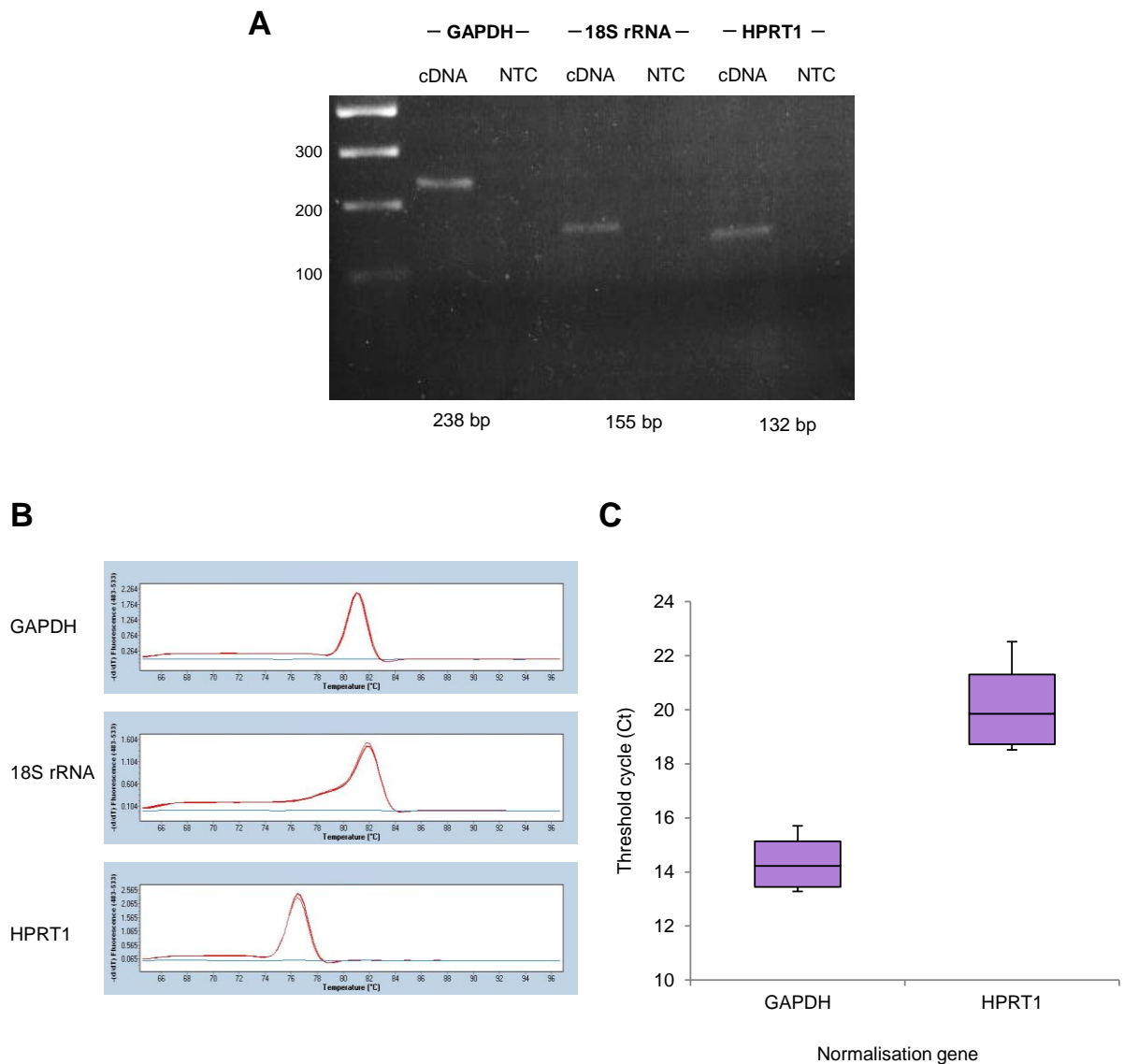


Figure 6.4 Validation of GAPDH as a suitable normalisation gene for qRT-PCR analysis

cDNA was reverse transcribed from mRNA extracted from U2OS cells and used in qRT-PCR reactions with primers against genes indicated. **A.** DNA products were separated on an agarose gel and visualised. Product size (bp) for each reaction is indicated, as well as DNA ladder markers (bp). **B.** Melting temperatures of DNA products was determined by subjecting DNA to increasing temperatures up to 95°C. Dissociation curves (red) represent the change in fluorescence as a function of time. Blue lines indicate the no template control (NTC). **C.** Box-plot graph represents the range of average Ct values obtained in HCEC, HCT116, HT29, SW480 and SW620 cell lines for GAPDH and HPRT1 normalisation genes. Median values are indicated as lines across box and lower and upper boxes indicate the 25th and 75th percentile. Whiskers represent maximum and minimum values.

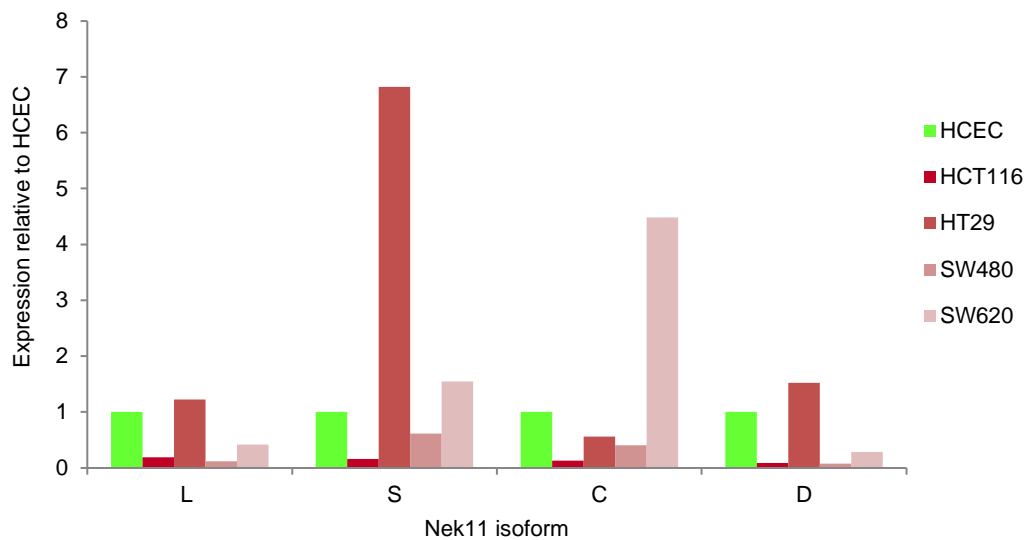


Figure 6.5 Expression of Nek11 isoforms in a panel of CRC cell lines compared to HCEC cells

mRNA was extracted from the cell lines indicated and used for qPCR with Nek11 isoform-specific primers. Reactions were set up in triplicate and resulting Ct values were averaged. Samples were then normalised against GAPDH and the difference in Ct values for colorectal cancer cell lines compared to HCEC was determined. Relative expression was calculated using $Q=2^{-\Delta\Delta C_t}$. These results represent one experiment.

6.2.2 Nek11 protein expression in colorectal cancer tissue compared to normal tissue

Having investigated Nek11 mRNA expression in colorectal cancer cell lines, we next wanted to examine Nek11 protein expression in colorectal tumour tissue. To do this, we first needed to test whether the antibodies available against Nek11 would allow detection of endogenous Nek11 protein in tissue samples. The polyclonal antibody (3216), generated in-house by Dr. Navdeep Sahota was tested first (Sahota, 2010). Due to the antigen it was raised against this antibody should recognise all Nek11 isoforms. In order to use the 3216 antibody to detect Nek11 by immunohistochemistry (IHC) studies, conditions for fixing and staining needed to be optimised. To begin, parental U2OS and GFP-Nek11L stable cells were pelleted and formalin-fixed and paraffin-embedded to produce cytoblocks from which sections were cut. Antigens from individual sections were retrieved by microwaving for 15 minutes in citrate buffer, pH 6.0. Sections were stained with a gradient of Nek11 antibody concentrations and, Ki-67, a proliferation marker (Figure 6.6A). At 1:100 or 1:500 the 3216 antibody gave strong staining of both parental and GFP-Nek11L cells. However, at a dilution of 1:1000, we were able to detect a weak stain of the U2OS parental cells and strong detection in the GFP-Nek11L cells. Closer examination revealed cytoplasmic staining of GFP-Nek11L, consistent with immunofluorescence data obtained previously (Figure 6.6B). This concentration was then used to stain a panel of normal versus colorectal tumour tissue (Figure 6.7A). It was noted by a Pathologist that staining was observed in both tissue types although the staining in normal tissue appeared to be marginally stronger. In addition, the tumour tissue exhibited strong staining towards the apical lumens but no evidence of specific staining to other tissue areas was observed (Figure 6.7B). However, as RNAi studies could not unambiguously confirm the specificity of this antibody by immunofluorescence, we decided to confirm these observations through using a second Nek11 antibody.

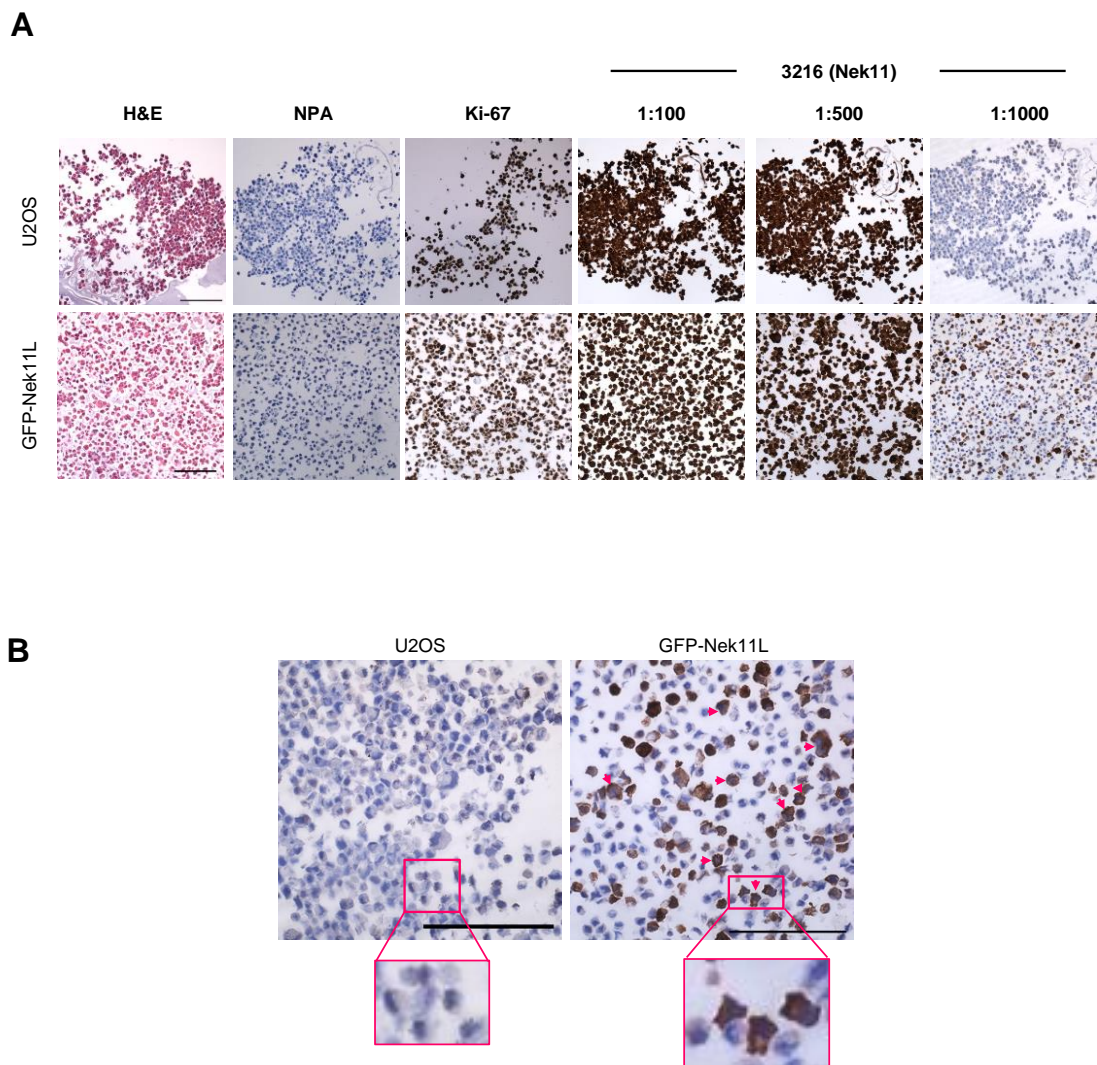


Figure 6.6 Optimization of the Nek11 antibody, 3216, for immunohistochemistry

A. U2OS parental and GFP-Nek11L stable cell lines were pelleted and fixed with formalin before being paraffin embedded. Sections were subjected to staining with either Ki-67, a proliferation marker, or Nek11 at the concentrations indicated (brown). NPA indicates no primary antibody. All sections were counterstained with haematoxylin to detect nuclei (blue). H&E represents additional staining with eosin to detect cytoplasm of cells (pink). Scale bar, 100 μ m. **B.** 40x magnification of cell pellet staining with Nek11 antibody (brown) from (A), at a dilution of 1 in a 1000. Scale bar, 100 μ m.

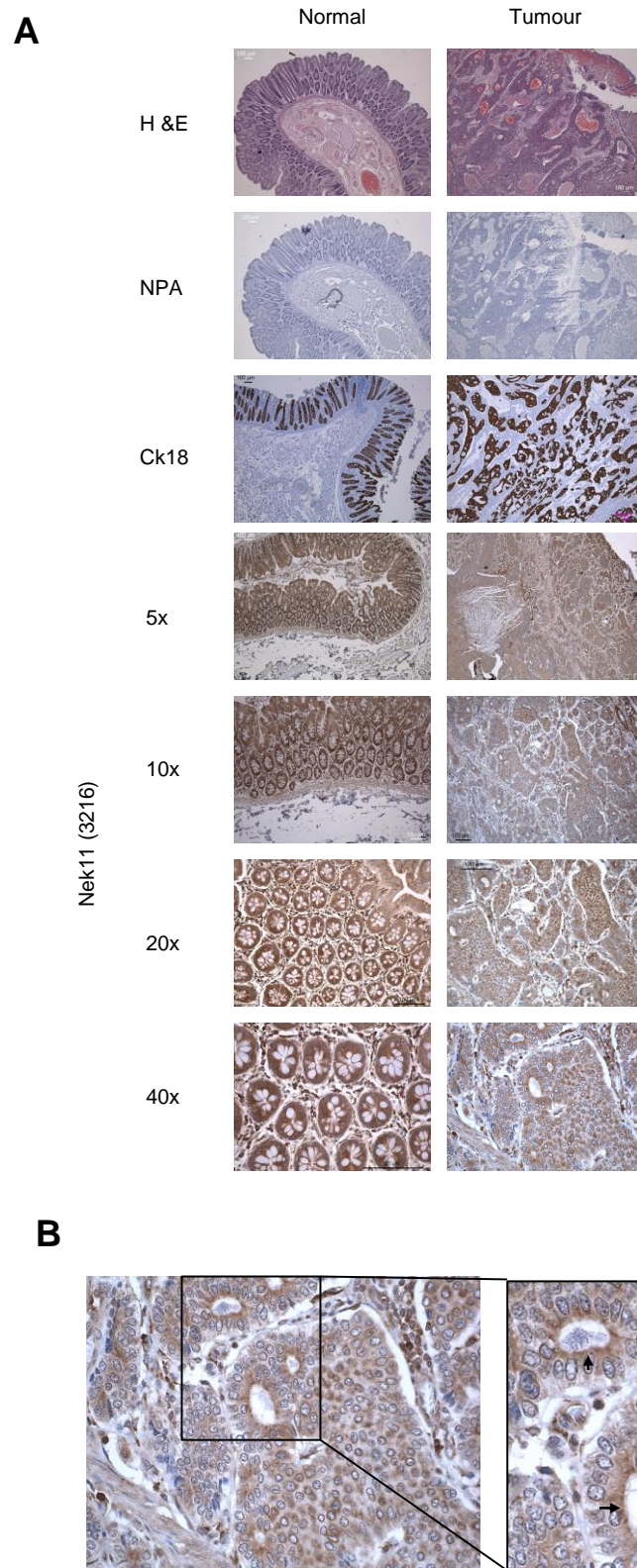


Figure 6.7 Expression of Nek11 in normal colorectal and colorectal cancer tissue

A. Sections from normal and tumour colorectal tissue were subjected to immunohistochemistry. Sections were either stained with haematoxylin (blue) and eosin (pink) (H&E) to detect nuclei and tissue, respectively; or against cytokeratin 18 (CK18, brown), or Nek11 (3216, 1:1000) (brown). NPA represents a no primary antibody control. All sections were counterstained with haematoxylin (blue). Nek11 stained samples are shown at various magnifications, as indicated. **B.** 40x magnification of tumour staining with Nek11 antibody as in A (left panel). Boxed region is blown up (right) and arrows indicate apical surfaces of lumen.

A commercially-available monoclonal antibody against Nek11 (Origene), was obtained that had been raised against the full-length Nek11L isoform. To test the specificity of this antibody by Western blot, lysates from GFP-Nek11L, S and C stable cell lines and cells transiently transfected with GFP-Nek11D were separated by SDS-PAGE and probed with Origene Nek11 and GFP antibodies (Figure 6.8A). Western blot analysis showed that the Origene antibody was only able to detect Nek11L and Nek11D isoforms. This suggests that the epitope it detects is contained within the region that is present within the Nek11L and Nek11D isoforms only (Figure 6.8B). U2OS cells were then fixed for IF analysis with the Origene antibody (Figure 6.8C). This revealed a cytoplasmic stain and is consistent with the cytoplasmic localisation observed in GFP-Nek11L and Nek11D stable cells. This antibody was then tested for IHC studies using U2OS and GFP-Nek11L cell sections as before (Figure 6.9). A dilution of 1:1000 stained the GFP-Nek11L cells strongly but only stained the U2OS cells weakly. Importantly, this staining was significantly reduced by pre-incubating the antibody with purified Nek11 protein supporting the conclusion that Nek11 is specifically detected with this antibody (Figure 6.10). However, IHC analysis to date on colorectal tumour tissue with this antibody has not resulted in any positive staining (data not shown).

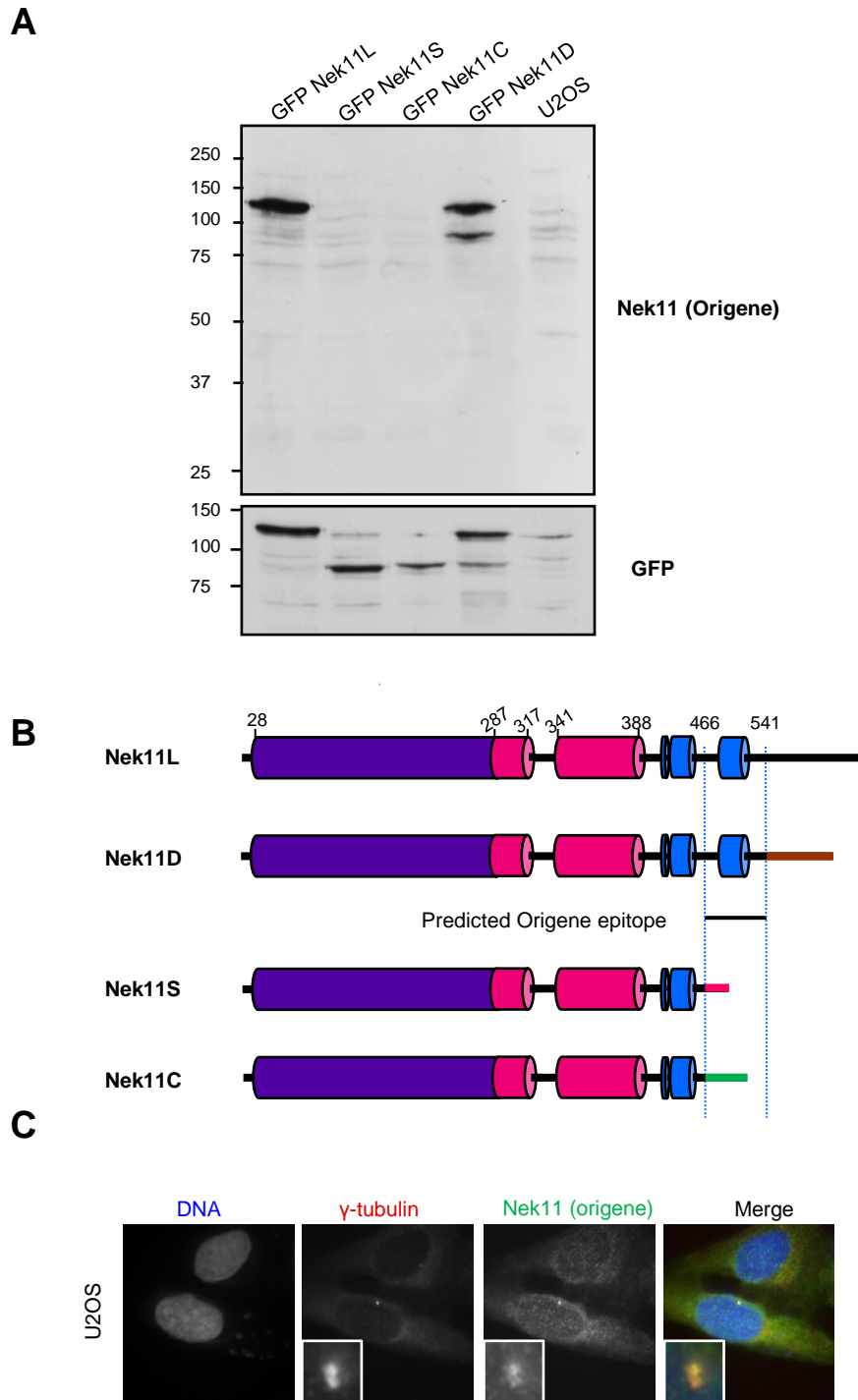


Figure 6.8 Nek11 monoclonal antibody, Origene, detects Nek11L and Nek11D isoforms only

A. GFP-Nek11L, S and C stable cell lines and U2OS cells transiently transfected with GFP-Nek11D were lysed in RIPA buffer and separated by SDS-PAGE. Blots were probed with antibodies against Nek11 (Origene) and GFP. Molecular weights (kDa) are indicated. **B.** Schematic representation of the Nek11 isoforms showing the region of Nek11L and Nek11D predicted to be recognized by the monoclonal Origene antibody. **C.** U2OS cells were fixed in methanol and stained for Nek11 (origene, green) and γ -tubulin (red). DNA was stained with Hoechst 33258 (blue).

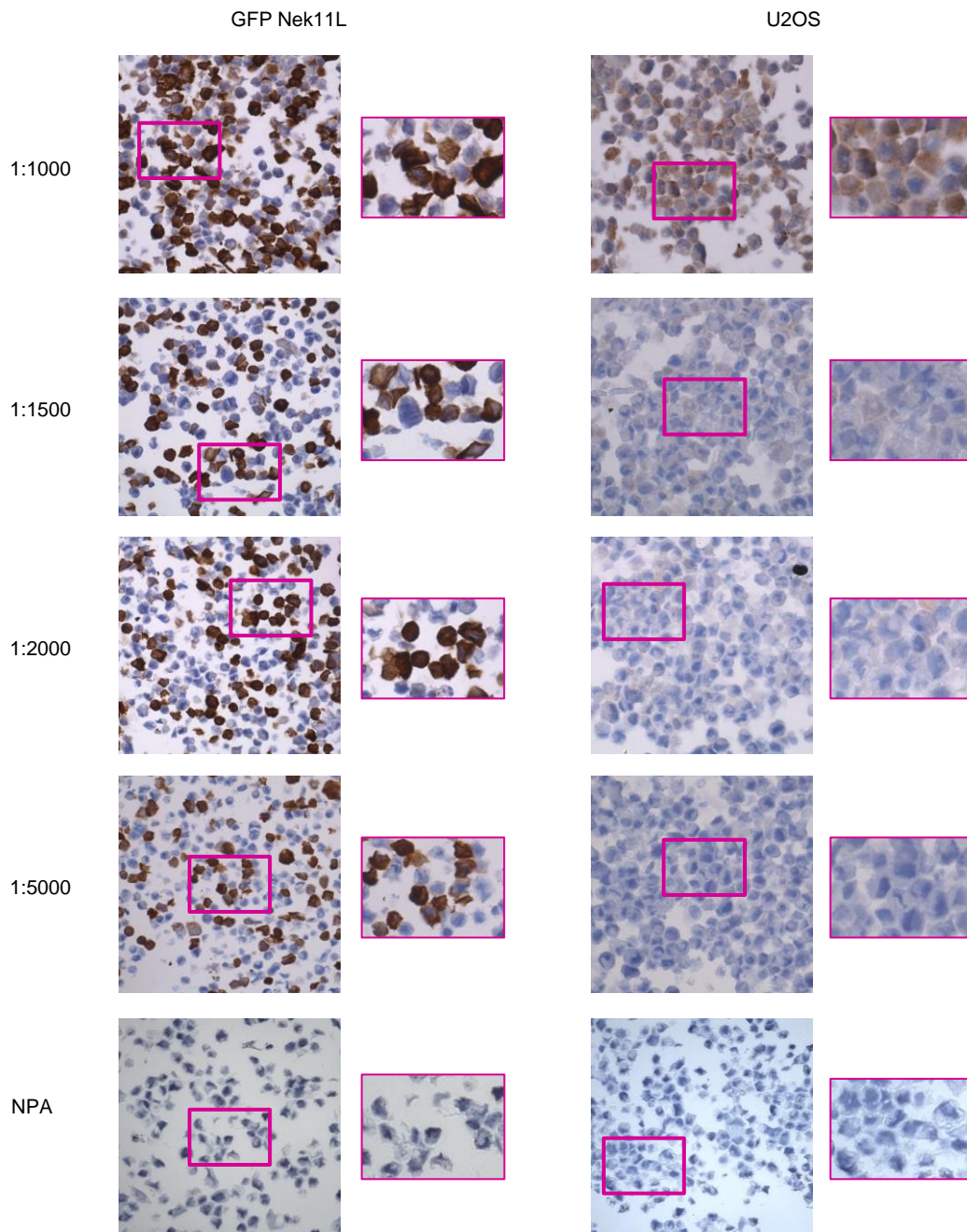


Figure 6.9 Optimization of the Origene Nek11 antibody for immunohistochemistry

U2OS and GFP-Nek11L stable cell lines were formalin-fixed and paraffin-embedded. Sections were subjected to staining with anti-Nek11 antibody from Origene at dilutions indicated (brown). NPA indicates no primary antibody. All sections were counterstained with haematoxylin to detect nuclei (blue). Magnified views of the regions within pink boxes are shown.

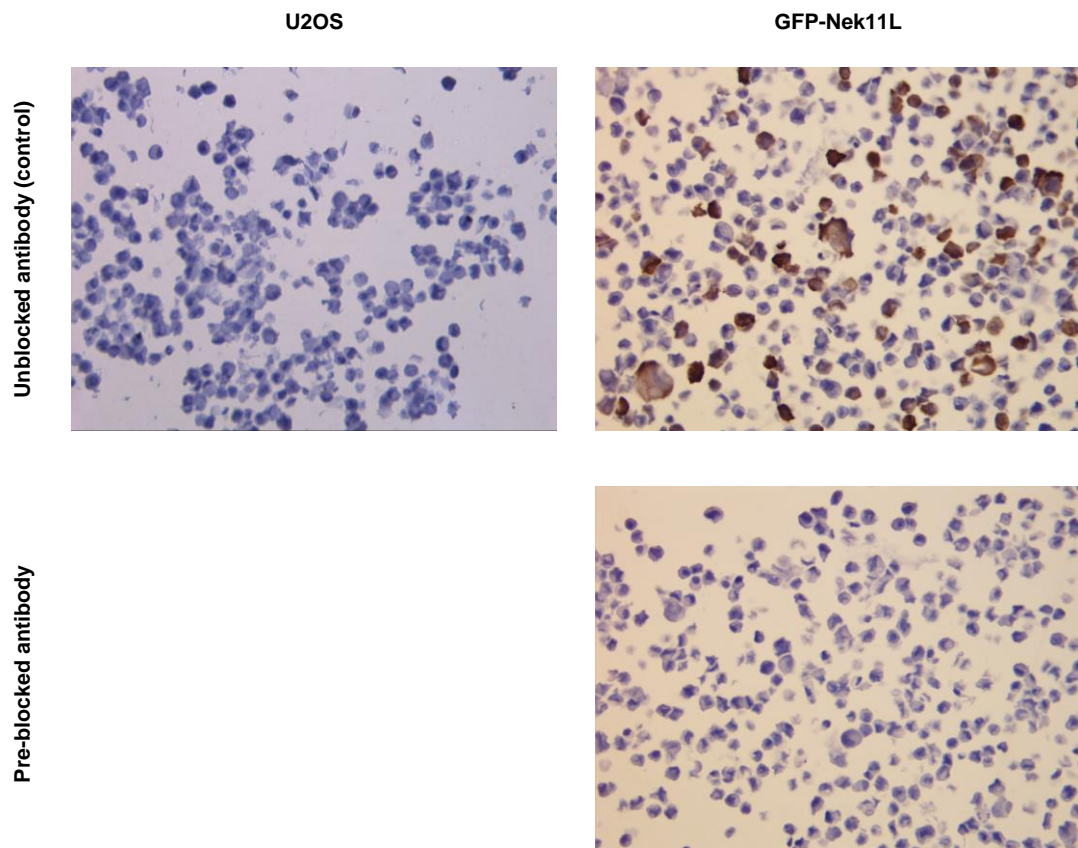


Figure 6.10 Competition assay with Origene antibody confirms detection of Nek11 is specific

Sections from U2OS and U2OS:GFP-Nek11L cell pellets were subjected to immunohistochemistry using the Origene antibody against Nek11 (brown). The upper two panels represent sections stained as normal with untreated antibody. The lower panel shows staining of a GFP-Nek11L section whereby the Origene antibody was first pre-incubated with 50 µg of purified Nek11 protein bound to nitrocellulose membrane, at 4°C overnight. Sections were counterstained with haematoxylin to detect nuclei (blue). Data kindly provided by Joon Wee Ho (unpublished).

6.3 Discussion

In this chapter, we have begun to examine the expression of Nek11 isoforms at the mRNA level in a panel of colorectal cancer cells and at the protein level in patient colorectal normal and tumour tissue via immunohistochemistry.

As previously discussed, the checkpoint machinery has become an increasingly attractive target for drug development. Therefore, we aimed to compare Nek11 mRNA and protein expression in normal and cancer cells and tissue to examine whether there may be some clinical benefit in targeting Nek11 in cancer cells. Previous mRNA studies have shown that Nek11 is expressed in a range of tissues and cancer cell lines (Noguchi *et al.*, 2002; Sahota, 2010). However, so far, no quantitative mRNA expression data had been obtained; furthermore, studies either concentrated on Nek11L or were not isoform-specific. Using qRT-PCR we show that all four Nek11 variants are expressed in a panel of colorectal cancer cells and an immortalised colorectal cell line. Results indicated that the Nek11L isoform was more predominant and Nek11C was the least abundant variant across the cell lines tested. This agrees with observations seen by Noguchi *et al.* (2002) whereby they detected higher expression of Nek11L compared to Nek11S. Two out of the four colorectal cancer cell lines used in mRNA expression studies revealed that all Nek11 isoforms were downregulated as compared to the control HCEC cell line. Nek11 promotes Cdc25A degradation therefore downregulation may be advantageous for tumour progression by causing an increase in Cdc25A protein levels and therefore resulting in uncontrolled cell division. These cell lines were derived from a more advanced tumour stage and so it would be interesting to look at Nek11 expression in a pre-cancerous lesion or early-stage tumour derived cell line.

Furthermore, the depletion studies carried out in Chapter 3 were done in HCT116 cells only, and our qRT-PCR data suggests that HCT116 cells express all Nek11 isoforms at a lower level compared to the HCEC cell line. Therefore, examination of the consequences of depletion in cells that express Nek11 at

higher levels may be of clinical interest. For example, the HT29 cell line expressed high levels of Nek11S and if these cells rely more heavily on Nek11, depletion could sensitise these cells to DNA damage induction more substantially than in HCT116 cells. It will be first important however to repeat mRNA expression studies since data obtained here are from single experiments.

Finally, to examine Nek11 expression in cancer tissue we employed immunohistochemistry. Two antibodies were used to detect Nek11, an in-house generated polyclonal antisera named 3216 and a commercial monoclonal antibody from Origene. Whilst the 3216 antibody is able to detect all Nek11 isoforms, analysis via Western blot and indirect immunofluorescence of the Origene antibody revealed specific detection of Nek11L and Nek11D isoforms. Importantly, both antibodies stain centrosomes. Hence, we propose that both antibodies are detecting endogenous Nek11 but with different isoform specificity.

Conditions for immunohistochemistry analysis with these antibodies were first optimised on sections generated from cell pellets that had been formalin-fixed and paraffin-embedded equivalent to the process of tissue preparation. Upon identifying a suitable antibody dilution, studies were carried out on tissue samples. These used normal colorectal and colorectal tumour samples obtained from the same patient to account for potential variation in expression of Nek11 between individuals and to act as an internal control. Staining of a number of sample sets from different patients with the 3216 antibody revealed that Nek11 was detected in both normal and tumour samples. The tumour samples showed slightly lower Nek11 expression when analysed by a pathologist. Furthermore, concentrated expression was observed on the apical surface of lumen structures in tumour samples, although the consequence of this is not yet known and to confirm these staining patterns a competition assay would need to be done. On the other hand, the specificity of the Origene antibody staining on the cell pellet samples was confirmed through a competition assay.

However, so far tissue staining has not revealed any positive staining. Additional optimisation of the technique could be investigated however, a larger cohort of tumour samples should first be stained at the conditions optimised for cell pellets. It may be that changes in Nek11 expression are not prevalent in the majority of colorectal tumours. This is also suggested by the previous expression study whereby 35% of colorectal tumours showed elevated Nek11 expression (Sorensen *et al.*, 2010).

There are a number of exciting avenues that the immunohistochemistry work could be taken. For example, it would be interesting to study Nek11 expression across different colorectal tumour grades compared to normal tissue to see whether expression is stage dependent as suggested by Sorensen *et al.* (2010). In addition, since Nek11 is activated in response to DNA damage it would also be interesting to examine its expression before and after radiotherapy to see whether there is a difference in expression levels, and therefore whether combination of radiotherapy with Nek11 inhibition would sensitise tumours.

There is also accumulating evidence that Nek11 is highly expressed in lung cancers. Oncomine database analysis by Dr. Joon Wee Ho (Fry lab) revealed high expression of Nek11 in squamous cell lung cancers. Furthermore, Nek11 mutations have been identified in ovarian, brain and lung tumours (Moniz *et al.*, 2011). Whether these mutations cause tumour progression through abrogation of the checkpoint by inactivation remains to be studied, but would significantly strengthen the concept of Nek11 as a therapeutic target for checkpoint inhibition.

CHAPTER 7 DISCUSSION

7.1 Does Nek11 have a role in the DNA damage response?

7.1.1 Nek11 is required for G2/M accumulation in response to DNA damaging agents

Activation of DNA damage cell cycle checkpoints in response to genotoxic stresses is crucial in order to allow time for DNA repair processes, and therefore maintain genome stability and prevent tumorigenesis (Ciccia & Elledge, 2010). It has been well established that in response to DNA damage, Chk1 phosphorylates Ser76 on Cdc25A that primes it for further phosphorylation at Ser82 and Ser88 leading to recruitment of the ubiquitin ligase SCF^{β-TrCP} and Cdc25A degradation. This keeps Cdk1/cyclin B inactive and results in G2/M arrest. A screen for novel components of the G2/M checkpoint identified Nek11 as the kinase that phosphorylates Cdc25A at these SCF^{β-TrCP} binding sites, following its activation by Chk1 (Melixetian *et al.*, 2009). However, this finding was questioned by a further study which suggested that it was not Nek11, but CK1α that was responsible for the phosphorylation and proteasomal degradation of Cdc25A in response to DNA damage by IR (Honaker & Piwnicka-Worms, 2010; Piao *et al.*, 2011). In this study we have demonstrated that Nek11 is a key component of the G2/M DNA damage checkpoint and is required for successful cell cycle arrest in response to different forms of DNA damage, including DSBs and inter- and intrastrand DNA crosslinks. This fits with data from previous studies whereby Nek11 activity was increased in response to both genotoxic chemicals and DNA replication inhibitors (Noguchi *et al.*, 2002).

We investigated the role of Nek11 in the colorectal carcinoma-derived cell line, HCT116, since expression of Nek11 was reported to be elevated in colorectal adenomas and carcinomas (Sorensen *et al.*, 2010). Using two individual siRNA oligonucleotides to deplete Nek11 we found that Nek11 is required for the G2/M arrest in response to DNA damaging agents, including IR, and the chemotherapeutically relevant agents, irinotecan and oxaliplatin. We also

directly compared these responses in isogenic p53-null HCT116 cells and found that Nek11 was also required for G2/M checkpoint activation in response to both IR and irinotecan in these cells. This indicates that p53 is not necessary for the Nek11-dependent cell cycle response to these treatments. However, treatment with oxaliplatin, did not lead to a significant G2/M arrest in p53-null cells and Nek11 depletion had no effect on the percentage of cells at this stage. An explanation for this is that oxaliplatin induced arrest is p53-dependent (Arango *et al.*, 2004; Toscano *et al.*, 2007). Therefore, the combination of a Nek11 drug with oxaliplatin treatment would not be an ideal treatment for p53-null or mutant tumours.

The DDR mechanism acts to prevent tumorigenesis through maintaining genomic stability. Indeed, during early stages of cancer progression, components of the DDR are often upregulated, but then downregulated in late stage cancers perhaps as a mechanism of resistance and to obtain a proliferative advantage. This is also the case for Nek11 since expression studies revealed that Nek11 was more highly expressed in adenomas compared to carcinomas (Sorensen *et al.*, 2010). Therefore, to expand on these studies investigation of the role of Nek11 in cells derived from various stages of colorectal cancer progression would reveal whether early stages tumours become more sensitive to DNA damage in combination with Nek11 depletion. Furthermore, it will also be important to investigate the role for Nek11 in other colorectal cancer cell lines, in primary colorectal cancer tissue and in cells derived from other cancer types. One starting point would be lung cancer cell lines, since expression database analyses revealed that Nek11 expression is elevated in lung tumours (Joon Wee Ho and Andrew Fry, unpublished data).

7.1.2 Nek11 is required for cell survival

Interestingly, in addition to its requirement at the G2/M checkpoint, we also found by Annexin V and clonogenic assays that Nek11 depletion in HCT116 cells results in the induction of apoptosis and inhibition of long-term cell survival,

respectively. This was observed in both the presence or absence of DNA damage. Hence, HCT116 cells also rely on the presence of Nek11 for normal proliferation. Interestingly, Chk1, the upstream kinase of Nek11, and a well-validated target for cancer drug development, is also required for the viability of normal cells. Importantly, depletion of Nek11 in combination with IR resulted in an increased sensitivity of these cells with many undergoing apoptosis. Indeed, we suspect that cells that fail to arrest in G2/M don't simply continue with cell cycle progression but are actively removed by apoptosis. Therefore, Nek11 does represent a potentially interesting target for drug development, particularly in combination treatments with DNA damaging agents. Further studies will be required though to examine toxicity in normal cells and determine whether a therapeutic window for treatments exists.

7.2 What's the relevance of different Nek11 isoform expression?

Previous studies had identified the expression of two alternatively spliced isoforms: Nek11 Long (L) and Nek11 Short (S) (Noguchi *et al.*, 2002). However data characterising these isoforms remained very sparse. Here we describe the expression of a further two isoforms: Nek11C and Nek11D. The four variants share amino acid identity up to residue 466 after which the C-terminal sequences diverges. Through generation of U2OS stable cell lines expressing each of these variants as well as a kinase-dead version of Nek11L we investigated individual Nek11 isoform behaviour to gain insight into the importance and potential mechanisms of action for each.

Using qRT-PCR we show that each of the Nek11 isoforms are expressed across a range of colorectal cancer cell lines, with some isoforms showing elevated expression in particular cell types when compared to HCEC cells, an immortalised colorectal cell line. Interestingly, we show that in HT29 cells the expression of Nek11S is much higher compared to the other cell lines. Using isoform specific oligonucleotides to deplete individual isoforms revealed that

depletion of Nek11S in HCT116 cells results in a greater abrogation of the checkpoint compared to depletion of Nek11L/D. Whilst this indicates that Nek11S plays an important and active role within the G2/M checkpoint we do not yet know whether it is the more active isoform. It could be that Nek11S protein levels are more abundant in these cells and hence depletion of Nek11S results in a greater abrogation of the checkpoint in response to DNA damage. Indeed, the in-house generated Nek11 antibody revealed greater expression of the shorter isoform in U2OS cells than the longer isoforms. With regards to DNA damage checkpoint activation, future work should investigate whether depletion of Nek11S leads generally to increased sensitisation to DNA damage.

7.3 What's the purpose of nucleocytoplasmic shuttling of Nek11?

Previous localisation studies identified Nek11 to localise to nuclei and nucleoli during interphase (Noguchi *et al.*, 2002; Noguchi *et al.*, 2004). However, these studies did not address specific isoforms. Using the stable cell lines, we show that the Nek11 isoforms exhibit distinct localisation patterns with the two longer isoforms, Nek11L and Nek11D, exhibiting mainly cytoplasmic distribution and the shorter isoforms, Nek11S and Nek11C, also showing localisation to nuclei. This suggests that the Nek11 isoforms may be playing distinct roles during cell cycle control. Indeed, we found that the Nek11D isoform was degraded by the proteasome in cells, but for what reason remains to be elucidated. Through the use of a nuclear export inhibitor, LMB, we show that the cytoplasmic distribution of the Nek11 isoforms results from rapid nucleocytoplasmic shuttling since treatment with LMB results in the accumulation of Nek11 protein in the nucleus. Through generation of truncation mutants, we identified regions within the C-terminal non-catalytic domain responsible for both nuclear import and export.

In response to DNA damage, sensor and mediator proteins recruit a vast number of proteins to sites of the DNA lesion to promote DNA repair and amplify the DDR signal to downstream effector proteins. We therefore,

examined the effect of DNA damage induced by IR on the localisation of Nek11 over a 24 hour time-course. We found that the bulk of Nek11 protein localisation remained unchanged, but at late time points after DNA damage induction there was apparent recruitment of Nek11L to DNA damage foci. This exciting finding suggests that Nek11 does not play an immediate response in the detection of DNA damage but more likely a role later in the DDR, perhaps in DNA repair. Interestingly, our mass-spectrometry data indicated Ku70 as a potential Nek11 interacting partner. Ku70 along with its partner Ku80 localises to sites of DSBs to mediate DNA repair through NHEJ, so this could suggest a potential novel mechanism for Nek11 in this pathway. This could be examined through co-localisation with other markers of NHEJ as well as analysis of Nek11L localisation in cells with defective NHEJ repair pathways. In addition, the efficiency of DNA repair via comet assays in Nek11 depleted cells exposed to DNA damage could be examined.

We propose that the nucleocytoplasmic shuttling of Nek11 is required for at least some of its DDR roles, for example in DNA repair. However the proposed upstream regulator and downstream substrate of Nek11, i.e. Chk1 and Cdc25A, although mainly nuclear also exhibit nucleocytoplasmic shuttling. Hence, it is equally plausible that some its DDR functions are exerted in the cytoplasm.

7.4 Why does Nek11 overexpression result in aneuploidy?

Using the U2OS:Nek11 stable cell lines and flow cytometry we found that overexpression of Nek11L but not the kinase-inactive version, results in an increased population of cells at G2/M. This suggests that Nek11 plays a role in normal cell cycle progression in an activity dependent manner. How this occurs is not yet known, although this could occur through controlling the stability of Cdc25A to ensure the timely progression into mitosis. Interestingly however, we also show that overexpression of Nek11 results in the formation of polyploid cells. This suggests that increased Nek11 activity either prevents cytokinesis or, more likely, causes endoreduplication as a result of delayed cell cycle

progression (Toettcher *et al.*, 2009). Again, this supports a role for Nek11, like Chk1, in controlling cell cycle progression even in the absence of specific damage.

7.5 Is Nek11 a validated chemotherapeutic target?

Our findings that Nek11 is required for successful induction of G2/M DNA damage checkpoint in response to a variety of DNA damaging agents makes it a potentially interesting drug target. One increasingly attractive method to target cancer cells is through the use of synthetic lethality. This exploits defects commonly found in cancer cells such as loss of the G1/S checkpoint. Inhibition of key players of the G2/M checkpoint through targeted agents, followed by exposure to DNA damaging agents, would lead to selective cancer cell death. Normal cells will have the remaining G1/S checkpoint to arrest and repair their DNA damage and so would not be killed. In the clinic inhibitors against Chk1 have already been developed and used in this way.

In this study, we compared the survival of cells depleted of Nek11 in cells via apoptotic and clonogenic assays and assessed whether this depended on the p53 status. Whilst loss of Nek11 led to G2/M checkpoint abrogation in both p53 wild-type and null cells, there was no significant increase in sensitivity in response to DNA damaging agents in the p53-null cells. It may well be that given the essential role of p53 in apoptosis that efficient apoptosis was not induced in this cell type despite loss of the G1/S checkpoint. Equally, it could be that these cells underwent cell death via mitotic catastrophe, although this remains to be experimentally determined. It would therefore be interesting to explore the long-term consequences of depleting Nek11 in combination with DNA damaging agents in cells with other defects G1/S progression, such as loss of Rb.

Finally, based on the controversy over whether Nek11 or CK1 α is responsible for targeting Cdc25A for destruction, it will be interesting to compare the

consequence of Nek11 depletion with CK1 α inhibition, as well as a combination of both, in different cells and in response to different genotoxic stresses.

7.6 Concluding remarks

The first aim of this study was to identify whether Nek11 plays an active role within the DNA damage response given the contradictory reports. Here, we have confirmed that Nek11 is required not only for G2/M arrest in response to a number of DNA damaging agents including IR, oxaliplatin and irinotecan, but also for cell survival in the absence of DNA damage in the colorectal tumour cell line, HCT116. Moreover, combination of DNA damaging agents with Nek11 depletion shows loss of cell survival and inability to proliferate. This adds weight to the hypothesis that Nek11 is an interesting potential drug target for cancer therapy. The second aim was to explore the underlying mechanisms through which Nek11 might contribute to cell cycle control. Here, we uncovered new insights into the control of its subcellular localization and observed that Nek11 can both interact with components of the NHEJ DNA repair pathway and localizes to sites of DNA damage at times when repair is expected to be taking place (Figure 7.1). Clearly much work remains though to determine the precise roles of Nek11 in cells and how it contributes to the DDR in normal and cancer cells.

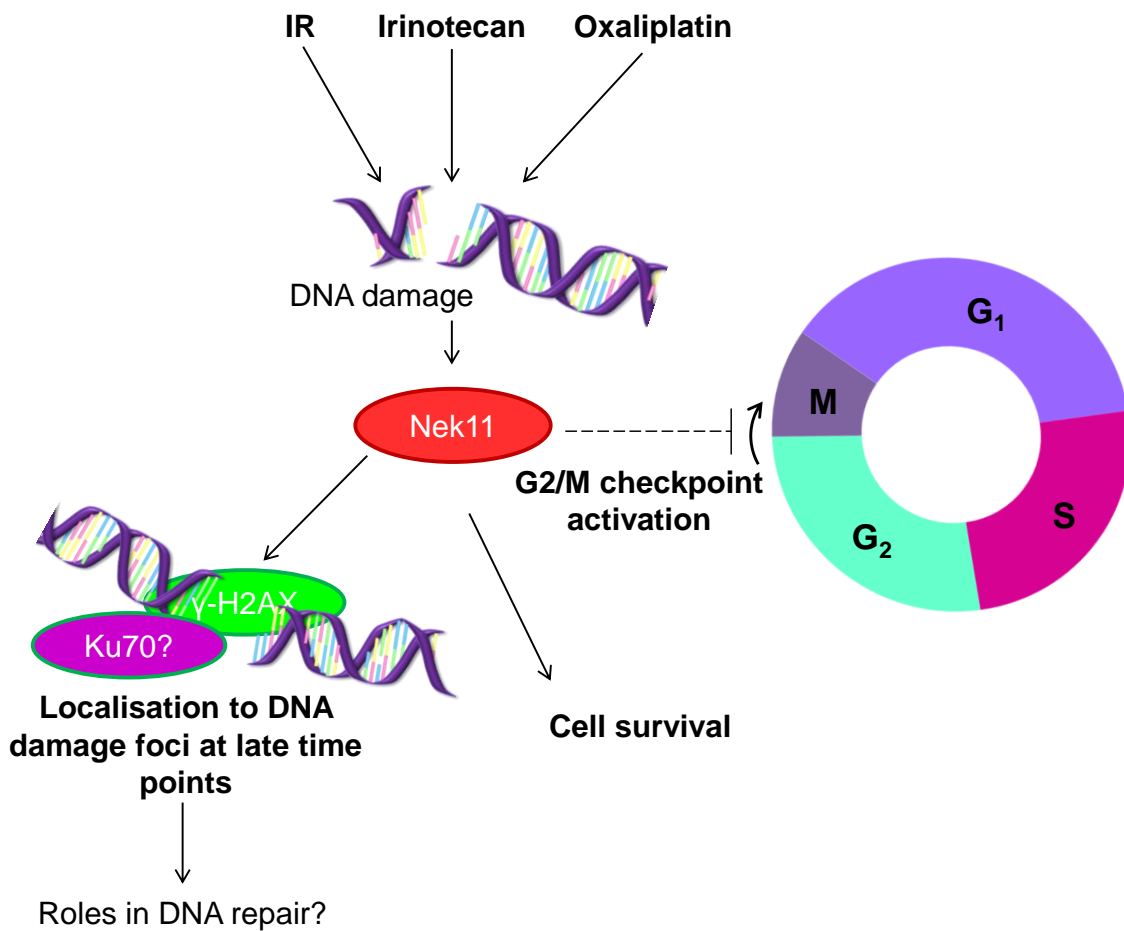


Figure 7.1 Cellular roles and mechanisms for Nek11

Nek11 plays an important role in the activation of the G2/M DNA damage checkpoint in response to a number of DNA damaging agents and is required for cell survival. Furthermore, localisation to sites of DNA damage at late time points suggests a role for Nek11 later on in the DDR pathways with roles in DNA repair being an attractive possibility.

CHAPTER 8 BIBLIOGRAPHY

Abraham, R.T., 2001. Cell cycle checkpoint signaling through the ATM and ATR kinases. *Genes & Development*. **15**, 2177-2196.

Acs, K., Luijsterburg, M.S., Ackermann, L., Salomons, F.A., Hoppe, T., Dantuma, N.P., 2011. The AAA-ATPase VCP/p97 promotes 53BP1 recruitment by removing L3MBTL1 from DNA double-strand breaks. *Nature Structural & Molecular Biology*. **18**, 1345-1350.

Agarwal, M.L., Agarwal, A., Taylor, W.R., Stark, G.R., 1995. p53 controls both the G2/M and the G1 cell cycle checkpoints and mediates reversible growth arrest in human fibroblasts. *Proceedings of the National Academy of Sciences of the United States of America*. **92**, 8493-8497.

Ahn, J.Y., Schwarz, J.K., Piwnica-Worms, H., Canman, C.E., 2000. Threonine 68 phosphorylation by ataxia telangiectasia mutated is required for efficient activation of Chk2 in response to ionizing radiation. *Cancer Research*. **60**, 5934-5936.

Arango, D., Wilson, A.J., Shi, Q., Corner, G.A., Aranes, M.J., Nicholas, C., Lesser, M., Mariadason, J.M., Augenlicht, L.H., 2004. Molecular mechanisms of action and prediction of response to oxaliplatin in colorectal cancer cells. *British Journal of Cancer*. **91**, 1931-1946.

Arnold, C.N., Goel, A., Blum, H.E., Boland, C.R., 2005. Molecular pathogenesis of colorectal cancer: implications for molecular diagnosis. *Cancer*. **104**, 2035-2047.

Bahe, S., Stierhof, Y.D., Wilkinson, C.J., Leiss, F., Nigg, E.A., 2005. Rootletin forms centriole-associated filaments and functions in centrosome cohesion. *The Journal of Cell Biology*. **171**, 27-33.

Baker, S.J., Preisinger, A.C., Jessup, J.M., Paraskeva, C., Markowitz, S., Willson, J.K., Hamilton, S., Vogelstein, B., 1990. P53 Gene Mutations Occur in Combination with 17p Allelic Deletions as Late Events in Colorectal Tumorigenesis. *Cancer Research*. **50**, 7717-7722.

Bakkenist, C.J. & Kastan, M.B., 2003. DNA damage activates ATM through intermolecular autophosphorylation and dimer dissociation. *Nature*. **421**, 499-506.

Ballinger, A.B. & Anggiansah, C., 2007. Colorectal cancer. *BMJ (Clinical Research Ed.)*. **335**, 715-718.

Bartek, J. & Lukas, J., 2003. Chk1 and Chk2 kinases in checkpoint control and cancer. *Cancer Cell*. **3**, 421-429.

- Bartek, J., Lukas, J., Bartkova, J., 2007. DNA damage response as an anti-cancer barrier: damage threshold and the concept of 'conditional haploinsufficiency'. *Cell Cycle (Georgetown, Tex.)*. **6**, 2344-2347.
- Bartkova, J., Horejsi, Z., Koed, K., Kramer, A., Tort, F., Zieger, K., Guldborg, P., Sehested, M., Nesland, J.M., Lukas, C., Orntoft, T., Lukas, J., Bartek, J., 2005. DNA damage response as a candidate anti-cancer barrier in early human tumorigenesis. *Nature*. **434**, 864-870.
- Belham, C., Roig, J., Caldwell, J.A., Aoyama, Y., Kemp, B.E., Comb, M., Avruch, J., 2003. A mitotic cascade of NIMA family kinases. Nerc1/Nek9 activates the Nek6 and Nek7 kinases. *The Journal of Biological Chemistry*. **278**, 34897-34909.
- Bergen, L.G., Upshall, A., Morris, N.R., 1984. S-phase, G2, and nuclear division mutants of *Aspergillus nidulans*. *Journal of Bacteriology*. **159**, 114-119.
- Berggard, T., Linse, S., James, P., 2007. Methods for the detection and analysis of protein-protein interactions. *Proteomics*. **7**, 2833-2842.
- Bladen, C.L., Udayakumar, D., Takeda, Y., Dynan, W.S., 2005. Identification of the polypyrimidine tract binding protein-associated splicing factor.p54(nrb) complex as a candidate DNA double-strand break rejoining factor. *The Journal of Biological Chemistry*. **280**, 5205-5210.
- Bleoo, S., Sun, X., Hendzel, M.J., Rowe, J.M., Packer, M., Godbout, R., 2001. Association of human DEAD box protein DDX1 with a cleavage stimulation factor involved in 3'-end processing of pre-mRNA. *Molecular Biology of the Cell*. **12**, 3046-3059.
- Boulon, S., Westman, B.J., Hutten, S., Boisvert, F.M., Lamond, A.I., 2010. The nucleolus under stress. *Molecular Cell*. **40**, 216-227.
- Brenner, H., Kloor, M., Pox, C.P., 2014. Colorectal cancer. *Lancet*. **383**, 1490-1502.
- Bridge, G., Rashid, S., Martin, S.A., 2014. DNA mismatch repair and oxidative DNA damage: implications for cancer biology and treatment. *Cancers*. **6**, 1597-1614.
- Brown, E.J. & Baltimore, D., 2003. Essential and dispensable roles of ATR in cell cycle arrest and genome maintenance. *Genes & Development*. **17**, 615-628.
- Cadet, J., Berger, M., Douki, T., Ravanat, J.L., 1997. Oxidative damage to DNA: formation, measurement, and biological significance. *Reviews of Physiology, Biochemistry and Pharmacology*. **131**, 1-87.

Campisi, J. & d'Adda di Fagagna, F., 2007. Cellular senescence: when bad things happen to good cells. *Nature Reviews.Molecular Cell Biology*. **8**, 729-740.

Candiano, G., Bruschi, M., Musante, L., Santucci, L., Ghiggeri, G.M., Carnemolla, B., Orecchia, P., Zardi, L., Righetti, P.G., 2004. Blue silver: a very sensitive colloidal Coomassie G-250 staining for proteome analysis. *Electrophoresis*. **25**, 1327-1333.

Cann, K.L. & Hicks, G.G., 2006. Absence of an immediate G1/S checkpoint in primary MEFs following gamma-irradiation identifies a novel checkpoint switch. *Cell Cycle (Georgetown, Tex.)*. **5**, 1823-1830.

Cao, S., Bhattacharya, A., Durrani, F.A., Fakhri, M., 2006. Irinotecan, oxaliplatin and raltitrexed for the treatment of advanced colorectal cancer. *Expert Opinion on Pharmacotherapy*. **7**, 687-703.

Cardoso, M.C., Leonhardt, H., Nadal-Ginard, B., 1993. Reversal of terminal differentiation and control of DNA replication: cyclin A and Cdk2 specifically localize at subnuclear sites of DNA replication. *Cell*. **74**, 979-992.

Celeste, A., Petersen, S., Romanienko, P.J., Fernandez-Capetillo, O., Chen, H.T., Sedelnikova, O.A., Reina-San-Martin, B., Coppola, V., Meffre, E., Difilippantonio, M.J., Redon, C., Pilch, D.R., Orlan, A., Eckhaus, M., Camerini-Otero, R.D., Tessarollo, L., Livak, F., Manova, K., Bonner, W.M., Nussenzweig, M.C., Nussenzweig, A., 2002. Genomic instability in mice lacking histone H2AX. *Science (New York, N.Y.)*. **296**, 922-927.

Center, M.M., Jemal, A., Smith, R.A., Ward, E., 2009. Worldwide variations in colorectal cancer. *CA: A Cancer Journal for Clinicians*. **59**, 366-378.

Chaki, M., Airik, R., Ghosh, A.K., Giles, R.H., Chen, R., Slaats, G.G., Wang, H., Hurd, T.W., Zhou, W., Cluckey, A., Gee, H.Y., Ramaswami, G., Hong, C.J., Hamilton, B.A., Cervenka, I., Ganji, R.S., Bryja, V., Arts, H.H., van Reeuwijk, J., Oud, M.M., Letteboer, S.J., Roepman, R., Husson, H., Ibraghimov-Beskrovnaya, O., Yasunaga, T., Walz, G., Eley, L., Sayer, J.A., Schermer, B., Liebau, M.C., Benzing, T., Le Corre, S., Drummond, I., Janssen, S., Allen, S.J., Natarajan, S., O'Toole, J.F., Attanasio, M., Saunier, S., Antignac, C., Koenekoop, R.K., Ren, H., Lopez, I., Nayir, A., Stoetzel, C., Dollfus, H., Massoudi, R., Gleeson, J.G., Andreoli, S.P., Doherty, D.G., Lindstrad, A., Golzio, C., Katsanis, N., Pape, L., Abboud, E.B., Al-Rajhi, A.A., Lewis, R.A., Omran, H., Lee, E.Y., Wang, S., Sekiguchi, J.M., Saunders, R., Johnson, C.A., Garner, E., Vanselow, K., Andersen, J.S., Shlomei, J., Nurnberg, G., Nurnberg, P., Levy, S., Smogorzewska, A., Otto, E.A., Hildebrandt, F., 2012. Exome capture reveals ZNF423 and CEP164 mutations, linking renal ciliopathies to DNA damage response signaling. *Cell*. **150**, 533-548.

Chang, J., Baloh, R.H., Milbrandt, J., 2009. The NIMA-family kinase Nek3 regulates microtubule acetylation in neurons. *Journal of Cell Science*. **122**, 2274-2282.

- Chen, A., Yanai, A., Arama, E., Kilfin, G., Motro, B., 1999. NIMA-related kinases: isolation and characterization of murine nek3 and nek4 cDNAs, and chromosomal localization of nek1, nek2 and nek3. *Gene*. **234**, 127-137.
- Chen, R.H., Waters, J.C., Salmon, E.D., Murray, A.W., 1996. Association of spindle assembly checkpoint component XMAP215 with unattached kinetochores. *Science (New York, N.Y.)*. **274**, 242-246.
- Chen, Y., Chen, C.F., Riley, D.J., Chen, P.L., 2011. Nek1 kinase functions in DNA damage response and checkpoint control through a pathway independent of ATM and ATR. *Cell Cycle (Georgetown, Tex.)*. **10**, 655-663.
- Chen, Y., Chen, P.L., Chen, C.F., Jiang, X., Riley, D.J., 2008a. Never-in-mitosis related kinase 1 functions in DNA damage response and checkpoint control. *Cell Cycle (Georgetown, Tex.)*. **7**, 3194-3201.
- Chen, Y., Chen, P.L., Chen, C.F., Jiang, X., Riley, D.J., 2008b. Never-in-mitosis related kinase 1 functions in DNA damage response and checkpoint control. *Cell Cycle (Georgetown, Tex.)*. **7**, 3194-3201.
- Choi, H.J., Lin, J.R., Vannier, J.B., Slaats, G.G., Kile, A.C., Paulsen, R.D., Manning, D.K., Beier, D.R., Giles, R.H., Boulton, S.J., Cimprich, K.A., 2013. NEK8 links the ATR-regulated replication stress response and S phase CDK activity to renal ciliopathies. *Molecular Cell*. **51**, 423-439.
- Christmann, M. & Kaina, B., 2013. Transcriptional regulation of human DNA repair genes following genotoxic stress: trigger mechanisms, inducible responses and genotoxic adaptation. *Nucleic Acids Research*. **41**, 8403-8420.
- Ciccio, A. & Elledge, S.J., 2010. The DNA damage response: making it safe to play with knives. *Molecular Cell*. **40**, 179-204.
- Clarke, A.R., Purdie, C.A., Harrison, D.J., Morris, R.G., Bird, C.C., Hooper, M.L., Wyllie, A.H., 1993. Thymocyte apoptosis induced by p53-dependent and independent pathways. *Nature*. **362**, 849-852.
- Cobrinik, D., 2005. Pocket proteins and cell cycle control. *Oncogene*. **24**, 2796-2809.
- Cohen, P., 2002. Protein kinases--the major drug targets of the twenty-first century? *Nature Reviews Drug Discovery*. **1**, 309-315.
- Connell-Crowley, L., Solomon, M.J., Wei, N., Harper, J.W., 1993. Phosphorylation independent activation of human cyclin-dependent kinase 2 by cyclin A in vitro. *Molecular Biology of the Cell*. **4**, 79-92.
- Cortez, D., Guntuku, S., Qin, J., Elledge, S.J., 2001. ATR and ATRIP: partners in checkpoint signaling. *Science (New York, N.Y.)*. **294**, 1713-1716.

d'Adda di Fagagna, F., 2008. Living on a break: cellular senescence as a DNA-damage response. *Nature Reviews.Cancer*. **8**, 512-522.

Daniely, Y., Dimitrova, D.D., Borowiec, J.A., 2002. Stress-dependent nucleolin mobilization mediated by p53-nucleolin complex formation. *Molecular and Cellular Biology*. **22**, 6014-6022.

Dannenbergh, J.H., van Rossum, A., Schuijff, L., te Riele, H., 2000. Ablation of the retinoblastoma gene family deregulates G(1) control causing immortalization and increased cell turnover under growth-restricting conditions. *Genes & Development*. **14**, 3051-3064.

David, S.S., O'Shea, V.L., Kundu, S., 2007. Base-excision repair of oxidative DNA damage. *Nature*. **447**, 941-950.

Davies, J.R., Osmani, A.H., De Souza, C.P., Bachewich, C., Osmani, S.A., 2004. Potential link between the NIMA mitotic kinase and nuclear membrane fission during mitotic exit in *Aspergillus nidulans*. *Eukaryotic Cell*. **3**, 1433-1444.

De Souza, C.P., Osmani, A.H., Wu, L.P., Spotts, J.L., Osmani, S.A., 2000. Mitotic histone H3 phosphorylation by the NIMA kinase in *Aspergillus nidulans*. *Cell*. **102**, 293-302.

Deckbar, D., Jeggo, P.A., Lobrich, M., 2011. Understanding the limitations of radiation-induced cell cycle checkpoints. *Critical Reviews in Biochemistry and Molecular Biology*. **46**, 271-283.

Deckbar, D., Stiff, T., Koch, B., Reis, C., Lobrich, M., Jeggo, P.A., 2010. The limitations of the G1-S checkpoint. *Cancer Research*. **70**, 4412-4421.

Dellaire, G. & Bazett-Jones, D.P., 2007. Beyond repair foci: subnuclear domains and the cellular response to DNA damage. *Cell Cycle (Georgetown, Tex.)*. **6**, 1864-1872.

Di Leonardo, A., Linke, S.P., Clarkin, K., Wahl, G.M., 1994. DNA damage triggers a prolonged p53-dependent G1 arrest and long-term induction of Cip1 in normal human fibroblasts. *Genes & Development*. **8**, 2540-2551.

Dinant, C., Ampatzidis-Michailidis, G., Lans, H., Tresini, M., Lagarou, A., Grosbart, M., Theil, A.F., van Cappellen, W.A., Kimura, H., Bartek, J., Fousteri, M., Houtsmuller, A.B., Vermeulen, W., Marteijn, J.A., 2013. Enhanced chromatin dynamics by FACT promotes transcriptional restart after UV-induced DNA damage. *Molecular Cell*. **51**, 469-479.

Donzelli, M. & Draetta, G.F., 2003. Regulating mammalian checkpoints through Cdc25 inactivation. *EMBO Reports*. **4**, 671-677.

Douillard, J.Y., Cunningham, D., Roth, A.D., Navarro, M., James, R.D., Karasek, P., Jandik, P., Iveson, T., Carmichael, J., Alakl, M., Gruia, G., Awad, L., Rougier, P., 2000. Irinotecan combined with fluorouracil compared with

fluorouracil alone as first-line treatment for metastatic colorectal cancer: a multicentre randomised trial. *Lancet*. **355**, 1041-1047.

Edmond, V., Moysan, E., Khochbin, S., Matthias, P., Brambilla, C., Brambilla, E., Gazzeri, S., Eymin, B., 2011. Acetylation and phosphorylation of SRSF2 control cell fate decision in response to cisplatin. *The EMBO Journal*. **30**, 510-523.

el-Deiry, W.S., Tokino, T., Velculescu, V.E., Levy, D.B., Parsons, R., Trent, J.M., Lin, D., Mercer, W.E., Kinzler, K.W., Vogelstein, B., 1993. WAF1, a potential mediator of p53 tumor suppression. *Cell*. **75**, 817-825.

Evans, T., Rosenthal, E.T., Youngblom, J., Distel, D., Hunt, T., 1983. Cyclin: a protein specified by maternal mRNA in sea urchin eggs that is destroyed at each cleavage division. *Cell*. **33**, 389-396.

Falck, J., Coates, J., Jackson, S.P., 2005. Conserved modes of recruitment of ATM, ATR and DNA-PKcs to sites of DNA damage. *Nature*. **434**, 605-611.

Faragher, A.J. & Fry, A.M., 2003. Nek2A kinase stimulates centrosome disjunction and is required for formation of bipolar mitotic spindles. *Molecular Biology of the Cell*. **14**, 2876-2889.

Fearon, E.R., 2011. Molecular genetics of colorectal cancer. *Annual Review of Pathology*. **6**, 479-507.

Fei, P. & El-Deiry, W.S., 2003. P53 and radiation responses. *Oncogene*. **22**, 5774-5783.

Ferlay, J., Shin, H.R., Bray, F., Forman, D., Mathers, C., Parkin, D.M., 2010. Estimates of worldwide burden of cancer in 2008: GLOBOCAN 2008. *International Journal of Cancer. Journal International Du Cancer*. **127**, 2893-2917.

Fernandez-Capetillo, O., Chen, H.T., Celeste, A., Ward, I., Romanienko, P.J., Morales, J.C., Naka, K., Xia, Z., Camerini-Otero, R.D., Motoyama, N., Carpenter, P.B., Bonner, W.M., Chen, J., Nussenzweig, A., 2002. DNA damage-induced G2-M checkpoint activation by histone H2AX and 53BP1. *Nature Cell Biology*. **4**, 993-997.

Fletcher, L., Cerniglia, G.J., Nigg, E.A., Yend, T.J., Muschel, R.J., 2004. Inhibition of centrosome separation after DNA damage: a role for Nek2. *Radiation Research*. **162**, 128-135.

Fletcher, L., Cerniglia, G.J., Yen, T.J., Muschel, R.J., 2005. Live cell imaging reveals distinct roles in cell cycle regulation for Nek2A and Nek2B. *Biochimica Et Biophysica Acta*. **1744**, 89-92.

- Forrest, A.R., Taylor, D., Grimmond, S., RIKEN GER Group, GSL Members, 2003. Exploration of the cell-cycle genes found within the RIKEN FANTOM2 data set. *Genome Research*. **13**, 1366-1375.
- Franken, N.A., Rodermond, H.M., Stap, J., Haveman, J., van Bree, C., 2006. Clonogenic assay of cells in vitro. *Nature Protocols*. **1**, 2315-2319.
- Fry, A.M., Mayor, T., Meraldi, P., Stierhof, Y.D., Tanaka, K., Nigg, E.A., 1998a. C-Nap1, a novel centrosomal coiled-coil protein and candidate substrate of the cell cycle-regulated protein kinase Nek2. *The Journal of Cell Biology*. **141**, 1563-1574.
- Fry, A.M., Meraldi, P., Nigg, E.A., 1998b. A centrosomal function for the human Nek2 protein kinase, a member of the NIMA family of cell cycle regulators. *The EMBO Journal*. **17**, 470-481.
- Fry, A.M., O'Regan, L., Sabir, S.R., Bayliss, R., 2012a. Cell cycle regulation by the NEK family of protein kinases. *Journal of Cell Science*. **125**, 4423-4433.
- Fry, A.M., O'Regan, L., Sabir, S.R., Bayliss, R., 2012b. Cell cycle regulation by the NEK family of protein kinases. *Journal of Cell Science*. **125**, 4423-4433.
- Fry, A.M., Schultz, S.J., Bartek, J., Nigg, E.A., 1995. Substrate specificity and cell cycle regulation of the Nek2 protein kinase, a potential human homolog of the mitotic regulator NIMA of *Aspergillus nidulans*. *The Journal of Biological Chemistry*. **270**, 12899-12905.
- Fuchs, C., Mitchell, E.P., Hoff, P.M., 2006. Irinotecan in the treatment of colorectal cancer. *Cancer Treatment Reviews*. **32**, 491-503.
- Gale, M., Jr & Parsons, M., 1993. A *Trypanosoma brucei* gene family encoding protein kinases with catalytic domains structurally related to Nek1 and NIMA. *Molecular and Biochemical Parasitology*. **59**, 111-121.
- Ganem, N.J., Storchova, Z., Pellman, D., 2007. Tetraploidy, aneuploidy and cancer. *Current Opinion in Genetics & Development*. **17**, 157-162.
- Gatei, M., Sloper, K., Sorensen, C., Syljuasen, R., Falck, J., Hobson, K., Savage, K., Lukas, J., Zhou, B.B., Bartek, J., Khanna, K.K., 2003. Ataxia-telangiectasia-mutated (ATM) and NBS1-dependent phosphorylation of Chk1 on Ser-317 in response to ionizing radiation. *The Journal of Biological Chemistry*. **278**, 14806-14811.
- Giacchetti, S., Perpoint, B., Zidani, R., Le Bail, N., Faggiuolo, R., Focan, C., Chollet, P., Llory, J.F., Letourneau, Y., Coudert, B., Bertheaut-Cvitkovic, F., Larregain-Fournier, D., Le Rol, A., Walter, S., Adam, R., Misset, J.L., Levi, F., 2000. Phase III multicenter randomized trial of oxaliplatin added to chronomodulated fluorouracil-leucovorin as first-line treatment of metastatic colorectal cancer. *Journal of Clinical Oncology : Official Journal of the American Society of Clinical Oncology*. **18**, 136-147.

- Gingras, A.C., Aebersold, R., Raught, B., 2005. Advances in protein complex analysis using mass spectrometry. *The Journal of Physiology*. **563**, 11-21.
- Ginzinger, D.G., 2002. Gene quantification using real-time quantitative PCR: an emerging technology hits the mainstream. *Experimental Hematology*. **30**, 503-512.
- Golomb, L., Volarevic, S., Oren, M., 2014. p53 and ribosome biogenesis stress: The essentials. *FEBS Letters*.
- Grallert, A. & Hagan, I.M., 2002. Schizosaccharomyces pombe NIMA-related kinase, Fin1, regulates spindle formation and an affinity of Polo for the SPB. *The EMBO Journal*. **21**, 3096-3107.
- Grallert, A., Krapp, A., Bagley, S., Simanis, V., Hagan, I.M., 2004. Recruitment of NIMA kinase shows that maturation of the S. pombe spindle-pole body occurs over consecutive cell cycles and reveals a role for NIMA in modulating SIN activity. *Genes & Development*. **18**, 1007-1021.
- Grothey, A. & Goldberg, R.M., 2004. A review of oxaliplatin and its clinical use in colorectal cancer. *Expert Opinion on Pharmacotherapy*. **5**, 2159-2170.
- Gullo, C., Au, M., Feng, G., Teoh, G., 2006. The biology of Ku and its potential oncogenic role in cancer. *Biochimica Et Biophysica Acta*. **1765**, 223-234.
- Ha, K., Takeda, Y., Dynan, W.S., 2011. Sequences in PSF/SFPQ mediate radioresistance and recruitment of PSF/SFPQ-containing complexes to DNA damage sites in human cells. *DNA Repair*. **10**, 252-259.
- Hames, R.S., Wattam, S.L., Yamano, H., Bacchieri, R., Fry, A.M., 2001. APC/C-mediated destruction of the centrosomal kinase Nek2A occurs in early mitosis and depends upon a cyclin A-type D-box. *The EMBO Journal*. **20**, 7117-7127.
- Harley, C.B., Futcher, A.B., Greider, C.W., 1990. Telomeres shorten during ageing of human fibroblasts. *Nature*. **345**, 458-460.
- Harper, J.W., Burton, J.L., Solomon, M.J., 2002. The anaphase-promoting complex: it's not just for mitosis any more. *Genes & Development*. **16**, 2179-2206.
- Hayflick, L., 1965. The Limited in Vitro Lifetime of Human Diploid Cell Strains. *Experimental Cell Research*. **37**, 614-636.
- Heo, K., Kim, H., Choi, S.H., Choi, J., Kim, K., Gu, J., Lieber, M.R., Yang, A.S., An, W., 2008. FACT-mediated exchange of histone variant H2AX regulated by phosphorylation of H2AX and ADP-ribosylation of Spt16. *Molecular Cell*. **30**, 86-97.

Herbig, U., Jobling, W.A., Chen, B.P., Chen, D.J., Sedivy, J.M., 2004. Telomere shortening triggers senescence of human cells through a pathway involving ATM, p53, and p21(CIP1), but not p16(INK4a). *Molecular Cell*. **14**, 501-513.

Hermeking, H., Lengauer, C., Polyak, K., He, T.C., Zhang, L., Thiagalingam, S., Kinzler, K.W., Vogelstein, B., 1997. 14-3-3 sigma is a p53-regulated inhibitor of G2/M progression. *Molecular Cell*. **1**, 3-11.

Hoeijmakers, J.H., 2001. Genome maintenance mechanisms for preventing cancer. *Nature*. **411**, 366-374.

Holland, P.M., Milne, A., Garka, K., Johnson, R.S., Willis, C., Sims, J.E., Rauch, C.T., Bird, T.A., Virca, G.D., 2002. Purification, cloning, and characterization of Nek8, a novel NIMA-related kinase, and its candidate substrate Bcd2. *The Journal of Biological Chemistry*. **277**, 16229-16240.

Honaker, Y. & Piwnicka-Worms, H., 2010. Casein kinase 1 functions as both penultimate and ultimate kinase in regulating Cdc25A destruction. *Oncogene*. **29**, 3324-3334.

Hoyt, M.A., Totis, L., Roberts, B.T., 1991. *S. cerevisiae* genes required for cell cycle arrest in response to loss of microtubule function. *Cell*. **66**, 507-517.

Huen, M.S. & Chen, J., 2008. The DNA damage response pathways: at the crossroad of protein modifications. *Cell Research*. **18**, 8-16.

Hwang, H.C. & Clurman, B.E., 2005. Cyclin E in normal and neoplastic cell cycles. *Oncogene*. **24**, 2776-2786.

Jackson, P.K., 2013. Nek8 couples renal ciliopathies to DNA damage and checkpoint control. *Molecular Cell*. **51**, 407-408.

Jackson, S.P. & Bartek, J., 2009. The DNA-damage response in human biology and disease. *Nature*. **461**, 1071-1078.

Jacobs, J.J. & de Lange, T., 2004. Significant role for p16INK4a in p53-independent telomere-directed senescence. *Current Biology : CB*. **14**, 2302-2308.

Janaswami, P.M., Birkenmeier, E.H., Cook, S.A., Rowe, L.B., Bronson, R.T., Davisson, M.T., 1997. Identification and genetic mapping of a new polycystic kidney disease on mouse chromosome 8. *Genomics*. **40**, 101-107.

Jones, D.G. & Rosamond, J., 1990. Isolation of a novel protein kinase-encoding gene from yeast by oligodeoxyribonucleotide probing. *Gene*. **90**, 87-92.

Kallstrom, G., Hedges, J., Johnson, A., 2003. The putative GTPases Nog1p and Lsg1p are required for 60S ribosomal subunit biogenesis and are localized to the nucleus and cytoplasm, respectively. *Molecular and Cellular Biology*. **23**, 4344-4355.

- Kandli, M., Feige, E., Chen, A., Kilfin, G., Motro, B., 2000. Isolation and characterization of two evolutionarily conserved murine kinases (Nek6 and nek7) related to the fungal mitotic regulator, NIMA. *Genomics*. **68**, 187-196.
- Kastan, M.B. & Bartek, J., 2004. Cell-cycle checkpoints and cancer. *Nature*. **432**, 316-323.
- Kastan, M.B., Onyekwere, O., Sidransky, D., Vogelstein, B., Craig, R.W., 1991. Participation of p53 protein in the cellular response to DNA damage. *Cancer Research*. **51**, 6304-6311.
- Keller, D.M., Zeng, X., Wang, Y., Zhang, Q.H., Kapoor, M., Shu, H., Goodman, R., Lozano, G., Zhao, Y., Lu, H., 2001. A DNA damage-induced p53 serine 392 kinase complex contains CK2, hSpt16, and SSRP1. *Molecular Cell*. **7**, 283-292.
- Kim, K., Dimitrova, D.D., Carta, K.M., Saxena, A., Daras, M., Borowiec, J.A., 2005. Novel checkpoint response to genotoxic stress mediated by nucleolin-replication protein a complex formation. *Molecular and Cellular Biology*. **25**, 2463-2474.
- Kim, S., Lee, K., Rhee, K., 2007. NEK7 is a centrosomal kinase critical for microtubule nucleation. *Biochemical and Biophysical Research Communications*. **360**, 56-62.
- Klaunig, J.E. & Kamendulis, L.M., 2004. The role of oxidative stress in carcinogenesis. *Annual Review of Pharmacology and Toxicology*. **44**, 239-267.
- Kobayashi, T. & Horiuchi, T., 1996. A yeast gene product, Fob1 protein, required for both replication fork blocking and recombinational hotspot activities. *Genes to Cells : Devoted to Molecular & Cellular Mechanisms*. **1**, 465-474.
- Kornev, A.P. & Taylor, S.S., 2010. Defining the conserved internal architecture of a protein kinase. *Biochimica Et Biophysica Acta*. **1804**, 440-444.
- Kosugi, S., Hasebe, M., Tomita, M., Yanagawa, H., 2009. Systematic identification of cell cycle-dependent yeast nucleocytoplasmic shuttling proteins by prediction of composite motifs. *Proceedings of the National Academy of Sciences of the United States of America*. **106**, 10171-10176.
- Krien, M.J., Bugg, S.J., Palatsides, M., Asouline, G., Morimyo, M., O'Connell, M.J., 1998. A NIMA homologue promotes chromatin condensation in fission yeast. *Journal of Cell Science*. **111 (Pt 7)**, 967-976.
- Krien, M.J., West, R.R., John, U.P., Koniaras, K., McIntosh, J.R., O'Connell, M.J., 2002. The fission yeast NIMA kinase Fin1p is required for spindle function and nuclear envelope integrity. *The EMBO Journal*. **21**, 1713-1722.
- la Cour, T., Gupta, R., Rapacki, K., Skriver, K., Poulsen, F.M., Brunak, S., 2003. NESbase version 1.0: a database of nuclear export signals. *Nucleic Acids Research*. **31**, 393-396.

- la Cour, T., Kiemer, L., Molgaard, A., Gupta, R., Skriver, K., Brunak, S., 2004. Analysis and prediction of leucine-rich nuclear export signals. *Protein Engineering, Design & Selection : PEDS*. **17**, 527-536.
- Lane, D.P., 1992. Cancer. p53, guardian of the genome. *Nature*. **358**, 15-16.
- Lao, V.V. & Grady, W.M., 2011. Epigenetics and colorectal cancer. *Nature Reviews.Gastroenterology & Hepatology*. **8**, 686-700.
- Lee, M.G. & Nurse, P., 1987. Complementation used to clone a human homologue of the fission yeast cell cycle control gene cdc2. *Nature*. **327**, 31-35.
- Lee, M.Y., Kim, H.J., Kim, M.A., Jee, H.J., Kim, A.J., Bae, Y.S., Park, J.I., Chung, J.H., Yun, J., 2008. Nek6 is involved in G2/M phase cell cycle arrest through DNA damage-induced phosphorylation. *Cell Cycle (Georgetown, Tex.)*. **7**, 2705-2709.
- Lee, S.E., Mitchell, R.A., Cheng, A., Hendrickson, E.A., 1997. Evidence for DNA-PK-dependent and -independent DNA double-strand break repair pathways in mammalian cells as a function of the cell cycle. *Molecular and Cellular Biology*. **17**, 1425-1433.
- Lee, S.H. & Kim, C.H., 2002. DNA-dependent protein kinase complex: a multifunctional protein in DNA repair and damage checkpoint. *Molecules and Cells*. **13**, 159-166.
- Lenzken, S.C., Loffreda, A., Barabino, S.M., 2013. RNA splicing: a new player in the DNA damage response. *International Journal of Cell Biology*. **2013**, 153634.
- Letwin, K., Mizzen, L., Motro, B., Ben-David, Y., Bernstein, A., Pawson, T., 1992. A mammalian dual specificity protein kinase, Nek1, is related to the NIMA cell cycle regulator and highly expressed in meiotic germ cells. *The EMBO Journal*. **11**, 3521-3531.
- Leva, V., Giuliano, S., Bardoni, A., Camerini, S., Crescenzi, M., Lisa, A., Biamonti, G., Montecucco, A., 2012. Phosphorylation of SRSF1 is modulated by replicational stress. *Nucleic Acids Research*. **40**, 1106-1117.
- Li, L., Monckton, E.A., Godbout, R., 2008. A role for DEAD box 1 at DNA double-strand breaks. *Molecular and Cellular Biology*. **28**, 6413-6425.
- Li, R. & Murray, A.W., 1991. Feedback control of mitosis in budding yeast. *Cell*. **66**, 519-531.
- Lichtenstein, P., Holm, N.V., Verkasalo, P.K., Iliadou, A., Kaprio, J., Koskenvuo, M., Pukkala, E., Skytthe, A., Hemminki, K., 2000. Environmental and heritable factors in the causation of cancer--analyses of cohorts of twins from Sweden, Denmark, and Finland. *The New England Journal of Medicine*. **343**, 78-85.

- Lieber, M.R., 2008. The mechanism of human nonhomologous DNA end joining. *The Journal of Biological Chemistry*. **283**, 1-5.
- Lindahl, T. & Barnes, D.E., 2000. Repair of endogenous DNA damage. *Cold Spring Harbor Symposia on Quantitative Biology*. **65**, 127-133.
- Liu, Q., Guntuku, S., Cui, X.S., Matsuoka, S., Cortez, D., Tamai, K., Luo, G., Carattini-Rivera, S., DeMayo, F., Bradley, A., Donehower, L.A., Elledge, S.J., 2000. Chk1 is an essential kinase that is regulated by Atr and required for the G(2)/M DNA damage checkpoint. *Genes & Development*. **14**, 1448-1459.
- Liu, S., Lu, W., Obara, T., Kuida, S., Lehoczky, J., Dewar, K., Drummond, I.A., Beier, D.R., 2002. A defect in a novel Nek-family kinase causes cystic kidney disease in the mouse and in zebrafish. *Development (Cambridge, England)*. **129**, 5839-5846.
- Livingstone, M., Ruan, H., Weiner, J., Clauser, K.R., Strack, P., Jin, S., Williams, A., Greulich, H., Gardner, J., Venere, M., Mochan, T.A., DiTullio, R.A., Jr, Moravcevic, K., Gorgoulis, V.G., Burkhardt, A., Halazonetis, T.D., 2005. Valosin-containing protein phosphorylation at Ser784 in response to DNA damage. *Cancer Research*. **65**, 7533-7540.
- Ljungman, M., 2010. The DNA damage response--repair or despair? *Environmental and Molecular Mutagenesis*. **51**, 879-889.
- Lobrich, M. & Jeggo, P.A., 2007. The impact of a negligent G2/M checkpoint on genomic instability and cancer induction. *Nature Reviews.Cancer*. **7**, 861-869.
- Lohka, M.J., Hayes, M.K., Maller, J.L., 1988. Purification of maturation-promoting factor, an intracellular regulator of early mitotic events. *Proceedings of the National Academy of Sciences of the United States of America*. **85**, 3009-3013.
- Long, J.C. & Caceres, J.F., 2009. The SR protein family of splicing factors: master regulators of gene expression. *The Biochemical Journal*. **417**, 15-27.
- Lou, Y., Yao, J., Zereshki, A., Dou, Z., Ahmed, K., Wang, H., Hu, J., Wang, Y., Yao, X., 2004. NEK2A interacts with MAD1 and possibly functions as a novel integrator of the spindle checkpoint signaling. *The Journal of Biological Chemistry*. **279**, 20049-20057.
- Lowe, S.W., Schmitt, E.M., Smith, S.W., Osborne, B.A., Jacks, T., 1993. P53 is Required for Radiation-Induced Apoptosis in Mouse Thymocytes. *Nature*. **362**, 847-849.
- Lu, K.P. & Hunter, T., 1995a. Evidence for a NIMA-like mitotic pathway in vertebrate cells. *Cell*. **81**, 413-424.
- Lu, K.P. & Hunter, T., 1995b. Evidence for a NIMA-like mitotic pathway in vertebrate cells. *Cell*. **81**, 413-424.

- Lu, K.P., Kemp, B.E., Means, A.R., 1994. Identification of substrate specificity determinants for the cell cycle-regulated NIMA protein kinase. *The Journal of Biological Chemistry*. **269**, 6603-6607.
- Ma, H.T. & Poon, R.Y., 2011. How protein kinases co-ordinate mitosis in animal cells. *The Biochemical Journal*. **435**, 17-31.
- Mahjoub, M.R., Montpetit, B., Zhao, L., Finst, R.J., Goh, B., Kim, A.C., Quarmby, L.M., 2002. The FA2 gene of *Chlamydomonas* encodes a NIMA family kinase with roles in cell cycle progression and microtubule severing during deflagellation. *Journal of Cell Science*. **115**, 1759-1768.
- Mahjoub, M.R., Trapp, M.L., Quarmby, L.M., 2005. NIMA-related kinases defective in murine models of polycystic kidney diseases localize to primary cilia and centrosomes. *Journal of the American Society of Nephrology : JASN*. **16**, 3485-3489.
- Malumbres, M., 2011. Physiological relevance of cell cycle kinases. *Physiological Reviews*. **91**, 973-1007.
- Malumbres, M. & Barbacid, M., 2005. Mammalian cyclin-dependent kinases. *Trends in Biochemical Sciences*. **30**, 630-641.
- Malumbres, M., Harlow, E., Hunt, T., Hunter, T., Lahti, J.M., Manning, G., Morgan, D.O., Tsai, L.H., Wolgemuth, D.J., 2009. Cyclin-dependent kinases: a family portrait. *Nature Cell Biology*. **11**, 1275-1276.
- Mandemaker, I., Vermeulen, W., Marteiijn, J., 2014. Role of chromatin remodeling during the transcriptional restart upon DNA damage. *Nucleus (Austin, Tex.)*. **5**, .
- Manning, G., Whyte, D.B., Martinez, R., Hunter, T., Sudarsanam, S., 2002. The protein kinase complement of the human genome. *Science (New York, N.Y.)*. **298**, 1912-1934.
- Masui, Y. & Markert, C.L., 1971. Cytoplasmic control of nuclear behavior during meiotic maturation of frog oocytes. *The Journal of Experimental Zoology*. **177**, 129-145.
- Matos, L.L., Trufelli, D.C., de Matos, M.G., da Silva Pinhal, M.A., 2010. Immunohistochemistry as an important tool in biomarkers detection and clinical practice. *Biomarker Insights*. **5**, 9-20.
- Matsuoka, S., Ballif, B.A., Smogorzewska, A., McDonald, E.R., 3rd, Hurov, K.E., Luo, J., Bakalarski, C.E., Zhao, Z., Solimini, N., Lerenthal, Y., Shiloh, Y., Gygi, S.P., Elledge, S.J., 2007a. ATM and ATR substrate analysis reveals extensive protein networks responsive to DNA damage. *Science (New York, N.Y.)*. **316**, 1160-1166.

Matsuoka, S., Ballif, B.A., Smogorzewska, A., McDonald, E.R.,3rd, Hurov, K.E., Luo, J., Bakalarski, C.E., Zhao, Z., Solimini, N., Lerenthal, Y., Shiloh, Y., Gygi, S.P., Elledge, S.J., 2007b. ATM and ATR substrate analysis reveals extensive protein networks responsive to DNA damage. *Science (New York, N.Y.)*. **316**, 1160-1166.

Matsuoka, S., Huang, M., Elledge, S.J., 1998. Linkage of ATM to cell cycle regulation by the Chk2 protein kinase. *Science (New York, N.Y.)*. **282**, 1893-1897.

Maya, R., Balass, M., Kim, S.T., Shkedy, D., Leal, J.F., Shifman, O., Moas, M., Buschmann, T., Ronai, Z., Shiloh, Y., Kastan, M.B., Katzir, E., Oren, M., 2001. ATM-dependent phosphorylation of Mdm2 on serine 395: role in p53 activation by DNA damage. *Genes & Development*. **15**, 1067-1077.

Meerang, M., Ritz, D., Paliwal, S., Garajova, Z., Bosshard, M., Mailand, N., Janscak, P., Hubscher, U., Meyer, H., Ramadan, K., 2011. The ubiquitin-selective segregase VCP/p97 orchestrates the response to DNA double-strand breaks. *Nature Cell Biology*. **13**, 1376-1382.

Meirelles, G.V., Perez, A.M., de Souza, E.E., Basei, F.L., Papa, P.F., Melo Hanchuk, T.D., Cardoso, V.B., Kobarg, J., 2014. "Stop Ne(c)king around": How interactomics contributes to functionally characterize Nek family kinases. *World Journal of Biological Chemistry*. **5**, 141-160.

Melixetian, M., Klein, D.K., Sorensen, C.S., Helin, K., 2009. NEK11 regulates CDC25A degradation and the IR-induced G2/M checkpoint. *Nature Cell Biology*. **11**, 1247-1253.

Mellacheruvu, D., Wright, Z., Couzens, A.L., Lambert, J.P., St-Denis, N.A., Li, T., Miteva, Y.V., Hauri, S., Sardiou, M.E., Low, T.Y., Halim, V.A., Bagshaw, R.D., Hubner, N.C., Al-Hakim, A., Bouchard, A., Faubert, D., Fermin, D., Dunham, W.H., Goudreault, M., Lin, Z.Y., Badillo, B.G., Pawson, T., Durocher, D., Coulombe, B., Aebersold, R., Superti-Furga, G., Colinge, J., Heck, A.J., Choi, H., Gstaiger, M., Mohammed, S., Cristea, I.M., Bennett, K.L., Washburn, M.P., Raught, B., Ewing, R.M., Gingras, A.C., Nesvizhskii, A.I., 2013. The CRAPome: a contaminant repository for affinity purification-mass spectrometry data. *Nature Methods*. **10**, 730-736.

Miller, S.L., Antico, G., Raghunath, P.N., Tomaszewski, J.E., Clevenger, C.V., 2007. Nek3 kinase regulates prolactin-mediated cytoskeletal reorganization and motility of breast cancer cells. *Oncogene*. **26**, 4668-4678.

Mongelard, F. & Bouvet, P., 2007. Nucleolin: a multiFACeTed protein. *Trends in Cell Biology*. **17**, 80-86.

Moniz, L., Dutt, P., Haider, N., Stambolic, V., 2011. Nek family of kinases in cell cycle, checkpoint control and cancer. *Cell Division*. **6**, 18.

- Moniz, L.S. & Stambolic, V., 2011. Nek10 mediates G2/M cell cycle arrest and MEK autoactivation in response to UV irradiation. *Molecular and Cellular Biology*. **31**, 30-42.
- Morgan, D.O., 1997. Cyclin-dependent kinases: engines, clocks, and microprocessors. *Annual Review of Cell and Developmental Biology*. **13**, 261-291.
- Morgan, D.O., 1995. Principles of CDK regulation. *Nature*. **374**, 131-134.
- Morozumi, Y., Takizawa, Y., Takaku, M., Kurumizaka, H., 2009. Human PSF binds to RAD51 and modulates its homologous-pairing and strand-exchange activities. *Nucleic Acids Research*. **37**, 4296-4307.
- Morris, N.R., 1975. Mitotic mutants of *Aspergillus nidulans*. *Genetical Research*. **26**, 237-254.
- Mosbech, A., Gibbs-Seymour, I., Kagias, K., Thorslund, T., Beli, P., Povlsen, L., Nielsen, S.V., Smedegaard, S., Sedgwick, G., Lukas, C., Hartmann-Petersen, R., Lukas, J., Choudhary, C., Pocock, R., Bekker-Jensen, S., Mailand, N., 2012. DVC1 (C1orf124) is a DNA damage-targeting p97 adaptor that promotes ubiquitin-dependent responses to replication blocks. *Nature Structural & Molecular Biology*. **19**, 1084-1092.
- Muller, H.J., 1927. Artificial Transmutation of the Gene. *Science (New York, N.Y.)*. **66**, 84-87.
- Murphy, D., 2002. Gene expression studies using microarrays: principles, problems, and prospects. *Advances in Physiology Education*. **26**, 256-270.
- Musacchio, A. & Salmon, E.D., 2007. The spindle-assembly checkpoint in space and time. *Nature Reviews.Molecular Cell Biology*. **8**, 379-393.
- Nguyen, C.L., Possemato, R., Bauerlein, E.L., Xie, A., Scully, R., Hahn, W.C., 2012. Nek4 regulates entry into replicative senescence and the response to DNA damage in human fibroblasts. *Molecular and Cellular Biology*. **32**, 3963-3977.
- Nicklas, R.B., 1997. How cells get the right chromosomes. *Science (New York, N.Y.)*. **275**, 632-637.
- Nigg, E.A., 2001. Mitotic kinases as regulators of cell division and its checkpoints. *Nature Reviews.Molecular Cell Biology*. **2**, 21-32.
- Niida, H. & Nakanishi, M., 2006. DNA damage checkpoints in mammals. *Mutagenesis*. **21**, 3-9.
- Noguchi, K., Fukazawa, H., Murakami, Y., Uehara, Y., 2004. Nucleolar Nek11 is a novel target of Nek2A in G1/S-arrested cells. *The Journal of Biological Chemistry*. **279**, 32716-32727.

- Noguchi, K., Fukazawa, H., Murakami, Y., Uehara, Y., 2002. Nek11, a new member of the NIMA family of kinases, involved in DNA replication and genotoxic stress responses. *The Journal of Biological Chemistry*. **277**, 39655-39665.
- Nurse, P., 2000. A long twentieth century of the cell cycle and beyond. *Cell*. **100**, 71-78.
- Nurse, P., 1997. Checkpoint pathways come of age. *Cell*. **91**, 865-867.
- Nurse, P., 1990. Universal control mechanism regulating onset of M-phase. *Nature*. **344**, 503-508.
- Oakley, B.R. & Morris, N.R., 1983. A mutation in *Aspergillus nidulans* that blocks the transition from interphase to prophase. *The Journal of Cell Biology*. **96**, 1155-1158.
- O'Connell, M.J. & Cimprich, K.A., 2005. G2 damage checkpoints: what is the turn-on? *Journal of Cell Science*. **118**, 1-6.
- O'Connell, M.J., Krien, M.J., Hunter, T., 2003a. Never say never. The NIMA-related protein kinases in mitotic control. *Trends in Cell Biology*. **13**, 221-228.
- O'Connell, M.J., Krien, M.J., Hunter, T., 2003b. Never say never. The NIMA-related protein kinases in mitotic control. *Trends in Cell Biology*. **13**, 221-228.
- O'Connell, M.J., Norbury, C., Nurse, P., 1994. Premature chromatin condensation upon accumulation of NIMA. *The EMBO Journal*. **13**, 4926-4937.
- O'Regan, L., Blot, J., Fry, A.M., 2007a. Mitotic regulation by NIMA-related kinases. *Cell Division*. **2**, 25.
- O'Regan, L., Blot, J., Fry, A.M., 2007b. Mitotic regulation by NIMA-related kinases. *Cell Division*. **2**, 25.
- O'Regan, L. & Fry, A.M., 2009. The Nek6 and Nek7 protein kinases are required for robust mitotic spindle formation and cytokinesis. *Molecular and Cellular Biology*. **29**, 3975-3990.
- Osmani, A.H., McGuire, S.L., Osmani, S.A., 1991a. Parallel activation of the NIMA and p34cdc2 cell cycle-regulated protein kinases is required to initiate mitosis in *A. nidulans*. *Cell*. **67**, 283-291.
- Osmani, A.H., O'Donnell, K., Pu, R.T., Osmani, S.A., 1991b. Activation of the nimA protein kinase plays a unique role during mitosis that cannot be bypassed by absence of the bimE checkpoint. *The EMBO Journal*. **10**, 2669-2679.
- Osmani, S.A., May, G.S., Morris, N.R., 1987. Regulation of the mRNA levels of nimA, a gene required for the G2-M transition in *Aspergillus nidulans*. *The Journal of Cell Biology*. **104**, 1495-1504.

- Osmani, S.A., Pu, R.T., Morris, N.R., 1988. Mitotic induction and maintenance by overexpression of a G2-specific gene that encodes a potential protein kinase. *Cell*. **53**, 237-244.
- Osmani, S.A. & Ye, X.S., 1996. Cell cycle regulation in *Aspergillus* by two protein kinases. *The Biochemical Journal*. **317 (Pt 3)**, 633-641.
- Otto, E.A., Trapp, M.L., Schultheiss, U.T., Helou, J., Quarmby, L.M., Hildebrandt, F., 2008. NEK8 mutations affect ciliary and centrosomal localization and may cause nephronophthisis. *Journal of the American Society of Nephrology : JASN*. **19**, 587-592.
- Painter, R.B. & Young, B.R., 1980. Radiosensitivity in ataxia-telangiectasia: a new explanation. *Proceedings of the National Academy of Sciences of the United States of America*. **77**, 7315-7317.
- Park, J.H., Jensen, B.C., Kifer, C.T., Parsons, M., 2001. A novel nucleolar G-protein conserved in eukaryotes. *Journal of Cell Science*. **114**, 173-185.
- Partridge, J.J., Lopreiato, J.O., Jr, Latterich, M., Indig, F.E., 2003. DNA damage modulates nucleolar interaction of the Werner protein with the AAA ATPase p97/VCP. *Molecular Biology of the Cell*. **14**, 4221-4229.
- Patton, J.G., Porro, E.B., Galceran, J., Tempst, P., Nadal-Ginard, B., 1993. Cloning and characterization of PSF, a novel pre-mRNA splicing factor. *Genes & Development*. **7**, 393-406.
- Paulsen, R.D., Soni, D.V., Wollman, R., Hahn, A.T., Yee, M.C., Guan, A., Hesley, J.A., Miller, S.C., Cromwell, E.F., Solow-Cordero, D.E., Meyer, T., Cimprich, K.A., 2009. A genome-wide siRNA screen reveals diverse cellular processes and pathways that mediate genome stability. *Molecular Cell*. **35**, 228-239.
- Pazour, G.J., Agrin, N., Leszyk, J., Witman, G.B., 2005. Proteomic analysis of a eukaryotic cilium. *The Journal of Cell Biology*. **170**, 103-113.
- Peeper, D.S., van der Eb, A.J., Zantema, A., 1994. The G1/S cell-cycle checkpoint in eukaryotic cells. *Biochimica Et Biophysica Acta*. **1198**, 215-230.
- Pelegri, A.L., Moura, D.J., Brenner, B.L., Ledur, P.F., Marques, G.P., Henriques, J.A., Saffi, J., Lenz, G., 2010. Nek1 silencing slows down DNA repair and blocks DNA damage-induced cell cycle arrest. *Mutagenesis*. **25**, 447-454.
- Peters, J.M., 2006. The anaphase promoting complex/cyclosome: a machine designed to destroy. *Nature Reviews.Molecular Cell Biology*. **7**, 644-656.
- Piao, S., Lee, S.J., Xu, Y., Gwak, J., Oh, S., Park, B.J., Ha, N.C., 2011. CK1epsilon targets Cdc25A for ubiquitin-mediated proteolysis under normal

- conditions and in response to checkpoint activation. *Cell Cycle (Georgetown, Tex.)*. **10**, 531-537.
- Polci, R., Peng, A., Chen, P.L., Riley, D.J., Chen, Y., 2004. NIMA-related protein kinase 1 is involved early in the ionizing radiation-induced DNA damage response. *Cancer Research*. **64**, 8800-8803.
- Pu, R.T. & Osmani, S.A., 1995a. Mitotic destruction of the cell cycle regulated NIMA protein kinase of *Aspergillus nidulans* is required for mitotic exit. *The EMBO Journal*. **14**, 995-1003.
- Pu, R.T. & Osmani, S.A., 1995b. Mitotic destruction of the cell cycle regulated NIMA protein kinase of *Aspergillus nidulans* is required for mitotic exit. *The EMBO Journal*. **14**, 995-1003.
- Pu, R.T., Xu, G., Wu, L., Vierula, J., O'Donnell, K., Ye, X.S., Osmani, S.A., 1995. Isolation of a functional homolog of the cell cycle-specific NIMA protein kinase of *Aspergillus nidulans* and functional analysis of conserved residues. *The Journal of Biological Chemistry*. **270**, 18110-18116.
- Rajesh, C., Baker, D.K., Pierce, A.J., Pittman, D.L., 2011. The splicing-factor related protein SFPQ/PSF interacts with RAD51D and is necessary for homology-directed repair and sister chromatid cohesion. *Nucleic Acids Research*. **39**, 132-145.
- Rao, P.N. & Johnson, R.T., 1970. Mammalian cell fusion: studies on the regulation of DNA synthesis and mitosis. *Nature*. **225**, 159-164.
- Reinhardt, H.C. & Yaffe, M.B., 2009. Kinases that control the cell cycle in response to DNA damage: Chk1, Chk2, and MK2. *Current Opinion in Cell Biology*. **21**, 245-255.
- Richards, M.W., O'Regan, L., Mas-Droux, C., Blot, J.M., Cheung, J., Hoelder, S., Fry, A.M., Bayliss, R., 2009. An autoinhibitory tyrosine motif in the cell-cycle-regulated Nek7 kinase is released through binding of Nek9. *Molecular Cell*. **36**, 560-570.
- Roig, J., Groen, A., Caldwell, J., Avruch, J., 2005. Active Nercc1 protein kinase concentrates at centrosomes early in mitosis and is necessary for proper spindle assembly. *Molecular Biology of the Cell*. **16**, 4827-4840.
- Roig, J., Mikhailov, A., Belham, C., Avruch, J., 2002. Nercc1, a mammalian NIMA-family kinase, binds the Ran GTPase and regulates mitotic progression. *Genes & Development*. **16**, 1640-1658.
- Roos, W.P. & Kaina, B., 2013. DNA damage-induced cell death: from specific DNA lesions to the DNA damage response and apoptosis. *Cancer Letters*. **332**, 237-248.

Rothenberg, M.L., 1997. Topoisomerase I inhibitors: review and update. *Annals of Oncology : Official Journal of the European Society for Medical Oncology / ESMO*. **8**, 837-855.

Sage, J., Mulligan, G.J., Attardi, L.D., Miller, A., Chen, S., Williams, B., Theodorou, E., Jacks, T., 2000. Targeted disruption of the three Rb-related genes leads to loss of G(1) control and immortalization. *Genes & Development*. **14**, 3037-3050.

Sahota, N.K., 2010. Cell cycle studies on the human Nek3, Nek5 and Nek11 protein kinases. Unpublished PhD thesis ed. University of Leicester.

Salaun, P., Rannou, Y., Prigent, C., 2008. Cdk1, Plks, Auroras, and Neks: the mitotic bodyguards. *Advances in Experimental Medicine and Biology*. **617**, 41-56.

Salton, M., Lerenthal, Y., Wang, S.Y., Chen, D.J., Shiloh, Y., 2010. Involvement of Matrin 3 and SFPQ/NONO in the DNA damage response. *Cell Cycle (Georgetown, Tex.)*. **9**, 1568-1576.

Savage, K.I., Gorski, J.J., Barros, E.M., Irwin, G.W., Manti, L., Powell, A.J., Pellagatti, A., Lukashchuk, N., McCance, D.J., McCluggage, W.G., Schettino, G., Salto-Tellez, M., Boulwood, J., Richard, D.J., McDade, S.S., Harkin, D.P., 2014. Identification of a BRCA1-mRNA splicing complex required for efficient DNA repair and maintenance of genomic stability. *Molecular Cell*. **54**, 445-459.

Saxena, A., Rorie, C.J., Dimitrova, D., Daniely, Y., Borowiec, J.A., 2006. Nucleolin inhibits Hdm2 by multiple pathways leading to p53 stabilization. *Oncogene*. **25**, 7274-7288.

Schultz, S.J., Fry, A.M., Sutterlin, C., Ried, T., Nigg, E.A., 1994a. Cell cycle-dependent expression of Nek2, a novel human protein kinase related to the NIMA mitotic regulator of *Aspergillus nidulans*. *Cell Growth & Differentiation : The Molecular Biology Journal of the American Association for Cancer Research*. **5**, 625-635.

Schultz, S.J., Fry, A.M., Sutterlin, C., Ried, T., Nigg, E.A., 1994b. Cell cycle-dependent expression of Nek2, a novel human protein kinase related to the NIMA mitotic regulator of *Aspergillus nidulans*. *Cell Growth & Differentiation : The Molecular Biology Journal of the American Association for Cancer Research*. **5**, 625-635.

Schultz, S.J. & Nigg, E.A., 1993. Identification of 21 novel human protein kinases, including 3 members of a family related to the cell cycle regulator nimA of *Aspergillus nidulans*. *Cell Growth & Differentiation : The Molecular Biology Journal of the American Association for Cancer Research*. **4**, 821-830.

Shalom, O., Shalva, N., Altschuler, Y., Motro, B., 2008. The mammalian Nek1 kinase is involved in primary cilium formation. *FEBS Letters*. **582**, 1465-1470.

- Shaw, P. & Brown, J., 2012. Nucleoli: composition, function, and dynamics. *Plant Physiology*. **158**, 44-51.
- Shechter, D., Costanzo, V., Gautier, J., 2004. ATR and ATM regulate the timing of DNA replication origin firing. *Nature Cell Biology*. **6**, 648-655.
- Sherr, C.J. & Roberts, J.M., 1999. CDK inhibitors: positive and negative regulators of G1-phase progression. *Genes & Development*. **13**, 1501-1512.
- Smith, L.A., Bukanov, N.O., Husson, H., Russo, R.J., Barry, T.C., Taylor, A.L., Beier, D.R., Ibraghimov-Beskrovnaya, O., 2006. Development of polycystic kidney disease in juvenile cystic kidney mice: insights into pathogenesis, ciliary abnormalities, and common features with human disease. *Journal of the American Society of Nephrology : JASN*. **17**, 2821-2831.
- Smith, L.D. & Ecker, R.E., 1969. Role of the oocyte nucleus in physiological maturation in *Rana pipiens*. *Developmental Biology*. **19**, 281-309.
- Sohara, E., Luo, Y., Zhang, J., Manning, D.K., Beier, D.R., Zhou, J., 2008. Nek8 regulates the expression and localization of polycystin-1 and polycystin-2. *Journal of the American Society of Nephrology : JASN*. **19**, 469-476.
- Sorensen, C.S., Melixetian, M., Klein, D.K., Helin, K., 2010. NEK11: linking CHK1 and CDC25A in DNA damage checkpoint signaling. *Cell Cycle (Georgetown, Tex.)*. **9**, 450-455.
- Sorensen, C.S., Syljuasen, R.G., Falck, J., Schroeder, T., Ronnstrand, L., Khanna, K.K., Zhou, B.B., Bartek, J., Lukas, J., 2003. Chk1 regulates the S phase checkpoint by coupling the physiological turnover and ionizing radiation-induced accelerated proteolysis of Cdc25A. *Cancer Cell*. **3**, 247-258.
- Stark, G.R. & Taylor, W.R., 2006. Control of the G2/M transition. *Molecular Biotechnology*. **32**, 227-248.
- Surpili, M.J., Delben, T.M., Kobarg, J., 2003. Identification of proteins that interact with the central coiled-coil region of the human protein kinase NEK1. *Biochemistry*. **42**, 15369-15376.
- Tan, B.C. & Lee, S.C., 2004. Nek9, a novel FACT-associated protein, modulates interphase progression. *The Journal of Biological Chemistry*. **279**, 9321-9330.
- Tanaka, K. & Nigg, E.A., 1999. Cloning and characterization of the murine Nek3 protein kinase, a novel member of the NIMA family of putative cell cycle regulators. *The Journal of Biological Chemistry*. **274**, 13491-13497.
- Taylor, W.R. & Stark, G.R., 2001. Regulation of the G2/M transition by p53. *Oncogene*. **20**, 1803-1815.

Toettcher, J.E., Loewer, A., Ostheimer, G.J., Yaffe, M.B., Tidor, B., Lahav, G., 2009. Distinct mechanisms act in concert to mediate cell cycle arrest. *Proceedings of the National Academy of Sciences of the United States of America*. **106**, 785-790.

Toscano, F., Parmentier, B., Fajoui, Z.E., Estornes, Y., Chayvialle, J.A., Saurin, J.C., Abello, J., 2007. P53 Dependent and Independent Sensitivity to Oxaliplatin of Colon Cancer Cells. *Biochemical Pharmacology*. **74**, 392-406.

Trinkle-Mulcahy, L., Boulon, S., Lam, Y.W., Urcia, R., Boisvert, F.M., Vandermoere, F., Morrice, N.A., Swift, S., Rothbauer, U., Leonhardt, H., Lamond, A., 2008. Identifying specific protein interaction partners using quantitative mass spectrometry and bead proteomes. *The Journal of Cell Biology*. **183**, 223-239.

Ubersax, J.A., Woodbury, E.L., Quang, P.N., Paraz, M., Blethrow, J.D., Shah, K., Shokat, K.M., Morgan, D.O., 2003. Targets of the cyclin-dependent kinase Cdk1. *Nature*. **425**, 859-864.

Uetz, P., Giot, L., Cagney, G., Mansfield, T.A., Judson, R.S., Knight, J.R., Lockshon, D., Narayan, V., Srinivasan, M., Pochart, P., Qureshi-Emili, A., Li, Y., Godwin, B., Conover, D., Kalbfleisch, T., Vijayadamodar, G., Yang, M., Johnston, M., Fields, S., Rothberg, J.M., 2000. A comprehensive analysis of protein-protein interactions in *Saccharomyces cerevisiae*. *Nature*. **403**, 623-627.

Upadhyaya, P., Birkenmeier, E.H., Birkenmeier, C.S., Barker, J.E., 2000. Mutations in a NIMA-related kinase gene, Nek1, cause pleiotropic effects including a progressive polycystic kidney disease in mice. *Proceedings of the National Academy of Sciences of the United States of America*. **97**, 217-221.

Vermes, I., Haanen, C., Steffens-Nakken, H., Reutelingsperger, C., 1995. A novel assay for apoptosis. Flow cytometric detection of phosphatidylserine expression on early apoptotic cells using fluorescein labelled Annexin V. *Journal of Immunological Methods*. **184**, 39-51.

Vogler, C., Homan, S., Pung, A., Thorpe, C., Barker, J., Birkenmeier, E.H., Upadhyaya, P., 1999. Clinical and pathologic findings in two new allelic murine models of polycystic kidney disease. *Journal of the American Society of Nephrology : JASN*. **10**, 2534-2539.

Wang, J., Chen, J., Gong, Z., 2013. TopBP1 controls BLM protein level to maintain genome stability. *Molecular Cell*. **52**, 667-678.

Wang, Q., Song, C., Li, C.C., 2004. Molecular perspectives on p97-VCP: progress in understanding its structure and diverse biological functions. *Journal of Structural Biology*. **146**, 44-57.

Wang, X.W., Zhan, Q., Coursen, J.D., Khan, M.A., Kontny, H.U., Yu, L., Hollander, M.C., O'Connor, P.M., Fornace, A.J., Jr, Harris, C.C., 1999. GADD45

induction of a G2/M cell cycle checkpoint. *Proceedings of the National Academy of Sciences of the United States of America*. **96**, 3706-3711.

Weinert, T.A. & Hartwell, L.H., 1988. The RAD9 gene controls the cell cycle response to DNA damage in *Saccharomyces cerevisiae*. *Science (New York, N.Y.)*. **241**, 317-322.

Weiss, W., Weiland, F., Gorg, A., 2009. Protein detection and quantitation technologies for gel-based proteome analysis. *Methods in Molecular Biology (Clifton, N.J.)*. **564**, 59-82.

Wen, W., Meinkoth, J.L., Tsien, R.Y., Taylor, S.S., 1995. Identification of a signal for rapid export of proteins from the nucleus. *Cell*. **82**, 463-473.

White, M.C. & Quarmby, L.M., 2008. The NIMA-family kinase, Nek1 affects the stability of centrosomes and ciliogenesis. *BMC Cell Biology*. **9**, 29-2121-9-29.

Wilke, H.J. & Van Cutsem, E., 2003. Current treatments and future perspectives in colorectal and gastric cancer. *Annals of Oncology : Official Journal of the European Society for Medical Oncology / ESMO*. **14 Suppl 2**, ii49-55.

Wogan, G.N., Hecht, S.S., Felton, J.S., Conney, A.H., Loeb, L.A., 2004. Environmental and chemical carcinogenesis. *Seminars in Cancer Biology*. **14**, 473-486.

Wong, M.L. & Medrano, J.F., 2005. Real-time PCR for mRNA quantitation. *BioTechniques*. **39**, 75-85.

Wu, L., Osmani, S.A., Mirabito, P.M., 1998. A role for NIMA in the nuclear localization of cyclin B in *Aspergillus nidulans*. *The Journal of Cell Biology*. **141**, 1575-1587.

Xiao, Z., Chen, Z., Gunasekera, A.H., Sowin, T.J., Rosenberg, S.H., Fesik, S., Zhang, H., 2003. Chk1 Mediates S and G2 Arrests through Cdc25A Degradation in Response to DNA-damaging Agents. *Journal of Biological Chemistry*. **278**, 21767-21773.

Xiong, Y. & Beach, D., 1991. Population explosion in the cyclin family. *Current Biology : CB*. **1**, 362-364.

Yin, M.J., Shao, L., Voehringer, D., Smeal, T., Jallal, B., 2003. The serine/threonine kinase Nek6 is required for cell cycle progression through mitosis. *The Journal of Biological Chemistry*. **278**, 52454-52460.

Yissachar, N., Salem, H., Tennenbaum, T., Motro, B., 2006. Nek7 kinase is enriched at the centrosome, and is required for proper spindle assembly and mitotic progression. *FEBS Letters*. **580**, 6489-6495.

Yoder, B.K., 2007. Role of primary cilia in the pathogenesis of polycystic kidney disease. *Journal of the American Society of Nephrology : JASN*. **18**, 1381-1388.

Zhang, H., Wang, Q., Kajino, K., Greene, M.I., 2000. VCP, a weak ATPase involved in multiple cellular events, interacts physically with BRCA1 in the nucleus of living cells. *DNA and Cell Biology*. **19**, 253-263.

Zhao, H. & Piwnica-Worms, H., 2001. ATR-mediated checkpoint pathways regulate phosphorylation and activation of human Chk1. *Molecular and Cellular Biology*. **21**, 4129-4139.

Zhou, B.B. & Elledge, S.J., 2000. The DNA damage response: putting checkpoints in perspective. *Nature*. **408**, 433-439.

Zimber, A., Nguyen, Q.D., Gespach, C., 2004. Nuclear bodies and compartments: functional roles and cellular signalling in health and disease. *Cellular Signalling*. **16**, 1085-1104.

Zou, L. & Elledge, S.J., 2003. Sensing DNA damage through ATRIP recognition of RPA-ssDNA complexes. *Science (New York, N.Y.)*. **300**, 1542-1548.